SOME STUDIES ON EXCITED STATES BY E.S.R.

David D. Reekie

A Thesis Submitted for the Degree of PhD
at the
University of St Andrews

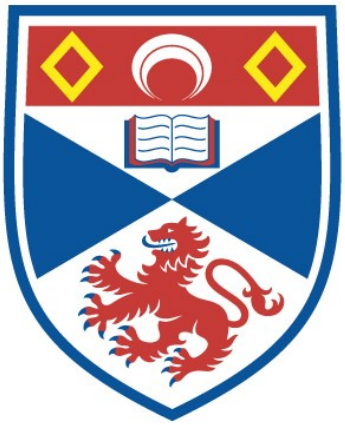

1966

SOME STUDIES ON EXCITED STATES BY E.S.R.

ProQuest LLC.
789 East Eisenhower Parkway
P.O. Box 1346
Ann Arbor, MI 48106 – 1346

DECLARATION

I hereby declare that this thesis has been composed by me, is a record of work carried out by me and that it has not been previously presented for a higher degree.

CERTIFICATE

I certify that David Reekie, B.Sc., has spent at least nine terms as a research student in the Physical Laboratory of the United College of St. Salvator and St. Leonard in the University of St. Andrews, that he has fulfilled the conditions of Ordinance No. 51 of the University Court of St. Andrews and that he is qualified to submit the accompanying thesis in application for the Degree of Doctor of Philosophy.

(Supervisor)

CAREER

The author matriculated in October, 1956, in the United College of St. Salvator and St. Leonard in the University of St. Andrews, and followed a course leading to graduation in June 1960 with the degree of Bachelor of Science with Honours in Natural Philosophy, also being awarded the Class Medal and the Neil Arnott Award for Physics for that year. In the following October, he was admitted by the Senatus Academicus of the same University as a research student in the School of Natural Philosophy in the same college and until 1964, was engaged on the work described in this thesis. The author has now joined the Western Regional Hospitals Board of Scotland, Regional Physics Department, where he is engaged on a practical study of the possible applications of electron spin resonance as a diagnostic technique.

Frontispiece

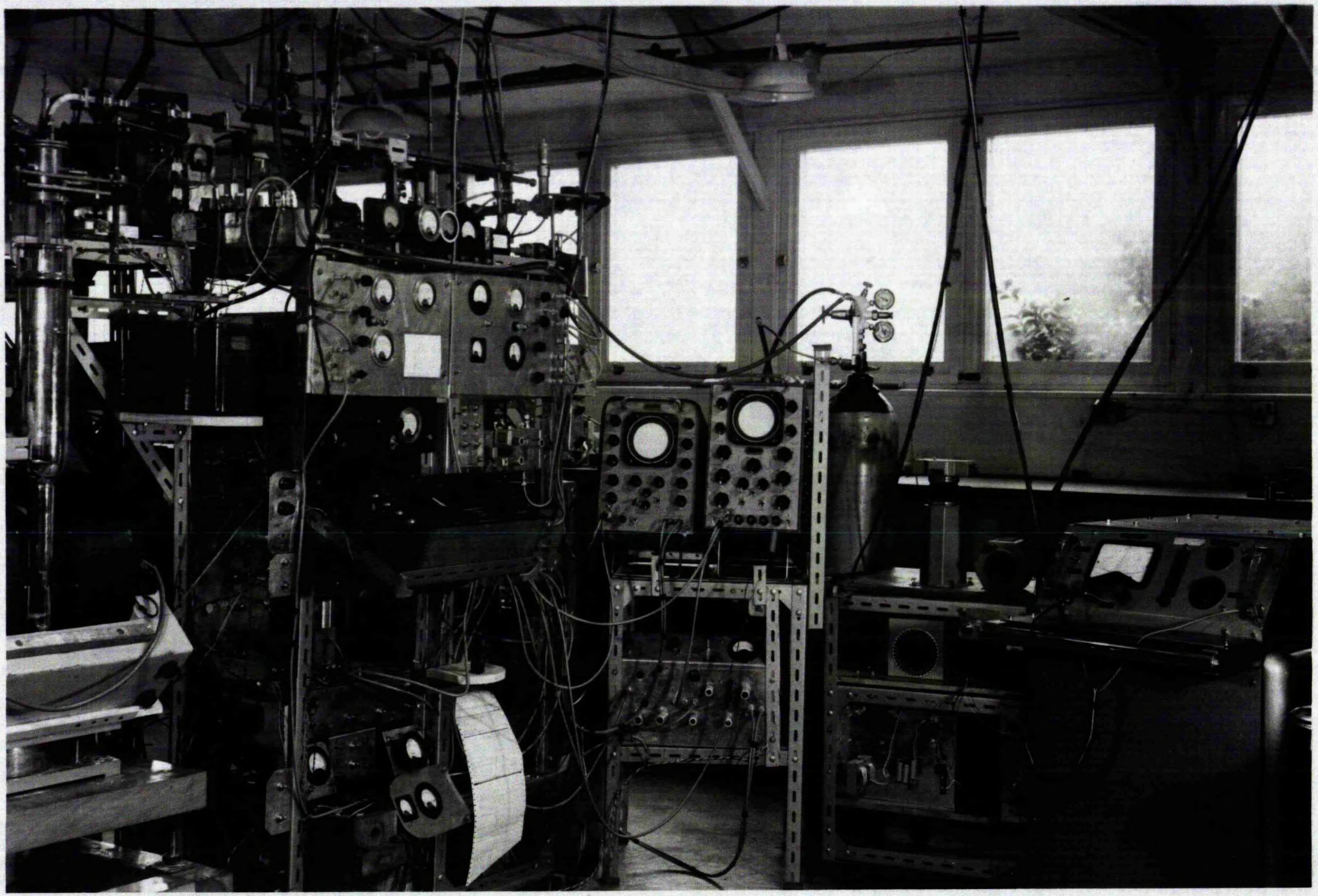

A general view of the apparatus

INDEX

CHAPTER I

INTRODUCTORY

The phenomenon of phosphorescence has intrigued investigators for decades, and many and varied have been the suggestions as to its origins. However, the advent of modern atomic physics and the quantum theory has narrowed the possibilities to a single mechansim, namely that the phosphorescent emission is due to electronic transitions in the sample. Until very recently the only method of investigation available to the experimenter was that of optical studies, and this to a large extent explains why nearly all the known phosphors are in the visible region of the spectrum. The optical investigations have revealed many interesting effects, and the volume of interest in this field is certainly not diminishing. In general, it has been found that only one electronic transition is responsible per molecule, suggesting that the excited electron would therefore be unpaired in spin, and hence should exhibit paramagnetism.

In 1944, Kasha showed the existence of paramagnetism in an organo-phosphor, performing an experiment of considerable technical difficulty, since only the very small change

in gross susceptibility could be measured and only at very low temperatures. Since 1946, however, microwave spectroscopy has offered fresh opportunities for detecting paramagnetism, although at the time the work contained in this thesis was begun little advantage had been taken of it. Since then, the use of microwave spectrometers has become more widespread, and indeed they have now acquired that supreme accolade of indispensibility - commercial production! Stoodley has recently commented that "the best way to understand a spectrometer is to build one" (R9), a comment which is adequately substantiated by some recent papers. An account of the design, construction and performance of the spectrometer used is given in Chapter III preceded by a short theoretical introduction to electron spin resonance (e.s.r.) in Chapter II.

Since this thesis was intended to be a basis for future continuing work, it was decided to make a general review of all phosphorescent materials with the exception of those which are impurity activated. As discussed in Chapter VI, this involved a lengthy study of the literature which often revealed that the information given was inadequate for an assessment of the phosphor's possibilities. It was obvious in many cases, however, that low temperature measurements would be necessary and the cryostats designed and used are discussed in Chapter IV. The experimental results and their evaluation are given in

Chapters VII, VIII and IX.

On various occasions the spectrometer was used to study materials which were quite unrelated to the general line of attack and some data on these substances is included in Chapter X. The thesis concludes with some comments and suggestions by the author for future work.

CHAPTER II

PARAMAGNETIC RESONANCE

II (a). **Introductory.** Paramagnetic substances may be grouped in the following categories: (1) atoms or ions possessing an unfilled inner electronic level, (2) atoms or molecules with an odd number of electrons, (3) metals and (4) molecules with independent unpaired spins or with coupled electrons of spin state 1.

The case of a completely free electron will be considered first, and the effect of perturbing influences will be added in subsequent sections. When the electrons are in a zero local magnetic field, the spins are randomly orientated and are of equal energy. If a steady (d.c.) magnetic field is applied to the spins, they align themselves either parallel or antiparallel to the applied field, no intermediate positions being allowed since the spin is quantized ($= \frac{1}{2}$, for a single electronic spin). The electrons therefore fall into two groups, of different energies, those lying parallel to the field having the lower energy.

The ratio of the distribution of the electrons between

these two states under equilibrium conditions follows the usual Maxwell-Boltzmann expression

$$N_a/N_p = \exp(-E_{ap}/kT) \qquad (2.1)$$

where N_p and N_a = the number of electrons lying parallel and antiparallel respectively to the magnetic field, E_{ap} = the energy gap between the two states and T = the absolute temperature. It can be seen from this equation that at all times there is an excess of electrons in the lower state.

The magnitude of E_{ap} is $2(\frac{1}{2} g\beta H)$, where β is the Bohr magneton and g is known as the spectroscopic splitting factor and has a value of 2.0023 for a completely free spin. So it is clear that the magnitude of the splitting is proportional to the applied magnetic field (H) acting on the electron.

If radiofrequency energy ($h\nu$) is applied to the system of spins, at right angles to the applied magnetic field, spins from the lower energy state can be stimulated to the higher energy state, and the sample may absorb power. The necessary condition for this resonant absorption is therefore:-

$$E_{ap} = h\nu = g\,H(\Delta S)\beta \qquad (2.2)$$

where ΔS is the change in spin quantum number.

From equation (2.1) it can be seen that the larger the applied magnetic field, the greater the power absorption by the sample and the easier to detect the phenomenon. In practice,

however, the efficiency of the detecting apparatus acts as a limiting factor on the frequency used (see Chapter III) and the optimum value is found to be around 10 Gc/s.

The field which can be usefully used is also a limiting factor, since a compromise has to be made between its strength and homogeneity. It is obvious from (2.2) that if H varies by dH over the sample volume, a set of absorptions relevant to H + dH will be obtained. This would appear as a broadening of the resonance, which is generally unacceptable. A variation of .1 gauss over 1 cc. was considered adequate for the work in this thesis, although for many studies this is not the case. At 3500 gauss (the field corresponding to 10 Gc/s.) this homogeneity can be attained without great difficulty.

II (b). Temperature variation. From equation (2.1) it can also be seen that the intensity of the absorption is temperature dependent. On lowering the temperature from 300°K to 80°K there is a gain of 4 in the number of excess spins, while on cooling to 1.2°K the gain is 180 times. So the benefits of working with liquid helium can be quite considerable, provided saturation does not occur (see below).

II (c). Effects caused by the presence of the host lattice.

(c) 1. Spin-lattice relaxation. When the electron is raised to an excited state it must return to the ground state. There are

various mechanisms by which this can occur, known as relaxation processes, the most common being known as "spin-lattice" relaxation, in which the spin energy is lost by interactions with the lattice. This mechanism has a characteristic decay time known as the "spin-lattice relaxation time." If this is long (i.e. the interaction is weak) saturation of the upper state ($N_a = N_p$) can occur, and so the net absorption of power by the sample decreases. Since this condition is more likely at the centre of the resonance line than in the wings, the observed result is a broadening of the line. This effect is more common in free radical studies, and can be made worse by lowering the temperature, since this reduces the amplitude of the lattice vibrations. The reverse effect is also possible, i.e. very short relaxation times, which also leads to a broadening of the resonance since the electrons involved do not have sufficient time to reach thermal equilibrium.

(c) 2. <u>the Spin Hamiltonian</u>. An assembly of spins in a lattice are subject to various other interactions both with the lattice and themselves. These interactions can be described by the following Hamiltonian:-

$$W = W_F + V + W_{LS} + W_{SS} + \mu_B \underline{H}(\underline{L} + 2\underline{S}) + W_N - g_I \mu_N \underline{I}.\underline{H}. \qquad (2.3)$$

where W_F = that portion of the energy of a free ion which is not dependent on spin. ($\sim 10^5 cm^{-1}$).

V = the electrostatic energy due to the crystalline field ($\sim 10^4 cm^{-1}$).

W_{LS} = the interaction due to the coupling of the spin and the orbital motions (spin-orbit coupling) ($\sim 10^2 cm^{-1}$).

W_{SS} = the spin-spin interaction ($\sim 1 cm^{-1}$).

$\mu_B \underline{H}(\underline{L} + 2\underline{S})$ = the interaction with the applied field ($\sim 1 cm^{-1}$).

W_N = the interaction of the spin magnetic moment with nuclear spins (if any) ($\sim 10^{-2} cm^{-1}$).

$g_I \mu_N \underline{I} \cdot \underline{H}$ = the energy of the nucleus in the magnetic field ($\sim 10^{-3} cm^{-1}$).

For crystalline fields of high symmetry, the manner of the splitting of the orbital levels can often by predicted by group theory. In general only the lowest orbital state will be populated at room temperature, although spin degeneracy may remain. For an atom in a given state, g is given by

$$g = \frac{3}{2} + \frac{S(S+1) - L(L+1)}{2J(J+1)} \qquad (2.4)$$

where L and S are the orbital and spin quantum numbers. If $L = 0$, $g = 2$ and any deviation from this value can be attributed to a residual spin-orbit coupling.

The crystalline field may also be responsible for further splitting through the spin-orbit coupling, since if the spin quantum number is 1 or more, the spin degeneracy may be lifted

in the absence of a magnetic field. This splitting, known as zero-field splitting, may affect each magnetic level in a different way, so that the energy relationships between the various levels may be different from that expected. Using a fixed frequency, the various $dM = 1$ transitions will therefore appear at different field strengths and this effect is known as fine structure. It is therefore often helpful in cases where the fine structure is complex, to study the spectrum using different energy gaps (E_{ap}) (i.e. using different microwave frequencies).

For any number of odd electrons in a molecule, Kramer's theorem predicts that the lowest energy state will always be spin degenerate, so that in these cases, e.s.r. is always possible in principle.

For work on spin resonance phenomena, the Hamiltonian given in (2.3) can be transformed to one containing only spin components, and experimentally observed quantities can then be expressed as the parameters. This "spin Hamiltonian" can be written as a generalized operator expression, but if the crystal has axial symmetry along an axis (e.g. the z-axis) it can be simplified considerably to:-

$$\begin{aligned}\mathcal{H} = {} & \mu_B(g_{\parallel}H_zS_z + g_{\perp}(H_xS_x + H_yS_y)) + D(S_z^2 - \frac{S(S+1)}{3}) \\ & + AI_zS_z + B(I_xS_x + I_yS_y) + Q'(I_z^2 - \frac{I(I+1)}{3}) \\ & - g_I\mu_N\underline{H}\cdot\underline{I} \end{aligned} \qquad (2.5)$$

where (2S+1) is the multiplicity of the level under consideration. D is the fine structure constant, I_j are the components of the nuclear spin and A and B are the hyperfine structure constants (see below). The term involving Q' represents the quadrupole interactions, but these were not observed in the present work and need not be considered in detail.

For an arbitrary angle ϕ, between an axis of symmetry and the applied field, the observed g-value of a line is given by:-

$$g^2 = g_{//}^2 \cos^2\phi + g_{\perp}^2 \sin^2\phi \qquad (2.6)$$

(c) 3. Hyperfine structure. (h.f.s.). The terms A and B in equation (2.5) arise from the interaction of the electronic spin with the nuclear spin on any atom lying within its spatial orbit. This limits the effect to certain atoms such as H, N Cu, etc. which possess a nuclear spin and excluding such common atoms as C^{12} and O^{16}. No h.f.s. was directly observed in the experiments reported later, although the presence of unresolved components was detected.

For the observation of h.f.s., conditions similar to those required for the observation of e.s.r. must be fulfilled, e.g. field homogeneity, magnetic modulation amplitude (both d.c. and r.f. (III (k) 1)), relaxation time, dilution (II (c) 4) and the use of the correct medium. The last condition was the limiting one in most of the work discussed later. In the crystalline phase, the anisotropy of the electronic spin transition does not

matter, while for liquid samples the rapid tumbling of the molecules averages this component to zero. But in a glassy matrix neither of these conditions is fulfilled and the line is therefore broadened. The unresolved h.f.s. can therefore act as an additional broadening mechansim.

(c) 4. Other line-width mechanisms. Two other mechanisms which are often important in e.s.r. studies and which have not yet been mentioned are "dipole-dipole" and exchange interactions. The former, which results in a broadening of the line due to the dipolar interactions between neighbouring spins is discussed fully in (X (c) 3), while the latter is a quantum mechanical effect which in general leads to line broadening. In the special case of identical spins, however, the exchange interactions can lead to considerable line narrowing. The line-shape is narrowed at the half-power points and increased in the wings, so that the resulting curve approximates more closely to that of a Lorentzian distribution than to the normal Gaussian one. Both these interactions can be reduced by dilution in either a diamagnetic isomorphic host crystal or a diamagnetic solvent which may be frozen into a glassy or crystalline state.

CHAPTER III

THE SPECTROMETER

III (a). Design considerations for optimum sensitivity.

The magnetic susceptibility χ of a paramagnetic substance is proportional to the number of spins and can be written in terms of a real part χ' and an imaginary part χ''. Changes in χ'' can be detected as changes in the microwave power absorbed by the sample, while changes in χ' appear as changes in frequency.

In a spectrometer using a reflection cavity, changes in χ' may be detected since the reflected wave may interact with the incident wave. These waves are usually carefully adjusted so that they cancel out, but if the frequency of the incident wave shifts, this condition may no longer be maintained, and the resulting signal can appear as a spurious absorption change. In this spectrometer, the klystron frequency is kept constant (see III (d) 1) and the signal detected is due solely to changes in χ''.

Feher (Q1) has shown that for the minimum detectable number of spins, the following equation holds:-

$$\chi''_{min} \simeq \frac{1}{Q_o \pi \eta} \left[\frac{(N_m/L + F_A + t_D - 1)\, L.kT(\Delta\nu)}{2P_o} \right]^{\frac{1}{2}}$$

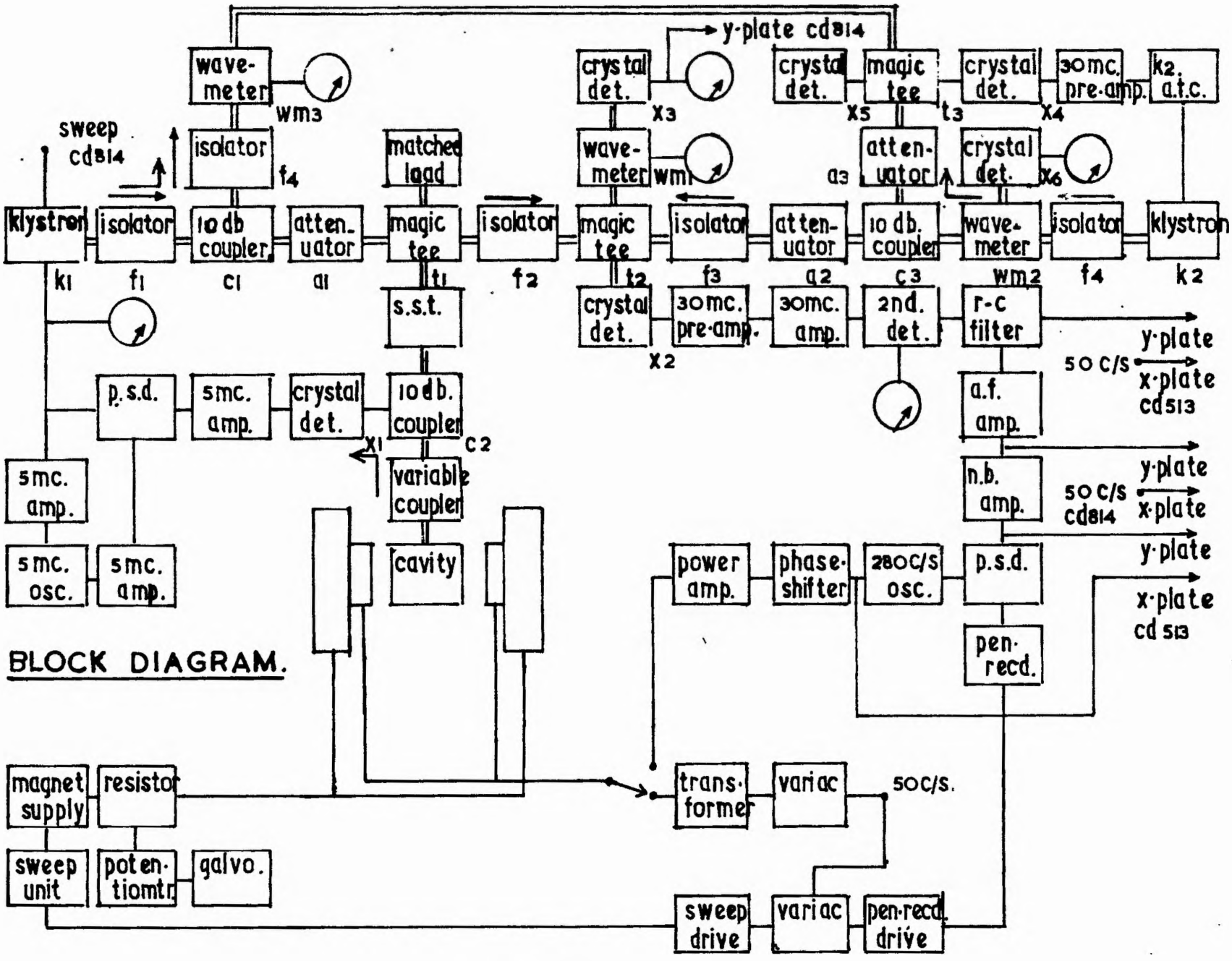
BLOCK DIAGRAM.
wave-meter
wm3
isolator
f4
sweep cd814
klystron
isolator
10 db coupler
atten-uator
magic tee
isolator
matched load
k1
f1
c1
a1
t1
f2
s.s.t.
p.s.d.
5mc. amp.
crystal det.
10 db. coupler
x1
c2
variable coupler
5mc. amp.
5mc. osc.
5mc. amp.
cavity
y-plate cd814
crystal det.
x3
wave-meter
wm1
magic tee
t2
crystal det.
x2
isolator
f3
30mc. pre-amp.
crystal det.
x5
magic tee
t3
atten-uator
a3
atten-uator
a2
30mc. amp.
crystal det.
x4
30mc. pre-amp.
k2. a.t.c.
crystal det.
x6
10 db. coupler
c3
2nd. det.
wave-meter
wm2
isolator
f4
klystron
k2
r-c filter
y-plate
50 c/s
x-plate
cd513
a.f. amp.
n.b. amp.
50 c/s
cd814
y-plate
x-plate
y-plate
x-plate
cd 513
power amp.
phase-shifter
280c/s osc.
p.s.d.
pen-recd.
magnet supply
resistor
sweep unit
poten-tiomtr.
galvo.
trans-former
variac
50c/s.
sweep drive
variac
pen-recd. drive

Figure III 1

where

Q_o = the unloaded Q-factor of the resonant cavity,

η = the filling factor, which depends on the field distribution in the cavity and in the sample,

N_m = incident noise from the microwave system,

L = the conversion loss of the crystal detector,

F_A = the noise figure of the amplifier,

t_D = the noise temperature of the crystal,

$\Delta\nu$ = the bandwidth of the detecting apparatus,

P_o = the microwave power supplied by the klystron.

The various factors will be discussed as they occur in the text.

There are at present two practical possibilities in the solution of equation (2,2), the use of either 3cm. (9Gc/s.) or 8mm. (35Gc/s.) equipment. Feher has shown that both give comparable sensitivities in terms of the above equation, but 8 mm. components are more expensive, demand closer workshop tolerances and need higher field strengths, so 3cm. (X-band) equipment was decided on.

A block diagram of the apparatus is given in Figure III 1 and was designed and built by the author.

III (b). <u>The microwave circuit</u>.

(b) 1. <u>The bridge</u>. The basic circuit consists of a

balanced bridge, using the isolation properties of a magic tee. These are such that at T1, with arm 2 matched and with a matched reflection cavity in arm 1, no signal is coupled from the E arm to the H arm. Variable phase-shift and attenuation are provided in arm 1 or 2, for fine control of the balancing. On e.s.r. absorption in the cavity, the power balance is altered, and a microwave signal proportional to this change will be directed along the H arm, where it is detected by a crystal. Superheterodyne detection of this signal is used to minimize the low frequency crystal noise (N_m/L). Feher has shown that this noise falls off as ν^{-1}, and is negligible at 30 Mc/s. the i.f. is produced by mixing the signal power with microwave power from a second klystron (K2); a second magic tee (T2) is used as the mixer and the i.f. voltage so produced at crystal (X2) is amplified by a tuned amplifier, and then detected by a valve detector.

(b) 2. Presentation of e.s.r. spectra. This can be done in two ways. Firstly, with a 50c/s. magnetic field modulation, the detected signal is applied to the Y-plates of a scope. A correctly phased 50c/s. signal is also applied to the X-plates, and the back trace is eliminated by a 50c/s. Z-modulation. A display, such as that shown in Figure III 8 (4), is then obtained. An R-C filter is used to define the bandwidth ($\Delta\nu$); 10^4c/s. is the commonly used value with this arrangement. The second method

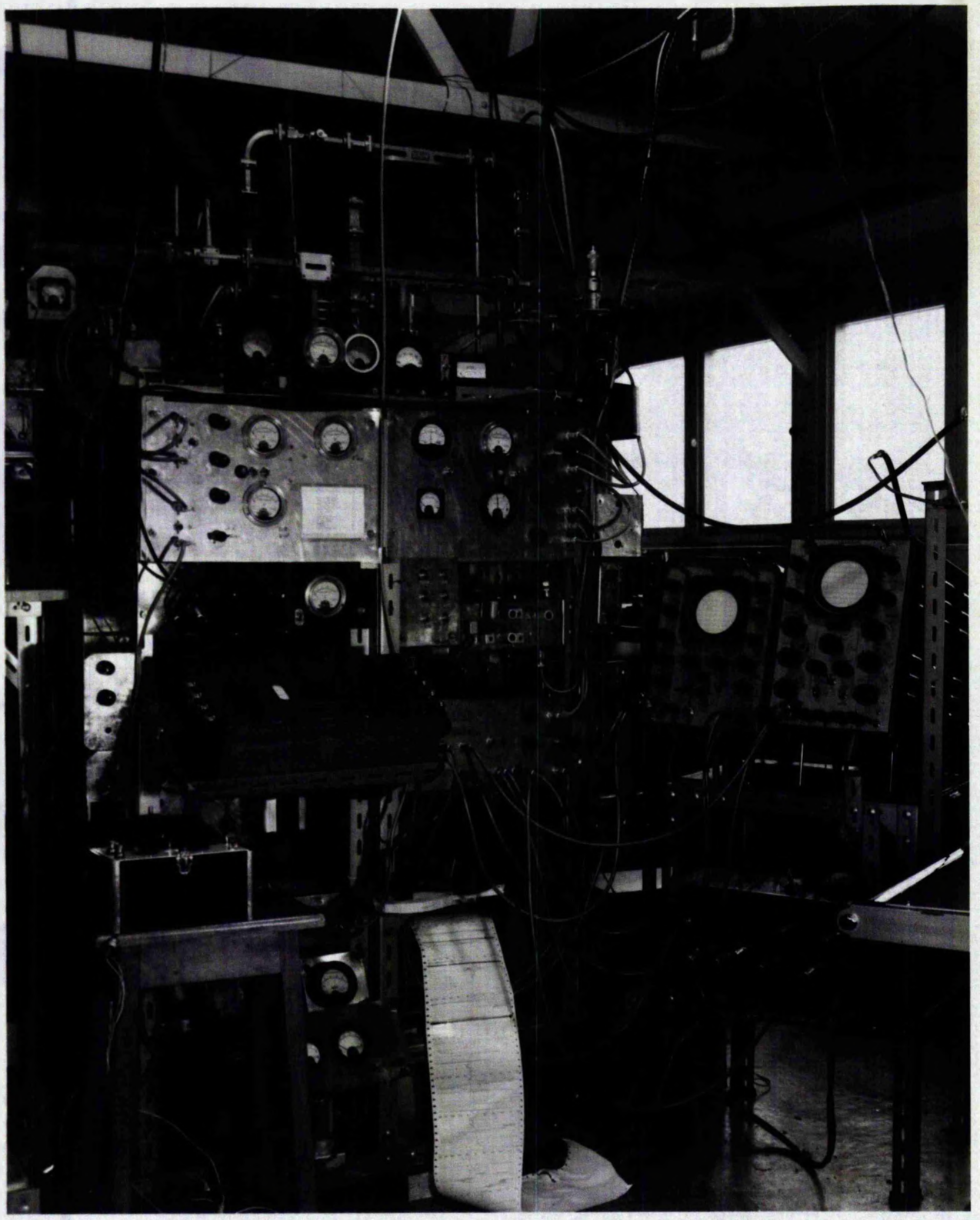

The electronic part of the apparatus

Figure III 2

is of greater sensitivity than the video method discussed above. If the output bandwidth is decreased to the order of 1c/s., it can be seen from equation (3.1) that a gain of 100 times is obtained. To achieve this bandwidth, a phase-sensitive detection system is used, the information being obtained in the form of a first derivative pen-recording.

(b) 3. Auxiliary circuits. An Automatic Frequency Control (K1.A.F.C.) is used to ensure that K1 and the cavity have the same resonant frequency, and a second system (K2.A.F.C.) to keep the i.f. constant at 30Mc/s.

III (c). Microwave components.

(c) 1. Klystrons. The klystrons used were English Electric model K302 (operating frequency = 9570 - 9085 Mc/s., mechanical tuning range = 30Mc/s., power output = 15mW.) D.C. heating was used to reduce 50c/s. pick-up. Ferrite isolators (Microwave Instruments) (forward attenuation = $\frac{1}{2}$db., reverse attenuation = 22db.) are used to reduce klystron pulling, caused by varying power reflections in the microwave circuitry.

(c) 2. Mounting. The waveguide system is mounted above eye-level as can be seen in Figure III 2; since it is rarely touched after the initial adjustment, this arrangement is convenient and allows the relevant meters to be placed at eye-level. The wave-guide used throughout is American X-band (.9" x .4" i.d.).

(c) 3. Magic tees. T1 is a Philips (PP4050X) model, which has a quoted 40db. decoupling between the E and H arms. However, it was found that this value could be greatly improved at a given frequency by inserting 3-stub tuners in the E and H arms. The frequency chosen was 9355Mc/s., as the klystron gives its maximum power output around this value. All other tunable components in the circuit were optimized at this frequency, and during operation of the spectrometer the resonant frequency of the cavity was adjusted to this value as closely as possible. This greatly facilitates the ease of operation.

Tees T2 and T3 were made in the workshop and are of a lower standard, but since their function is only microwave mixing, this is acceptable.

(c) 4. Detailed balancing of the arms 1 and 2 of T1. Since the detecting system is a null device, optimum sensitivity might be expected when the cavity is perfectly matched to the wave-guide. But this is an inherently unstable situation, and in practice a small (constant) mismatch is introduced to avoid this. However, this condition naturally varies from sample to sample, and some device for quick detailed balancing of the bridge is needed. Two methods were used:-

Sliding stub tuner and matched load. The matched load is a device (a wooden fish-tail, 12" long) which is capable of

absorbing most of the power falling on it and is placed in arm 2. The resultant standing wave in arms 1 and 2 can be minimized by judicious use of the sliding stub tuner (Microwave Instruments 32/1400) which is a post projecting into the microwave run and capable of both vertical and horizontal movement; this device must be used with care as the control is rather critical.

Attenuator and Phase-shifter. The device above is very frequency sensitive, and if the frequency of the cavity shifts during a pen-recording, the changes in the standing wave ratio lead to a drift in the base-line of the pen-recording. These effects can be reduced somewhat by use of a set-up which is less frequency sensitive. This is done by removing the matched load, removing the sliding stub from the waveguide and putting in arm 2 a phase-shifter (MI 32/2325), attenuator (MI 32/670) and a short circuit.

(c) 5. Crystals. The crystals used were BTH types CS3-A and CS3-B, depending on the mount used. The mount for M1 was a Philips PP4220X, the rest were made in the workshop.

(c) 6. Cavities. The cavity arm will be discussed in relationship with the cryostats, but the actual cavities used are discussed below.

As can be seen from equation (3.1) as high a Q-factor (consistent with K1 frequency stability) as possible is desirable,

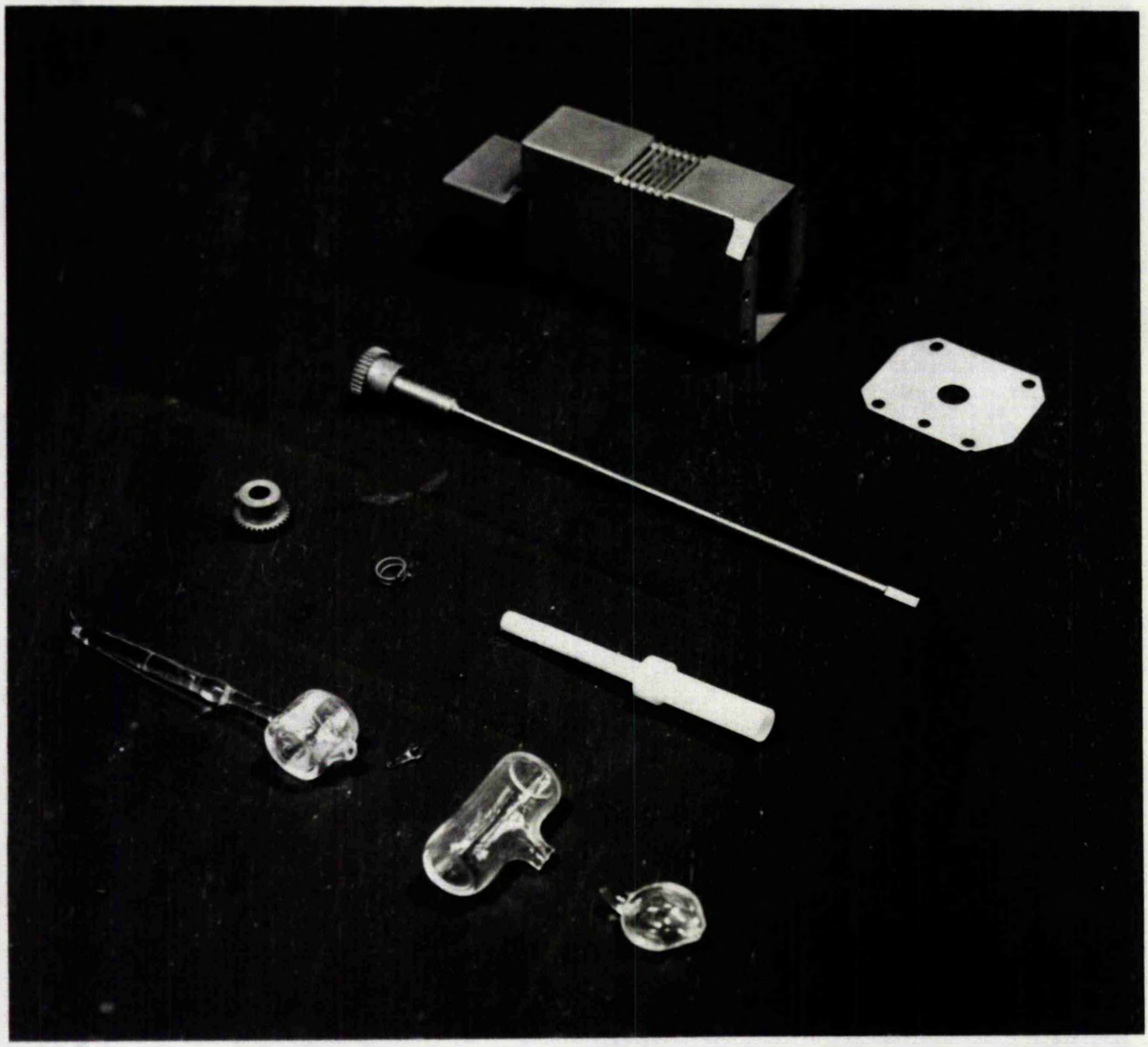

A typical cavity, complete with sample rotation mechanism. The three quartz sample holders are also shown.

Figure III 3.

but due to the limitations of the magnet pole-piece gap ($2\frac{1}{4}$") and the need to fit a cryostat into this gap as well, the only possibility is a H_{012} rectangular mode or a H_{11} cylindrical mode type; the requirements of maximum light input rule out the H_{11} mode, as the wall currents are unfavourable for cutting slits.

The dimensions of a H_{012} cavity are given by:-

$$\nu_{res} = \frac{c}{2\sqrt{\epsilon}} \left[\left(\frac{1}{a}\right)^2 + \left(\frac{2}{d}\right)^2 \right]^{\frac{1}{2}} \qquad (3.2)$$

where a = the broad face of the wave-guide (.9") and d = the length of the cavity. The $\sqrt{\epsilon}$ factor means that different cavities have to be made for the various dielectrics used (air; liquid nitrogen ($\epsilon = 1.4$); liquid helium (at 1.6°K, $\epsilon = 1.057$, $\tan\delta < 5\ 10^{-6}$(T71)). It is also desirable that the sample, which for maximum sensitivity should sit in the middle of the cavity, can be rotated through at least 360°, for measurement of anisotropic effects. To do this, the sample is mounted on a teflon tube (Figure III 3); the teflon, which passes through the E-field of the cavity, reduces the length by .10" to 1.7". Onto the teflon is screwed a gear-wheel, which meshes (1:1) with a similar gear-wheel, capable of rotation from outside the cavity arm by means of a non-magnetic stainless steel rod. In the case of the N_2 arm, a slow motion drive was fitted which has about $\frac{1}{2}^0$ resolution, while for the

He arm, a pointer and scale was used and here about 2^{o} resolution could be attained.

As it is desired to work at a fixed frequency (9355 Mc/s.) and as each sample has a different dielectric constant, some form of variable tuning had to be introduced. This was done by means of a quartz rod, entering at the E-bend and passing down the inside of the wave-guide.

The area exposed by the slits was determined by the solid angle of the incident light beam (see IV (b)). The optimum slit width was found by trial, and their direction is determined by that of the wall currents in the cavity. The slits are 1 mm. wide and $\frac{1}{2}$ mm. apart; if all the slits are removed, the Q-factor falls by a factor of 3, while the light input only goes up by 1.5. The slits are milled from the wave-guide and filed to a minimum thickness; the use of wires strung across the gap is not recommended as they may vibrate in the modulation field (R33). The cavities are bolted on to a flange on the wave-guide run by four 6 BA screws, which also serve to locate the coupling hole. The size of the coupling hole, which was made from .010" Cu, was found by trial for a particular sample. The cavities were silvered electrolytically to increase the Q-factor. The values attained for the various cavities were:-

$Q_{300^{o}K} = 3000$; $Q_{77^{o}K} = 4000$;

$Q_{1.6^{o}K} = 8000$ (both cavities); $Q_{gas\text{-}flow} = 3000$.

The gain in Q is due to the increasing wall conductivity at the lower temperatures. The values quoted are loaded Q values, measured at the half-power points by a high Q wavemeter.

(c) 7. Variable coupler. When the cavity arm was put into liquid nitrogen or helium, it was found that the coupling hole did not give reproducible results. (The main difficulty is not so much the loss in sensitivity from the mismatch, but that the Kl.A.F.C. circuit cannot function reliably when a considerable mismatch occurs. Adjusting the sliding stub tuner does not help as this does not affect the standing wave ratio between the cavity and the 10db. coupler). The problem was overcome by fitting a variable coupler; this is a device in which the broad dimension of the wave-guide is reduced below cut-off by means of metal strips bolted on the narrow face, and the length cut-off is varied by means of a piece of material whose dielectric constant is such as to make the wave-guide go above cut-off (R11, R12). In liquid helium, the variable coupler used at room temperature worked well, using teflon as the dielectric, but in liquid nitrogen, which has a much higher dielectric constant than air, the width of the metal strips had to be increased (from .2" to .3") and perspex used in place of teflon. The sensitivity of the spectrometer is completely unaffected by the presence of these devices, which are controlled by a stainless steel rod, passing out through the top plate. The change of

coupling is not very large, but is sufficient for the purpose.

(c) 8. Teflon filled wave-guide. The second problem associated with the immersion of the tail in a cryogenic liquid, is that when the liquid boils off, the level falls, setting up a varying reflection in that arm, with the result that, when pen-recording over several minutes, considerable base-line drift occurs. When the u.v. lamps were used, this effect became particularly serious. This difficulty has been overcome by filling up the inside of the wave-guide as completely as possible with teflon. A piece of teflon, 10" long, was made as tight a fit as possible, cooled in liquid nitrogen and pushed into position. This source of drift was then found to have been reduced to negligible proportions. As the loss factor of teflon is very small ($\tan\delta$ = .0003), the sensitivity of the spectrometer is unaffected. The plug was tapered at both ends to reduce reflections.

III (d). Kl.A.F.C.

(d) 1. Need for Kl.A.F.C. Klystrons, being unstabilized oscillators, are at all times subject to a certain amount of frequency drift. The manufacturers quote a maximum of 5Mc/s. Since a Q of 8000 corresponds to a half-power width of only 1Mc/s., obviously pen-recording for several minutes is impossible. The main troubles to be corrected are:-

(i) environmental thermal changes;

(ii) mains voltage changes;

(iii) 50c/s. pick-up on the repeller;

(iv) cavity resonance frequency drift (due to changes in the temperature of the cryogenic liquid and to rotation of the sample);

(v) microphonics.

The only way to correct for all these is to have a system which locks the klystron frequency to that of the cavity.

(d) 2. Outline of the method used. A small 5Mc/s. sinusoidal sweep is applied through a condenser to the reflector of Kl, and this amplitude modulation produces a frequency modulation of the klystron output power. The reflected power from the cavity will thus now also possess 5Mc/s. sidebands, whose amplitude and phase are dependent on the difference between the frequency of Kl and the cavity resonance frequency. The signal is coupled out of the cavity arm by means of a 10db. coupler and is detected at crystal Xl, whose output will thus contain a 5Mc/s. component. After amplification, the signal is phase-sensitively detected and the d.c. signal obtained fed onto the repeller of Kl. The more common method of stabilization, a modified Pound system (R5) uses a similar technique, modulating a crystal in arm 2. There is probably little to choose between them, although the Pound system will also correct for any changes occurring in arm 2 and also for changes caused by the sliding stub tuner. Klystron modulation systems have been mentioned by (R3, R4). Other systems using a separate reference cavity, or

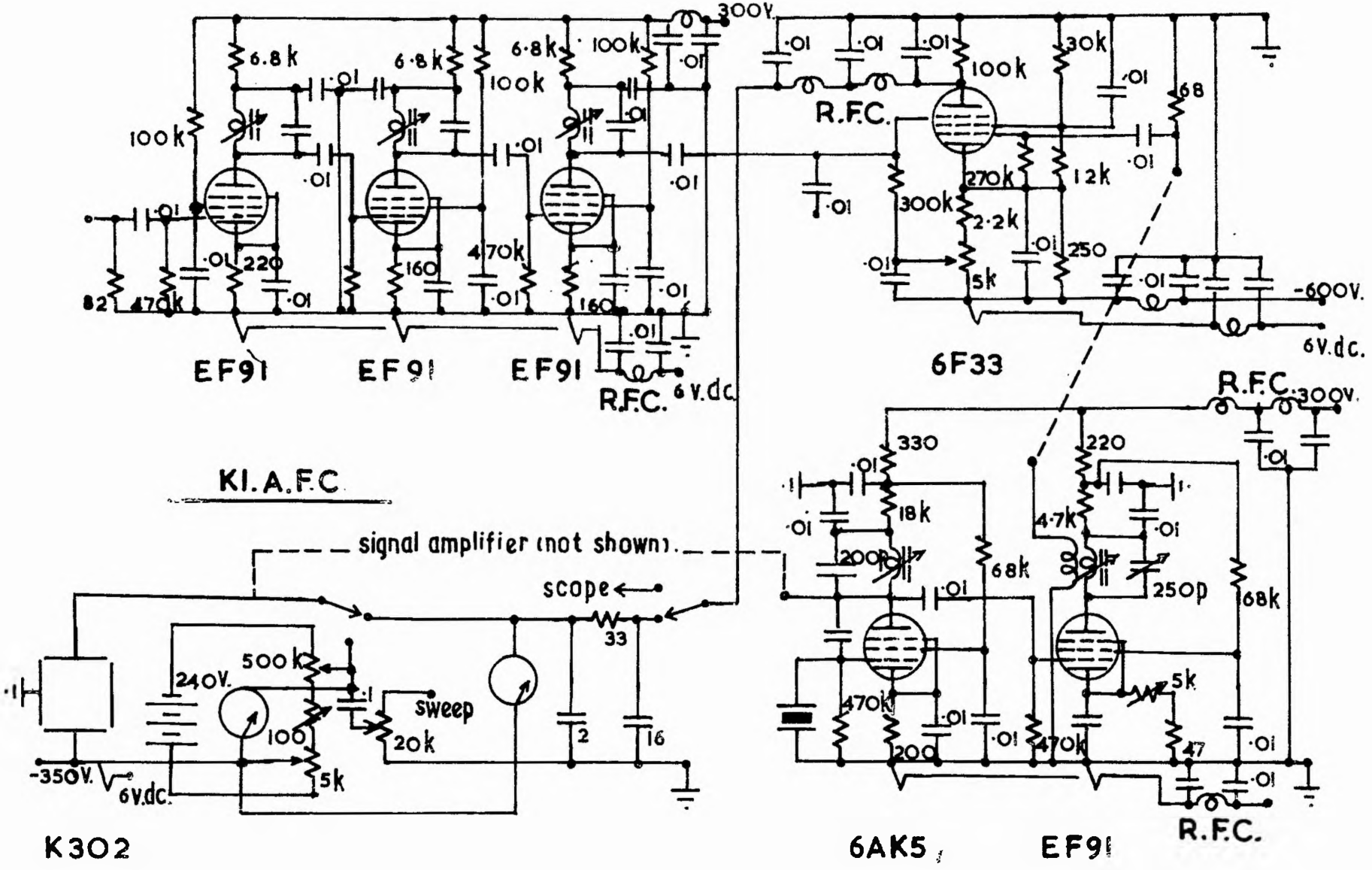
300V.
6.8k
100k
.01
220
160
470k
82
EF91
EF91
EF91
R.F.C.
6V.dc.
K1.A.F.C.
signal amplifier (not shown)
scope
33
500k
240V.
100
20k
5k
sweep
2
16
-350V.
6V.dc.
K302
R.F.C.
100k
30k
68
270k
12k
300k
2·2k
250
-600V.
6V.dc.
6F33
R.F.C.
300V.
330
18k
200p
68k
4·7k
250p
470k
200
47
6AK5
EF91
R.F.C.

Figure III 4

two cavities both offtuned and acting as a microwave discriminator (R6) or using mechanical tuning (R7) have little to recommend them in the present case.

For a theoretical discussion by the author of the circuit, in which the various design parameters are found, see Appendix 1.

(d) 3. Details of the Kl.A.F.C. loop. (Figures III 1 and 4).

(d) 3. 1. Oscillator. The 5Mc/s. signal is derived from a crystal oscillator, which is followed by two parallel amplifiers, which also act as buffer stages for the oscillator, and provide the klystron modulation and the reference signal for the phase-sensitive detector (P.S.D.). The signal amplifier has a phase and amplitude control, and is followed by a resistive cathode follower to reduce the signal amplitude to about 100 mv. (p.t.p.) The signal is then passed through a constant amplitude phase-shifter and permanently fed onto the repeller of Kl. The voltage for the reference signal is loosely coupled out of the amplifier tuned load and was adjusted to a maximum (20v. (p.t.p.)).

(d) 3.2. 5 Mc/s. Amplifier and P.S.D. The amplifier is a conventional 3-stage tuned-load amplifier and is built integral with the P.S.D., the whole unit being in a closed box. The P.S.D. is a single ended pentode, with the signal being fed onto grids 1 and 3. The anode load is so chosen that the quiescent output potential is approximately that of Kl repeller. A low-pass filter is fitted to eliminate 5Mc/s. in the output, preventing

regeneration. It was found that the amount of 50c/s. in the output could be greatly reduced by the use of d.c. heating, so the amplifier is heated by an Advance d.c. supply, and the P.S.D. by a trickle-charged battery.

(d) 3. 3. Kl operation. The klystron is run with the anode grounded, and the cathode at -300v. d.c. The repeller, at -450v. (approx.) can be run by batteries or by the Kl.A.F.C. A variable sweep, from a scope, can be applied when using the battery supply to assist the setting up procedure. The heater is run from an Advanced 6v. d.c. supply to minimise 50c/s. in the output.

(d) 3. 4. Setting-up procedure. Kl is swept as above and the output from crystal X3 displayed on the scope, CD 813 (Solartron). The klystron is manually tuned until the cavity mode is displayed symmetrically. The cavity resonance frequency is then tuned by the wavemeter WM1 (M.I. 32/2000). WM3 is also set to the same frequency, as on resonance WM1 gives no current output. The coupling hole is then adjusted to an optimum (Figure III 8 1.). The sweep amplitude is then reduced until only the centre portion is swept and the output from the P.S.D. is displayed on the scope, after the P.S.D. filter circuit (see below) has been disconnected. The phases of the tuned loads all round the loop are adjusted until the characteristic S-shape is found (Figure III 8 2), the correct slope having been determined by trial. The sweep is then switched off and the filter connected. By manual electronic

tuning, the cavity dip can be traced out on the crystal current meter (X3), while the S-shape is traced out by the M.A.F.C. meter. When the voltage is at a predetermined value (known to be that of the ropeller of K1) the switch is turned and the loop closed. The meter and M3 are then checked to ensure that the operation is correct. Closing this loop is the most difficult part of operating the spectrometer, due to the high gain of the loop, and the operation needs some experience before it can be done quickly.

(d) 3. 5. Bandwidth and stability of the loop. As is common with feedback loops, at certain frequencies the amplitude and phase changes round the loop are such that regeneration can occur. In the circuit built this occurred at a few kc/s. However, since the modulation frequency of the pen-recording system is 280c/s., it is not necessary to correct for changes occurring at higher frequencies than this, and consequently the bandwidth of the loop has been reduced to 300c/s. by means of an R-C filter. Due to the high anode load resistance used in the P.S.D., the condensers used in this filter must have a high leakage resistance, and conservatively rated good quality ones have been used.

The short-term stability of the loop, S, can be defined as $S = df_0/df$, where df_0 = the frequency drift without stabilization and df = that with stabilization. Using the method suggested

by Brown (S1), S was found to be 500, which compares reasonably with the value of 800 found for the Hirshon-Fraenkel system. The peak-to-peak voltage of the Kl.A.F.C. is 135v., and the voltage correction is 200v./Mc/s.

(d) 3. 6. Use of 5Mc/s. as the modulating frequency. (R35). The modulation frequency used is by no means arbitrary, since equation (2.2) can now be written as

$$h\nu \pm h(\nu \pm d\nu) = g\beta H \qquad (3.3)$$

or, since the field is normally varied, instead of the resonance being detected at H gauss, it is now also detected at H ± dH gauss.

For 5Mc/s., dH corresponds to 1.5 gauss, and this obviously could lead to serious broadening of the line. However, it must be remembered that the intensities of the resonances detected are proportional to the power input, which is given by $J_0(m_f)(\nu)$, $J_1(m_f)(\nu + d\nu)$ and J_1 is less than 2% of J_0 (for the definition of J_0 etc., see Appendix 1). Further discrimination is gained by using a narrow-band i.f. amplifier. In the amplifier used this leads to an extra 7db. discrimination. Also since the lines to be dealt with by this spectrometer were not expected to be less than 10 gauss, the effect of such broadening was considered to be negligible.

This was tested by examining the derivative spectra of a 3 gauss DPPH line, using another spectrometer in which stabilization

is effected by a Hirshon-Fraenkel method and applying a 5Mc/s. modulation to the klystron. No difference could be detected.

III (e). i.f. Amplification.

(e) 1. Amplifiers. The factors which have to be specified for the i.f. amplifiers are (i) frequency, (ii) bandwidth, (iii) gain, (iv) noise figure. A 30Mc/s. amplifier, with a bandwidth of 5M/cs., suits the restrictions on (i) and (ii) which have been discussed above. According to Fcher, a gain of 80db. is desirable, and the noise figure should be as low as possible. The amplifiers sold by Decca (30/14, 30/19) seemed to fit these requirements and a pre-amp (gain = 66db.) and an amplifier (gain = 86db.) with video detector were used. The quoted noise figure of the pre-amp is 2, but the input circuit of the pre-amp contains an 82 ohm grid-leak resistor, and theoretical calculation (R27, R28, R29) shows that this should lead to a noise figure of 15. Measurement with a Noise Meter (ex W.D. 108/16149) gave a value of 10 (almost the same as the amplifier). It was felt that it might not be desirable to alter the circuit and the pre-amp has been used in this state. The co-ax connection between the crystal X2 and the pre-amp was kept as short as possible and the pre-amp was sprung mounted. Gain controls were fitted to both, the variation being achieved by applying a 6v. d.c. variable potential across a cathode bias resistor of 330 ohm (i.e. 20mA). This supply is obtained from a trickle charged wet cell.

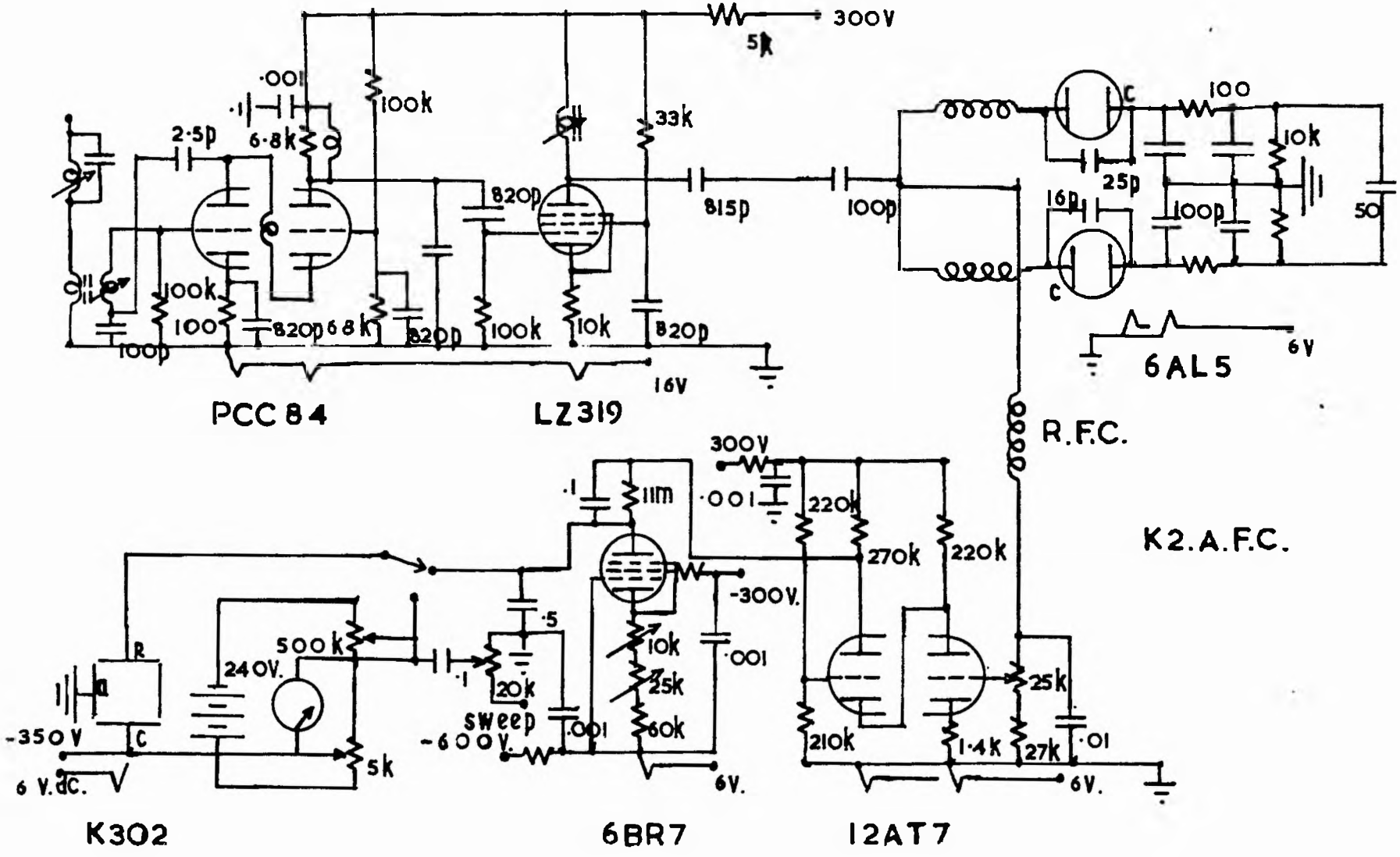
300V
5k
·001
·1
100k
6·8k
2·5p
33k
820p
815p
100p
100
10k
25p
16p
50
100k
100
820p
68k
820p
100k
10k
820p
100p
16V
PCC 84
LZ319
6AL5
6V
R.F.C.
K2.A.F.C.
300V
·1
11m
·001
220k
270k
220k
-300V.
·5
500k
240V.
10k
25k
60k
·001
20k
sweep
-600V.
·001
-350V
6 V.dc.
5k
210k
1·4k
25k
27k
·01
6V.
6V.
K302
6BR7
12AT7

Figure III 5

(e) 2. K2.A.F.C. The i.f. signal at 30Mc/s. is obtained from a second klystron (K2) at 9355 ± 30Mc/s. Since K1 follows the cavity frequency, if K2 were kept at a constant frequency, the beat frequency would drift, introducing amplitude and phase changes in the output signal from the i.f. amplifier. To avoid this, some form of feedback loop has to be built to keep the frequency difference at exactly 30Mc/s.

For a discussion of the constants involved, see Appendix 2.

(e) 3. K2.A.F.C. circuit. Figure III 5. The 30Mc/s. signal is obtained from K1 and K2 by means of 10db. couplers, C1 and C3, using a magic tee (T3) as a mixer. The signal thus obtained is of constant amplitude, and after detection by crystal X4, it is then amplified 30x using a modified T.V. pre-amp. (bandwidth 2Mc/s., Noise Figure = 5). The signal is then fed into a ratio detector with a Foster-Seely input; this device gives very little response to amplitude changes, which in the detector would appear as (spurious) frequency changes (T1). Two resonant coils are used, one tuned to 31Mc/s., the other to 29Mc/s. The signal is then amplified by a cascode d.c. amplifier, gain 100x. The quiescent potential at this point is around 250v., and this has to be fed onto the repeller of K2 at -450v. This is achieved by means of a constant current device. The 12Mohm anode load is bypassed by a condenser to allow the maximum correction for transient signals (T2). The amplitude of the d.c. signal is

approx. 90v., and the voltage correction is 50v./Mc/s. The bandwidth is 100c/s. The unit was built on a single chassis, and once set up at the correct frequency, it was sealed up so that no alterations other than voltage level setting are possible.

(e) 4. Setting-up procedure. K1 is swept, as before, over a small region of the cavity dip, and K2 manually tuned until the correct S-shaped curve is found (III 8.3). Then the K1.A.F.C. is set up as described previously and the second detector current is then maximized by progressive tuning of both manual and electronic tuning. The switch from K2 battery to K2.A.F.C. is then closed, and stabilization effected. The voltage level is adjusted slowly until the second detector shows the same value as before. This loop is easier to close as the loop gain is not so high.

III (f). Video detection.

(f) 1. Setting-up procedure. With both K1.A.F.C. and K2.A.F.C. circuits operative, the spectrometer can now be balanced by means of the sliding stub tuner, adjusting it until there is a minimum in the second detector current. The bridge is then slightly unbalanced to ensure that any e.s.r. absorption does not alter the match from overcoupled to undercoupled, as this would lead to a phase change in the detected signal, giving a spurious result. The detected i.f. signal is then fed through an R-C filter of bandwidth 10^4c/s., and the signal observed on

A. F. AMPLIFIER.

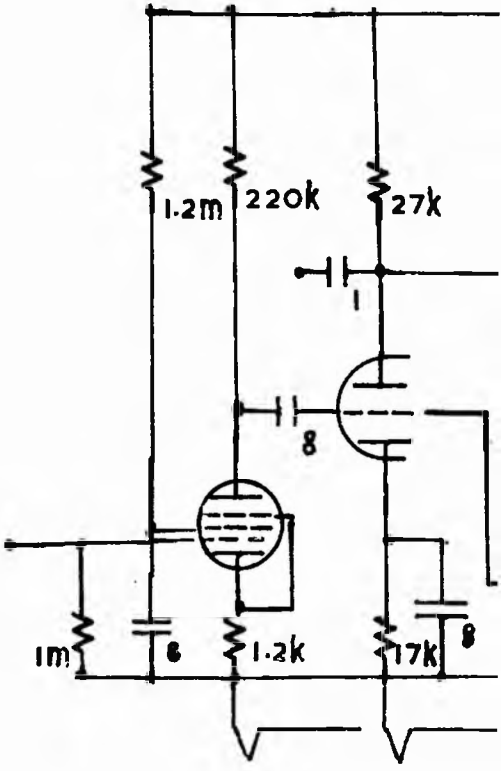

6BR7

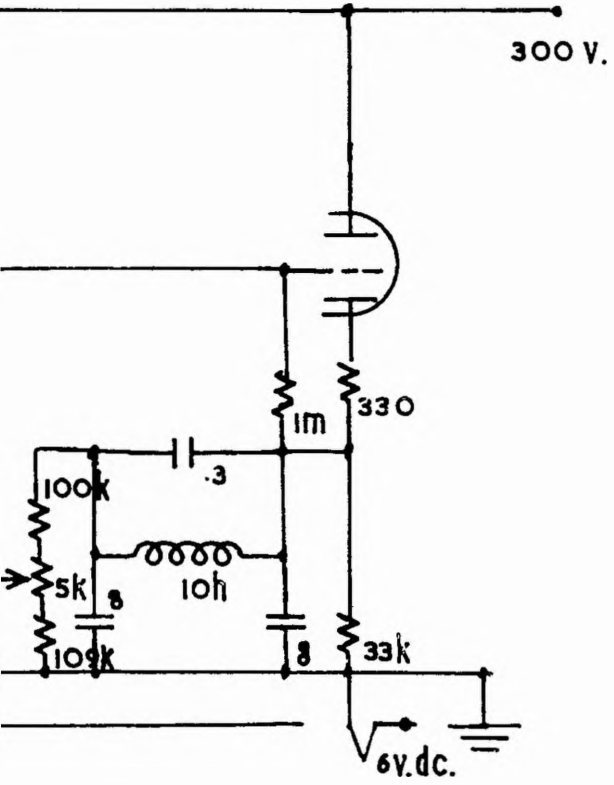

Figure III 6

a scope (Solartron CD 513), 1mv./cm. range.

The signal is then given some further a.f. amplification and displayed on scope CD 814, 30mv./cm.

(f) 2. Audio amplifier. Figure III 6. This is a two-stage amplifier, the second stage having a feedback loop, designed to minimize low frequency oscillations. These are caused by slow vibrations of the cavity arm and can be annoying when the signal is displayed on a scope.

(f) 3. e.s.r. absorption display. With a 50c/s. magnetic field modulation, the absorption can now be observed. An external 50c/s. signal is applied to the X-plates of the scopes and is phased so as to centre the absorption. The back trace is eliminated by a 50c/s. Z-modulation. (Figure III 8.4).

(f) 4. Reference cavity. In lining up the spectrometer a reference is used. This consists of a complete cavity arm which can be coupled in, replacing the normal cavity arm. It is kept permanently set up with a known sample of 4 10^{15} spins D.P.P.H. It is not possible to use the sample alone, since in the case of a helium run it is not possible to change the sample. Since the sample is khown it is possible to check the performance of the spectrometer before each liquid helium experiment.

III (g). Phase-sensitive detection.

(g) 1. Method. The magnetic field is modulated at 280 c/s. to a value less than the line width, and simultaneously swept

280 c/s OSCILLATOR & PHASE-SHIFTER.

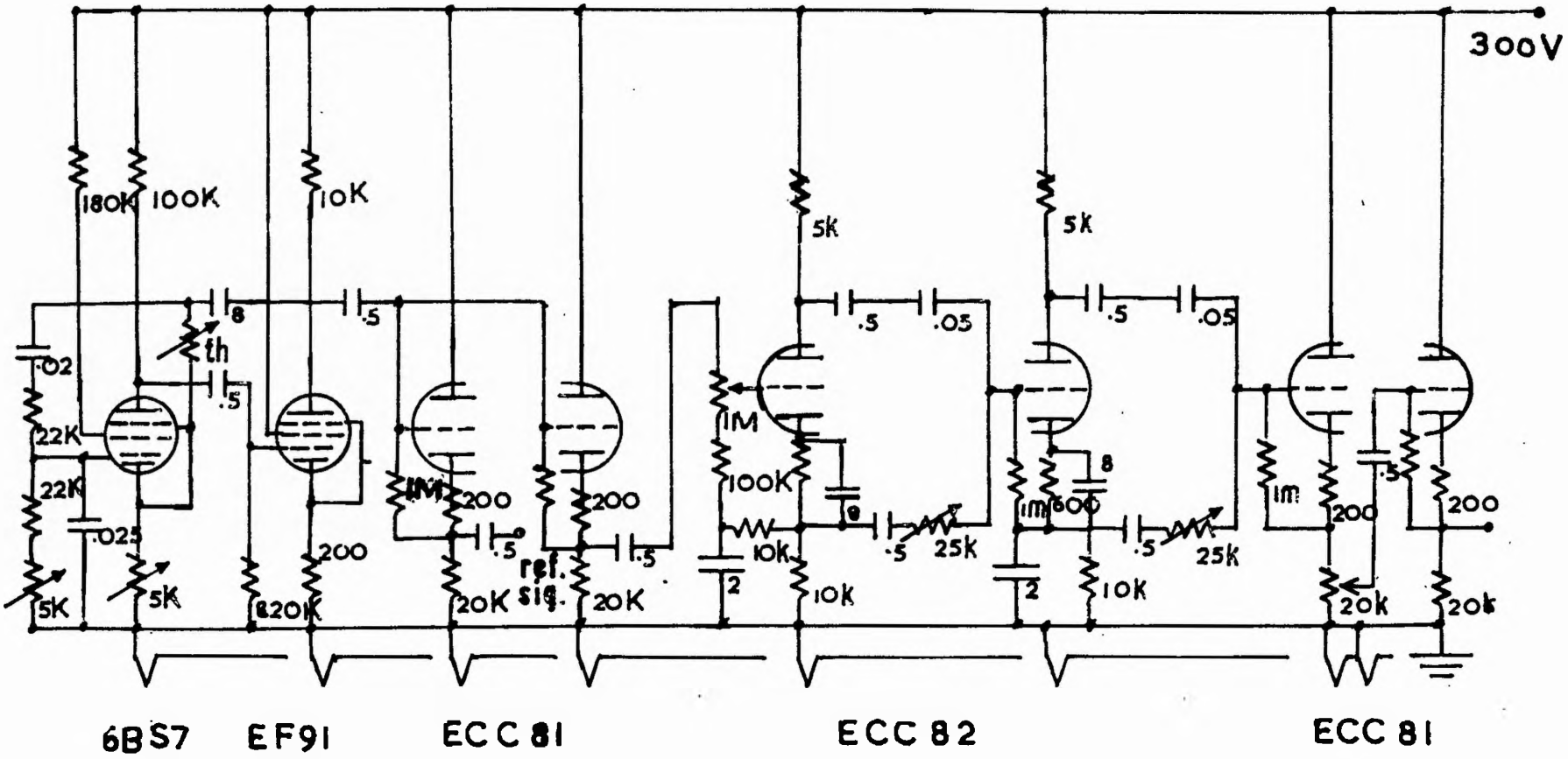

Figure III 7

slowly with a linear sweep through the absorption line. The 280c/s. signal is taken from the a.f. amplifier and further amplified by a narrow-band amplifier tuned to 280c/s., and detected by a phase-sensitive detector. The spectra are displayed on a pen-recorder as a first derivative signal.

(g) 2. 280c/s. oscillator, phase-shifter and power amplifier. (Figure III 7).

The oscillator is of the Wien-bridge type, with thermistor stabilization (T3). For a discussion of the stability requirements, see Appendix 3. The oscillator is fitted with a frequency and amplitude control, and when these are correctly set it gives a steady sine wave output. The oscillator is followed by two cathode followers, one giving an output used as a reference, the other acting as a buffer leading to the phase-shifter. The phase-shifter consists of two identical stages, which give a combined phase-shift of 270°, without affecting the amplitude of the signal, and it is followed by two cathode followers, the first of which is used as a gain control. The output is fed into a power amplifier (T4), which is used to drive the sweep coils, with a maximum current output of 20mA.

(g) 3. 280c/s. narrow-band amplifier and phase-sensitive detector.

To reduce the effect of harmonics of 50c/s., the amplifier has a bandwidth of a few cycles. At this low frequency, a twin-tee type of amplifier was used, of the same design as that in (S1).

Figure III 8

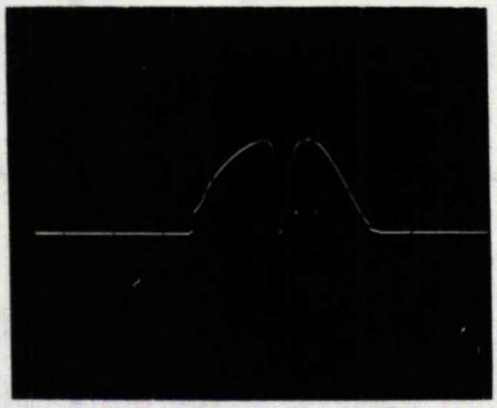

8.1 display obtained at X2 when the repeller of K1 is swept with a linearly increasing voltage. Thus the trace shows the power output of K1 as a function of frequency. The sharp dip in power is due to a matched cavity. (Q = 4000).

8.2 upper trace (on left): bottom of cavity dip in 8.1 (expanded) (Y-scale = 50mv/graticule division.)
lower trace: S-shaped curve from K1.A.F.C. (Y-scale = 50v/graticule division.)

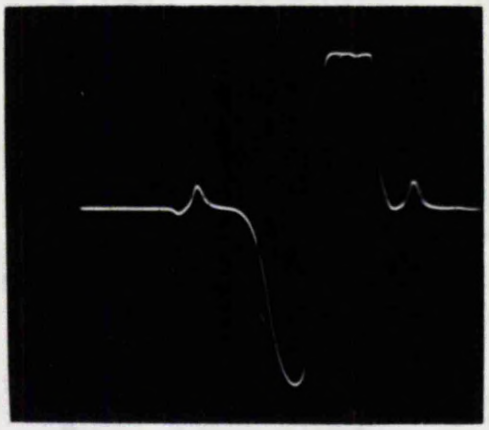

8.3 the S-shaped curve from K2.A.F.C. (Y-scale = 10v/graticule division). The two small peaks are caused by the 5Mc/s. mod^{n}. (K1 was swept as in 8.1 to obtain this trace.)

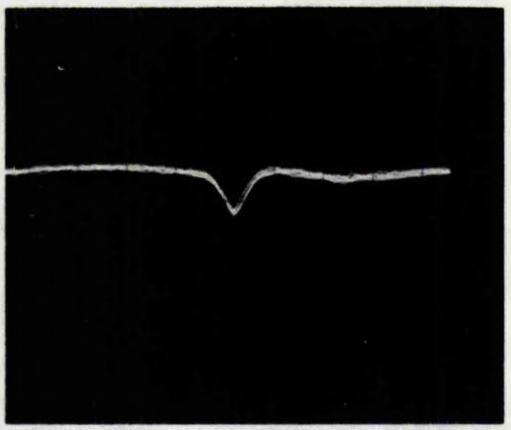

8.4 e.s.r. absorption signal from 10^{16} spins D.P.P.H. at room temp. (bandwidth = 10^{4}c/s.)

The gain is 10^4 and the bandwidth 3.5c/s. This amplifier is somewhat valve dependent, and care has to be taken in its use. (See Appendix 3). In this type of amplifier, the frequency selectivity is obtained by means of heavy negative feedback at all frequencies other than that desired. This means that the amplifier has an inherent tendency to oscillate. In practice, the amplifier was mounted as far away from the sweep coils as possible, and orientated for minimum pick-up. As the P.S.D. was also built on the same chassis, a mu-metal screen was inserted to cut down the pick-up from the reference. The P.S.D. is of the Schuster type (T5), and the output is fed into an Evershed & Vignoles pen-recorder (.5 - 0 - .5 mA).

(g) 4. Setting-up procedure. The output of the narrow-band amplifier is fed onto the Y-plates of scope CD 513. With the time base running free, the output is maximized by adjusting the frequency control of the oscillator. The time-base is then driven by an external 280c/s. sweep, provided by the P.S.D. reference signal. The sliding stub tuner is then given a fine adjustment until the trace on the scope is a straight line and the pen-recorder balanced. The field is varied until the resonance line is observed, as a flip over of the trace from  to  shape. The field is then swept at a set rate and the pen-recording obtained is compared against a standard from the reference specimen. The gain of the amplifier

is varied until equality is reached. The field is then turned well off resonance, and the no input signal is observed. If this is unsteady, the spectrometer is usually readjusted and realigned. The stability normally improves with time and is better in the evening. The main difficulties are usually transients associated with load switching on other spectrometers or on equipment in the main part of the building. There is very little that can be done about this except to wait until it ceases.

(g) 5. Stability. With the spectrometer at maximum gain, the noise level was found to be 1 division of the pen-recorder graph paper (100 divisions full-scale). By manually de-tuning the klystron, this can be shown to be equivalent to a frequency drift of 20kc/s., which is almost the design stability of the spectrometer. This stability can be achieved over a six minute period.

III (h). Stabilized power supplies.

(h) 1. Mains input and earthing. The input to the electronic side of the spectrometer was fitted with a 15kW stabilized transformer. The apparatus is earthed to a metal plate below the floor of the building.

(h) 2. Stabilized power supplies. (d.c.).

	Voltage	Current	Ripple
(1)	+ 300v.	300mA.	1.0 mv.
(2)	+ 300v.	250mA.	1.3 mv.
(3)	+ 300v.	200mA.	1.0 mv.
(4)	- 640v.	20mA.	.7 mv.
(5)	- 540v.	30mA.	.5 mv.
(6)	- 300v.	60mA.	1.0 mv.
(7)	+ 150v.	200mA.	1.0 mv.
(8)	85v.	100mA.	10. mv.

The power supplies (1) - (5) are of the same basic design as (S2). The output resistance is 2 ohms, and regulation for a 12% mains voltage change = 20).

(7) is a transistorized model (International Electronics, DSM2).

(8) is of a simpler design and is used for supplying the slow sweep voltage.

Two 6v.d.c. Advance power supplies are also used.

III (i). The Magnet

(i) 1. Types used. Two magnets were used, as available:-

Newport Instruments	Type E	7"
	Type E	7" shimmed

The latter magnet was used in all the work quoted in the results. The inhomogeneity of the field in the first model is .2 oe/cm. parallel to the pole pieces, and .4 oe/cm. perpendicular. For

details of the construction and inhomogeneity measurements, see (S4). The inhomogeneity of the second magnet has not been measured, but should be better than the first. The second magnet is also water-cooled, which helps the stability and field calibration. Both can be rotated through 360° and are mounted on trollies, running on rails, so that they can be moved to other spectrometers.

(i) 2. Magnet power supply. This is provided by a Newport Instruments Type B, Mk II supply, with specifications:-

Current stability = ± 1 in 10^4 for a 4% mains change.

Ripple field = .5 oe.

Controllable current range = .5 - 9. amp.

or 5. - 13. amp.

(i) 3. Measurement of field strength. A .01 ohm resistance was fitted in series with the magnet coils, and the voltage developed over this was measured by a potentiometer (Tinsley 3387B) and galvanometer (Tinsley .5 μA. f.s.d.). The resistance was initially calibrated using a proton resonance meter (S3), making allowance for the hysteresis, and a calibration graph drawn. The field can be read to an accuracy of ± 4 oe., as checked against DPPH samples. For a further verification of the accuracy of the calibration see Chapter VII.

(i) 4. Slow sweep generators.

Small field sweep. The power supply has a facility that if a slowly varying voltage is fed into the supply's control amplifier, the output current will also vary. The variation in voltage is obtained from a 1K, 40 turn Helipot, working from an 80v.d.c. floating supply (since the input terminals to the control unit are also floating). The helipot is driven by a 22v. a.c. motor through a reduction gear train, and is fitted with microswitches to prevent damage to the wiper arm. The following possibilities are available:-

Time of sweep = 2 min., 6 min.

Amplitude of sweep = 90,200,341 and 500 oe.

Direction of sweep = repetitive or alternate.

The mains input to the motor and to the pen-recorder drive are taken off a variac (Philiac 2 amp.). This was found to be desirable as otherwise the sudden current surge on starting tends to cause an unbalance in the pen-recording system.

The sweep is reasonably linear up to 200 oe, but after this it becomes less so. It was found that if the voltage was applied in the reverse polarity, better linearity was obtained.

Full field variation. The above device is of no use when a field of over 400 oe. is needed. A full field sweep was obtained by using the remote control facility on the power supply. A slow motion drive motor was used to rotate the wiper arm of a

large diameter 20K pot. Latterly an electronic integrator was fitted in place of the resistance.

(i) 5. Magnetic field modulation. The 50c/s. or 280c/s. field modulation is applied through a Helmholtz pair of coils, mounted in parallel with the magnet coils. The 50c/s. sweep is applied through a Variac and a 3:1 step-up autotransformer. The maximum sweep which can be applied at 50c/s. is 380 oe., while at 280c/s. the maximum is 10.5 oe. A diode and voltmeter were fitted across the output of the 280c/s. power amplifier, and the voltmeter was calibrated in oe., so that the 280c/s. modulation depth can be easily varied.

III (j). Sensitivity of the spectrometer.

(j) 1. Practical measurement. The absolute sensitivity of the spectrometer was measured by observing the Signal to Noise ratio (S:N) of a series of samples of a known free radical (di-phenyl-picryl-hydrazyl) at various concentrations.

On video, at 300°K, a S:N::1:1 was given by $5\ 10^{14}$dH spins.

On pen-recording, a gain of at least 10^2 is attained, and on lowering the temperature to 1.4°K there is a further gain of $5\ 10^2$ (due to an increase in both the Boltzmann distribution and the cavity Q.) This therefore leads to an absolute sensitivity for the spectrometer, at 1.4°K, of

$5\ 10^9$ dH spins (optimum modulation depth, infinite recording time).

In practice, it is possible to detect the presence of a line which has a S:N ratio of less than unity, on video, but with pen-recordings a S:N::10:1 is necessary for a useful recording. In general, it can be taken that if a line is not detectable on video, it is unlikely to appear on pen-recording, unless the line is very broad, since in this case it is not being properly swept by the 50c/s. modulation.

(j) 2. Theoretical estimation. Brown (S1) has given a method of calculating the absolute sensitivity. Using the values appropriate to this spectrometer, for an S:N::1:1 at 300°K, we should need only $7\ 10^{12}$ dH spins. As discussed in the original, this value is not attained in practice for a variety of reasons including principally the klystron noise sidebands beating with the signal from the other klystron. The use of a balanced mixer, to eliminate K2 noise sidebands together with a low noise i.f. amplifier could be expected to improve the sensitivity by a factor of 10 (R8).

The ultimate in sensitivity seems to have been reached by Smidt (R1) and Mishra (R2) who quote values of 10^{10} dH spins at room temperature, however these spectrometers lose a lot of flexibility in the process, e.g. Smidt uses a cavity in parallel with the sample cavity to eliminate K1 noise, and this would obviously be difficult to use in the present experiment where the cavity frequency varies.

The particularly long cavity arm which has to be used is an additional source of microphonics, however the results show that the spectrometer is up to the design standard.

III (k). Evaluation of spectra.

(k) 1. Errors in observed quantities. When the spectra have been obtained from the spectrometer, there still remains the measurement of the relevant quantities. In this section, these are discussed, and the errors, both systematic and random, are evaluated.

The major quantities to be obtained from a spectrum in the first instance are:-

(i) line-width

(ii) g-value (or some similar quantity)

(iii) signal intensity

(iv) line-shape (including h.f.s.).

Line-width. It is now customary in e.s.r. work to define the line-width of an absorption line as the distance between the points of maximum slope rather than between the half-power points, since a first derivative presentation gives this information directly. In the following experiments, generally a magnetic field sweep was used where the rate of change of field with time was known, and so the line-width could be directly measured off the pen-recording using a travelling microscope.

The major random error in this step is in deciding exactly where the turning points of the first derivative occur. The possible error is estimated at 5%. There may also be a systematic error which is discussed below.

g-value. To calculate the g-value, it is necessary to measure both the operating frequency and the field strength at the cross-over point on the first derivative tracing. Since it is very difficult to measure the cross-over point while the line is still being traced out, the field strength was measured at the beginning of the trace. The extra field to the cross-over point is again measured by a travelling microscope. The random error in this measurement is variable, depending on the sweep rate used, but in general it is small compared to the error in measuring the absolute field strength of ± 4 oe. (See III (i) 3). The error in measurement of the frequency is ± 2 Mc/s. in 9500 Mc/s., and can be ignored.

(k) 2. Systematic error in line-width and g-value measurements. In all spectrometers, when pen-recording, the output bandwidth is kept very small. Generally this is achieved by an R-C circuit with a long time-constant, in the final stage of the P.S.D. Since a condenser, both on charging and discharging, follows an exponential law, it follows that the output is never a perfect reproduction of the input. The general effect is shown

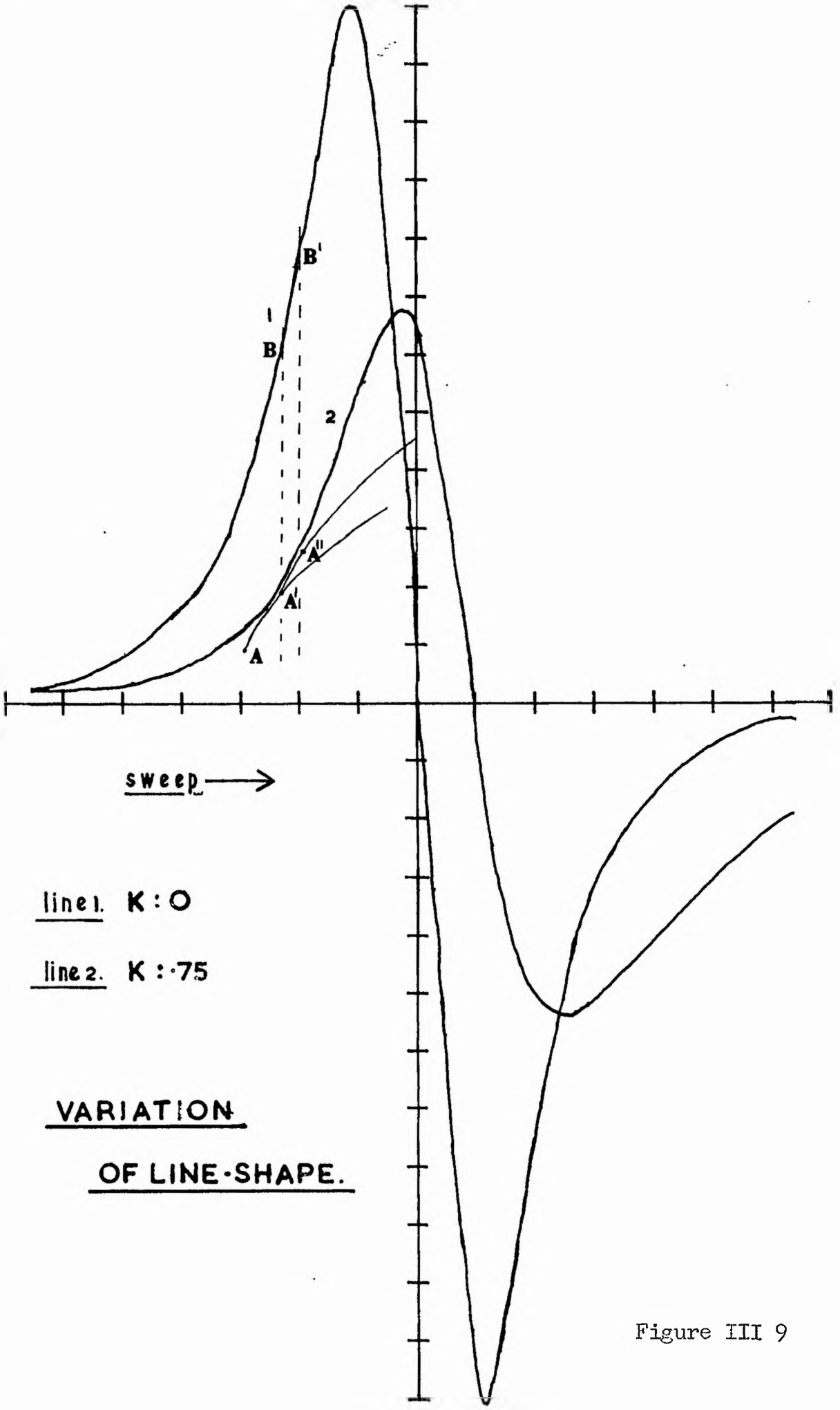

line 1. K : O

line 2. K : ·75

VARIATION

OF LINE-SHAPE.

Figure III 9

qualitatively in Figure III 9 for a Gaussian line, where it can be seen that several important changes result in the observed line-shape. These are:-

(i) Shift of the cross-over point of the line

(ii) Shift of both peaks.

(iii) Distortion of the line-shape

(iv) Increase in the line-width

(v) Decrease in signal intensity.

This graph was obtained by drawing the charging curve for a given time-constant at a point A, and using the value attained where this curve crosses the abscissa of point B as the start of the charging curve for this new impressed voltage. For accuracy, the step A - B was made as small as possible.

It is clear from the above that in certain circumstances, the values of the quantities (i) - (v) taken directly from a pen-recording may be in serious error. As far as the author is aware, the problem does not seem to have been discussed before, and may explain the varied results obtained in similar experiments by different authors (e.g. see Chapter VII).

In order to clarify the situation, the author proposes to discuss these effects in terms of a single dimensionless quantity, K, where

$$K = \frac{dH/dt}{\text{line-width/time-constant}} \qquad (3.4)$$

LINE-WIDTH VARIATION.

AS A FUNCTION OF K.

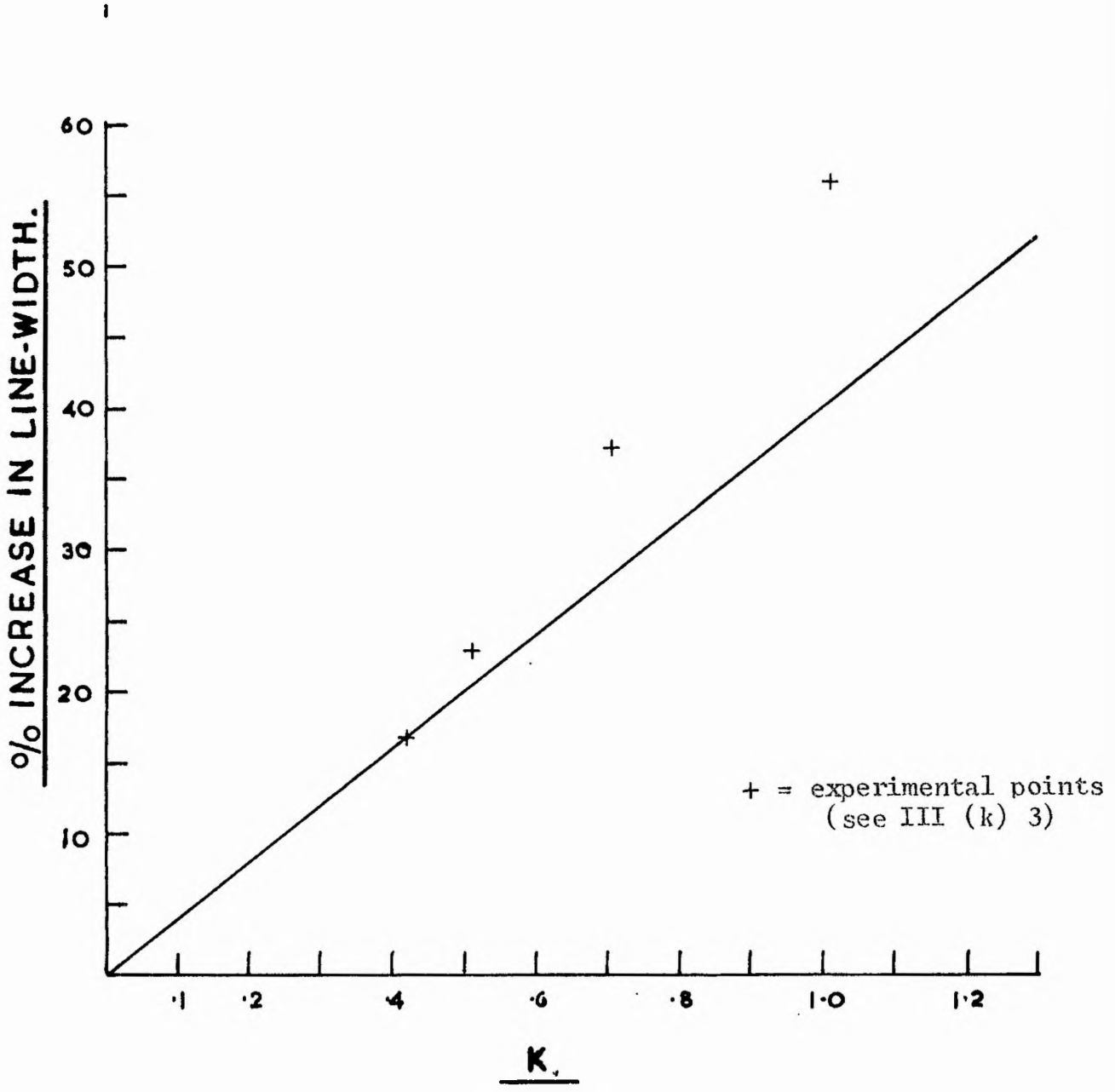

Figure III 10

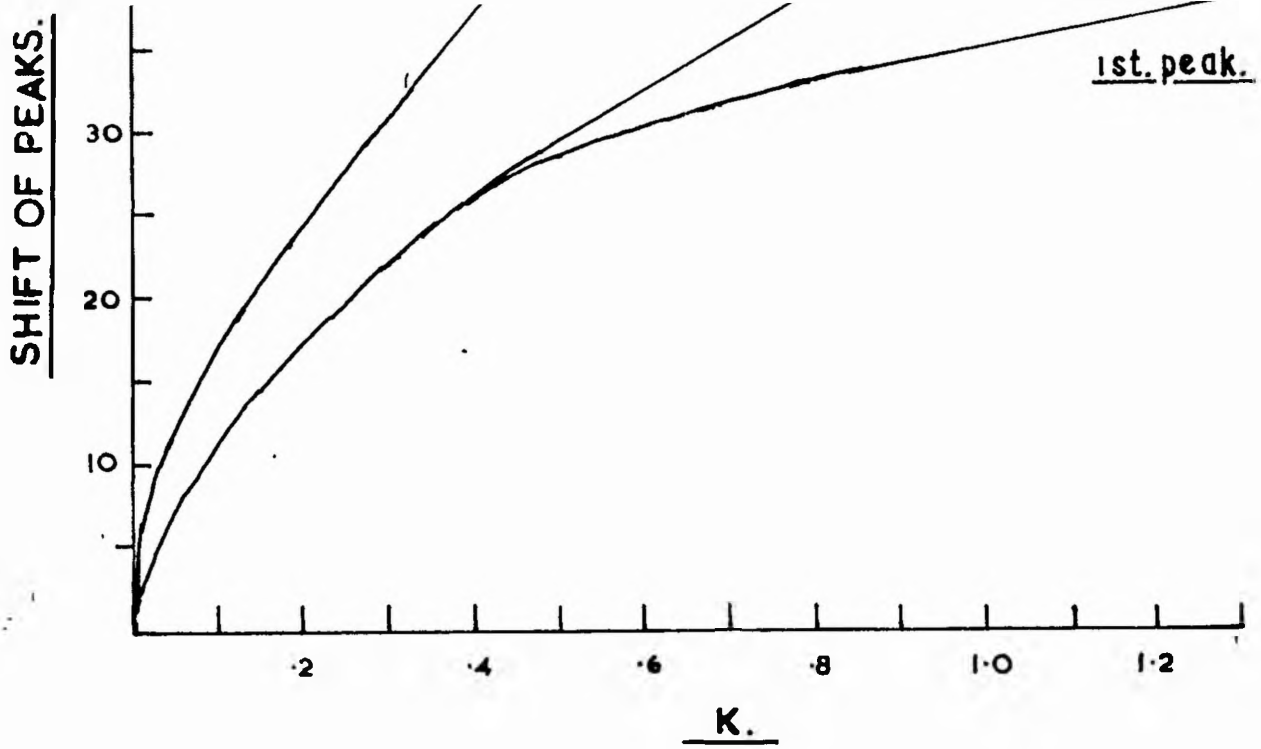

Figure III 11

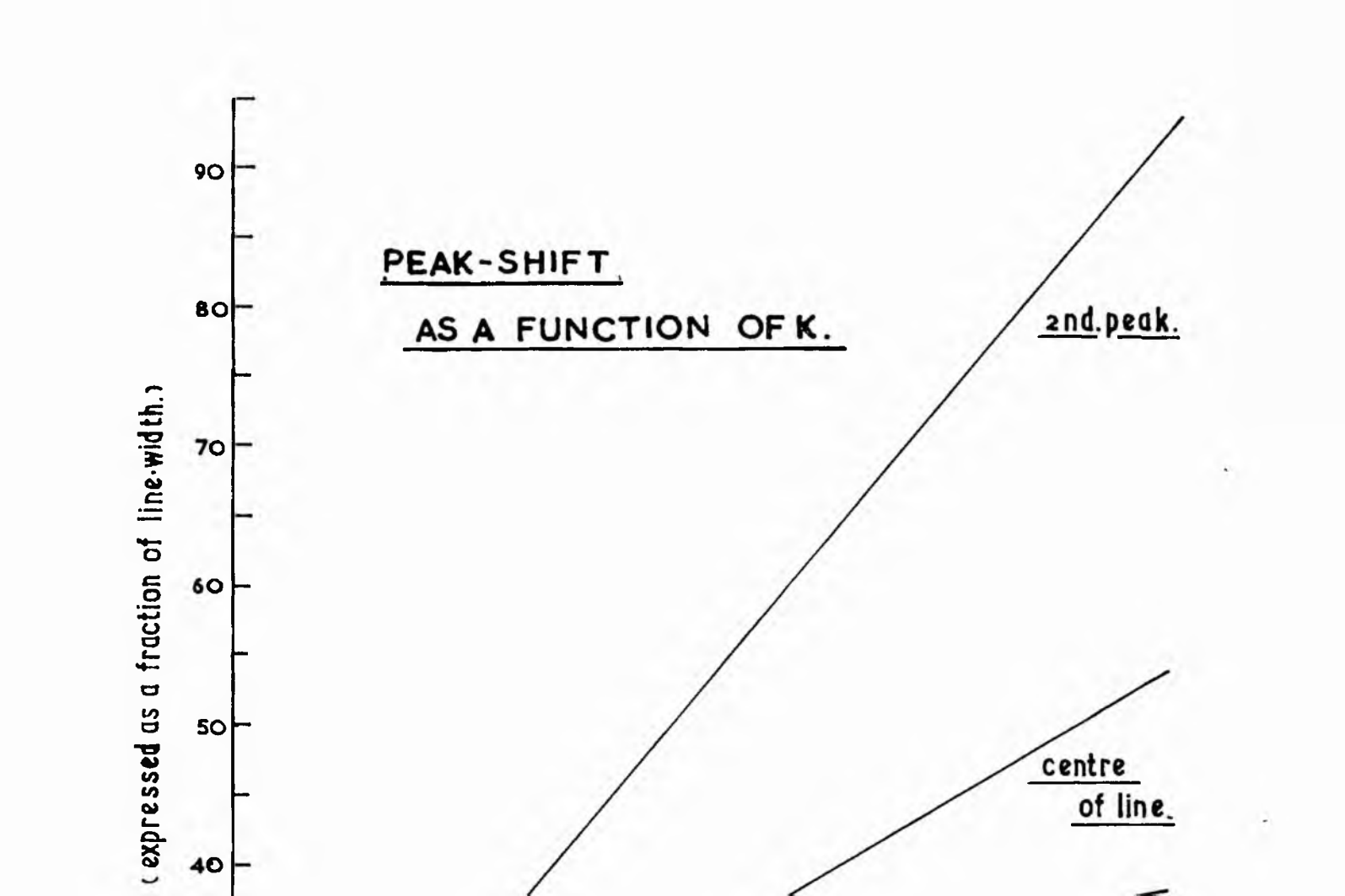
PEAK-SHIFT
AS A FUNCTION OF K.
2nd. peak.
centre
of line.
90
80
70
60
50
40
(expressed as a fraction of line-width.)

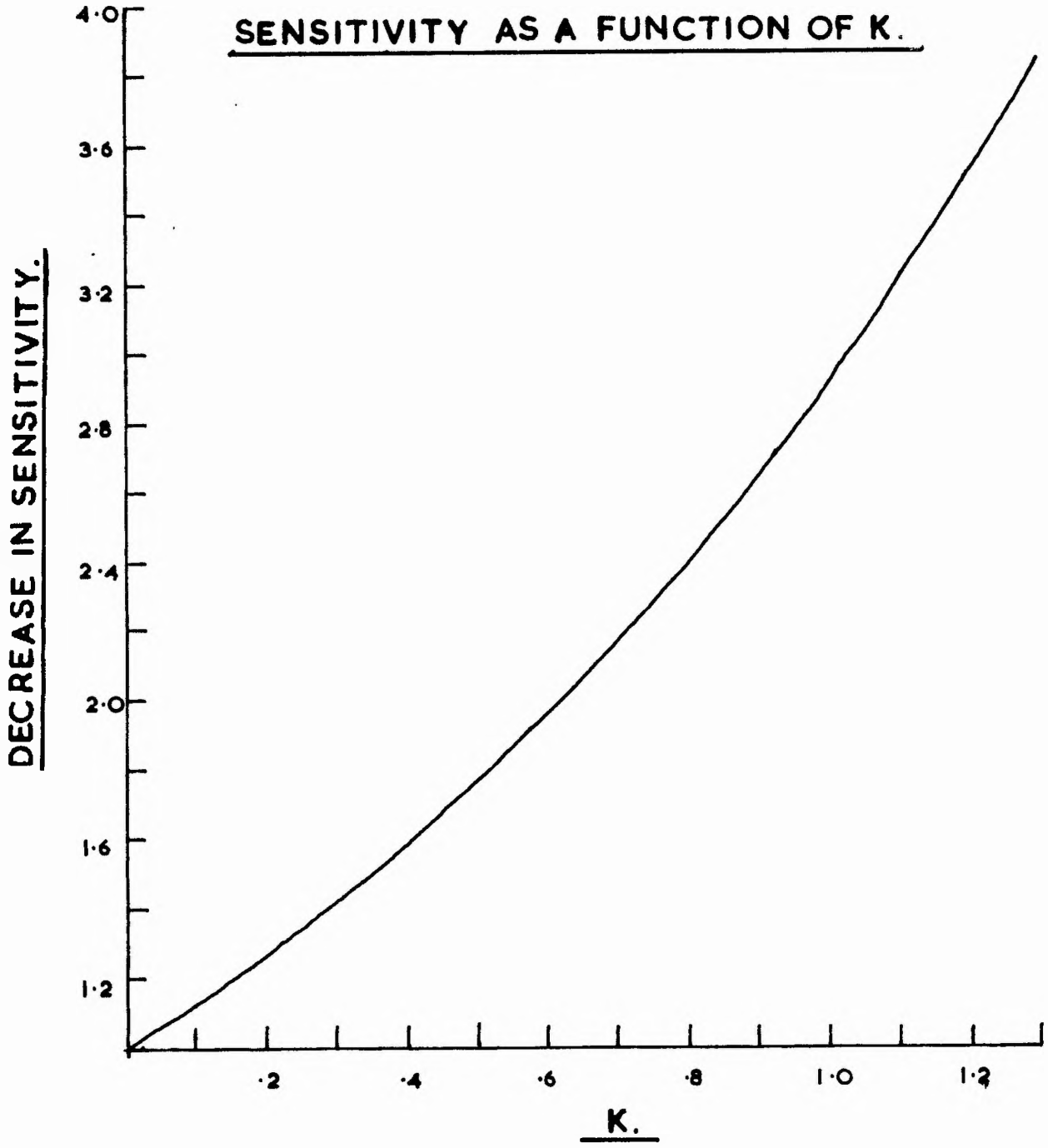

Figure III 12

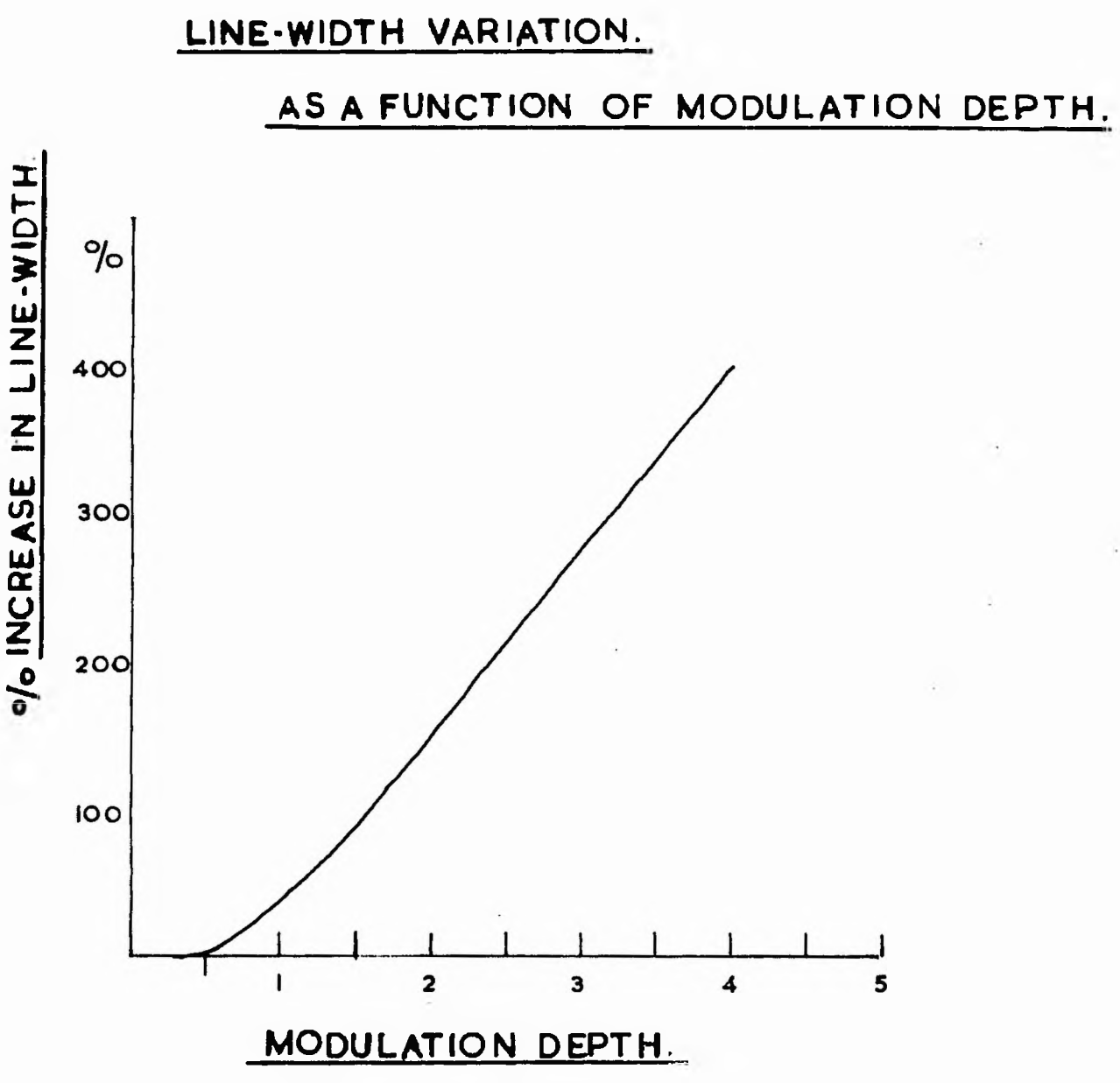

Figure III 13

SENSITIVITY AS A FUNCTION OF MODULATION DEPTH.

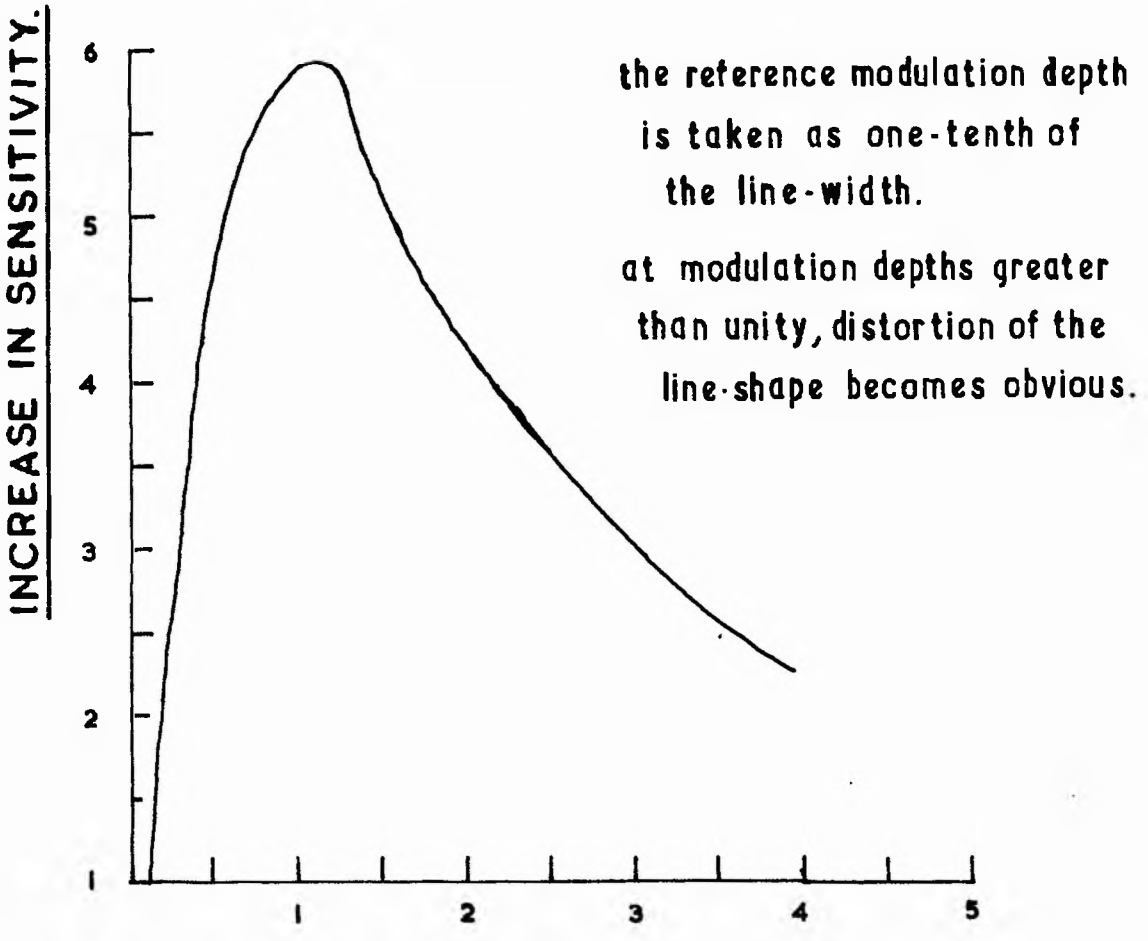

the reference modulation depth is taken as one-tenth of the line-width.

at modulation depths greater than unity, distortion of the line-shape becomes obvious.

Figure III 14

K therefore includes the three independent variables in any pen-recording. By graphical integration of a standard Gaussian first derivative line, a series of derivatives were drawn for various values of K. The relevant details mentioned above were found and the results plotted graphically against K. The graphs for the increase in line-width (Figure III 10), shift of peaks and of cross-over point from the true values (Figure III 11) and decrease in sensitivity (Figure III 12) were plotted.

By use of these graphs it is possible to reduce all pen-recordings to a standard value, and to find the true field values involved. The graphs are also very useful for making estimates in advance of the optimum sweep rates which should be used, which can result in a considerable time saving.

A similar procedure was carried out on a standard Gaussian line to determine quantitatively the effect on line-width and sensitivity of the modulation depth. Figures III 13 and 14 show these variations. These graphs were useful in deciding on modulation depth values and also give a means of reducing different spectra to a standard value.

(k) 3. Experimental verification. During one of the runs on the pure Naphthalene triplet line, the effect of altering K was checked. In this case dI/dt was altered. The pen-recordings are shown in Figure III 15 and the results on Figure III 10. The slight discrepancy at higher K values is

Figure III 15. Variation of spectra with K.

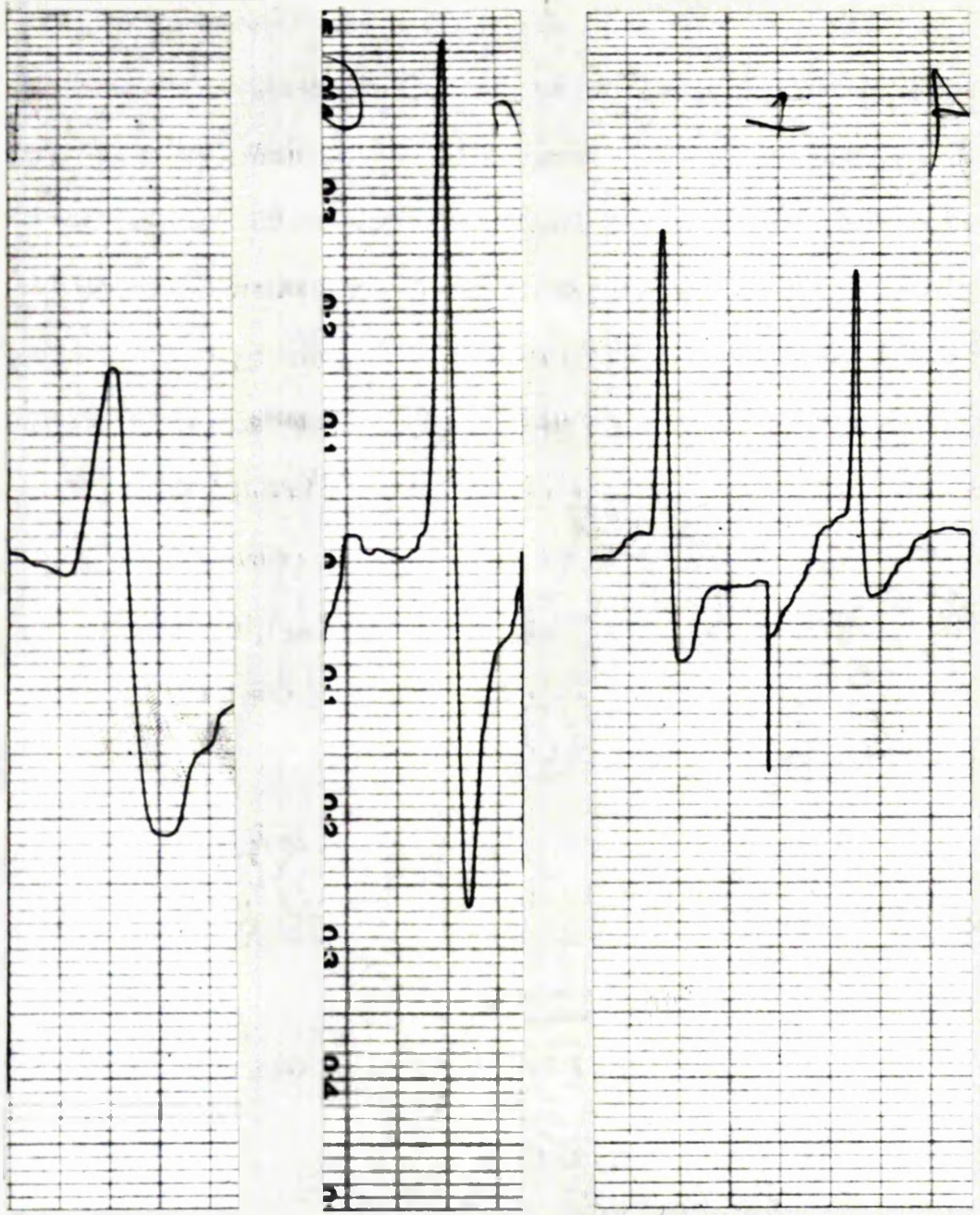

Sample : naphthalene/benzophenone. These pen-recordings are taken from Exp. 2 on Figure VII 4.

K = .18; = .4 ; = .71 ; = 1.0

dH/dt = .75; = 1.6 ; = 2.83 ; = 4.1 oe/sec.

H increasing from left to right in each recording.

The recordings are not all at the same spectrometer gain.

Paper speed : 1 division (6.25mm.) corresponds to ~30 sec.

due partly to the error in measuring the line-width at the higher dH/dt rates and partly to the non-Gaussian shape of this resonance line. However they illustrate the trend quite well. The graphs were used in the work on the triplet state, since the short experimental time of an hour made it desirable to use faster dH/dt rates (up to K = .15).

(k) 4. Estimation of spin-density in a sample. Theoretically the spin-density in a sample can be obtained by evaluation of equation (3.1), but as shown in III (j) 2 this cannot be done with any precision. So an experimental calibration has to be made using a known free radical, and then using (3.1) to modify the proportionality factor, i.e.

$$\frac{S_u:N\ (dH_k)}{S_k:N\ (dH_u)} = \frac{U}{K} \cdot \frac{Q_k\ \eta_k (P_{ok})^{\frac{1}{2}}\ (T_u \Delta\nu_u)^{\frac{1}{2}}}{Q_u\ \eta_u (P_{ou})^{\frac{1}{2}}\ (T_k \Delta\nu_k)^{\frac{1}{2}}} \qquad (3.5)$$

where U and K are the unknown and known spin densities respectively.

So, the estimation of the spin density involves the following factors:-

(i) S:N ratio
(ii) line-width
(iii) cavity Q
(iv) temperature, bandwidth, microwave power and filling factor
(v) absolute sensitivity.

In addition

(vi) the observed S:N is dependent on the modulation depth and the K-value used.

(i) Measurement of the S/N ratio is by no means accurate, especially from a pen-recording. In practice, the line is usually recorded several times and compared. The error is about 20% (estimated).

(ii) If the line-width is taken off a pen-recording, the error in determining the maximum is about 1 oe. in a 20 oe. line, but this can vary depending on the experimental conditions. The error is on average about 5%.

(iii) The Q varies from sample to sample, and on orientation. The method used for measuring the Q during a run is not very sensitive, and the error is about 10%.

(iv) Errors in these quantities can normally be made negligible by using the same experimental conditions for both unknown and reference samples, since they are purely mechanical conditions under the operator's control.

(v) The errors (i) and (ii) also come into the absolute calibration, although the method used minimizes these (III (j) 1). There is also some error in the standard samples. The value obtained is estimated to be within 20%.

(vi) This error can be corrected for by the use of the method outlined in (III (k) 2).

From the above section, it can be seen that, although the errors are well known, there is little that can be done to

improve the situation. The error in a given estimation would seem to be around ± 40%.

This value compares with an estimate made from the results of several authors, discussed in (R21), where a figure of 50% was found.

According to (R23) DPPH (the usual calibrating agent) may contain up to 20% of the solvent of crystallization, leading to a variable error in calibration. Yariv & Gordon (R26) have discussed a method of measuring the absolute sensitivity involving the changes in the reflection coefficient of the cavity, but the method is far too tedious for day-to-day estimations.

It is also possible to cut down the errors in evaluation of the spectra by using a two-sample cavity, with the reference sample situated in a different field strength to the unknown. The intensity of the absorption can be measured more directly by an evaluation of the first moment of the derivative curve, although considerable error is introduced by the indeterminacy of the wings of the curve (R34). This method would appear to suffer from errors in making a standard at very low concentrations of a comparable intensity to the signal involved. In the experiments carried out, the signal concentration was not considered to be a particularly vital factor and the accuracy attained is sufficient.

III (1). Empty cavity effect. When the spectrometer was operated in liquid helium, a strong broad line appeared. The constants are:-

g = 2.06 ± .02; line-width = 200 ± 25 oe.;

apparent number of spins = at least 10^{15} (difficult to estimate because of the large width and intensity).

The origin of this line is obscure, and it was not found possible to cure it. The line still appeared even when the cavity was completely empty (except for liquid helium) and appeared with both cavities. The quartz tuning rod was completely withdrawn and the line appeared on both 50c/s. and 280c/s. modulation. No trace of the line could be found at liquid nitrogen or room temperatures, showing at least that it was not due to the electronic side of the apparatus. The only conclusion therefore is that the effect is due either to the liquid helium or is a consequence of the low temperatures (and high sensitivies) involved.

A similar effect is reported (R22, 05) to be a common feature of all high sensitivity spectrometers. It is said that the effect can be cured by the introduction of dielectric tuning stubs inserted in the narrow face of the cavity, but no further information is given. Time did not permit trying this solution. In many of the experiments which were conducted at g = 4 field values, this line was of course irrelevant. In

those conducted at g = 2 (VIII (2)), on video a narrow line would have been obvious if superimposed on the broad line. Pen-recording at maximum gain in this region is however almost impossible.

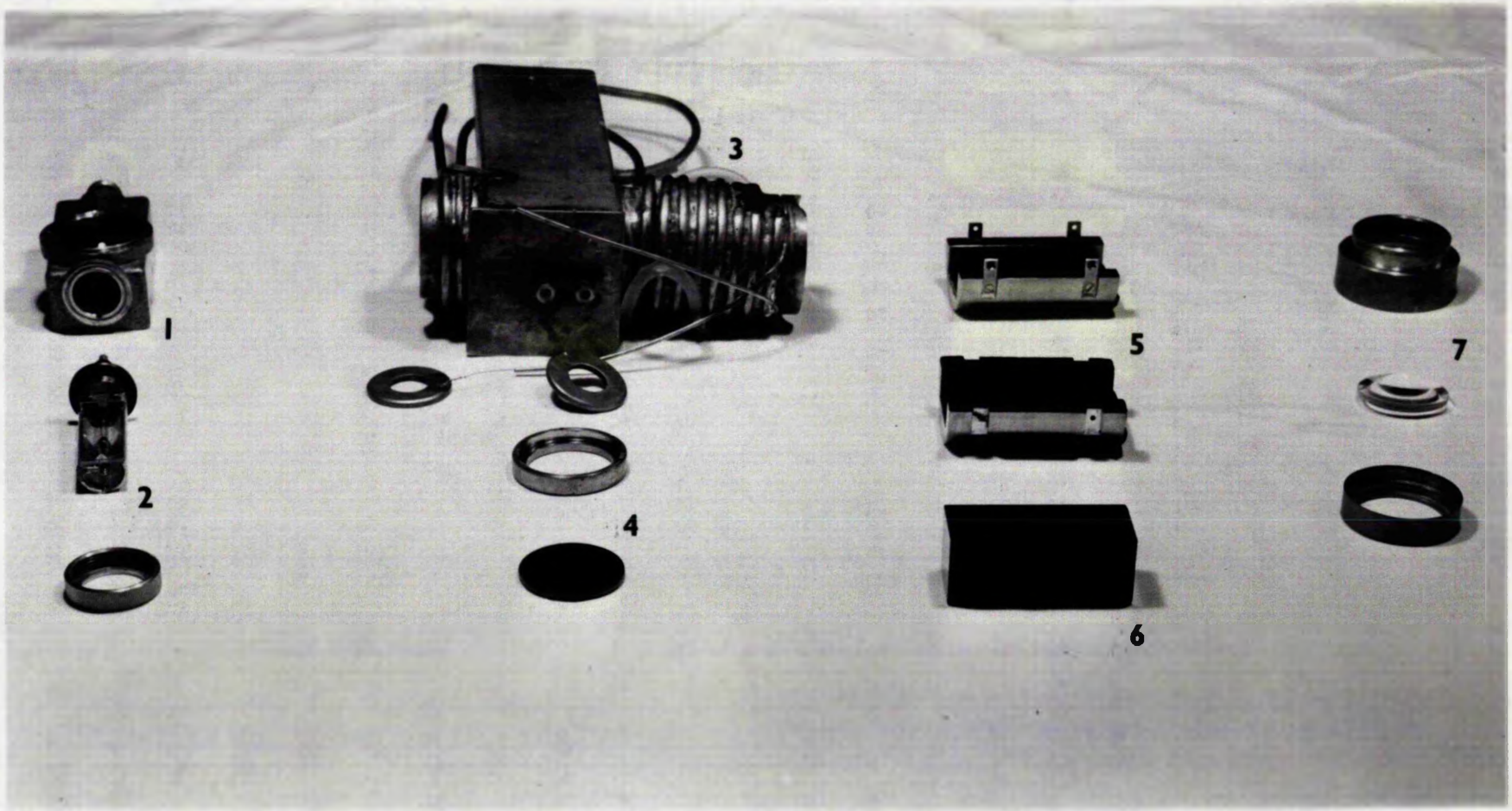

Figure IV 1 High-pressure mercury lamp and filters

1) lamp holder for 2) high-pressure lamp. 3) liquid filter container (showing external water-cooling coils and prism rotation mechanism). 4) Chance glass filter and holder (push-fit inside longer barrel). 5) brass mounting for 6) calcite prism. 7) quartz lens and holder (push-fit on to longer barrel) (an extra glass filter can be mounted on this holder if needed).

CHAPTER IV

OPTICS AND CRYOGENICS

IV (a). Light sources

(a) 1. Medium-pressure mercury lamp. This lamp is a Hanovia 500W a.c. air-cooled discharge lamp, and is supplied with its own control unit. The discharge tube obtained was U-shaped, and since forced air cooling caused the cavity to vibrate, natural convection was used. This lamp generates a lot of ozone and is unpleasant to work with. The light output was found by using an Uranyl Oxalate actinometer method (T11, T12). A replica of the optical path was set up, and by use of a suitable filter the energy in a single emission band could be found. At 3660A, the number of quanta per second falling on the sample is $(1 \pm .2)\ 10^{15}$. By means of a comparative table supplied by the makers, the energy in any other band can be readily estimated, e.g. at 2500A, the intensity is reduced to $3\ 10^{14}$ quanta/sec.

(a) 2. High-pressure mercury lamp. This lamp was bought at a later date when it became apparent that for work being done on the triplet state of organic molecules, the medium pressure

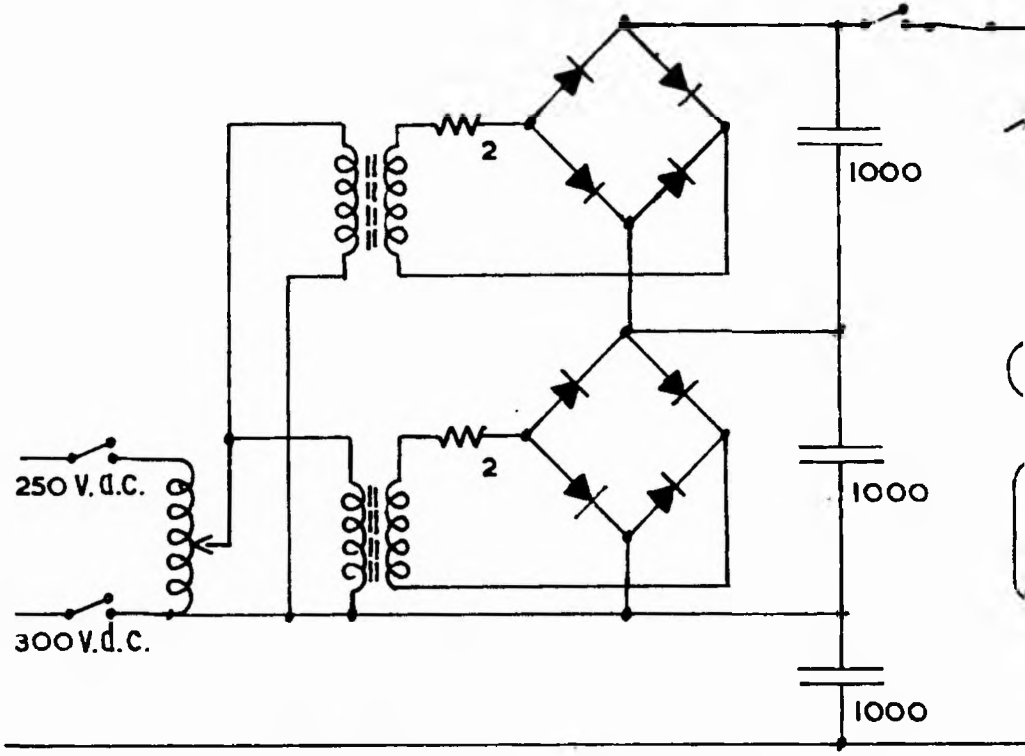

High-pressure Lamp Power Supply.

Figure IV 2

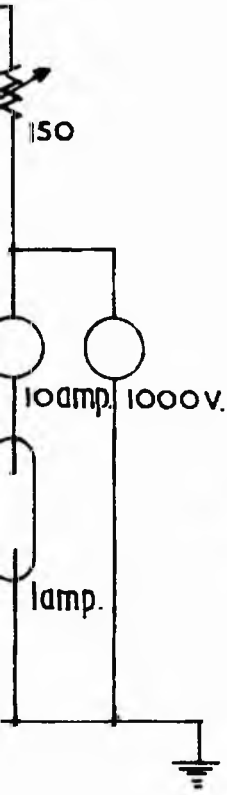

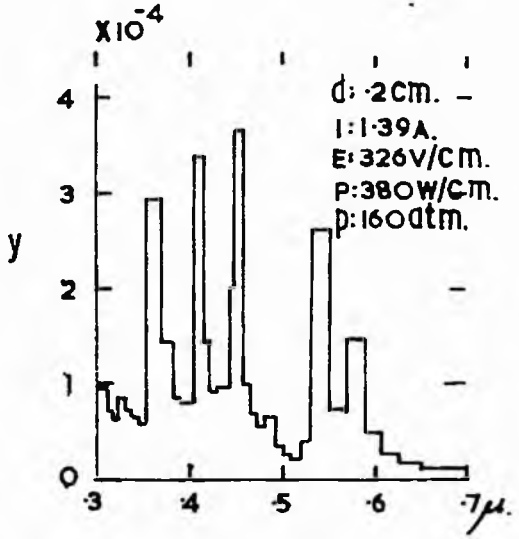

$$\int y\,d\lambda = \frac{P_{rad.}}{P}$$

y: radiation energy per Å per watt input.

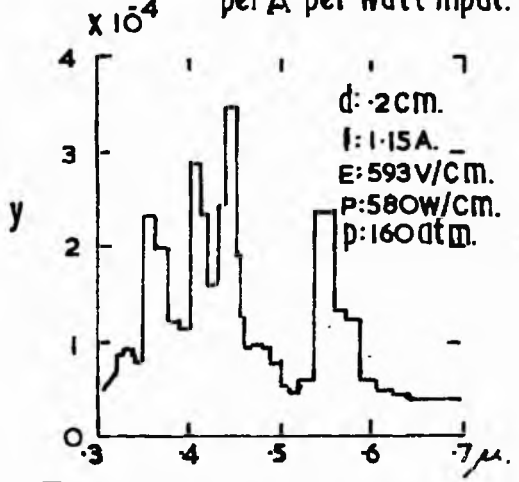

Typical output spectra of high-pressure lamps.

lamp was inadequate. The lamp chosen was a Philips 1000W.d.c. water-cooled type, which appears to be the only one of this class generally available in this country. The makers seem reluctant to part with them, and considerable time was lost in getting the lamp, replacements and details of the operating characteristics. The lamps are supplied with their own housing (Figure IV 1) and the windows are quartz (they were checked on a spectrograph (fortunately!)). The lamp is cooled by a water flow of 1 gallon per minute.

(a) 3. d.c. power supply. A power supply had to be built for the lamp as there was none available in the department, and the commercial 6-phase transformer/rectifier suggested by the makers was too expensive. The circuit shown (Figure IV 2) operates successfully, and the lamps seem to have their stated performance (50 hours lifetime at 2 hours/switching). The voltage over the lamp fluctuates by up to 50v. during normal running.

(a) 4. High-pressure lamp performance and filters. The high pressure lamp increases the light output because of the increased wattage, increased efficiency and because its small tube area (1.5 x .4 cm.) permits the profitable use of a reflector. Figure IV 2 shows the output spectrum of the nearest comparable lamp that could be found in the literature. (T60, T62). The

performance below 3000A is not known exactly, but it is thought to fall off rapidly. This is confirmed by observations on the triphenylene triplet line (Chapter VII), where at 3200A, a line of S:N::30:1 was observed, but at 2500A the line cannot be observed at an S:N::1:1. The AH-6 super-high pressure lamp which is used by American authors is comprehensively reviewed in (T63) and is stated to run at 110 atmospheres. This lamp radiates some 100 watts at wavelengths shorter than 3200A and 30 watts shorter than 2800A. As can be seen in Figure IV 2, the amount of visible and infra-red given out by high-pressure lamps (in contrast to the medium pressure type) is considerable (about 500W), so a filter is necessary with both cryostats. Figure IV 1 shows the one constructed, using a combination of liquid and Chance glass filters. The liquid container is 5cm. long, with quartz windows held on with Araldite. The filter contains cooling coils, which are also led around the tubing. In operation the filter has been found to be very effective and the temperature of the solutions used does not rise more than 5°C. Two Chance glass filters can be fitted, one between the liquid filter and the prism, the other after the lens (helium dewar only).

The following filter combinations (T21, T22) were used:-

Filter. (solvent = distilled water)		Pass-band.
(F.C.I.)	5cm. $CuSO_4$ (saturated)	3400 -5300A.

(F.C.2.)	F.C.1 + Chance OXI	3400 - 3800A.
(F.C.3.)	F.C.1 + Chance OX7	2800 - 3800A.
(F.C.4.)	F.C.1 + Chance OB10	3800 - 4600A.
(F.C.5.)	5cm. $K_2Cr(SO_4)_2.12H_2O$ (30gm/l.)	3000 - 3500A.
(F.C.6.)	5cm. $NiSO_4.6H_2O$ (240gm/l.) + $CoSO_4.7H_2O$ (45gm/l.)	2400 - 3200A.
(F.C.7.)	F.C.6. + 1 cm. KI.	2400 - 2800A.

Time did not permit an accurate evaluation of the light output of the high-pressure lamp using the actinometer method. However, by observing the boil off rate of liquid helium with and without the lamp on, a rough estimate of the number of quanta entering the cavity can be made. For F.C.2, the heat input is 210mW, leading to an estimated $2\ 10^{17}$ quanta/sec. This represents a considerable gain over the medium pressure lamp at this wavelength.

IV (b). Optical system.

(b) 1. Lens. The optical system was designed in the first instance for the medium pressure lamp. This U-shaped lamp presents a radiant area of 6 x 2 cm. toward the sample. The U is too wide to go between the magnet coils, and the distance between the object and image is therefore fixed at 22cm. Further restrictions are also imposed by the magnet gap, by the sample size and by the cavity width. After a mathematical

and practical investigation, it was found that the maximum light is gathered by a 30D lens of 1.5" diameter. A quartz lens of this size was obtained from Optical Works Limited (London). When the medium pressure lamp was used, a $\frac{1}{4}$" iron plate (with an appropriate slot) had to be bolted across the magnet, otherwise the stray field from the magnet "blew" the lamp out at fields in excess of 2500 oe. This plate was unnecessary with the high pressure lamp, which operated satisfactorily up to 6000 oe. This lamp however has to be mounted horizontally and so it cannot be brought any closer to the sample than the other. The filter takes up all the space between the lamp and the cryostat.

(b) 2. Prism. In some experiments, the use of a polarizing prism was necessary. A 1" square-ended calcite prism was obtained from Hilger & Watts; the prism is some 3" long and, together with a brass mount, is shown in Figure IV 1. The simple rotation device for turning the prism through angles up to 180° can also be seen. About 100mW are dissipated in it with most filter combinations, but no heating was observed. The 1" aperture is slightly less than the entrance pupil at the point where it is situated, but the light loss is small. The light transmission of the prism unit at 3200Å (F.C.5) was approximately 25%; this was found from the decrease in signal intensity when observing the triphenylene triplet absorption.

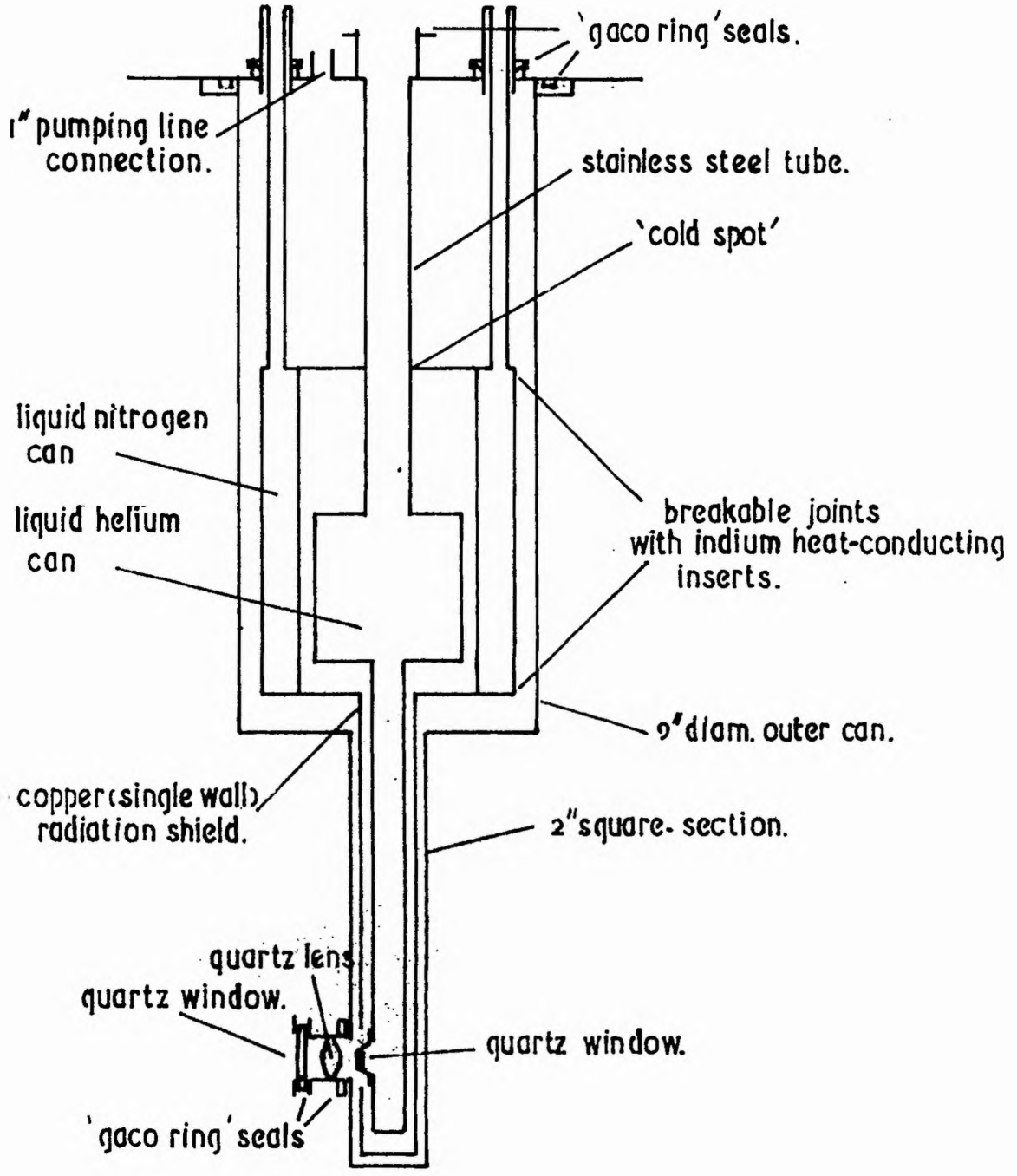

Metal cryostat assembly (schematic)

construction: brass except where indicated.
joints : soft-soldered.

Figure IV 3

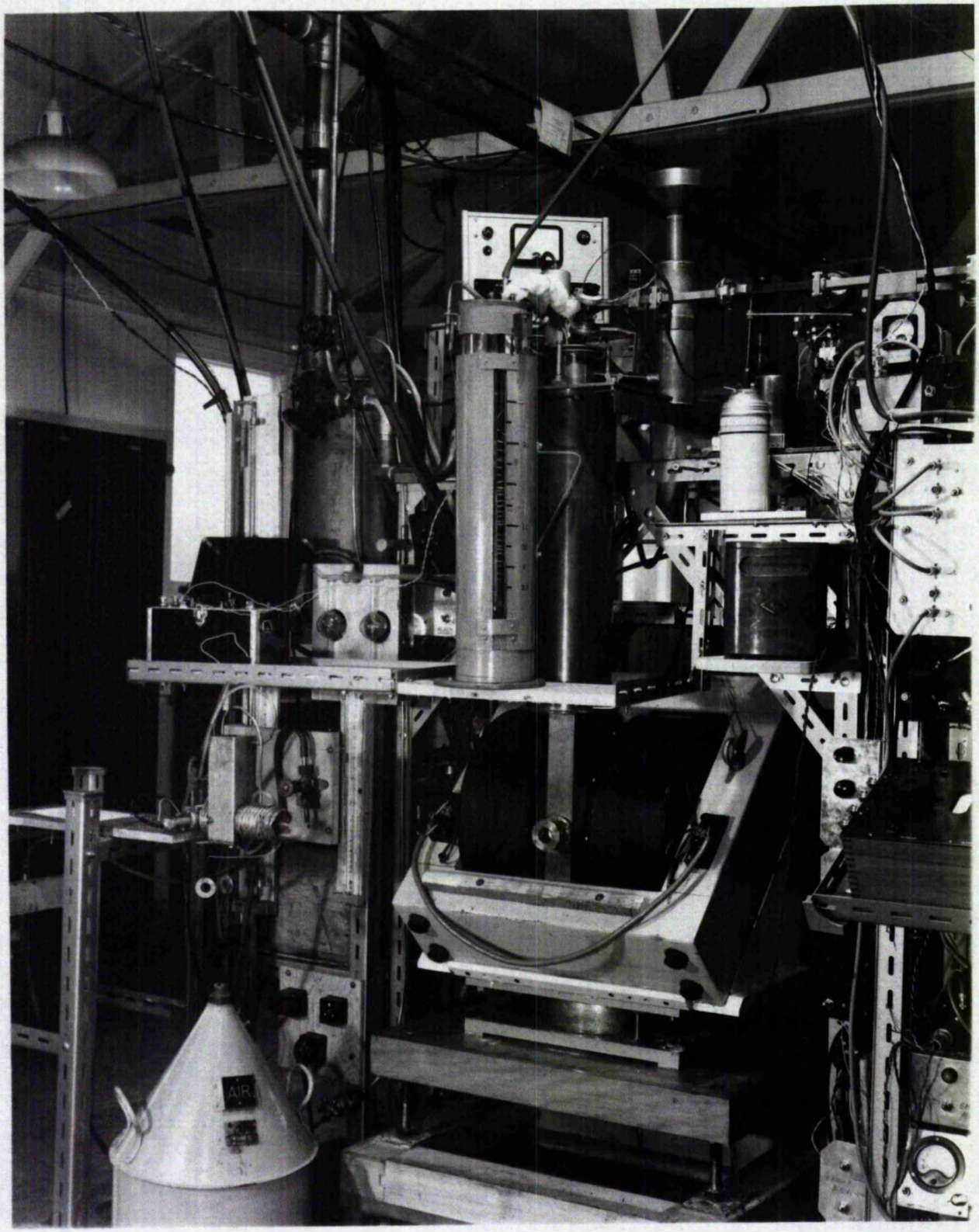

Figure IV 4

The cryogenic side of the apparatus, showing the metal cryostat set up for gas-flow operation.

The manufacturers quote 20% transmission at 2500A.

(b) 3. Sample holders. The quartz sample holders used can be seen in Figure III 3. They were made in the department.

The volumes are:-

2mm. long	.16 ± .01 cc.	(s1)
6mm. long	.40 ± .01 cc.	(s2)
2cm. long	.96 ± .01 cc.	(s3)

IV (c). The metal cryostat

(c) 1. Purpose. When the project was started, it was realized that for maximum flexibility, wavelengths down to 2500A were needed, necessitating the use of quartz. Two possibilities exist, either an all quartz dewar or a metal one with quartz windows. The main problem with the former was that the tolerances offered on commercial tubing were too large and also the difficulty of working large diameter quartz tubing with the facilities available. Accordingly a metal dewar, which seemed the easier proposition, was built.

(c) 2. General design. A drawing of the cryostat built is given in Figure IV 3, and a photograph of the mounting etc. in Figure IV 4. The design follows the normal pattern for such dewars, e.g. (T32). The cryostat, which is made of brass except where indicated, consists of a single walled Helium can, joined to the top plate by a stainless steel tube. The volume of this

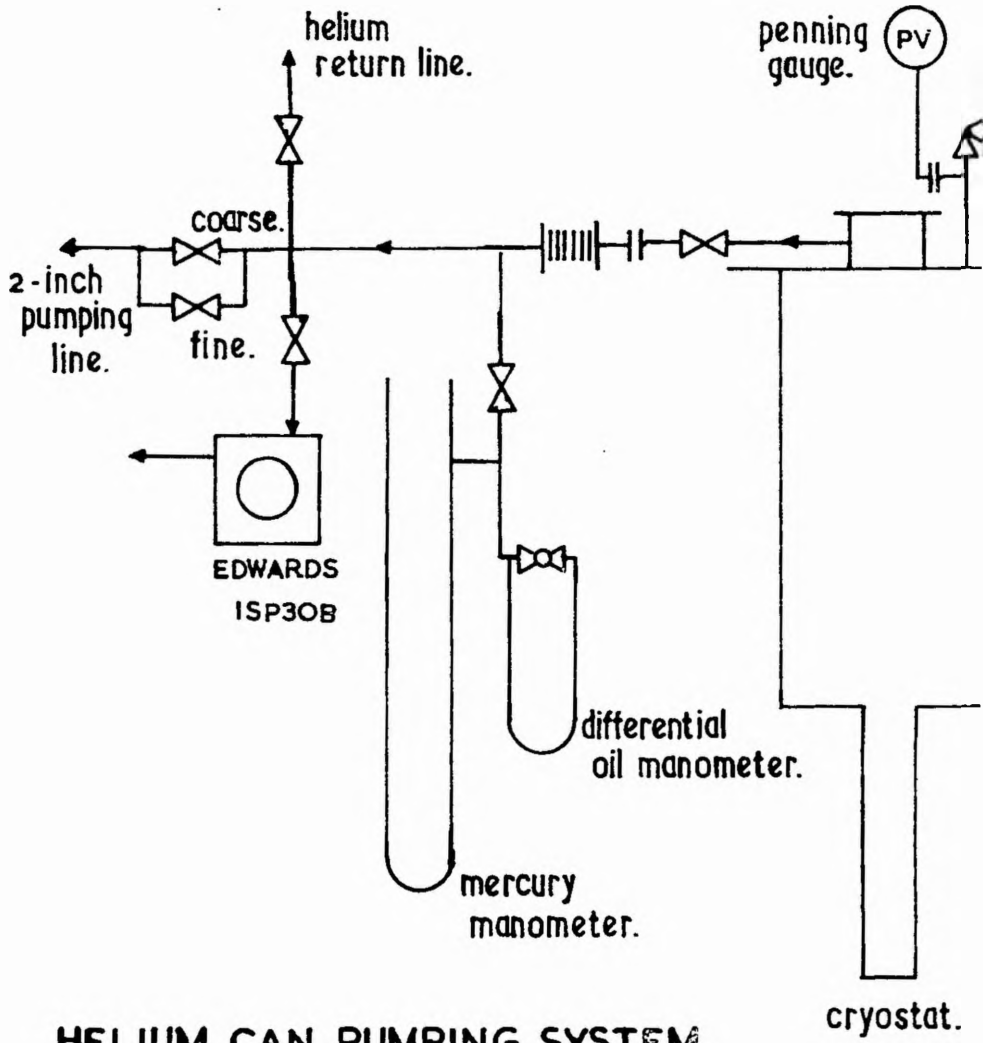

HELIUM CAN PUMPING SYSTEM.

Figure IV 5

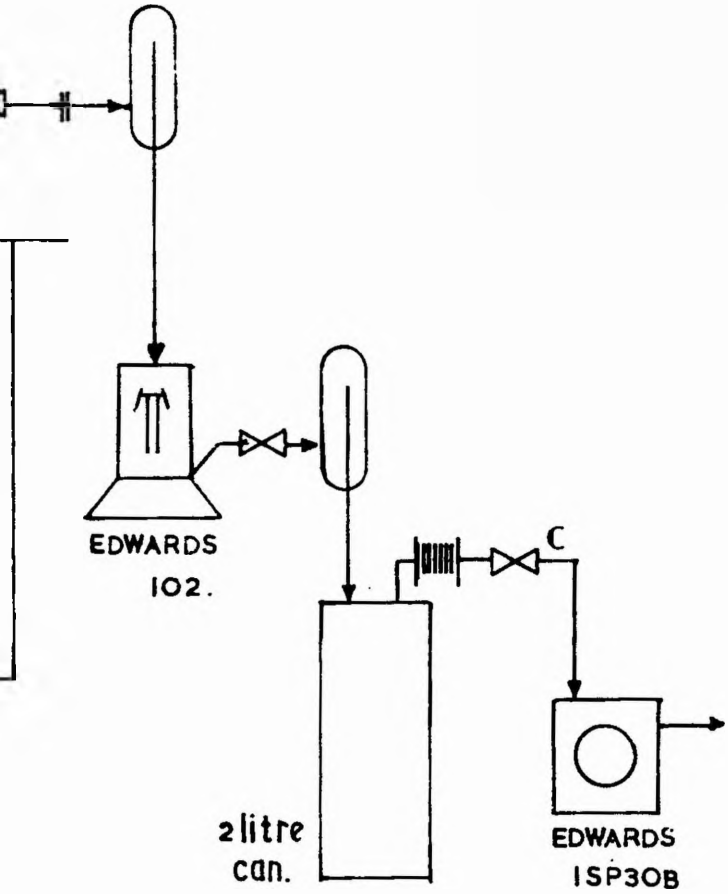

HIGH-VACUUM
CAN PUMPING SYSTEM

can and its tail is about 1 litre. The can is surrounded by an annular can, which when filled with liquid nitrogen, acts as a radiation shield. The shield is connected by a plate to the stainless steel tube in order to provide a cold spot, which shortens the stainless steel tubing to a practical length. The lower end of the liquid nitrogen can is connected to a single-walled copper tube which encases the helium can tail. This tube is split to allow the cryostat to be dismantled. The whole assembly is surrounded by an outer can at room temperature. All breakable vacuum joints are at room temperature and sealing is effected using Gaco rings. The pumping system is shown in Figure IV 5. The best vacuum attained on pumping is $2\ 10^{-5}$ torr. When the liquid nitrogen can is filled, the vacuum is improved to better than 10^{-6} torr.

The quartz window on the outer can is housed in the projecting barrel and the quartz lens is housed inside it, since due to its feather edge it cannot be used as a vacuum tight window. There is no window on the radiation shield, while that on the helium can is to the design of Roberts (T31). The diameter of this window is fixed by the light cone to be 15.5mm., and the rest of the design is governed by this consideration. The window was sealed onto a .010" annealed spun copper foil by Araldite (Mk 1). The copper foil is soldered onto the brass

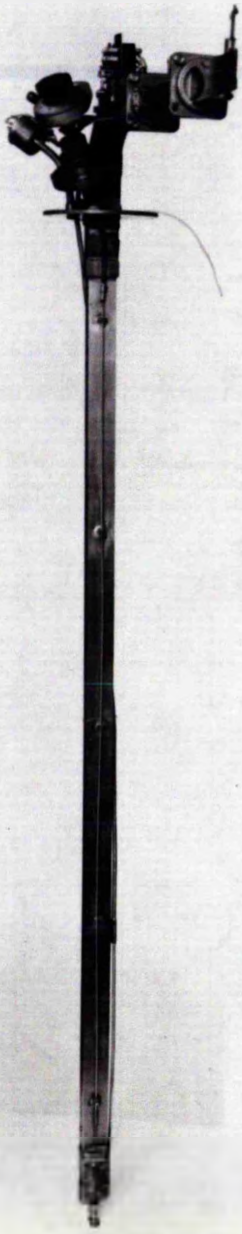

Figure IV 6.
Cavity arm for
metal cryostat
(showing slow-
motion drive.)

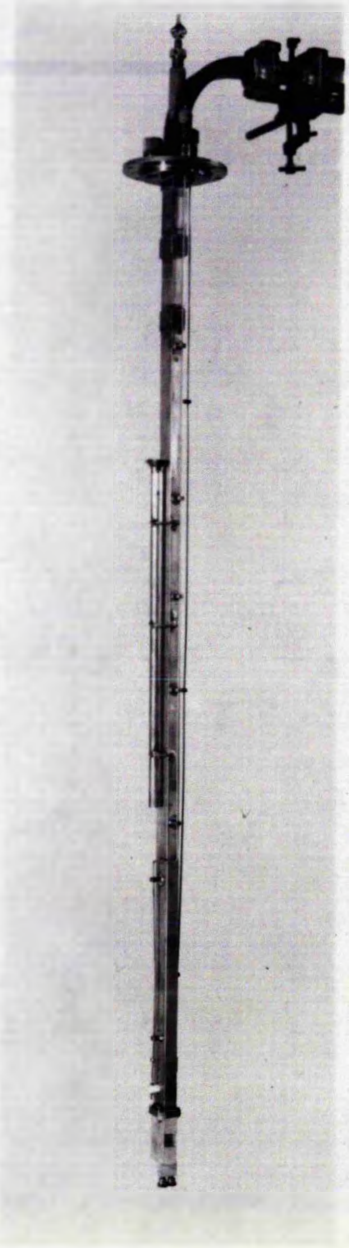

Figure IV 7.

Cavity arm for

glass cryostat.

tail with Wood's metal. The window has proved reliable after repeated pressure and temperature cycling. The complete cryostat weighs about 56 lbs.

The cavity arm is shown in Figure IV 6. The wave-guide between the top-plate flanges and the cavity is .020" stainless steel; as this o.d. is less than that of the brass wave-guide, a connecting piece had to be made. Since gaseous helium has to be conserved, the helium can also has to be made vacuum tight (2 torr.). The helium pumping system is shown in Figure IV 5. Also shown on the cavity arm is an electrical vacuum to air connection (glass-to-metal seal), which can be used for thermocouples, etc. (a similar facility is fitted to the high vacuum can). The top end of the sample turning mechanism is also shown. The gear wheel at the foot is connected to a stainless steel rod which runs up the broad side of the wave-guide and is connected at the top to a slow-motion drive by a flexible cable. The slow-motion drive, which has a reduction ratio of 6.25:1, is turned by a 12-turn counter, graduated 0 - 100. The tube which can be seen at the back was used for the gas-flow system (IV (c) 2). In Figure IV 7 (which is the glass cryostat arm) there can be seen the variable coupler connection and also the guide tube for channelling the liquid helium down into the tail. Both cavity arms are connected to the main wave-guide run by means of a short

section of flexible wave-guide (W. H. Sanders, "Flexiguide") with a quick release coupling. This allows easy demounting of the cryostat, and gives a little freedom in adjusting the cryostats in the magnet gap. The method of filling cryostats has been adequately discussed in (S4) and further details can be found there.

In practice this cryostat proved difficult to fill, due to the gas in the tail acting as a cushion for the liquid dropping down. However, even when filled, the cryostat was found to have a very large heat leak (about 200mW); this means that 1 litre of liquid helium lasts about 1 hour (after pumping). This is too short to be of any use. The reason for the heat leak is not known exactly, heat leak calculations for both conduction and radiation do not reveal any major errors in the design (T33). The temperatures at various points in the cryostat were measured by thermocouples, again revealing nothing unexpected. If the helium can and the nitrogen can are both filled with liquid nitrogen, there is still a boil off rate of about 150mW observed (measured by timing a soap bubble traversing a known volume). The trouble would seem to lie between either the tolerances in the tail section being so tight that the heat leak estimates are wrong or that insufficient heat conduction from the cold spot on the stainless steel tube occurs and possibly that the tube is of substandard quality.

At this point, the author decided that the development problems associated with the cryostat were too time consuming. It was obvious that fairly drastic alterations were needed and from previous experiences in getting work done in the workshop and the troubles of making the cryostat leak tight again, it was decided to leave the cryostat as it was and to use it for liquid nitrogen work.

(Since the author finished experimental work, for mechanical reasons the cryostat has been stripped down and rebuilt. Recently it has been tried out again and held liquid helium for eight hours - a value approaching the design specification.)

IV (d). The glass cryostat. Glass dewars had been used for some time in the department and an existing set were converted for use with this apparatus. For details of the dewars see (35); they can be seen mounted in the frontispiece. The dewars are made of Monax glass and the transmission characteristics were measured on a quartz spectrograph. The results showed that below 3300A appreciable absorption occurs, but it was known by this time that for much of the work planned at liquid helium temperatures, wavelengths shorter than this were not needed. The dewars were resilvered so that a clear ring was left around the cavity. They proved very reliable in operation and many runs were performed with them. The clear ring increases the heat input a

little, but a run can last up to six hours at 1.4°K (no a.v. input). The spectrometer normally needs about an hour to set up and to settle down (due to thermal drifts after pumping); so this leaves five hours' experimental time, but if the high pressure lamp is used, this cuts the running time to one and a quarter hours. The cryostat was invariably used at the minimum temperature which could be reached with the pumping facilities available (1.4°K); with the lamp on, the temperature rose to about 1.5°K. Even small changes in pressure (.5 torr.) are sufficient to cause a considerable base-line drift on the pen-recordings, and on days when other people were also using the same pumping line, pen-recording at maximum sensitivity was often made difficult (for even although the pressure change is instantaneous, the sample and cavity take some time to drift to the new temperature. In a one hour run, this is rather serious). Above the lambda point, bubbling in the cavity makes pen-recording impossible; in fact, even when pumping at maximum speed, it was on occasion possible to induce local boiling of the helium around the sample when using the high-pressure lamp and F.S.2. This could be detected by the consequent frequency change of the K.A.F.C.; the only solution was to reduce the light input until this stopped.

As the height of this cryostat was slightly different from the metal one, a separate cavity arm (Figure IV 7) was used.

An extra piece of flexible wave-guide was used to connect the cavity arm to the main spectrometer with minimum power reflection.

IV (e). Operation at 77°K.

(e) 1. Cavity filled with liquid nitrogen. In this method, liquid nitrogen was poured into the inner can of the metal dewar and allowed to fill the cavity. Since the dielectric constant of liquid nitrogen is 1.4, the cavity had to be much shorter in length than the others. The nitrogen, of course, bubbles constantly, but this was cured by pumping the nitrogen to a pressure of about 140 torr. At this pressure, the nitrogen stops boiling, but care has to be used for if the pressure falls to 100 torr., the nitrogen solidifies. The 1 litre inner can was connected in parallel with a 20 litre (empty) can to increase the volume being pumped and so helping to even out fluctuations in the pumping rate, control of which was done by a series of 2 Saunders valves and 2 needle valves. The general operation was, however, not particularly successful, the pressure having to be kept constant to within .2 torr. The higher heat capacity of the liquid nitrogen resulted in an even longer time to reach a stable equilibrium temperature than with liquid helium. This system was finally abandoned in favour of the gas-flow method described below.

(c) 2. Gas-flow method. The circuit is shown in Figures IV 4 and 6 and V 1A. Nitrogen gas from a cylinder is passed through a reducing valve and the flow rate metered. The gas then passes through a wide bore liquid nitrogen trap which removes most of the water vapour present (which is quite considerable) and then into a cooling coil also immersed in liquid nitrogen. The coil is made of about 20 feet of $\frac{1}{8}$" Cu-Ni tubing. The gas then passes through a small filter of glass-wool, which removes any ice which has been carried through by the gas (if this is not done, the quartz window in the helium can soon gets snowed up). The gas is then passed through a tube running down the cavity arm and directed onto the sample through a $\frac{1}{4}$" hole in the wall opposite that bearing the slits. A thermocouple (copper-constantan) is situated in the gas-flow where it enters the cavity and the e.m.f. developed is read on a Doran Mini-thermocouple potentiometer. The reference temperature is 0°C. The thermocouple was put in this position as it was found rather difficult to mount it directly in the cavity on to a sample which was being rotated. The temperature accuracy is $\pm$ 5°K, but this is adequate in the measurements made. The cooling coil was quite efficient, and a flow rate of 10 l/min. was sufficient to liquify the gas-stream. The normal flow rate, corresponding to a temperature of about 100°K, was about 8 l/min. at a pressure of 3 p.s.i.,

while the liquid nitrogen consumption was about 1 l/hr. Since there is only dry gas now passing through the cavity, slight variations in the flow rate do not affect the resonant frequency of the cavity, and pen-recording is quite easy. Samples could be changed in about thirty minutes.

The liquid nitrogen can of the cryostat was, of course, filled and the cryostat continuously pumped. Since the rotary pump caused the cavity to vibrate, the line was closed at valve C (Figure IV 5), and the diffusion pump allowed to work into a 2 litre can, until the back pressure rose too high for it to operate (about 10 torr.); this normally did not occur under two hours. A liquid nitrogen trap is used to increase this working time, since the plastic vacuum tubing used tends to degass.

CHAPTER V

SAMPLES : PREPARATION AND OPTICAL STUDIES

V (a). Purity. The samples used were of the highest quality commercially available; it is fully appreciated that this is no guarantee of purity, but since the work involved was, in the first instance, exploratory, further purification was not carried out. In particular, the purifying of organic compounds was felt to be a problem for a competent chemist with the proper facilities.

V (b). Crystal-growing techniques.

(b) 1. Water bath. Crystal growing is still an art rather than a science, but a few general references are given in (T41, T42, T43, T44). A study of these will reveal that each crystal has to be tackled on its own, however all the crystals which it had been decided to study were capable of being grown from aqueous solution. A water bath was built, using a Mercury-Toluene thermostat to acuate a "Sunvic" relay (F102-301 modified). Heating was provided by 2 150W lamps (one of which was just sufficient to maintain the temperature in case of failure) and the bath was continuously stirred. The temperature was constant

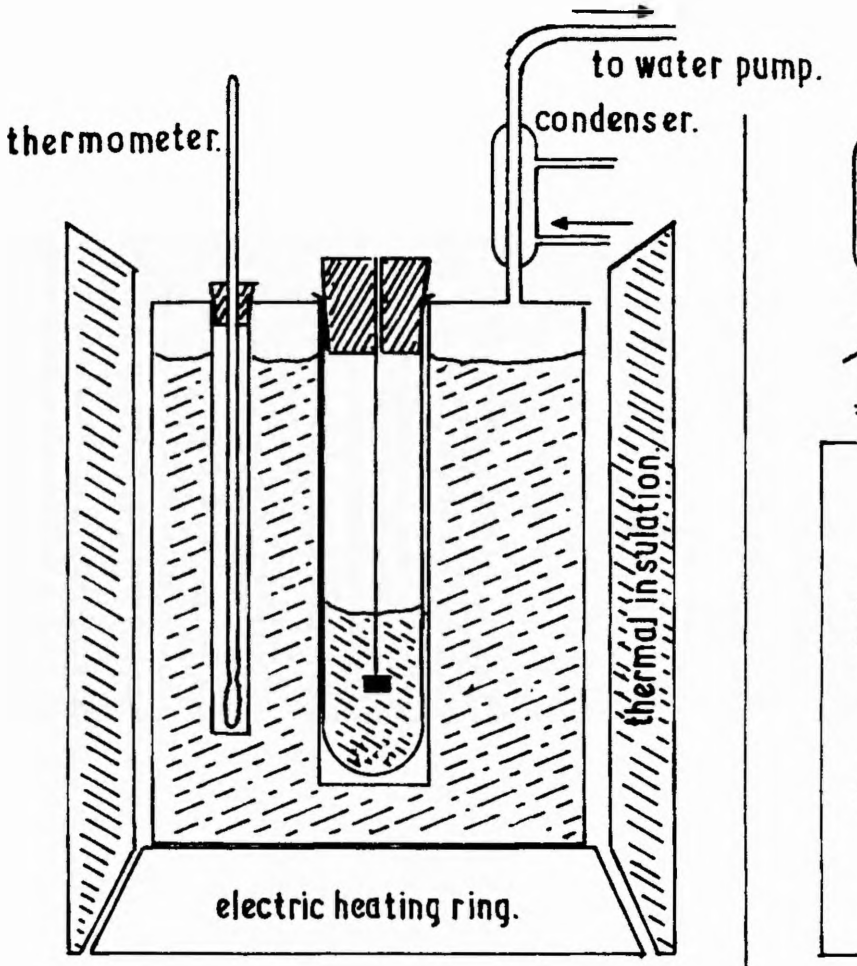

KCl(TlCl) CRYSTAL BATH.

Figure V 1

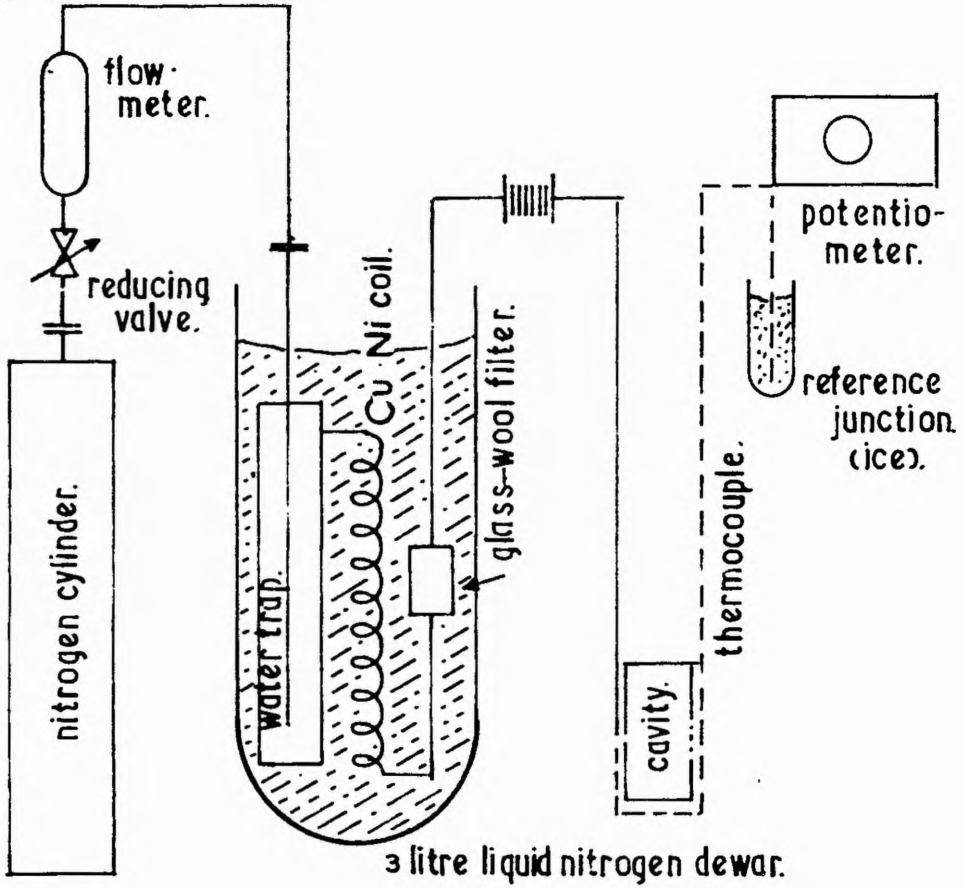

GAS-FLOW SYSTEM.

Figure V 1A

to $\pm$ .02°C. between 21 - 29°C. By gradually lowering the temperature, single crystals of the desired size were grown of $BaPt(CN)_4 \cdot 2H_2O$, $UO_2(NO_3)_2 \cdot 6H_2O$ and $K_2UO_2(NO_3)_4$.

(b) 2. Single crystals of KCl(TlCl). (see 01). Pringsheim prepared this salt by co-precipitation from a boiling solution of water saturated with KCl and TlCl; only the first 5% of the precipitate being collected. The author managed to grow single crystals by the method shown in Figure V 1. A saturated boiling solution is put in a glass test-tube and corked with a bung having a very small hole drilled through it. The test-tube is hung in a sealed double-boiler, heated by an electric ring of sufficient power to keep the water in the boiler at 100°C. The pressure over the water is then lowered by means of a water-pump to about 98°C, so that no boiling can occur in the test-tube (otherwise the solution splashes and the salt is deposited on the cooler walls as a powder). With the condenser fitted the water loss from the boiler is negligible, and the whole apparatus is left for a week or so. The water in the test-tube gradually evaporates and reasonably sized single crystals are formed on the piece of thread.

As far as the author is aware, up to the present all KCl(TlCl) single crystals used have been grown from the melt, so this method may be of some interest.

PHOTOMULTIPLIER CIRCUIT.

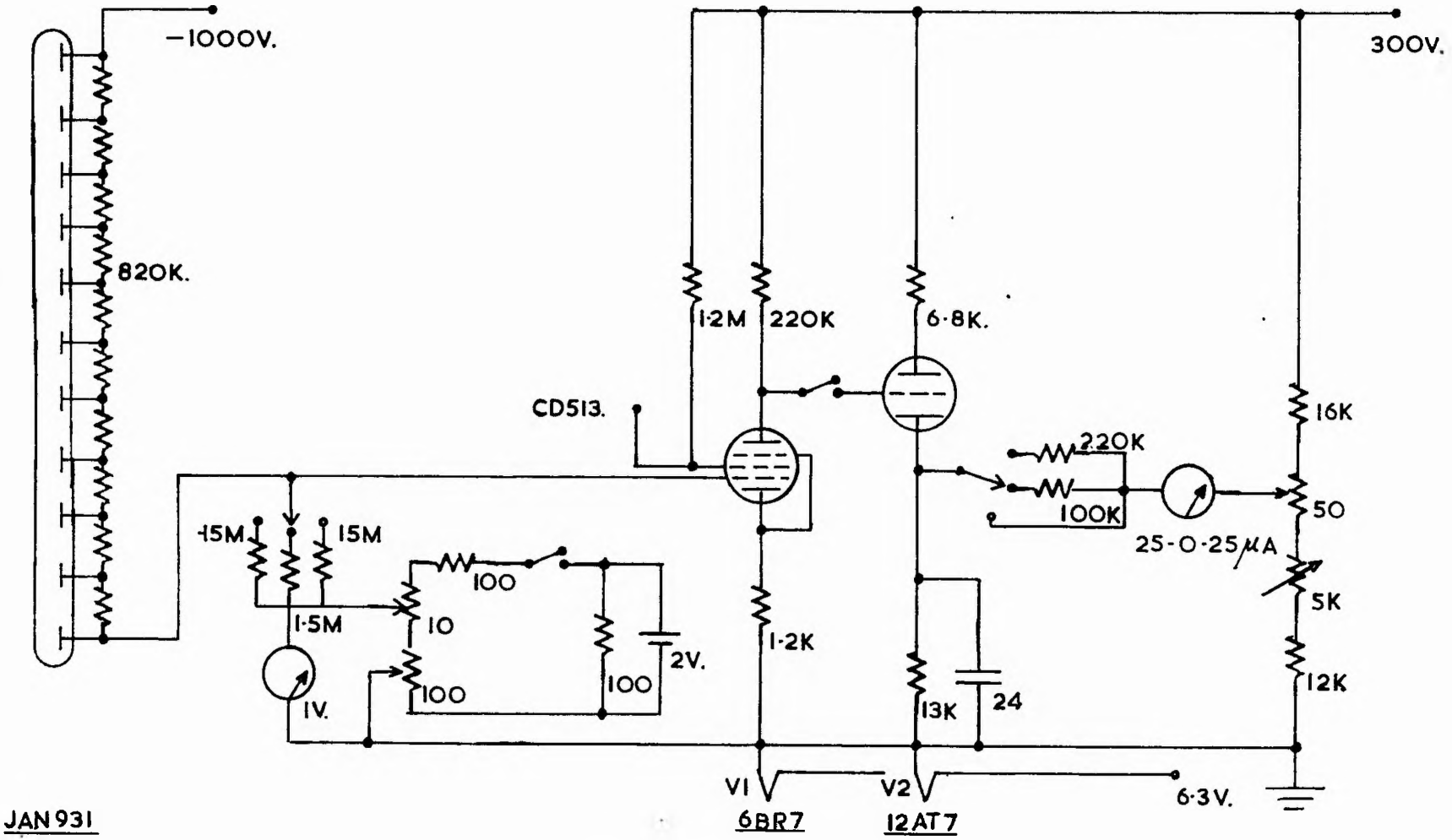

Figure V 2

V (c). Measurement of phosphorescence decay and thermoluminescence. As will be shown later in the thesis, it was often necessary to measure the phosphorescent and thermoluminescent emissions from various samples. The time-scales involved with the various samples ranged from a few milliseconds to over an hour. The amplifier circuit and recording techniques devised by the author allowed these widely varying conditions to be readily dealt with.

The circuit of the photomultiplier and amplifier used is given in Figure V 2. Two methods were possible, depending on the length of the decay period being measured. For short decay times, V_2 was disconnected and the output from the screen grid of V_1 (since a greater stage gain was obtained from this grid than from the anode) displayed on scope CD 513. The slowest time base on this scope is 11 seconds, and this is adequate for organic substances studied. The trace is recorded photographically (camera: Langholm-Thomson, Series 105). A shutter arrangement was used which cut off the irradiating light and exposed the photomultiplier tube.

For longer recording times, the slow sweep system for the magnet (III (i) 4) was used to give 2 and 6 minute linear sweeps, or the timebase could be disconnected and a cine-camera used. (Gossor). For even longer recording times than this, the whole

of the amplifier circuit was used. The bridge circuit formed by V_2 and the resistance chain was balanced with zero light input; the tube was then exposed to the phosphorescence and the bridge rebalanced by applying a reverse potential to the grid of V_1. This potential was then read on a meter or potentiometer. This method was used for measuring the decay time and thermoluminescence of $BaPt(CN)_4.2H_2O$. It is also possible to calculate approximately the number of quanta given out by the sample. A discussion of the analysis is given in Appendix 4.

For thermoluminescence measurements, the metal cryostat was used for slow warming rates and a quartz dewar (12" long, 1 cm. diameter) was used for faster rates. The temperature was measured by a thermocouple attached to the crystal.

CHAPTER VI

REVIEW OF OPTICAL AND E.S.R. WORK ON LUMINESCENCE

It is proposed in this chapter to indicate briefly previous work by other authors which provided a starting point for the work contained in this thesis.

VI (a). Literature. Luminescent properties of materials have been studied since about 1850 and a great deal of information has been obtained. Unfortunately, most of it - up to the 1930's at least - is almost valueless. This is due mainly to the various investigators having no clear idea of the mechanisms involved, and so the information they recorded is quite haphazard and often irrelevant. In particular, the presence of impurities was not understood, and the work of Lenard (who dominated much of the thinking from 1900-25) is a good example of this. With the arrival of quantum and crystal field theories, the basic mechanism was begun to be appreciated, and the more recent work has stemmed from this. The problem nevertheless has still proved intractable, and no generally unifying theory has been proposed.

The generally quoted standard text is by Pringsheim (PO), which was published in 1947 (although the material is only up

to 1938) and is sadly out of date, in addition to being verbose. (This view is not held by all, e.g. Smaller (1964) (A23) has described it as "an excellent monograph"). More recent work will be mentioned below.

An example of the general confusion surrounding luminescence occurs straightaway in defining fluorescence and phosphorescence - the terms are used quite indiscriminately in many cases. It should also be noted that "a phosphor" is a material which phosphoresces - or fluoresces - or both!

The above situation makes it very difficult to gather material relevant to the problem at hand, and obviously involves one in a great deal of cross-checking.

VI (b). Jablonskii diagram. In very general terms, when the exciting light is incident on a molecule and there is absorption by the molecule, an electron is raised from a lower to a higher excited stated. If this upper state represents an unstable configuration, the electron quickly returns to the ground state, and the probable lifetime of this state can be shown to be $<10^{-8}$ sec. (F11). The electron can return to the ground state in either a single transition or a series of smaller ones. The energy released in the single transition type normally occurs as a flash of visible light, and this phenomenon is known as fluorescence, while in the multiple transition type the energy emitted per transition is much smaller (generally in the far infra-red),

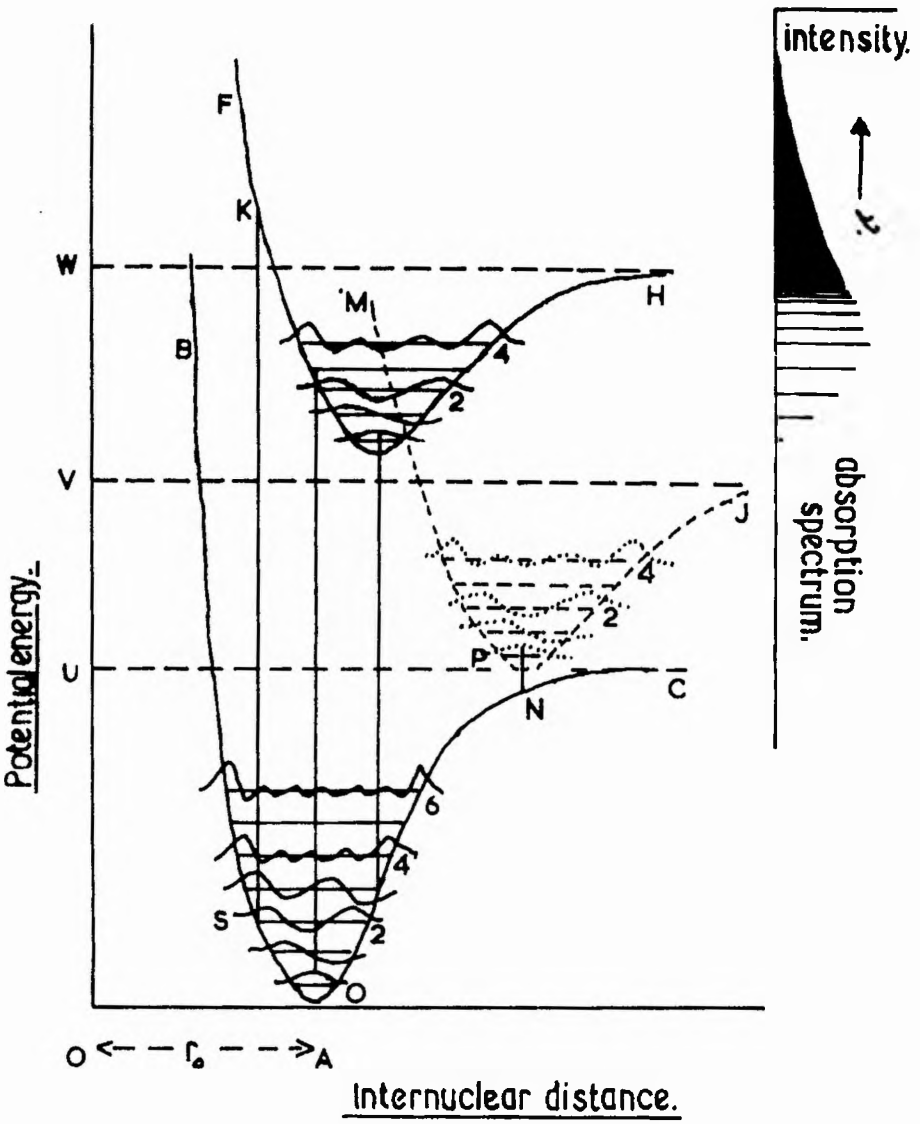

Jablonskii diagram.

Figure VI 1

and so this type is often known as a "radiationless transition". If the excited state represents a stable configuration, the electron is permanently trapped and there will be no emission. Finally, if the state is metastable, it will be released after a given time and the resulting emission is known as phosphorescence. The above definition of phosphorescence and fluorescence (i.e. whether or not the electron enters a metastable state) is quite rigorous, but if the lifetime of the electron in the metastable state approaches that of its possible lifetime in an ordinary excited state, it often becomes difficult to distinguish between the two by spectroscopic methods (see below). It is quite possible for both types of emission to occur with the same exciting wavelength.

It is more instructive to represent the above discussion schematically by a diagram, Figure VI 1, due to Jablonskii (B5). The diagram shows a plot of the potential energy of the ground (B), first excited (F) and a metastable (M) state of a molecule against a generalized co-ordinate of distance. The horizontal lines indicate various vibrational levels. Since the first excited state is one of greater energy than the ground state, the position of the minimum is generally farther from the centre than that of the ground state, as shown. The lines representing absorption and emission are drawn vertically on the diagram (Franck-Condon principle). The number of vibrational quanta

emitted after both absorption and emission is of the order of 10-100. Thus the emitted light is always of lower energy than the absorbed light (Stokes' Law; this law can be violated if the absorption process is a two-photon one (E91).) For phosphorescent emission, the transition from the metastable state to the ground one can occur either via the first excited state or directly; so phosphorescent light can have either the same wavelength as the fluorescent emission or longer.

It has proved possible in a few cases to calculate these configurational diagrams for fluorescence phenomena and to make a few predictions, but generally they are drawn schematically (L3B).

VI (c). Apparatus limitations. An e.s.r. spectrometer is in theory capable of detecting unpaired electrons in a sample, and hence any electron in the excited states mentioned above. There is a serious limitation to this however, as can be seen by constructing an equation, balancing the steady state concentration of spins in the excited state to the number of spins that can be detected by the spectrometer:-

$$\phi . A . \tau = N.W.S.$$

where ϕ = light flux, at the appropriate wavelength, in quanta/sec.

A = the product of the fractional absorption of light by the sample and the phosphorescence/fluorescence ratio.

τ = decay time of the phosphor (in seconds). (τ is defined in VI (d) 3).

N = number of spins detectable by the apparatus, at unit line-width.

W = line-width of the e.s.r. signal.

S = S:N ratio of the e.s.r. signal.

Since the value of N is obtained empirically (III (j) 1), this equation is only valid when the e.s.r. absorption of the phosphor has the same characteristics as the calibrating sample, i.e. it should have a Lorentzian line-shape and "spin-lattice relaxation" effects should be unimportant.

A S:N::10:1 is necessary for any useful work, and the line-width is unlikely to be less than 10 gauss in the type of experiments planned, so the R.H.S. $\geqslant 10^{12}$. The L.H.S. is more difficult to estimate, but in a favourable case A may be .01 and $\phi = 10^{17}$ at 3660A, so the minimum value for τ is .001 sec., and may well be greater than this. However, it is obvious that fluorescence and short-period phosphorescence cannot be studied by e.s.r.

VI (d). <u>Types of phosphorescence mechanisms</u>. Since the time-scale has been fixed, only mechanisms involving the metastable state are of immediate interest. There are two broad possibilities involving this state:- either the excited electron is completely removed from the molecule (Class 1) or it is localized on the molecule (Class 2). This classification of the various phosphors (and the sub-divisions introduced below) is due to the author.

(d) 1. Class 1 phosphors. The metastable state in this class is caused by traps in the crystals, such as:-

dislocations	(Class 1A)
lattice vacancies	(Class 1B)
isomorphic foreign atoms embedded in the lattice	(Class 1C)

This class contains almost all the commercial phosphors and almost all phosphors of long duration. These phosphors are often a combination of A, B and C. For example, 1A is typified by the Lenard school of research, where all the phosphors studied were fired at 2000°C; this treatment naturally leads to severe dislocations in the crystal structure. Class 1B is exhibited by naturally discoloured NaCl (P4). Class 1C is often prepared along with Class 1A, although KCl(TlCl) is a possible example (C1).

However, as a class these phosphors are not of great interest in the present work, since the phosphorescent centres are in general non-uniform and randomly distributed, so that any e.s.r. absorption is likely to be isotropic. For interest, a selection of the varied types of phosphors in this class is given in Appendix 5.

(d) 2. Class 2. In this class a basically different situation arises, since the phosphorescence is due to a forbidden transition within the molecule. Under these circumstances, there is no necessity to disturb the crystal lattice and the possibility of an ordered structure of phosphorescent centres exists. The class

can be divided into five groups:-

Class 2A = organic molecules (nearly all containing planar condensed aromatic ring systems).

2B = Cr and Mn doped crystals, etc.

2C = rare-earth doped crystals.

2D = platinocyanide salts.

2E = uranyl salts.

The individual properties of these phosphors will be discussed below. (Tungstate ($WO_4^=$) phosphors are often quoted as belonging to Class 2 phosphors, but recent work has shown that the phosphorescence is due to a trapping mechanism, the decay time being proportional to sec^{-1}., i.e. a bimolecular mechanism (see IX (a) 1) (N10, N11).

(d) 3. Classification of a given phosphor. This is a difficult problem, and in general the following facts need to be known:- composition, method of preparation, nature and quantity of impurities, absorption, fluorescence and phosphorescence spectra, temperature variation of decay lifetime and thermoluminescence. Unfortunately, it is rare for all these facts to be available, and it is often difficult to draw a definite conclusion. It is also possible for a Class 1 phosphor to stimulate Class 2 phosphorescence in a crystal if the absorption band of the Class 2 phosphor overlaps the emission band of the Class 1 phosphor.

The form of the decay of the phosphorescent emission and

also its temperature dependence often provide useful guides. In the case of Class 2 phosphors, since the return of the electron to the ground state is governed by the spin-forbiddenness of this transition, the emission intensity (I) will have an exponential form:-

$$I = I_o \exp(-pt) \qquad (6.2)$$

where p is a constant (related to the transition probability) with the dimensions of frequency. The decay time (τ) of a phosphor, which has an exponential decay, is defined as the time taken for the emission intensity to fall to 1/e of its original value.

In Class II, there is no forbidden transition, but instead the electron has to receive a quantum of energy of the correct value in order to escape. In the simplest case, this leads to an emission which has the following form:-

$$I = I_o \exp(-E/kT) \qquad (6.3)$$

where E = the potential energy of the trap (in ev.) and T = the temperature (^oK). The above equation is occasionally obeyed, but more often the decay law is modified due to retrapping and/or a spread of energy levels - situations which do not occur with Class 2 phosphors. Some examples of the various forms of the decay laws are given in (IX (a) 1). In the case of phosphors with non-exponential decay curves, τ is not explicitly defined

(since the shape of the curve can now vary during the decay, as it will depend on the number and energies of the traps filled).

As can be seen above, if the temperature of a Class I phosphor is varied, the decay-time varies (for further discussion of this point, see IX (a) 1,) while for a Class 2 phosphor, this is not the case, since here the transition is purely quantum mechanical in nature and is not dependent on lattice interactions. Slight variations may in fact be found as it is possible for the lattice vibrations to have some effect but in general not more than a factor of 2 or 3 between $300^{o}K$ and $1^{o}K$. So the form of the decay curve is almost entirely determined by p, and is independent of the conditions of excitation such as intensity, wave-length and duration of excitation.

Further points of difference are that Class 2 phosphors should have decay characteristics which are largely independent of the host matrix (if any), that they may well be non-photoconducting and that the fluorescence and phosphorescence bands should be separate (although this separation need not be large).

(d) 4. Comments. As has been stated before, the whole field of phosphors is in need of re-examination and classification. For

example, 99% of the phosphors mentioned in the literature emit in the visible region of the spectrum, but this proportion seems unduly high, so it is quite possible that a number of phosphors which would yield interesting results by e.s.r. techniques have been overlooked. An interesting field which seems to have had little study is that of silicon phosphors of the ring type (P8).

VI (e). E.S.R. work on Class 1 phosphors. The first phosphors to be investigated were of the SrS double activated type. The earliest attempts were made by Low (C1) on SrS(Eu, Sm) and SrS:SrSe(Eu, Sm), with little success. The main trouble with this particular phosphor is that the Eu gives an e.s.r. signal when the sample is unirradiated, so that on irradiation, the number of spins contributing to this resonance decreases - a much more difficult situation to detect, due to the difficulties in keeping the spectrometer gain steady when the light is shone on to the sample. The variation was finally detected by Dubinin (C2), who found that the number of active centres was only 10% of the total number of activator ions. However, as can be appreciated, little of interest can be gathered from this sort of experiment. In a later paper they observed the effect of the addition of fluxes (C3). Recently this subject has been taken up again by Garlick (C4), studying the entry of Mn^{2+} into CaF and SrF phosphors. This is a continuation of earlier work (C5) on many phosphors of the general type ZnX(Mn) where

$X = GeO_4$, $(PO_4)_2$, Al_2O_4, S, SiO_4 or B_2O_3. On irradiating these phosphors, no significant change in the e.s.r. signal from the Mn^{2+} was obtained and no new lines observed.

Work has also been reported recently on polycrystalline ZnS(Ga) (C8) and also on single crystals of cubic (Zn/Al) (C9). In the latter case the signal was frozen in at 77°K and was stimulated by 3660A illumination. These phosphors are interesting as the resonance was observed in the excited state, and it has been possible to make some deductions on the lattice site and its distortions.

Kallman (C10) has reported the observation of a resonance in a few selected ZnS(Cd) crystals after stimulation, although the spin density observed was much less than the optical spin density. They attribute this discrepancy to a coupling between the trapped electrons and the ionized activators, forming a singlet state.

A photosensitive centre has been detected in CdS(Cu, Ga), when the Cu concentration is greater than that of the Ga and is ascribed to a filled Ga trap. (C11).

VI (f). E.S.R. work on Class 2A phosphors.

(f) 1. Mechanism of Class 2A phosphors. The phosphors of this type are numerically very large, the more common members being mentioned in Appendix 6. The phosphorescent state of those materials can normally only be observed by e.s.r. when the phosphor is dissolved in an inert

matrix to reduce the dipolar broadening. The host lattice can be either crystalline or glassy, and must satisfy the following conditions:-

(i) insignificant absorption in the phosphor absorption band,

(ii) (preferably) small absorption in the phosphor emission band,

(iii) stability under the exciting radiation and

(iv) chemical inertness toward the phosphor.

The mechanisms involved in the phosphorescent process are similar in all cases and can be briefly described as follows:- (see Figure VI 1).

(i) Initially the molecule is in an unexcited state (B) and the orbital electrons are in their lowest molecular orbitals; this state is a diamagnetic singlet.

(ii) The exciting light raises an electron to the first excited molecular orbital level (F). As no spin change has taken place, this state is also diamagnetic.

(iii) Excess vibrational energy is rapidly lost to the surrounding lattice and the electron quickly ($\sim 10^{-11}$ sec.) falls to the lowest vibrational level.

(iv) Return to the ground state can then take place giving the usual fluorescence phenomena.

(v) Or the electron can cross over into the state M, and this is known as "inter-system crossing". In Figure VI 1, the probability

distribution of an electron in the various vibrational levels is shown. At points near the curve F, for example, it can be seen that the electron has a lesser probability of being there, but when it is near this point it has a very low kinetic energy, and if this point is also a region of low kinetic energy for states M, it is possible for the electron to enter this state, and by (rapid) vibrational deactivation it falls to point P. In these organic crystals, this state M can only be provided by the first triplet state (i.e. one in which the electron spins are parallel). By Hund's rule, at least one triplet-state must always have an energy less than that of the first excited state. For the electron to enter the triplet state implies a spin change for one of the electrons, and the reason for this breakdown in the spin conservation laws is in part due to the fact that the laws do not hold strictly for "radiationless transitions" and partly to the magnetic effect of heavy atoms and other unpaired electrons (E72). The number of electrons which make this transition is however somewhat surprising, e.g. in the case of phenanthrene it appears to be as high as 50%.

(vi) When the electron is in the triplet state there is no easy way for it to return to the ground state and it is temporarily trapped. Spin reversal does of course finally occur and the electron returns to the ground state, via the path P-N-A, with possible visible light emission, depending on the potential

change P-N. McLure has shown the effect of spin-orbit coupling on the forbiddenness of this transition by observing the effect on lifetime of the substitution of different heavy atom groups (F, Cl, Br and I) on Naphthalene derivatives. He showed that the relative lifetimes were in the approximate ratio to be expected from the spin-orbit coupling data (E5).

There still remains an anomaly in that the intersystem crossover of the excited singlet to triplet has a high probability, while the triplet to ground singlet probability remains very low. Pariser (B6) has attempted to resolve the problem by the introduction of another 2-fold degeneracy in the electronic designation and by judicious use of this increased number of states can provide an explanation of the anomaly.

The possibility of the triplet state mechanism was first discussed by Kasha & Lewis (E13) in 1944, and the paramagnetism of the state was first demonstrated by the former using a magnetic susceptibility balance (E60). The absorption spectra of the triplet state has also been investigated using flash photolysis techniques. (E26).

(f) 2. <u>E.S.R. work on the triplet state</u>. The e.s.r. absorption of the triplet state was first observed in 1960 by Hutchison and Mangum (A3), using naphthalene as the phosphor in a host matrix of durene. Single crystals of this kind had been studied

optically by McLure (E87), who had shown that the naphthalene molecules lie in an ordered manner relative to the host lattice. Because of this ordered structure, it was therefore possible to study the anisotropy of the triplet state of this molecule. The results showed that these dM = 1 transitions had a large anisotropy (2000 oe.). Since there are two possible dM = 1 transitions, two absorption lines were observed (h.f.s. was also observed, superimposed on these two lines) (A1).

Subsequent work, however, has not followed this method because of the difficulty of obtaining suitable host crystals, and the problem of determining the impurity orientation. Another reason was the discovery by de Groot and van der Waals (A4), using the same phosphor, of the dM = 2 transition. This transition, which strictly should be forbidden, turned out to be partially allowed, with an intensity of about one-hundredth of the dM = 1 transitions. However, the e.s.r. absorption turned out to be much less anisotropic than the dM = 1 transitions, and the same authors soon showed that the line could be detected in a glassy solution, usually frozen at 77°K (A5). The results will be discussed in Chapter VII and here it will only be pointed out that since the spin transition is 2 in this case, the magnetic field to obtain resonance at a given frequency is halved, i.e. it is about 1500 oe. The "half-field" resonance is a very useful property, as it eliminates the problem of spurious

resonances due to, for example, free radicals created in the solvent by the u.v. irradiation.

The discovery of a simple method of observing the triplet state lead to the examination of a wide range of these phosphors, but since the line is anistropically broadened, the amount of information which can be obtained is limited. Some of the more important phosphors which have been recorded are noted in Appendix 6. The latest work published uses Perspex as the host matrix and this material has the advantage of being able to be used at all temperatures up to 400°K (A19).

The dM = 1 transition has also been reported in glassy solution (A8), 100-fold weaker than the dM = 2 transitions; the resonance being observed in spite of the large anisotropy, because of a sharp change in the number of absorbing molecules at the extreme field values. Naturally the line was broadened by unresolved h.f.s. and did not reveal any additional information. Recently, however, theoretical papers have been published on the line shapes of these transitions (B7, B8) and the conclusions drawn are very interesting. There is little doubt that these papers indicate the direction in which immediate developments in this field will occur.

Other experiments in this field have used the dM = 2 transition as a tool. For example, Farmer (A10) has detected energy

transfer between the triplet states of two independent phosphors, the ones used being benzophenone and naphthalene. The absorption spectrum of naphthalene stops at 3100A, but that of benzophenone extends as far as 3800A, and has an extinction coefficient $\log \epsilon = 2.5$ at 3500A (See Appendix 6). It was discovered during optical studies by Terenin & Ermolaev (E30) that if the sample was irradiated at 3500A, it was still possible to stimulate the naphthalene phosphorescence. Benzophenone has a very large Q_{phos}/Q_{fl} ratio and they postulated that energy transfer between the triplet states of the two phosphors was occurring. The argument that association complexes between the compounds was the true cause was countered by observing (i) no decrease in the lifetime of the naphthalene triplet state, (ii) no change in the phosphorescence spectrum, (iii) no change in the absorption spectrum and (iv) no sensitized phosphorescence from strongly polar molecules equally likely to associate with naphthalene (e.g. benzoic acid). (Compare these observations with those on Naphthalene/T.C.P.A. phosphors in Chapter VII). The effect has been observed with several other energy donors and acceptors. The e.s.r. observations, by Farmer, confirmed this interpretation by observing the unchanged naphthalene absorption. The transfer of energy has also been studied by e.s.r. in the case of phenanthrene to naphthalene in single crystals of biphenyl (All) and even a two-stage transfer using indole as the intermediate between

diphenylamine and fluorene (A23).

VI (g). E.S.R. work on Class 2B phosphors. The substance which has received most attention in this group has been ruby ($Al_2O_3(Cr^{3+})$). In this case the phosphorescence is due to a forbidden transition in the chromium ion. However the short-life time of a few milli-seconds precludes any study of this class in the present apparatus. All the phosphors in this group have a similar decay period. A further difficulty is that the chromium impurity gives rise to broad ground-state resonances (C21). The e.s.r. absorption resonances were detected by an ingenious method which measured changes in the optical absorption of the various levels as the magnetic field was varied while keeping the microwave signal at a constant frequency (C22, C23). Although this method is very sensitive, it has several drawbacks, amongst them being the need for a sharp (optical) absorption line. No work was done on phosphors in this group by the author.

VI (h). E.S.R. work on Classes 2C, 2D and 2E. No work has been reported on these phosphors and a description of the optical properties is given in Chapter IX, along with the experimental work done on them by the author.

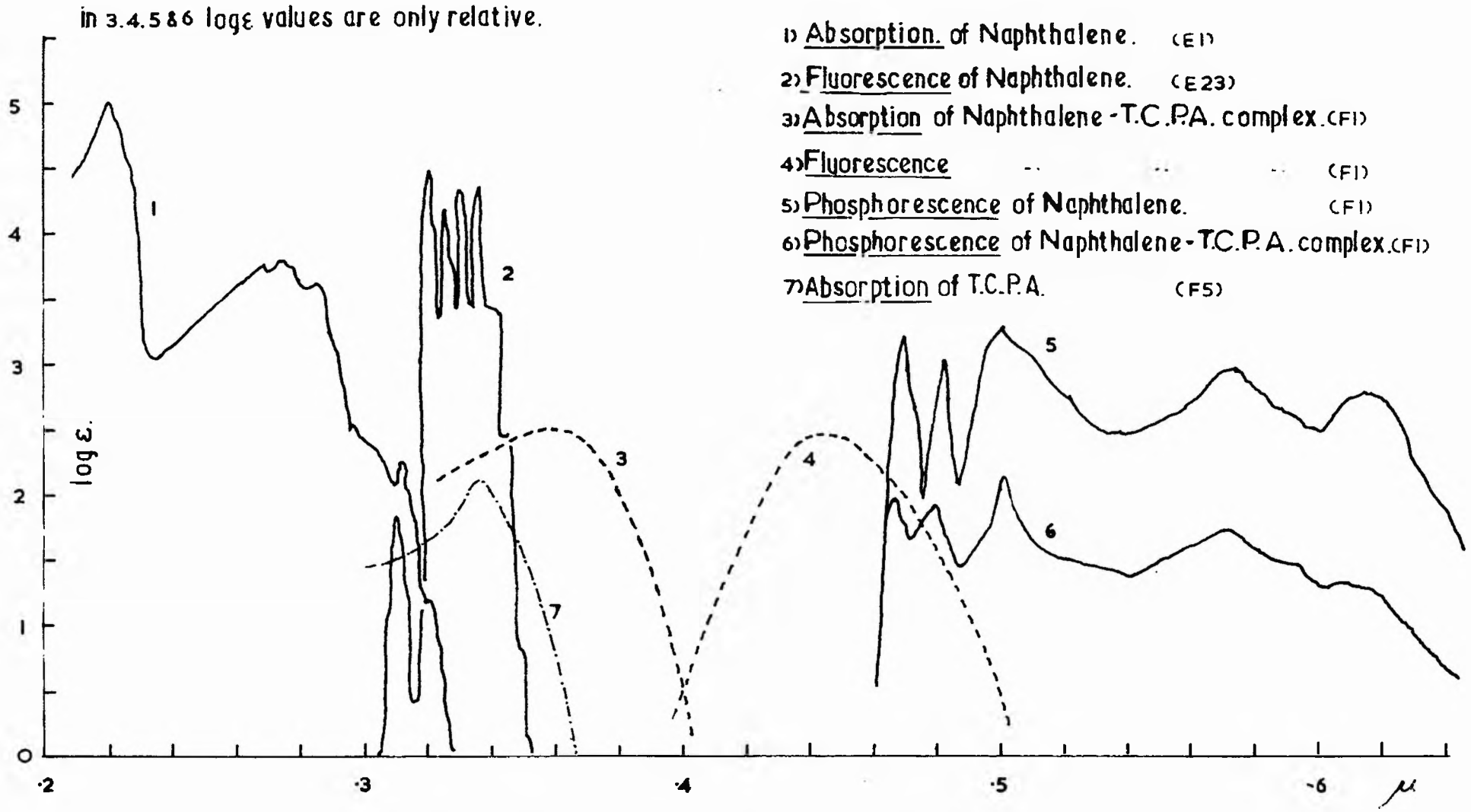

Spectral Detail of Naphthalene-T.C.P.A. complex.

Figure VII 1

CHAPTER VII

Experimental work by the author on Molecular Complexes

VII (a). Introductory

In this chapter some work which has been done on several aromatic hydrocarbons will be discussed. As mentioned previously (VI (f)), these substances provide a wide, but inter-related, series of Class 2 phosphors. The author has used the techniques of electron spin resonance to study the excited states of charge-transfer complexes of the donor-acceptor type. In the experiments conducted, various aromatic hydrocarbons were used as the donor component in complexes having the same acceptor. As discussed in the following review of previous optical studies of complexes (VII (b) 1), which is included in this chapter for convenience, the mechanism involved in these complexes was not clear. The work reported here clarifies the situation, and has also thrown new light on the problem of energy transfer.

VII (b). Previous work on charge-transfer complexes.

(b) 1. Review of optical work. When two substances, one of which (the acceptor) has a strong electron affinity and the other (the donor) which has a zero or negative electron affinity are brought together, either in gaseous or liquid phase, a

molecular complex can be formed in suitable cases, e.g. where there is no chemical reaction. The complex may, therefore, be stable (or semi-stable) and often gives rise to a completely new optical absorption band, which usually has a lower excitation energy than either of the two components separately (see Figure VII 1).

Reid was the first to notice a general parallelism between the triplet-singlet emission spectra of complexes with organic acceptors and donors when irradiated in their complex absorption band, and the triplet-singlet emission spectra of the uncomplexed donor compound (F8, see Figure VII 1). He concluded from his studies that the triplet level of the donor was almost unaffected energy-wise in the complexing process.

Recently Czekalla (F2) investigated complexes of hexamethylbenzene with each of eight different acceptor molecules in turn. He showed that the charge-transfer absorption band of the complex decreased in energy (i.e. underwent a red-shift) as the electron affinity of the acceptor increased, and also that the fluorescence emission spectra also underwent a similar red-shift, so that in each case the energy relationship between the absorption and emission bands was maintained. There seems little doubt that the fluorescent emission is from a charge-transfer singlet state. For the particular complexes of the type aromatic hydrocarbon (e.g. naphthalene) - tetra-chloro-phthallic-anhydride (T.C.P.A.), Czekalla found that it was possible to distinguish,

after excitation in the charge-transfer absorption band, two emission spectra, one the mirror image of the charge-transfer absorption ($\tau = 10^{-9}$ sec.) and the other corresponding to the phosphorescence of the aromatic hydrocarbon (with a reduced life-time). Since it was not possible to stimulate the phosphorescence of the uncomplexed donor substance at this wavelength (see Figure VII 1), his theory that "absorption in the charge-transfer band is followed by either the converse emission or intersystem crossing to a dissociative level of the complex which yields the aromatic in its first excited triplet state, leading to the normal aromatic phosphorescence" seemed to be a reasonable interpretation of the mechanism. Work by McGlynn (F3) also endorsed this view.

However, in a later paper, McGlynn (F4) has proposed exactly the opposite point of view. In the example he studied (anthracene-trinitrobenzene (T.N.B.)) he found that the skeletal breathing, symmetric and C-C bond stretching vibrations all have a decreased frequency of some 3%. From his experimental work, he was therefore compelled to conclude that "the excess energy of the dissociative triplet is dissipated and that reformation of the complex occurs in its excited triplet state in a time shorter than the lifetime of the triplet of free anthracene."

(b) 2. Charge-transfer theory. The theory of charge-transfer absorption is based on the work of Mulliken (F12) who considered

the interaction of a no-bond ground state $\psi_0(D,A)$ and a polar excited state $\psi_1(D^+ - A^-)$ to produce a stabilized ground state

$$\psi_0' = \psi_0(D,A) + \lambda\psi_1(D^+ - A^-)$$

and an excited, charge-transfer state

$$\psi_1' = \psi_1(D^+ - A^-) + \mu\psi_0(D,A) \qquad [\lambda,\mu \ll 1]$$

Mulliken used these wave-functions to calculate the charge-transfer transition moment. In many applications, the experimental results obtained were consistent with the theoretical predictions, but in others it failed. For example, the theory predicts that the stability of the complex should increase linearly with the intensity of the charge-transfer band, but in practice, for most series, a decrease is found to take place.

Murrell (F11) has proposed an alternative explanation whereby the intensity of the charge-transfer bands is derived from excited states of the donor or acceptor, and is dependent on the intensity of the absorption bands of the acceptor and/or donor. According to this theory, an electron is transferred from an excited orbital of the donor (d^*) to an excited orbital of the acceptor (a^*). (A similar state exists if a (d) electron is transferred to an (a^*) orbital or a (d) electron to an (a) orbital.)

Since the "starred" orbitals occupy a greater volume than the "unstarred", it can be seen qualitatively that the (d^*a^*)

overlap might be quite large. A combination of energy and overlap considerations suggests that the charge-transfer state almost certainly takes on more donor excited-state character than ground-state character. It may have more acceptor excited state character also.

The e.s.r. data presented later shows clearly that in the complexes studied the donor excited-state is distorted, in agreement with this latter theory.

(b) 3. E.S.R. studies. As far as the author is aware there is no report of e.s.r. studies on aromatic hydrocarbon -T.C.P.A. complexes.

Some work has been done on other charge-transfer complexes, which showed e.s.r. absorption in the ground state (e.g. see (X a)) for some substances studied by the author).

Bijl (D5) has reported on an extensive series of biradical molecular compounds in powder form. These particular complexes were formed from a range of phenylene diamines (donors) with halogenated quinones (acceptors). It was found that the concentration of the paramagnetism in the complexes generally increased with the strength of the donor-acceptor tendency, and that the spin-concentration was independent of temperature. In these particular complexes, the e.s.r. absorption was thought to arise from a ground-state triplet but only $dM = 1$ transitions were observed.

Other workers have reported e.s.r. resonances from perylene-iodine, perylene-o-chloranil and carbazole-chloranil (D4). In the carbazole complex, the e.s.r. signal was shown not to be directly associated with the donor-acceptor pair, but confined to the solid state.

The resonances observed by the above authors were all of the $\Delta M = 1$ transition, observed at the free spin value, and are unrelated to the type of complex discussed in this thesis.

In the experimental work mentioned in this chapter, the resonances observed were due to the $\Delta M = 2$ transition of the triplet state. Such "half-field" resonances are very useful in e.s.r. studies since they enable an unambiguous interpretation of the cause of the resonances to be made.

VII (c). Choice of suitable complexes. Czekalla (F1, F2) has listed the following hydrocarbons as forming complexes of the type to be discussed in this chapter:- durene, hexamethylbenzene, naphthalene, phenanthrene, anthracene, coronene and 1,2-benzanthracene. Of these substances, however, only naphthalene, phenanthrene and coronene have a lifetime suitable for the spectrometer (VI (c); e.s.r. of durene has not been observed.)

The original work also listed several acceptors:- di-chloro-phthallic-anhydride, tetra-chloro-phthallic-anhydride (T.C.P.A.), tetra-bromo-phthallic-anhydride (in order of

Data on T.C.P.A. complexes.

Phosphor.	abs.	fl.	phos.	τ sec.	$\frac{Q_{ph.}}{Q_{fl}}$	ε
Naphthalene.	3100A. E1. l.w.l.	3300 A. E23. max.	4750A. F1. S.W.l.	E4 2·5	E4 ·1	
Naphthalene-T.C.P.A.	3600A. F1. max	4400A. F1. max.	red shift. 100A.	F1 1·6	F5 [·5]	F5 1000 max.
Phenanthrene	3500A. E1. l.w.l.	3470A. E3. S.W.l.	4600A. E3. S.W.l.	E5 3·3		
Phenanthrene-T.C.P.A.	3480A. F1 max.	4650A. F1. max.	red shift 440A.	F1 1·8		
Coronene	4300 A. E1. l.w.l.		5300A. E50. S.W.l.	E50 9		
Coronene-T.C.P.A.	3900 A. F5. max.			F1 5·1		

l.w.l./s.w.l. = long/short wave limit.

Figure VII 2

E.S.R. absorption data for TRIPHENYLENE.

Ref.	Solvent.	Temp.	Conc.	D/hc cm^{-1}	Line-width. oe.
	Alphanol 79	90K.	·003M.	·1358 ± ·0015.	16 ± 1.
A5.	Alphanol 79.	~77K.	~·003M.	·1353 ± ·0015.	18.
A9.	E.P.A.	~77K.		·1353 ± ·0015	7·9 ± ·7
B1.	theoretical.			·081	

$D^* = D$ (symmetric molecule.)

Figure VII 3

increasing acceptor strength.) It was decided to try these experiments with T.C.P.A. as it alone of these acceptors is commercially available. In addition, more optical data was available for complexes using T.C.P.A.

Optical data on the three complexes chosen is given in Figure VII 2. Data on T.C.P.A. is given in Figure VII 1 and Appendix 6.

VII (d). Presentation of Data. Before going on to consider the experimental work which was done, it is necessary to outline the quantities which were measured in the e.s.r. experiments. These have been mentioned before (III (k) 1) as line-width, line-shape (including h.f.s.) and g-value. The line-width and line-shape were dealt with in the manner discussed in (III (k) 1), but the "g-value" measurement was not made, and a quantity known as $\underline{D}^{*}$ was found instead. The derivation of this quantity is discussed in the following section, and the practical relevance of $\underline{D}^{*}$ is emphasized.

(d) 1. Derivation of $\underline{D}^{*}$. The theory of e.s.r. absorption in crystals has been dealt with in (II (c) 2). For the case of molecules possessing two spins (i.e. a spin 1 state) Griffith has shown that the behaviour of the energy levels can be described by the spin Hamiltonian:-

$$\mathcal{H}_s = g\beta \underline{H}.\underline{S} + DS_z^2 + E(S_x^2 - S_y^2) \qquad (7.1)$$

where D and E are the fine structure constants and the S_i are components of the spin vector. The energy levels and their transition probabilities have been calculated (B10).

de Groot and van der Waals, after their discovery of the forbidden transition in naphthalene, coronene etc., presented a detailed development of the above Hamiltonian when applied to these substances (A5). They considered the transition probabilities when the microwave magnetic field was both parallel and perpendicular to the static magnetic field. The transition probabilities were determined as functions of the random orientation of the spin vector. When the microwave magnetic field is perpendicular to the steady magnetic field (the arrangement used by the author) their work showed that a single peak, with the observed asymmetry, should be detected. In a first derivative presentation, this asymmetry leads to a sharp peak on the low field side, denoted as H_{min} (see Figure VII 13). For the case of $E \ll D$ and provided that $D/h\nu < \frac{2}{3}$, H_{min} is given by the relation

$$D^* = \left[D^2 + 3E^2 \right]^{\frac{1}{2}} = 3\left[\tfrac{1}{4}(h\nu)^2 - (g\beta H_{min})^2 \right]^{\frac{1}{2}} \qquad (7.2)$$

In many recent papers by American authors, it appears to have become customary to express the values of D^*, D and E in units of cm^{-1}. These units are dimensionally incorrect and D^*, D and E should be divided by hc before they can be expressed in these

units. In the present text, the notation $\underline{D}^{*}$, $\underline{D}$ and $\underline{E}$ has been used to denote this division.

One of the most useful aspects of the work on organophosphors has been the use of the experimental results obtained as end points for theoretical calculations, enabling various orbital waveform functions to be tested. In calculations of the dipolar interaction, the r^{-3} dependence, however, causes difficulties in the correct evaluation.

McConnell has shown that the Pauli Exclusion Principle confines electrons of parallel spin to orbitals which are anti-symmetric in their space variables. The perturbation energy which has to be evaluated is

$$\int \psi_T \mathcal{H}_S \psi_T \cdot d\tau \qquad (7.3)$$

with

$$\psi = \left[a(1)b(2) - b(1)a(2)\right]$$

In this case, a and b are the p_z orbitals of the two carbon atoms which have a bond axis in the z-direction.

The parameters D and E are expressible in terms of the expectation values

$$D = -\frac{3}{4}\frac{g^2\beta^2}{hc}\left\langle \psi \left| \frac{3z_{12}^2 - r_{12}^2}{r_{12}^5} \right| \psi \right\rangle \qquad (7.4)$$

$$E = -\frac{3}{4}\frac{g^2\beta^2}{hc}\left\langle \psi \left| \frac{3(x_{12}^2 - y_{12}^2)}{r_{12}^5} \right| \psi \right\rangle \qquad (7.5)$$

E.S.R. experiments conducted on aromatic/tetra-chloro-phthallic-anhydride complexes.

Exp.No.	Phosphor.	Solvent.	Concentration. Phosphor/T.C.P.A.	Sample size.	Lamp.	Filter.	Comments.
1	Naphthalene/Benzophenone	iso-Propyl-ether/iso-Pentane.	·01/·01M.	S1.	HIGH PRESSURE.	F.C.2.	An E.S.R. absorption line was observed in each experiment at H~ 1500 oe. ν ~ 9300 Mc/s.
2	"	" " "	·05/·05M.	S1	"	"	"
3	Naphthalene-T.C.P.A.	di-Ethyl-ether.	·005/·005M.	S2.	"	"	"
4	"	Toluene.	·02/·01M.	S1.	"	"	"
5	"	di-Ethyl-ether.	·005/·001M.	S2.	"	"	"
6	"	Toluene.	·05/·01M.	S1.	"	"	"
7	Coronene.	Ethanol.	·001M.	S2.	"	F.C.3.	"
8	Coronene-T.C.P.A.	Toluene.	·003/·003M.	S1.	"	F.C.2.	"
9	Phenanthrene.	iso-Propanol.	·005M.	S2.	"	F.C.3.	"
10	Phenanthrene-T.C.P.A.	" "	·005/·005M	S1.	"	F.C.2.	"
11	"	" "	·005/·0025M.	S2.	"	F.C.2&3.	"

Figure VII 4

Since the zero-field splitting is thus the result of first order anisotropies in the electron correlations, current theoretical work has been directed towards predicting the known values of $\underline{D}$ and $\underline{E}$.

In the preceding paragraphs, an experimental method of accurately determining $\underline{D}^{*}$ has been discussed, and the relationship which $\underline{D}^{*}$ bears to the actual spin orbit has been emphasized. Thus it can be seen that a measurement of $\underline{D}^{*}$ (or changes in $\underline{D}^{*}$) may be a great help in determining the spatial location of the orbit of the spin (or changes in it).

In this situation, therefore, measurements of $\underline{D}$ and $\underline{E}$ are of considerably more practical significance than a measurement of g. The very long lifetime (τ) of the metastable state is a clear indication that lattice interactions with the electron must be small. Thus a g-value very close to the free-spin value can be expected (see A1); a measurement of the g-value is therefore unlikely to be significant. The strong dependence of $\underline{D}$ on the z-coordinate and of $\underline{E}$ on the x-y plane is an important point and has been used in the interpretation of the data presented later in this chapter.

VII (e). E.S.R. work. The author carried out six different experiments which are listed in Figure VII 4. The substances were first checked optically to ensure that complexing was in fact taking place. The phosphorescent decay was measured using

Figure VII 5. Oscilloscope traces of visible emission from various substances.

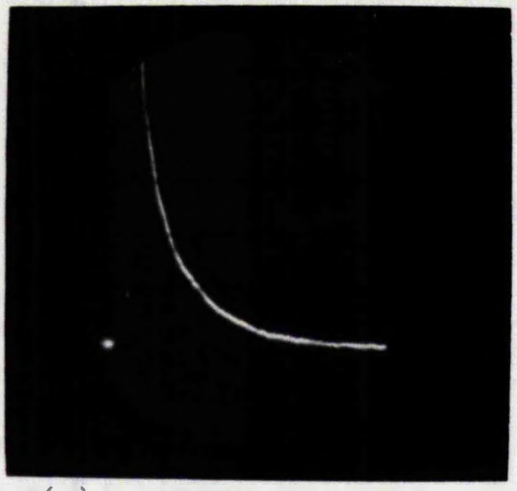

5(a).
Phosphor : naphthalene-T.C.P.A.
Solvent : iso-propyl-ether.
(Y-scale : 2v./grat. div.)

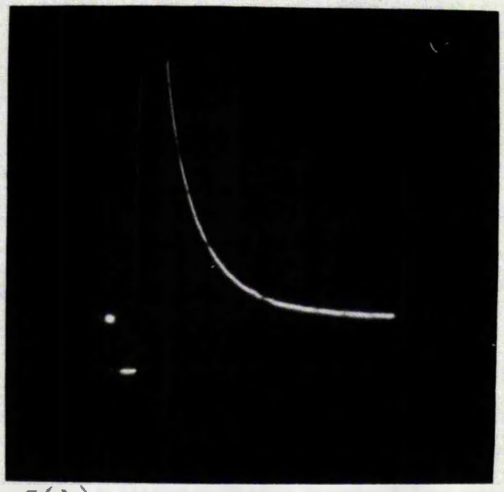

5(b).
Phosphor : naphthalene-T.C.P.A.
Solvent : toluene.
(Y-scale : 5v./grat. div.)

In (a) - (f) are shown the phosphorescent emissions from various organo-phosphors. The samples were all irradiated at 77°K with 3660A light. The X-scale is approx. 11 secs. (total).

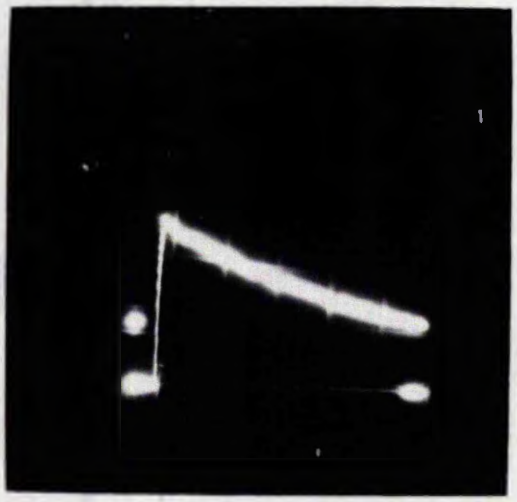

5(c).
Phosphor : coronene.
Solvent : ethanol.
(Y-scale : 5v./grat. div.)

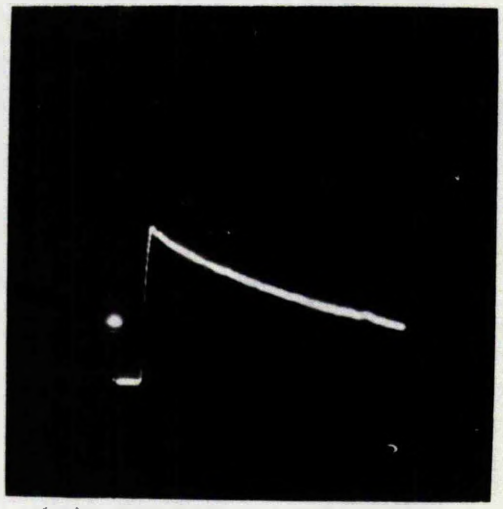

5(d).
Phosphor : coronene-T.C.P.A.
Solvent : ethanol
(Y-scale : 5v./grat. div.)

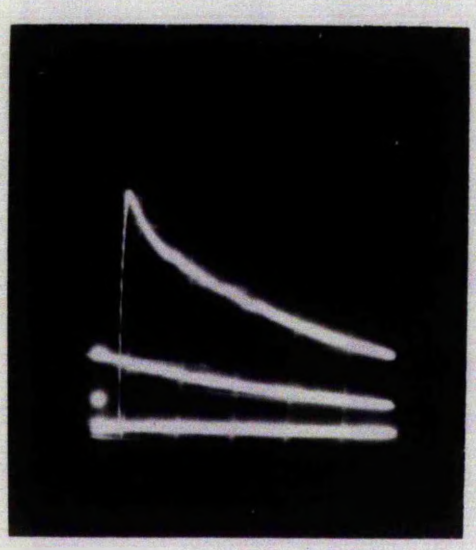

5(e).

Phosphor : coronene.

Solvent : toluene.

(Y-scale : 10v./grat. div.)

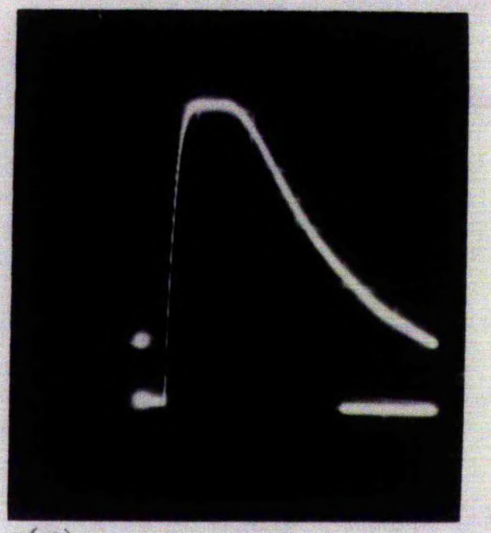

5(f).

Phosphor : coronene-T.C.P.A.

Solvent : toluene

(Y-scale : 10v./grat. div.)

5(g).

Triboluminescence of uranyl nitrate hexahydrate.

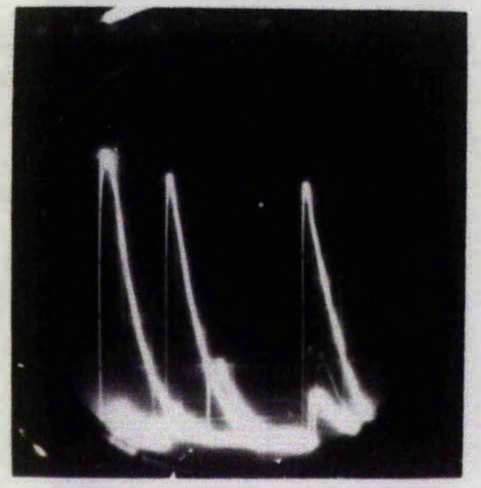

Sample warming up from 77°K.

X-scale : .025 sec. (total) (approx.)

5(h).

Thermoluminescence of diPotassium uranyl nitrate.

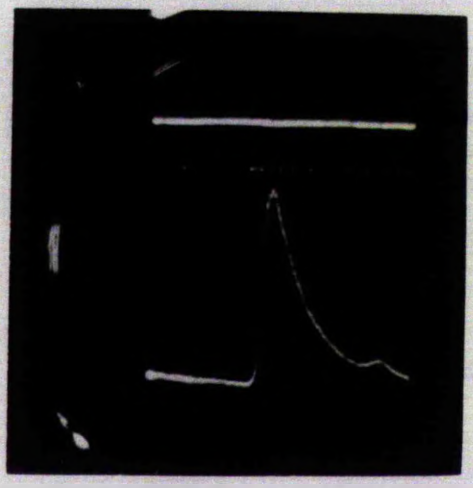

Sample warming up from 77°K.

X-scale : 2 minutes (total).

(the dots represent temperature calibration points.)

the apparatus discussed in (V (c)), and some of the photographs taken are shown in Figure VII 5. The details of these photographs are explained in VII (g) 3.

The e.s.r. experiments were carried out at a temperature of 1.6°K, in contrast to those previously reported by other authors which have all been done at 77°K or above (with one exception). For this reason, it was therefore necessary to examine both the pure and the complexed substances. The e.s.r. observations which were made from the various experimental data are:-

i) Temperature variation of $\underline{D}^{*}$ for the uncomplexed substance. (VII (g) 1).

ii) Temperature variation of linewidth for the uncomplexed substance. (VII (g) 2).

iii) Determination of the existence of an e.s.r. absorption signal from the complex on irradiation in the charge-transfer band. (VII (g) 3).

iv) Variation of $\underline{D}^{*}$ between the complexed and uncomplexed substances. (VII (g) 4).

v) Variation of line-width and line-shape between the complexed and uncomplexed substances. (VII (g) 5).

vi) Variation in line-width due to various acceptor-donor concentration ratios. (VII (g) 6).

It must be emphasized that in most cases the experiments

listed were duplicated, and that in every case the results quoted are drawn from a series of pen-recordings.

In the case of naphthalene, the glass dewars do not permit irradiation in the absorption band; benzophenone was therefore used as an energy transferring agent (VI (f) 2). With phenanthrene and coronene, it was possible to stimulate the phosphorescence using the glass dewars.

VII (f). Accuracy of the measurements of line-width and D^{*}.

Line-width. The error in the measured line-width has been discussed in (III (k) 1). With these particular samples, the asymmetrical line-shape means that it is more difficult to determine the position of the high-field maximum than that of H_{min}. The total error, including the correction for K-factor, for a 20 gauss line, is estimated to be ± 1 gauss.

D^{*}. The error in D^{*} is part absolute and part random. The absolute error is caused by errors in the magnetic field and frequency calibrations. The error in the magnetic field is ± 3 gauss, while that in frequency is ± 1 Mc/s. Random error occurs in reading the wavemeter scale, ± 1 Mc/s., and in determining the position of H_{min}, ± 1 gauss. (The value of H_{min} is found in the same manner as is the g-value (III (k) 1).) The spectrum must also be corrected for field-shift of the H_{min} peak (III (k) 2), since otherwise it leads to an absolute error.

For the values of field, frequency and $\underline{D}^*$ used in these experiments:-

an error of ± 5 g. leads to an error in $\underline{D}^*$ of ± .002 cm^{-1}.

" " " " 4 g. " " " " " " " " .0015 cm^{-1}.

" " " " 1 " " " " " " " " .0004 cm^{-1}.

" " " " 1 Mc/s." " " " " " " " .0001 cm^{-1}.

For this spectrometer, therefore, the total error in $\underline{D}^*$ may be ± .0015 cm^{-1}. In those experiments where only changes in $\underline{D}^*$ are considered, the error is somewhat less, but due to the method of field calibration the error may be not less than ± .0010 cm^{-1}.

Since the value of $\underline{D}^*$ can be compared with other published results, a control experiment was carried out. Triphenylene in Alphanol 79 (a commercially available mixture of primary alkanols) was used to obtain a direct comparison with a similar experiment by de Groot and van der Waals. The results are given in Figure VII 3, and show very close agreement.

In Figures VII 7 and 8, it will be noticed that the values of $\underline{D}^*$ obtained by Foerster (A18) are .004 cm^{-1}. less than those obtained by other authors - this seems to be due to an error in his field calibration, and these values have been disregarded for this reason. It will be noted also that some other authors quote an error of ± .0002 and .0004 cm^{-1}. for their measurements, - in the present author's opinion these values seem to be optimistic.

D^* & Linewidth measurements for NAPHTHALENE.

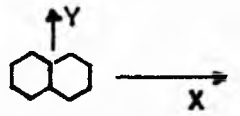

Exp. No.	Ref.	Sample.	Solvent.	Temp.	Conc.	$\underline{D}^* = (\underline{D}^2 + 3\underline{E}^2)^{1/2}$ cm.$^{-1}$	Line-width. oe.	Mod oe.
	A9.	Naphthalene.	E.P.A. & Methanol.	77K.		·1049 ± ·0015.	[11·2 ± ·7.]*	—
	A5.		Alphanol 79.	77K.	~·02M.	·1050	22 ± 1.	7·1
	A19.		Lucite.	77K.		·1063 ± ·0004	14·1	—
	A1.		Durene crystal.	77K.	~·02M.	$\underline{D}$ = ·1008 ± ·0007. $\underline{E}$ = ·0138 ± ·0002.	~20.	—
	A20.		Durene crystal.	77K. 4·2 1·7	~1·5M %	$\underline{D}_{77}$ = ·0995 $\underline{D}_{4\cdot2}$ = ·1049	17 $(H_0 n^l z)_{4°K}$	15·
	B1.		theoretical.			·1029		
1&2.			iso-Propanol / iso-Pentane.	1·4K.	·01 & ·05	·1079 ± ·0015.	20 ± 1.	9
3		Naphthalene - T.C.P.A.	di-Ethyl-ether.	1·6K.	·0005	·1217 ± ·0015.	29 ± 1.	6·5

$\underline{D}^* = D^*/hc$. etc. *see text

Figure VII 6

D^* & Linewidth measurements for PHENANTHRENE.

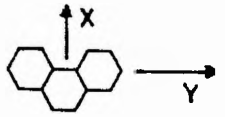

Exp No.	Ref.	Sample.	Solvent.	Temp.	Conc.	$D^* = (D^2 + E^2)^{1/2}$ cm^{-1}	Line-width. cm	Mod
	A9.	Phenanthrene.	E.P.A. or Methanol.	77K		·1335 ± ·0015	[12·2 ± ·7]*	—
	A18.		iso-Propanol.	77K.		[·129]*	[21]*	—
	A19.		Lucite.	77K.		·1336 ± ·0004	17 5	—
	A11.		Biphenyl.	77K		D = ·10044 ± ·00002. E = ·04657 ± ·00002		—
	B1.		theoretical.	77K		·1000		
9			iso-Propanol.	1·6K	·005M	·1392 ± ·0015	15·2 ± 1	6·5
10.		Phenanthrene-T.C.P.A.	iso-Propanol.	1·6K	·005M	·1442 ± ·0015	16·3 ± 1	8

D^* D^*/hc. etc. *see text

Figure VII 7

D^* & Linewidth measurements for CORONENE.†

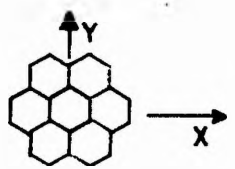

Exp. No.	Ref.	Sample.	Solvent.	Temp.	Conc.	$\underline{D}^* = (\underline{D}^2 + 3\underline{E}^2)^{1/2}$ cm^{-1}	Line-width oe.	Mod.
	A9.	Coronene.	E.P.A. & Methanol.	77K.		·0971 ± ·0015.	[7±·7.]*	—
	A5.		Alphanol 79.	77K.	~·0005.	·097	14±1.	7-12
	A18.		Hexane & iso-Propyl-ether.	77K.		[·093.]*	unusual line shape. no textual comment	—
	A19.		Lucite.	77K.		·0983 ± ·0004.	9·5.	—
	B1.		theoretical.			·0522.		
7.			Ethanol.	1·6K.	·001M	·1030 ± ·0015.	12±1.	6·5
8.		Coronene-T.C.P.A.	Toluene.	1·5K.	·003M	·1044 ± ·0015.	28±1.	6·5

† since Coronene is symmetrical in the X & Y axes theoretically $E \equiv O$, so $D^* \equiv D$.

$\underline{D}^* = D^*/hc$. etc.

*see text

Figure VII 8

VII (g). Discussion of the experimental results obtained.

The D^* and line-width measurements for the six experiments, namely:- naphthalene, naphthalene-T.C.P.A.; phenanthrene, phenanthrene-T.C.P.A.; coronene, coronene-T.C.P.A. are given in Figures VII 6, 7 and 8. The solvents and the operating conditions used are also given. For comparison, the values obtained by other authors are also listed.

(g) 1. Temperature variation of D^* for the pure substances.

The values obtained for D^* at 1.6°K for coronene and naphthalene are plotted on Figure VII 9. Also shown on this figure are the values obtained by Thomson (A19) for these substances at various temperatures between 77° and 300°K. (Thomson's values were obtained using lucite as the host matrix, and have been corrected here to agree with the values obtained when a glassy solvent is used). The present work confirms that the slight increase in D^* with decrease in temperature is continued down to very low temperatures. It is clear that D^* does not level off to a steady value between 77° and 1.6°K, as has been suggested (see below).

The value obtained for naphthalene is in agreement with data recently published by Hornig and Hyde (A20), who have measured D at 77°K and 4°K, in a naphthalene-durene crystal. These authors quote an increase in D of 1%, but unfortunately do not quote the E variation.

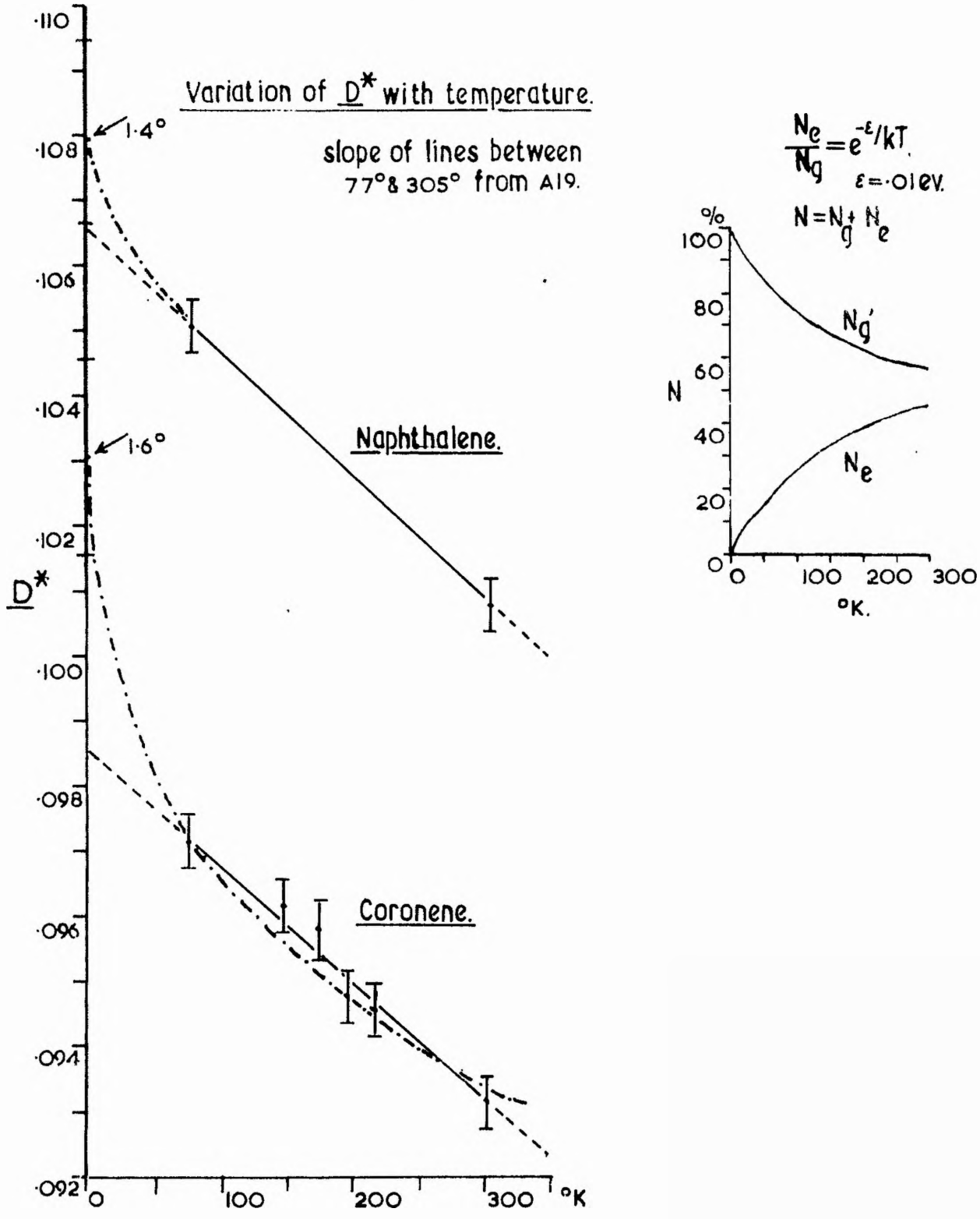
Variation of D* with temperature.
slope of lines between
77°& 305° from A19.
1·4°
1·6°
Naphthalene.
Coronene.
D*
·110
·108
·106
·104
·102
·100
·098
·096
·094
·092
0
100
200
300
°K
$\frac{N_e}{N_g} = e^{-\varepsilon/kT}$
ε=·01ev.
N=Ng+Ne
%
100
80
60
40
20
0
N
Ng'
Ne
0
100
200
300
°K.

Figure VII 9

The cause of this increase in $\underline{D}^*$ is still obscure, and several suggestions have been put forward. Thomson, for example, suggests that the variation is due to the decrease in population of higher vibrational levels as the temperature falls. Qualitatively, this would lead to a decrease in the average distance between the unpaired electrons and thus to a larger value of $\underline{D}$ and $\underline{E}$. The possibility of vibrational levels being depopulated has also been postulated from optical work, where it was found that the decay curve of the emission from some phosphors at 77°K was not strictly exponential (E75). The present measurements, however, at 1.4°K, disprove this theory as causing an increase in $\underline{D}^*$ for the following reasons:-

If the triplet vibrational levels were populated, the electrons in each level would obey a Boltzman distribution, i.e. $N_u/N_l = \exp(-\epsilon/kT)$. For a vibrational level with $\epsilon = .01$ ev., the fraction of electrons in each level has been plotted as a function of temperature in Figure VII 9. At 300°K, the number of spins in each vibrational level is approximately the same. The intensity of an e.s.r. absorption is directly proportional to the number of spins present, so that at 300°K, the absorption should consist of two lines of almost equal intensity. In Thomson's theory, these lines are synthesised to form the observed line of 20 gauss width. At 77°K, the ratio between the spin

populations has changed to 4:1, i.e. one of the "observed" lines should have become much less intense, and in Thomson's opinion, this decrease leads to a change in H_{min}, and hence in $\underline{D}^{M}$. The spectrometer, however, is capable of detecting only a very small difference in the absolute number of spins, particularly when the two absorption lines overlap - a ratio of about 5:1 being about the maximum (this statement is demonstrated in VII (g) 6). As a result of this lack of discrimination, if the temperature is lowered any further, the change in spin concentration will have no significant effect on the observed line-shape. In other words, below 77°K, the rate of change of $\underline{D}^{M}$ with temperature should fall to zero. Although a specific value of ϵ has been used in the above discussion, the argument is quite general, the only difference being that if a smaller value of ϵ is postulated, the rate of change of $\underline{D}^{M}$ with temperature will continue to be constant to lower temperatures. The experimental results, particularly for coronene, show that in fact the rate of change of $\underline{D}^{M}$ increases as the temperature falls.

In the present author's opinion, the most reasonable explanation seems to be that the change is due to temperature-dependent lattice interactions. It has been shown by e.s.r. that the electron has some interaction with the solvent (see VII (g) 5), but optical measurements on this problem (e.g. observation on the decay time of the phosphorescence) are rare,

and there seem to be none on glassy solutions at 4°K. All measurements at this temperature have been confined to single crystals (E12). Unfortunately the apparatus for the measurement of decay times could not be used, since the stray illumination from the large glass dewars was too high.

de Groot (A21) has recently observed a similar change in $\underline{D}^*$ on cooling benzene to 15°K, and suggests that this could be due to asymmetry in the benzene bond lengths, so that $\underline{E}$ is no longer zero.

The fact that coronene, which is a much larger molecule physically than naphthalene or benzene, and therefore more susceptible to lattice interactions, shows a greater change in $\underline{D}^*$ is possibly significant in this context (since changes in the quantity $(x^2 + y^2)$ will have a proportionally greater effect); but since there is very little data, it is not possible to draw a definite conclusion. Theoretical results have been included in Figures VII 6, 7 and 8 to show that help from this quarter is unlikely for some time yet.

(g) 2. Temperature variation of line-width of the pure substances. The linewidths of the substances examined are given in Figures VII 6, 7 and 8. As can be seen there, the values obtained in the present experiments for naphthalene and coronene at 1.6°K agree, within the experimental error, with those of de Groot at 77°K. Thus it seems that there is relatively little change

in line-width between these two temperatures. Since the observed line-width is mainly due to unresolved anisotropic components (see VII (g) 5), this result was to be expected.

The variation of line-width of these two substances has been measured recently by Thomson (A19) in the temperature range 77° - 300°K. In the case of naphthalene, he states that the line-width changes "by only 1 - 2%" (in quoting this figure, presumably he measured to an accuracy of .5%, i.e. .07 gauss; the S:N ratio of the signal at 305°K is quoted as 4:1). For coronene (in lucite) he found that the line-width decreased from 9.6 g. at 77°K to 8.4 g. at 305°K. There is no evidence at all of this increase being continued to lower temperatures (the author's values are both less than de Groot's).

The case of phenanthrene does show a decrease in line-width from the value quoted by (A18) of 21 g. at 77°K to 15 g. at 1.6°K in the same solvent. The line-width quoted from (A18) was measured from the published pen-recordings, which were made using a modulation depth of 12 g., which is far too high for a 15 g. line. As can be seen from Figure III 13, this leads to an increase in line-width of some 25%, so that any comparison is of dubious value.

It will have been noticed in Figures VII 6, 7 and 8, that the line-width values quoted by Smaller (A9) are considerably different (about one-half) from those quoted by other authors.

The reason for this discrepancy is that he uses a spectrometer which gives a "second-order derivative" presentation. The values quoted are presumably the half-width of the low-field (sharp) peak. Since he does not mention the magnitude of either of the modulation depths used, it is difficult to estimate what relation these line-widths bear to the customary "first-derivative" line-widths. This discrepancy has not been discussed by other authors who quote and use these results. (See also VII (g) 5).

(g) 3. E.S.R. studies on the complexed substances. For each of the complexes studied, that is, naphthalene-T.C.P.A., phenanthrene-T.C.P.A. and coronene-T.C.P.A., an absorption line was detected. The observed line was quite stable over the period of the experiment.

Details of the values of D^{*} and line-width found for these complexes are given in Figures VII 6, 7 and 8, while the detailed differences between these values and those obtained for the pure substances are discussed in the following sections, (g) 4, 5 and 6.

It must be emphasized, however, that in each case the complex e.s.r. absorption bears a reasonably close relationship to the e.s.r. absorption of the respective donor, i.e. the triplet state of the complex has a large amount of donor character. The changes in D^{*} and line-width, however, do show

that the triplet state of the donor is significantly affected on complexing. Since the e.s.r. technique employed here observes only the excited state of the molecule (and not the combined effect of the ground and excited states as is the case with optical techniques), the observed change in the e.s.r. absorption spectrum on complexing indicates that the triplet state in these complexes cannot be dissociative as Ozekalla suggested (VII (b) 1), but must be associative as suggested by the later work of McGlynn.

In none of the phosphors was a line observed which could be attributed to strong complexing, such as was mentioned in (VII (b) 3). Such a line was not expected since Ozekalla (F2) gives the acceptor strengths as:-

T.C.P.A. < T.N.B. < dichloroquinone < chloranil < (dichloro-dicyano-quinone), which indicates that T.C.P.A. is a fairly weak acceptor.

No absorption line, other than that attributed to the $dM = 2$ transition of the complexes was found when the samples were irradiated (except that discussed in VIII (a)).

Although a careful check was made, in none of the experiments was an e.s.r. absorption attributable to T.C.P.A. noted. Since the value of H_{min} for each of the complexes is appreciably different, there is no possibility of the resonances which were observed being partly due to this cause.

(g) 3.a. Saturation. The e.s.r. spectra were checked for saturation, by reducing both the light input and the microwave power level. There was certainly no optical saturation and, as far as could be ascertained, no microwave saturation. (A6B; see Ch. XI). Due to the method of Kl.A.F.C. stabilization adopted it is unfortunately not possible to obtain a very wide range of microwave power input ($\sim$ 10 db down on the 7mW. normally incident on the sample is the minimum consistent with stable Kl.A.F.C. operation).

In principle, at least, it should be possible to check for e.s.r. saturation using equation 6.1. Evaluation of this equation is, in the case of these phosphors, rather difficult. Since naphthalene-T.C.P.A. is the complex about which most information is available, it will be used as an example.

The L.H.S. ($\phi.A.\tau$) of equation 6.1 will be considered first. ϕ (= 2.10^{17} quanta/sec.) and τ (= 1.5 sec.) are known but A has to be estimated. A is the product of the absorbing power of the sample and the ratio of phosphorescent to fluorescent emission for the stimulated electron.

The absorption of the sample is given by $(1 - 10^{-\epsilon cd})$, where ϵ is the molar extinction coefficient, c the concentration in gram mol./litre, and d the thickness traversed by the light. Values of ϵ are difficult to obtain for molecular complexes since ϵ is no longer an independent function, but is concentration

dependent. By taking a series of results over varying donor-acceptor concentrations, using a Benesi-Hildebrand plot (F10), a value of ϵ can be found (F7, F9).

With ϵ = 800 at 3600A, c = .005M and d = .6 cm. (the conditions in exp. 3) almost all the incident light is absorbed. If the product is less than this value, the fraction absorbed falls off rapidly (T12). (Not every donor molecule in an equimolar solution will necessarily be complexed - Czekalla quotes 50%).

The value of Q_{phos}/Q_{fl} for the complex, when irradiated in the complex absorption band, has not been published, although Czekalla has remarked (F2) that the ratio seems similar to that for pure naphthalene (~.1). The value published by McGlynn (F5) was measured using light well within the absorption band of pure naphthalene and the value of Q_{fl} was found at 3200A. This value is, therefore, not comparable. It should also be pointed out that in using the Q_{phos}/Q_{fl} ratio to determine the fraction of the absorbed light entering the triplet state any spins which may return to the ground state by a radiationless transition from the metastable state are ignored, although de Groot (A7) has found that both optical and e.s.r. signals of various aromatic substances have the same decay times.

Combining all the quantities mentioned above, the L.H.S. is found to equal approximately $3\ 10^{16}$ spins.

The R.M.S. is also difficult to evaluate accurately. W (= 29 g) and S (including K-factor correction = 35:1) are straightforward, but the value of N to be used needs some consideration. The basic value is 10^{10} spins (after correction for the differences in mod^{n}. depths used is considered (Figure III 14)), but while the e.s.r. absorption used to calibrate the spectrometer was D.P.P.H., the complex line is non-Lorentzian and is related to the dM = 2 transition, not the dM = 1.

The effect of the non-Lorentzian line-shape is difficult to estimate, but a factor of 5 may cover it reasonably well. With regard to the dM = 2 transition, the spin population (assuming a Boltzman distribution is obeyed) is divided among the three levels in the proportions given by

$$N_i = \frac{N \exp(-E_i/kT)}{\sum_{j=1,2,3} \exp(-E_j/kT)} \qquad (7.6)$$

Since zero-field splittings affect the energy level distribution, it cannot be assumed that the energy difference between the + 1 and 0 spin states is equal to that between the 0 and - 1 states. Without going into the matter in greater detail, since the accuracy required does not warrant it, it appears that in the case of naphthalene the sensitivity should be reduced by a factor of 2. (see A1).

A further consequence of the dM = 2 transition is that the - 1 to + 1 spin transition is not fully allowed, unlike the D.P.P.H. transition which is (f ~ 1). de Groot has indicated that for the dM = 2 transition f ~ .01.

When all the above factors are taken into account, it is found that the R.H.S. equals approximately 10^{16} spins.

Bearing in mind all the approximations made in this calculation, the discrepancy between the two sides of equation 6.1 is not significant, and seems to indicate that little or no e.s.r. saturation occurred. The above example also illustrates the difficulties involved in trying to estimate beforehand whether or not a particular experiment is feasible.

(g) 3.b. Solvents used. As can be seen, several solvents have been used. Previous work has shown that the effect of the solvent on the measured quantities is very small. Several solvents were used because T.C.P.A. is a relatively insoluble compound in many normally used solvents. The complexes were each checked using the photomultiplier-tube circuit and the decay times compared with a reference using iso-propyl-ether as the solvent (F1). The intensity of any phosphorescence of the T.C.P.A. alone was also measured to ensure that it had no significant effect on the complex decay curve (see Figure VII 1). Examples of the photographs taken are shown in Figure VII 5. 5a and 5b show the increase in emission intensity of the complex using different

solvents (because of the increased solubility of T.C.P.A. in the latter); 5c and 5d show an example in which complexing is inhibited; while 5e and 5f show the effect of complexing on a particular substance. The solvents used in each e.s.r. experiment were those which gave the maximum light emission compatible with the correct decay time for the complex.

In the course of these optical studies, it was found that carbazole also apparently complexed with T.C.P.A., having a decay time of 5.5 sec. when complexed compared with 8 sec. for the pure substance. Unfortunately time did not permit a study by e.s.r. of this particular complex.

(g) 4. Variation of D^* on complexing. As can be seen from Figures 6, 7 and 8, D^* for the complexes was found to differ from the values found for the uncomplexed substances. The actual changes are:-

complex	dD^*
naphthalene-T.C.P.A.	+ .0138 cm^{-1}.
phenanthrene-T.C.P.A.	+ .0050 cm^{-1}.
coronene-T.C.P.A.	+ .0014 cm^{-1}.

In each case the value of D^* shows an increase on complexing, which may be due either to a change in D or E or to a combination of changes in D and E. In the case of coronene, where $E = 0$, the change in D^* is small, and this could indicate that the effect is mainly concerned with the E component.

A consideration of equation 7.4 shows that an increase in $\underline{D}$ would result from a reduction in the electron orbit, while an increase in $\underline{E}$ would result from either a symmetrical decrease or an asymmetrical change in the x-y plane of the electron's orbit. Bernstein (B1) has noted that in the range of distances 1.4 - 2.8 A, $\underline{D}$ and $\underline{E}$ both decrease monotonically at the rate of about 1% (.001 cm^{-1}.) per .01A increase in R_{12} - this implies about .1A change in R_{12} in the case of naphthalene. (See Figure A8.2).

There is also another piece of experimental evidence, based on the optical observations, which suggests a change in $\underline{E}$ rather than $\underline{D}$. When the donor substances are complexed, the 0 - 0 transition of the phosphorescent emission is shifted to a lower wavelength (red-shift). Czekalla has published details of the magnitude of this change for naphthalene and phenanthrene and these values are given in Figure VII 2. Such a red-shift implies that either the triplet orbital level is closer to the ground state (change along z-axis) and/or the triplet level has a different orbit in the x-y plane when complexed as compared with its orbital when it is pure, i.e. the red-shift should indicate a shift in $\underline{D}$ and/or $\underline{E}$ in the e.s.r. spectra.

A critical evaluation of the experimental evidence on the changes in $\underline{D}^{*}$ and red-shift is given in Appendix 8. On the basis of this study there appears, in fact, to be considerable

distortion in the x-y plane.

The next step in this discussion is to consider what physical arrangement of the two interacting molecules would be most likely to produce an x-y plane distortion of the triplet state.

Since the energy transfer between the two molecules must involve an overlap of π-electron orbitals, there are only two possible orientations of the T.C.P.A. molecule with respect to the donor:-

In both, the T.C.P.A. molecule is orientated with its x-y plane parallel to the x-y plane of the donor, but in one case the molecules are separated along the z-axis while in the other, they are separated along the x- or y- axis. Murrell (F11) has shown that both of these positions can lead to π-electron energy transfer.

The question as to which of these orbitals should be considered the preferred one has been discussed by Mulliken (F12). His theory predicts that orientation which involves separation along the z-axis.

When the molecules are in the orientation involving separation along the z-axis, the interaction of the two π-orbitals should lead to a delocalization of the electron in this (i.e. z-axis) direction, i.e. when in this orientation, there should be some decrease in the D component. However,

since the T.C.P.A. molecule is by no means isomorphic with any of the donor molecules, x-y distortion is also likely, and might be expected to be quite large. A significant change in $\underline{D}^*$ is therefore probable, but it is not possible from this argument to predict the sign of the change. In contrast, the other orientation (i.e. that in which the molecules are separated along the x- or y-axes) would provide a delocalization of the x-y plane of the triplet state, but should not significantly alter the z-axis displacement, i.e. it would lead to a change in $\underline{E}$ rather than in $\underline{D}$. Since the area of overlap in the latter case is of necessity rather small, the change in $\underline{E}$ may also be expected to be small.

The e.s.r. studies suggest that the T.C.P.A. molecules line up with their molecular (x-y) planes parallel and directly above (i.e. displaced along the z-axis).

Experimental optical work (polarization and X-ray measurements) has suggested that this is in fact the case for π-electron acceptors (which includes T.C.P.A.). Samples which have been studied in this way include benzene, naphthalene and anthracene in complexes with tri-nitro-benzene; phenol and quinol with benzo-quinone; hexamethylbenzene with chloranil. These samples were crystalline and, as the various authors point out, the molecules are subject to other considerations (such as close-packing) so that this finding is by no means conclusive (F11, F13, F14).

The question of the preferred orientation is continued in the following sections (g) 5 and 6, in which further experimental evidence is discussed.

(g) 5. Variations of line-width and line-shape for the complexed phosphors. In Figures VII 6, 7 and 8, the values for the line-width of the resonance obtained from the various complexes are given. The percentage changes are:-

complexed phosphor	change in line-width
naphthalene	45% (increase)
phenanthrene	6% "
coronene	130% "

These variations do not show any direct relationship with the p^{**} variations discussed in the previous section. However, this is not too surprising, for the variation in line-width is a far less sensitive test than the variation in p^{**}, since the natural line-width of the transition is known to be obscured by anisotropic effects. de Groot, for example, has published pen-recordings of the naphthalene $dM = 2$ transition in a durene crystal (A4), where it can be seen that in certain directions the line-width can be as low as 9 oe. (mod$^{n.}$ 7 oe.). The line-width of 9 oe. has been shown, by deuteration of the phosphor, to be largely due to nuclear magnetic interactions. (In most cases, deuteration of the solvent gave a further reduction, showing that the

triplet orbit is influenced to some extent by the solvent (A23)).

From an analysis of the line-shape of the $\Delta M = 2$ transition based on the theory given by de Groot (A5), it would seem that a second order anisotropy effect determines the observed line-width. This implies that the line-width should be dependent on the magnitude of the zero-field splitting.

de Groot has worked out the line-shape theory in detail only for molecules with $\underline{E} = 0$. The author has found that, for the series: benzene, triphenylene and coronene (i.e. molecules with $E = 0$), the published data obeys the relationship suggested by de Groot's theory, viz. $\underline{D} = k$ [line-width] . $k = [.012\ cm^{-1}/$ gauss] . For molecules where $\underline{E} \neq 0$, the situation becomes very complex, and an estimation of the line-width would demand a knowledge of the absolute magnitudes of both $\underline{D}$ and $\underline{E}$ (B12). It does appear, however, that the line-width depends on $\underline{E}$ in the first order (unlike $\underline{D}^2$) and hence the relative signs of $\underline{D}$ and $\underline{E}$ are important.

Smaller (A21) has also considered this situation, using his own measurements of line-width. Unfortunately, his values are taken from a "second derivative" presentation, and since he was trying to fit them to a theory in which the line-width is defined in terms of the "first derivative" presentation, the lack of correlation which he found is not unexpected.

The changes in line-width, which the author has recorded on complexing coronene and naphthalene are much greater than would be predicted for a change in D alone if one uses the relationship found between benzene, triphenylene and coronene as a guide. This result again could suggest therefore that there is considerable E distortion of the triplet excited state.

Line-shapes of the complexes. Line-shapes are even more difficult to handle than the line-widths dealt with above, and for the same reasons, although (A4) has derived a probable line-shape. A comparison of the pen-recordings given in Figure VII 13, for the various substances before and after complexing with T.C.P.A., shows that in each case the same characteristic form is observed, and there is certainly no radical difference observed.

The observed similarity is an important point, since the uncomplexed line-shape is due to the summation of $\Delta M = 2$ transitions in three dimensions, the complexed line may be assumed to be the result of a similar summation. This conclusion, of necessity, implies that the D and E variations for each individual complexed molecule are the same, i.e. the T.C.P.A. molecules must orientate themselves similarly with respect to the donor molecules. A similar conclusion has also been made from optical studies (F13, F14).

Variation of D^* & Line-width with Concentration.

Exp.No.	Concentration. Naphthalene.	T.C.P.A.	D^* cm^{-1}	Line-width. oe.	Mod^n
3	·005 M	·005 M	1217 ± ·0015	29 ± 1	6·5
4	·02 M	·01 M	·1195 ± ·0015	46 ± 1	9
5	·005 M	·001 M	·1101 ± ·0015	20 ± 1	6·5
6	·05 M	·01 M	not measured accurately.	20 ± 1	9
1	·01 M	—	·1083 ± ·0015	20 ± 1	9
2	·05 M	—	·1079 ± ·0015	20 ± 1	9

Figure VII 10

Variation of D^* & Line-width with Concentration.

Exp.No.	Concentration. Phenanthrene	T.C.P.A.	D^* cm^{-1}	Line-width. oe.	Mod^n
9	·005M	—	·1392 ± ·0015	15 ± 1	6·5
10	·005M	·005M	·1442 ± ·0015	16 ± 1	8
11	·005M	·0025M	·1461 ± ·0020	27 ± 2	6·5

Figure VII 11

(g) 6. A concentration effect observed with the complexes.

In this section, some unexpected results, obtained when the proportion of acceptor to donor molecules in the sample was varied, are discussed. This particular study arose when several experiments on the naphthalene-T.C.P.A. complex gave conflicting results. These results are tabulated in Figure VII 10, and as can be seen they show a quite surprising variation.

The values of $\underline{P}^{x}$ and line-width found in exps. 5 and 6, are obviously directly comparable with those obtained from naphthalene alone, but, as has been stated earlier (VII (e)), it was simply not possible to stimulate the naphthalene phosphorescence since the glass dewars do not pass light of the required wavelength.

Exp. 4 also posed a problem, for here the value of $\underline{P}^{x}$ obtained was comparable to the value obtained from the complex, but the line-width was considerably larger.

The solution was finally found by a close scrutiny of the pen-recordings taken in exp. 4, for they revealed a point of inflexion between the two peaks which is absent in recordings from the other experiments. In these recordings (see Figure VII 13), the noise level is as great as this inflexion, but careful checking of the spectra revealed no correlation whatsoever between the noise peaks in the various spectra, while

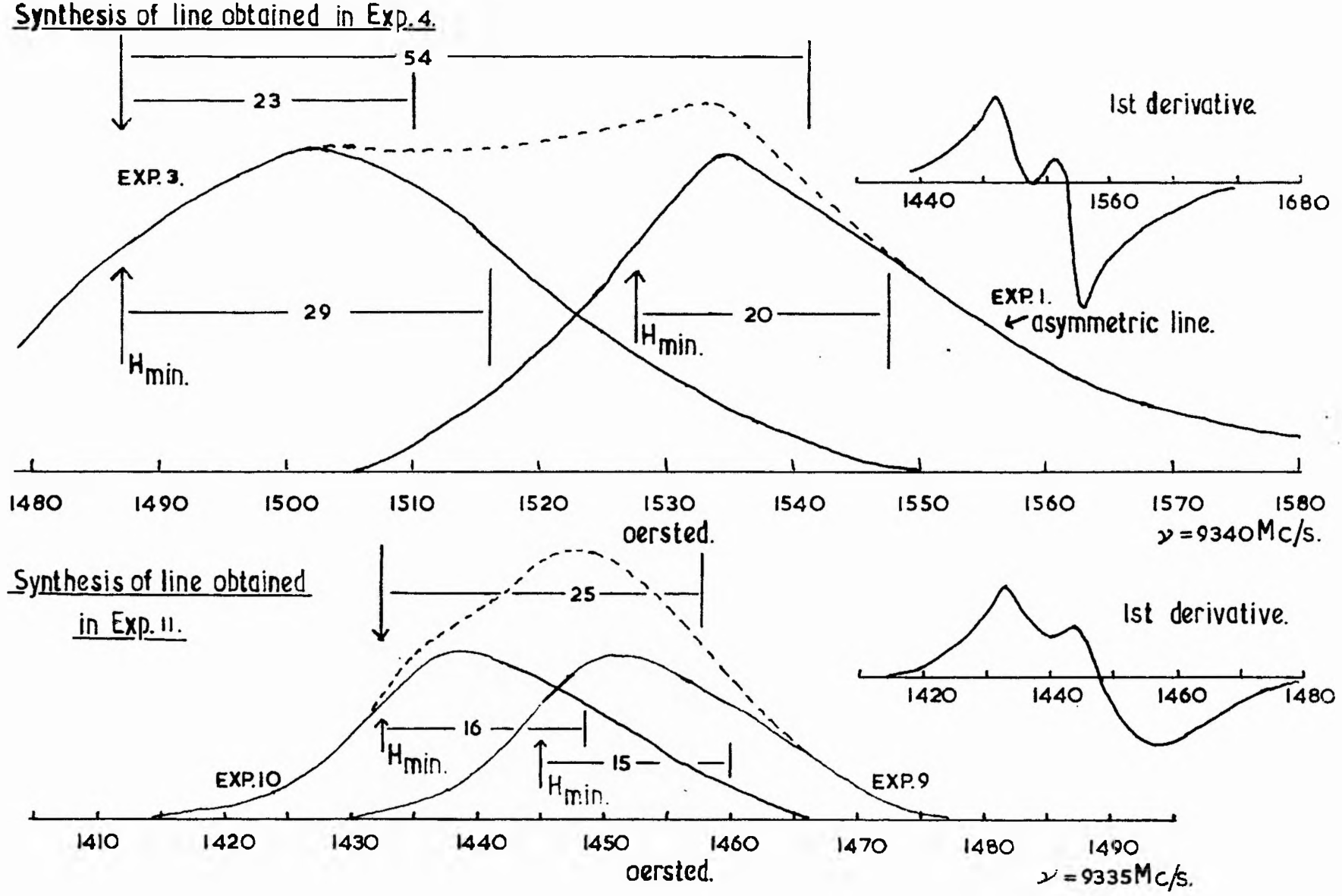

Figure VII 12

there was excellent agreement with the position of the point of inflexion (taken both with the field increasing and decreasing).

This small inflexion suggests that the line which had been observed might possibly be the result of the synthesis of a pure naphthalene line and a naphthalene complex line. In Figure VII 12, both lines have been drawn out, and the combined line-shape found; as can be seen the first derivative of this synthesized line compares directly with the line-shape found in exp. 4. The plot is qualitative only because the low signal to noise ratio obtained for the first derivative curve of the complex in exp. 3 does not permit a very accurate integration to be carried out. However, the essential features found in exp. 3 are reproduced.

An experiment (No. 11) was carried out with phenanthrene-T.C.P.A. to see if a similar situation would arise. The results are shown in Figure VII 11, and a synthesis of the line-shape is given in Figure VII 12. It must be pointed out, however, that since it is possible to excite the phenanthrene resonance using F.C.3, it is also possible that the resonance was stimulated using F.C.2 whose band-pass is quite close - although no such absorption is detectable from the pen-recordings in exp. 10 (see Figure VII 13). (The sensitivity of the apparatus was similar in both cases).

Figure VII 13

These pen-recordings have been selected as typical examples of the spectra obtained in the various experiments discussed in this chapter. Where possible, recordings taken at the same K-value ($\sim .2$) have been selected to help comparison. A fairly high K-value has been used in order to show the complete line-shape as far as possible, and the spectra are arranged so that in each case the magnetic field sweep increases from left to right. The small field sweep (see III (i) 4) was used throughout and the time of the sweep was 2 minutes, so that 1 division of the paper (6.25mm.) corresponds to $\sim$ 30 sec.

Figure VII 13

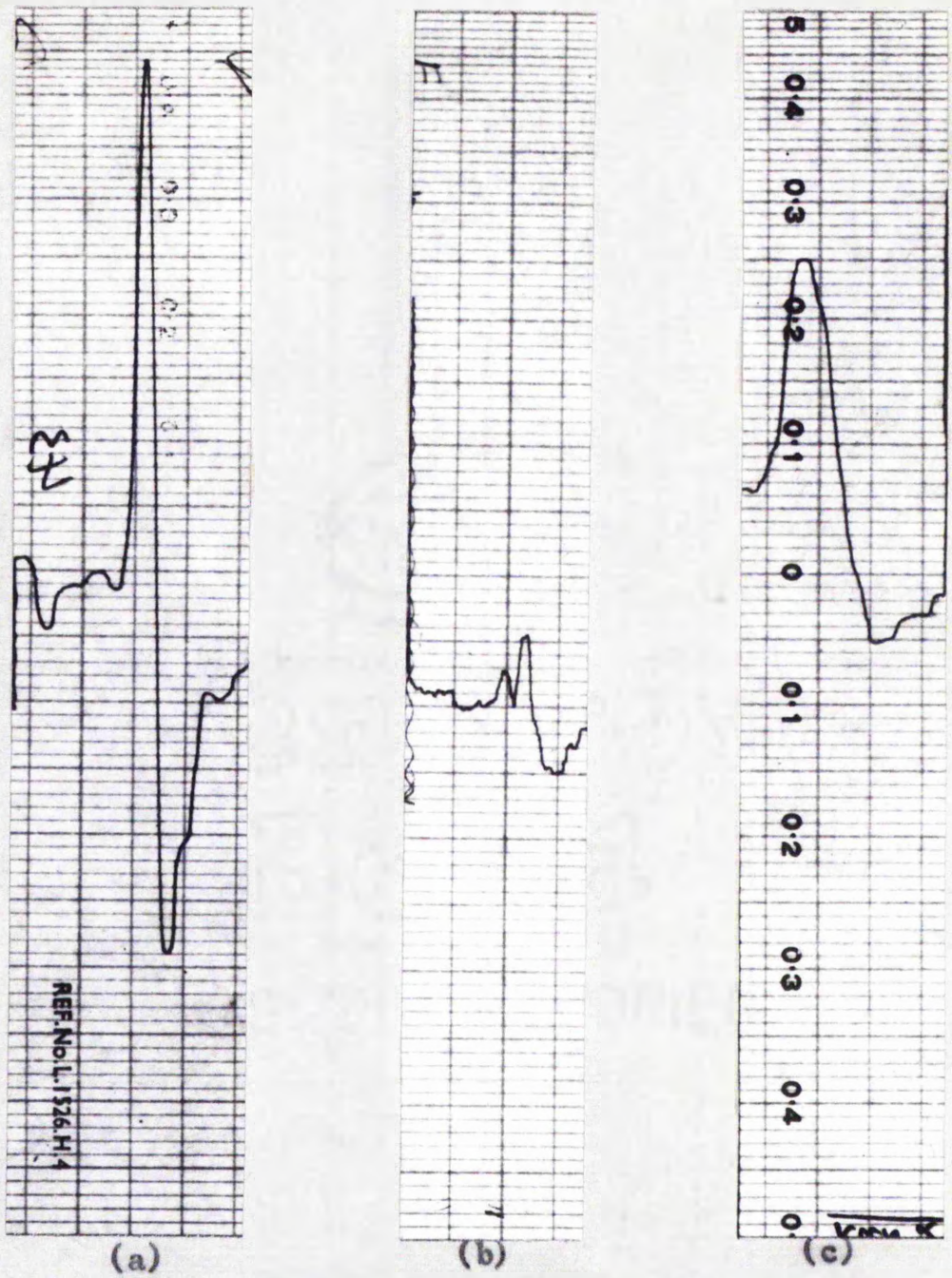

Samples: (a) naphthalene/benzophenone; (b) and (c) naphthalene/T.C.P.A.

For details of the experimental conditions see Figures VII 4 and 6, where (a) is from Exp. No. 2, (b) from Exp. No. 3 and (c) from a repeat exp. of Exp. No. 3. Also for (a), K = .4, dH/dt = 1.62 oe/sec., (see also Figure III 15), for (b) K = .05, dH/dt = 1.62 oe/sec., and for (c) K = .13 and dH/dt = .73 oe/sec.

Figure VII 13

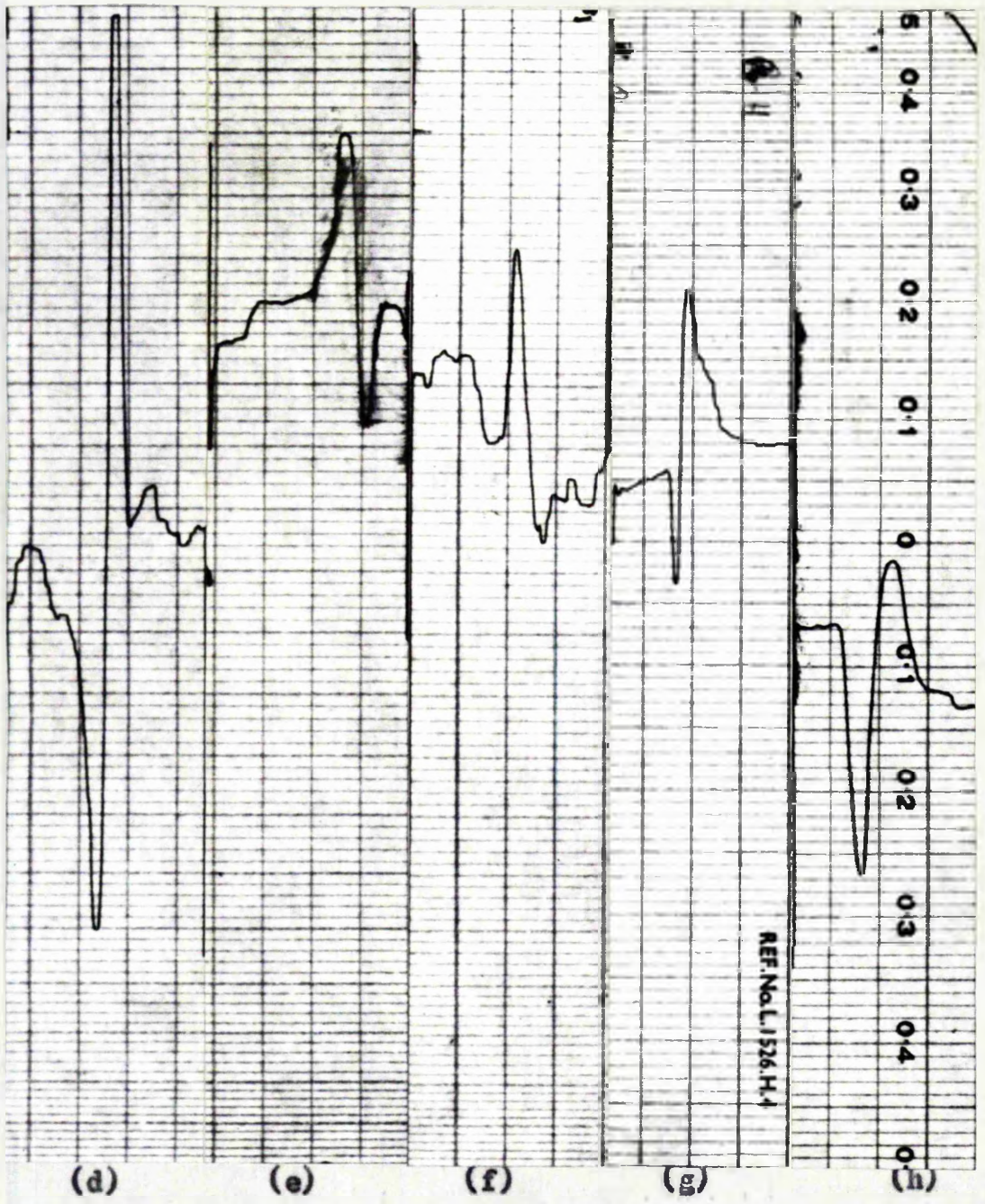

Samples: (d) phenanthrene (Exp. No. 9), (e) and (f) phenanthrene/T.C.P.A. (Exp. No. 10 and 11(F.C.2)), (g) coronene (Exp. No. 7), (h) coronene/T.C.P.A. (Exp. No. 8). For details of the exp. conditions, see figures VII 4, 7, 8, and 11. For (d), K = .2, dH/dt = 1.62, for (e), K = .4, dH/dt = 1.62(spectrum recorded with field sweep decreasing), for (f), K = .05, dH/dt = 1.62, for (g), K = .16, dH/dt = 1.62, and for (h), K = .27, dH/dt = 1.62 oe/sec.

Figure VII 13

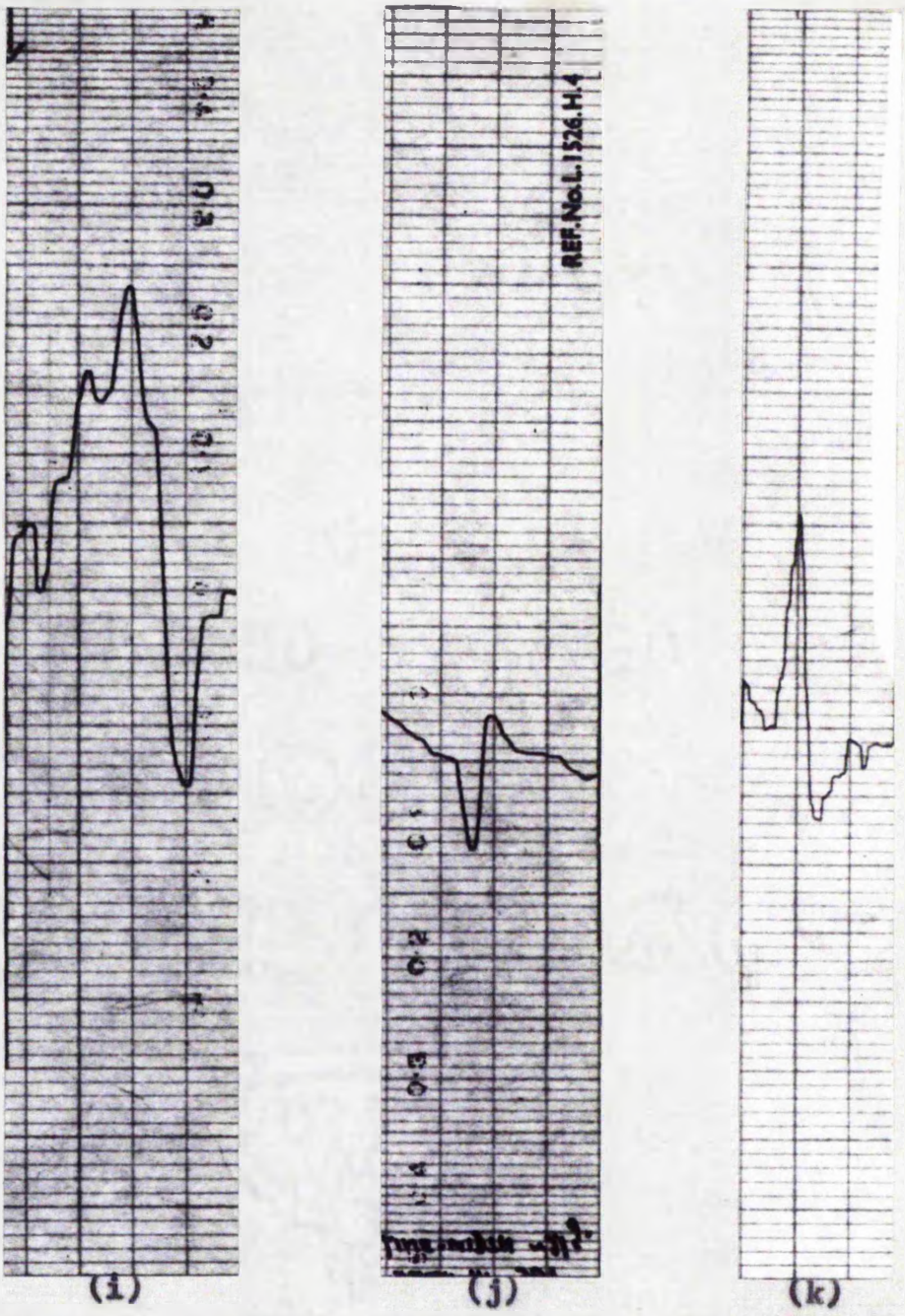

Samples: naphthalene/T.C.P.A. These recordings are examples of the concentration effects (VII (g) 6) and are taken from (i) Exp. No. 4, (j) Exp. No. 6 and (k) Exp. No. 5. For other details see Figures VII 4 and 10. For (i), K = .17, dH/dt = 1.62 oe/sec., for (j), K = .55, dH/dt = 2.77 oe/sec., and for (k), K = .16 and dH/dt = 1.62 oe/sec.

In both experiments it should be noted that the region over which it becomes possible to detect both resonances is limited - if the intensity of one falls to any less than one-half of the other, pen-recording will hardly reveal the presence of the smaller absorption line, no matter how much the modulation depth is reduced.

The effect seems to be dependent on the ratio of the donor molecules to that of the T.C.P.A. molecules, rather than the absolute concentration, as is shown by exps. 5 and 6. It was not possible to extend the work to lower concentrations because of the loss in sensitivity.

The samples were also checked optically, using the p.m. tube arrangement. It was found that, for a sample containing .05M naphthalene and .02M T.C.P.A., a decay time of about 2 secs. was obtained. The decay time for pure naphthalene is 2.5 sec., and that of the complex, 1.5 sec., so that this value is intermediate between these two cases, and supports the e.s.r. interpretation above.

Corollary. The above experimental observation of two distinct e.s.r. lines occurring at the same time poses some interesting problems on the mechanisms of energy transfer and complexing. In previous work involving optical studies, the distinction has always been made of considering one or other as the possible mechanism, but not both acting at the same time.

It is also relevant to note here that the energy transfer seems to be between naphthalene-T.C.P.A. complex and pure naphthalene, and not between T.C.P.A. and pure naphthalene. A study of the absorption coefficient of T.C.P.A. shows that it is rather small ($\epsilon \sim 30$) in the region being irradiated (e.g. see Figure VII 1 and compare with the calculation of light absorption in (g) 3 (a)). For uncomplexed T.C.P.A. therefore, the Q_{phos}/Q_{fl} ratio would require to have an unusually large value for a long decay period phosphor. Bearing in mind also the observation above that the effect appears to be dependent on the ratio, rather than the absolute value, of the concentrations, it seems reasonable to rule out the possibility of isolated uncomplexed T.C.P.A. molecules being responsible for the observed results.

The method of energy transfer is important when the relative positions of the naphthalene and the T.C.P.A. molecules are considered. The question of energy transfer has already been mentioned in (VI (f) 2) in connection with the naphthalene/benzophenone phosphor. The choice of mechanism between resonance transfer and molecular complexing was resolved in favour of the former.

Dexter (B11) has recently discussed in detail this choice of mechanism and has shown that, in the case of the energy transfer mechanism, the variation of the intensity of the

phosphorescence of the acceptor with acceptor concentration would be quadratic. He also considered the theory of weak complexing, possibly by C-T forces or London dispersion forces, and in this case he showed that the Benesi-Hildebrand constant (K_{BH}) becomes the rate constant for the above variation in signal intensity. (N.B. in the context of this paragraph the term "donor" is to be taken as referring to a naphthalene/T.C.N.A. complex molecule). The variation in signal intensity should be linear, with the constant of proportionality equal to $(K_{BH})^{-1}$. Chowdhury (F9) has found $K_{BH} = 2.8$. The experimental evidence shows that the e.s.r. absorption signal increase of the pure naphthalene (exps. 3, 4 and 5) is at least twice as great when the concentration is doubled. This seems, therefore, to support a resonance transfer mechanism.

Smaller has recently performed some e.s.r. studies (A23) on this subject and has drawn the conclusion that a weak complexing mechanism was responsible. He drew this conclusion indirectly from the behaviour of the phosphors on deuteration and on the variation of e.s.r. spin concentration as compared with the variations in phosphorescent emission discussed by Dexter. There is no reported e.s.r. detection of a complex in any of his studies.

The present experimental work is relevant here, because it has shown that, in a case where weak complexing is known to exist (from optical studies) the e.s.r. absorption has a different value of $\underline{D}^{**}$ and line-width. These facts appear to throw doubt on the interpretation given by Smaller to his results.

A second point of interest arises, particularly from the results in exp. 4, from the ability to separate two e.s.r. absorption lines in the intermediate case. The fact that the two lines can be so distinctly picked out can be interpreted only as due to the interacting molecules being in completely different fixed positions in both cases, so that two different mechanisms can occur; otherwise a general smearing out of the resonance line would have been expected. In particular this conclusion seems, in the author's opinion, to rule out some proposed mechanisms regarding energy transfer, for example, that suggested by Terenin of a random arrangement of molecules possibly within a certain sphere of action.

The fact that the "energy transfer" mechanism becomes apparent only when the donor concentration is greater than the acceptor concentration suggests that the position for this mechanism is less preferred than that for complexing.

The problem is to decide what these preferred positions are, and at the moment this can only be fairly speculative.

It has been suggested by the author from the e.s.r. data on complexes (VII (g) 4, 5) that the T.C.P.A. molecules cause a distortion in the x-y plane of the phosphor, i.e. that the T.C.P.A. molecules line up with their molecular plane parallel to that of the acceptor and located on the acceptor's z-axis. It would appear reasonable to assign this arrangement of the interacting molecules as one of the preferred positions. The other preferred position, i.e. when the T.C.P.A. molecular plane lies parallel to and in the same plane as the acceptor molecule, would then be associated with energy transfer.

Roy and El-Sayed (E36) have recently shown that in the case of deuterated phenanthrene and benzophenone the most probable configuration is that in which the molecular plane of the phenanthrene is parallel to the benzophenone axis, but of course they could not determine by optical methods in which planes the interacting molecules lie.

It has been suggested by Terenin (E30) that the "energy transfer" mechanism could depend more on the spatial overlap of the triplet wave functions than the energy overlap. In the position suggested above for this mechanism there could be some π-orbital interaction.

(g) 7. <u>E.S.R. triplet state and optical lifetime studies on the complexes</u>. Due to the rather low signal intensities involved it was possible only to make tentative observations on

the decay time of the e.s.r. signals, and as far as could be judged, they seemed to be in reasonable agreement with the optical values.

The phosphorescent emission decay curves of the naphthalene-T.C.P.A. complex were measured at 77° and 20°K, to find out if there was any temperature dependence. No significant variation was observed, indicating that the mechanism governing this emission is of the spin-forbidden transition type and not a lattice-trapping type (as was expected).

VII (h). Concluding remarks.

In the above studies, e.s.r. techniques have been used to examine weak donor-acceptor molecular complexes. These complexes are currently the subject of optical and theoretical studies, and the addition of a new technique by which to study them should be welcome.

As can be appreciated, there is considerable scope for further e.s.r. research in this field. In particular, the individual variations of D and E are matters of great importance. Since this research project was completed, some theoretical papers have shown how this can be achieved by using the $\Delta M = 1$ transitions in a glass. The sensitivity of the apparatus, however, would have to be increased in order to achieve this (see Ch. XI). The use of deuterated

donor molecules would also be desirable, as this should both reduce the e.s.r. line-width and increase the spin density (by increasing the life-time of the excited state).

The temperature variations of the uncomplexed substances have also been discussed, and in this case also the separation of the D and E variations is a matter of importance. The use of a plastic host medium for this study has much to commend it, since the temperature range 1.6° - 350°K could be studied with one sample. In this context, the possibility of using a stretched plastic medium to align the molecules would seem to have interesting possibilities.

The difficulties involved in using the published results of other authors have also been shown quite clearly in this chapter. It must be emphasized that (as demonstrated above) great care has to be taken in selecting results quoted by other authors, and a careful consideration of the finer points of e.s.r. spectra-recording is necessary. If possible, all relevant data should be obtained on the same spectrometer, thus eliminating many of the uncertainties.

CHAPTER VIII

E.S.R. studies on other organic substances.

VIII (a). A solvent e.s.r. absorption.

An absorption line was observed at g = 2 on irradiating di-ethyl-ether (the solvent used in exps. 3 and 5 in Ch. VII) with u.v. light (F.C.2) at liquid helium temperatures. This solvent was not used in experiments at other temperatures. The resonance line was quite stable after irradiation had ceased and seems to be due to a free radical being created in the solvent, as can be inferred from the following constants:-

$g = 2.009 \pm .003$

line-width = 19 ± 2 oe. (mod^{n}. 6 oe.)

spin-density = 1 in $5\ 10^{9}$ ether molecules.

The radical did not appear in other experiments where other solvents were used (see Figures VII 4 and VIII 1), so that it seems to be a property of this particular solvent.

A single weak absorption line has been reported (C6) after prolonged short wave-length u.v. irradiation of both methyl and ethyl alcohols (the author did not observe the ethanol line under the conditions of exp. 7 in Ch. VII). These lines showed some hyper-fine structure (which

disappeared as the irradiation continued) and this structure could be related to the spectrum expected from methyl and ethyl radicals. No structure was observed on the di-ethyl-ether line, and since little information can be gained from such a line, it is not possible to draw conclusions about the nature of the radical, although it seems likely that it is similar to those formed in methanol and ethanol.

VIII (b). Experiments with polarized light.

It has been pointed out in the previous chapter that although the dM = 2 transition is very useful, much more information could be obtained by observing the dM = 1 transitions, and in this section the author discusses a method by which he attempted to do this.

Since the dM = 1 transitions have a large anisotropy, the transitions have only been observed directly in doped crystals where the molecules are lined up in an ordered manner. It is not easy to find a suitable host lattice for each organic substance and growing the crystals from the melt can be a difficult and tedious process. The author tried a combination of two methods to achieve a "crystal" effect from a frozen solvent. The methods used involved (i) a crystallizing solvent and (ii) photoselection.

(i) Crystallizing solvents. The use of special solvents was initially suggested from a series of optical studies by

Sh'polskii (E50) on n-paraffins (n-pentane - n-undecane) as solvents for a variety of aromatic phosphors, where a striking change was observed in the emission spectra (both fluorescence and phosphorescence). Instead of the spectra being broad and diffuse as found with other solvents, they showed evidence of considerable line narrowing. The effect (now known as "quasi-linear spectra") has since been used successfully to elucidate the vibrational frequencies in many phosphors. The line-narrowing is thought to be due to the crystallization of these n-paraffins on cooling. Since the n-paraffins are linear molecules, each aromatic molecule is thought to enter into the lattice displacing several paraffin molecules, so that the aromatic molecule is effectively lined up in the solvent.

The author thought that this might be a possible method of obtaining a sample in which the phosphor was sufficiently lined up to overcome the large anisotropy of the $\Delta M = 1$ transition. Since the crystals formed are probably microcrystalline (this would not seriously affect Sh'polskii's studies) an additional method of lining up the molecules was used.

(ii) <u>Photoselection</u>. The method of photoselection has recently been extensively discussed by Albrecht (E81) for organic molecules, but the principle is quite simple:- the organic molecules used in this method are all planar benzene-ring compounds. For

molecules of this type, it is possible to define three mutually perpendicular axes. These axes are normally defined as:-

z-axis = perpendicular to the molecular plane.

y-axis = in the molecular plane, parallel to the shorter molecular axis (if any).

x-axis = mutually orthogonal to the other two.

Each axis has associated with it a transition probability for light absorption by the molecule. The energy of the light needed to stimulate a given transition depends on the molecule in question. In general, the energy needed to stimulate the transitions increases (i.e. a shorter wavelength) in the order x-, y-, z- directions (i.e. in the order of decreasing physical size of the molecules along the various axes). In theory, therefore, by using plane polarized light, the various axes in an ordered structure can be picked out by their different absorption bands as a function of wavelength. In practice, however, this ideal state is not found; overlap of the various spectra and mixed polarizations often occur. Only a limited amount of work has been published on this subject and good reviews are given in (E76, E78). According to these reviews, it would seem that the only two possible samples suitable for study in the author's spectrometer are phenanthrene and naphthalene. In phenanthrene, the two absorption bands, 3500 - 3000 A and 2950 - 2600 A, are said to be related to absorption

A list of experiments conducted using polarized light.

Exp. No.	Sample.	Solvent.	Conc.	Temp.	Sample holder.	Filter.
12	Phenanthrene.	iso-Propanol. n-Heptane .	·005 M. ·01 M.	77 K.	S 2.	F.C. 5 or 7.
13		iso-Propanol.	·005 M.	1·6K.	S 2.	F.C.3
14	Naphthalene.	n-Hexane.	·01 M.	77K.	S 2.	F.C.7.
15	Coronene.	n-Heptane.	·001 M.	1·6K.	S 2.	F.C.2.
16		Toluene.	·001 M.	1·6K.	S 2.	F.C. 2.
17	Carbazole.	iso-Propanol.	·005M.	77K.	S 2.	F.C.5.
18	Triphenylene.	Alphanol 79.	·003 M.	77K	S3.	F.C. 2.
19		n-Heptane.	·005 M.	77K.	S2.	F.C.5

Figure VIII 1

along the x and y axes respectively, while in naphthalene only one (y = 2850 - 2500 A) is said to be unique. Polarization of the phosphorescence of these two phosphors in glassy solution has recently been observed by using plane polarized exciting light within these bands (E82, E88).

E.S.R. work. Several e.s.r. experiments were conducted to see if any resonance could be detected. These were usually carried out as part of the experiments being done in connection with the T.C.P.A.-complexes and are listed in Figure VIII 1. It was for this reason that phosphors other than naphthalene and phenanthrene were also tried (the filter combinations used were decided on after a study of the absorption spectra). The polarizing prism used in these experiments has been discussed in IV (b) 2.

In none of these experiments was an absorption detected which could be attributed to a dM = 1 transition. As can be seen in Figure VIII 1, many of the experiments had to be done at 77°K due to the short wave-lengths involved, which of course reduced the sensitivity. There is unfortunately no record of the appropriate solvent for optical line-splitting with some of the samples.

Comments. It seems that the main difficulty with these experiments is that the photoselection method is inadequate. In some experiments, the dM = 2 transition was recorded both with

and without the polarizing prism and no difference in line-width could be detected. Since this line is built up from anisotropic components, it might have been expected to show some change.

Further practical difficulties are caused by the insertion of the polarizing prism reducing the light intensity by at least 60%, although since the dM = 1 transition is some 10x stronger than the dM = 2 one (A4) this loss might not be as serious as it seems. The most serious objection, however, is that polarized light is not sufficiently selective. Although one may arrange the incident light to be plane-polarized and of the correct wavelength so that only one molecular axis has a significant transition probability, this situation does not, of necessity, put any restriction on the spatial orientation of the other two axes with respect to the plane of polarization. In general, however, the transitions are usually polarized with respect to the molecular plane. But since the plane of the polarized light can always be resolved vectorially between the absorbing axis and an orthogonal one of the molecule, there is, therefore, in fact, a cosine variation in the number of molecules absorbing as a function of angle. The author had hoped that the lining up of the molecules by the crystalline solvent might be sufficient to limit this variation, but this does not seem to have been the case.

Kottis and Lefebrve(B12) have recently published a theoretical study on the line-shape of the dM = 2 transition in glassy solution when plane-polarized light is used. Their method was essentially an evaluation by computer of the points raised in the above paragraph, and they show that only a slight narrowing (and consequent intensity increase) of the line is to be expected for deuterated naphthalene. Deuterated naphthalene has a much narrower line-width than the substances tried by the author.

VIII (c). Anthracene, Stilbene and Durene.

Kallman (K90) has reported the existence of a phosphorescence with a long decay-time in these organic materials at room temperature when in the crystalline state. This phosphorescence was observed when the crystals were irradiated in their normal fluorescence band (~ 3600A) and is definitely unconnected with the triplet-singlet mechanism discussed in Chapter VII.

Since crystals of all three substances happened to be available, the author tried to find an e.s.r. absorption (at room temperature and using the appropriate filter) but no resonance could be detected. The crystals were rotated through 360° in two mutually orthogonal planes.

Kallman was unable to prove conclusively the exact cause of the phosphorescence, but suggested a continuous trap

distribution, probably caused by lattice dislocations (see IX (a)). A similar trap distribution has been postulated for the KCl(TlCl) crystals discussed in IX (e), and the conclusions drawn there (q.v.) regarding the feasibility of e.s.r. are also probably applicable in this case.

CHAPTER IX.

Inorganic Phosphors.

In this chapter, the results of experimental work, both optical and e.s.r., on a representative series of inorganic phosphors are recorded. The results are tabulated under the following headings:-

IX (b). Barium platinocyanide tetrahydrate.

(c). Uranyl nitrate hexahydrate.

(d). diPotassium uranyl nitrate.

(e). Potassium chloride (doped with thallous chloride).

(f). Lanthanum fluoride (doped with praseodymium).

These phosphors were chosen by the author as being the most suitable for the proposed experiments.

IX (a). Thermoluminescence. Before considering the experimental work on these phosphors, it is necessary to outline the derivation of the thermoluminescence formula used in the following sections. The phosphors discussed in Chapter VII are well established as examples of Class 2, but, from the evidence available, the phosphors considered in this section might have belonged to either section. As can be seen in the

following sections, thermoluminescence data can be useful in clarifying the situation.

Class 1 phosphors owe their long decay times to various trapping mechanisms. The Jablonskii diagram (Figure VI 1) is again helpful in explaining, in a general way, the characteristics of this class of phosphors. The state F should now be considered to be partly or wholly in the conduction band of the lattice. The level W represents an energy which, when exceeded, no longer holds the electron to the molecule. The electron, therefore, is free to wander through the lattice, gradually losing energy until it falls to an energy level J. It is then trapped in a state M and continues to lose energy until it falls to the lowest level. This potential hollow may be caused by a lattice vacancy, dislocation, etc. In Class 1 phosphors the transition P→N cannot occur, and so the only means of escape for the electron is by the path of entry, i.e. it has to receive sufficient stimulation to raise it to the conduction band again, where it may be trapped in a state F (leading to (possible) light emission) or it may fall into another state M (re-trapping). The stimulation PW is obviously less than AW, so that lower energy optical or thermal stimulation can be sufficient to empty the trap. The case of thermal stimulation is considered in the following section. While the electron is in the conduction band, it normally gives

rise to an electric current (photoconductivity).

The probability p of the transition PW occurring in unit time is given by

$$p = s \exp(-E/kT) \qquad (9.1)$$

in phosphors where re-trapping is negligible (s is a constant with the dimensions of frequency and is of the order of $10^9 sec^{-1}$ for most phosphors, and E is the energy separation of the transition PW). Solution of this equation as a function of time leads to an equation for emission intensity (I_t):-

$$I_t = n_o \, s \exp(-E/kT) \exp(-st \exp(-E/kT)) \qquad (9.2)$$

where n_o is the number of electrons initially trapped.

The decay time, τ, is defined as the time taken for I_t to fall to a value of 1/e of its original value.

If the sample, after irradiation at a temperature at which $\tau \rightarrow \infty$, is allowed to warm up at a rate of β^o/sec., then the variation of emission is given by:-

$$I_{t\beta} = n_o \, s \exp(-E/kT) \exp\left(-\int_{T_b}^{T_a} s \exp(-E/kT) \, dT \Big/ \beta\right) \qquad (9.3)$$

Solutions of this equation can be done graphically, and show that the emission reaches a maximum at some temperature ($T^{max\,o}K$) (L1).

The situation is often not as simple as that described above, and instead of a single trap depth E, there may be a distribution of traps, $N_E dE$, between E and E + dE.

In this case, $I_t = N_E kT/t$ (9.4)

Or possibly the distribution may be exponential, i.e. $N_E = A \exp(aE)$ whence

$$I_t = \text{constant}/\ t^{(akT + 1)} \quad (9.5)$$

When re-trapping is considered, the equations become more complex, since n_o is no longer a constant, and provide a wide range of solutions. In general, however, it has been found (in the few cases where a definite assessment could be made) that re-trapping is not significant.

The main point which it is desired to establish here is that it is possible to get a wide range of decay times from theoretical considerations. Hence it is very difficult to prove conclusively which trapping mechanism is involved in a given case.

Equation (9.3) as it stands is often difficult to handle experimentally and various authors have proposed simplifications. For example, Randall & Wilkins (L1) derived the following relation:-

$$E = T^{*}(1 + f(s, \beta\ ))\ k \log(s) \quad (9.6)$$

$$\log_{10}(t) = (\text{mantissa } (s))\ (T^{*}(1+f(s, \beta\ )) - T)/T \quad (9.7)$$

Curie (L3) gives:-

$$E\ (ev) = \frac{T^{*} - T_o(\ \beta\ /s)}{K(\ \beta\ /s)} \quad (9.8)$$

where K and T_o are read off from tables.

Grossweiner (L5) has suggested

$$E = 1.51\ k\ T^{*}\ T'/(T^{*} - T') \qquad (9.9)$$

where T' is the temperature on the low temperature side of the glow curve at which the intensity is one-half the maximum intensity. This equation does not depend explicitly on s and is said to be accurate to 5%.

Wrzesinska (L4) has discussed other methods of finding E, including the use of different warming rates.

IX (b). Barium platinocyanide tetrahydrate.

(b) 1. Introductory. The family of platinocyanides $(Pt(CN)_4)^{--}$ was first studied in detail by Levy (G1) in 1909, who found that many members of the series had a strong fluorescence, which was attributed to the platinocyanide group. Pauling, in his work on chemical bonding, showed that the $Pt(CN)_4$ group should be planar, with the platinum ion at the centre of a square formed by C-N groups (G2), and this structure has been borne out by X-ray analysis (G3). Pauling has also shown theoretically that the C-N bond lies in the same plane as the platinum ion, although it has been suggested from experimental evidence that the bond is perpendicular to the plane (G4). The matter does not appear to have been fully resolved.

Barium platinocyanide is the best known member of the series and has a strong green fluorescence at room temperature;

it is also known to have a long duration phosphorescence at low temperatures, which was first observed by Dewar in 1894 (G7). However, although the substance is well known, it does not seem to have received a great deal of attention. Very little information is available about the phosphorescence of the salt and the author studied this emission using the apparatus discussed in (V (c)).

The work discussed in the following pages was done on the barium salt as it is commercially available. Other salts can be formed by double decomposition with the appropriate cyanide or sulphate. Several of these were prepared by the author (e.g. magnesium and sodium salts (the pentahydrate of the former exhibits a most striking dichroism)), but the products obtained were of low purity and facilities for further purification were not available.

The barium salt crystallises readily as greenish yellow crystals belonging to the monoclinic system (a:b:c:: .8693:1: .4793, $\beta = 103^{\circ}\ 54'$). Two modifications exist depending on whether the salt is crystallized from acidic or neutral/alkaline solution, the latter form being more stable.

The absorption and fluorescence emission spectra of the barium salt (crystalline) have been recently studied by Moncuit and Poulet (G8) at room temperature, who give the following values:-

	Absorption		Emission
	λ_{max}	f(osc.strength)	λ_{max}
$\perp$ to $Pt(CN)_4$ plane	4400 A	1.	5200 A
// " "	2630	- (weak)	5180/5000 A.

These authors studied a series of platinocyanides (Mg, Ba, Ca and Sr) and found that while the λ_{max} of the absorption perpendicular to the $Pt(CN)_4$ plane varied through the series (5550 to 3530 A), the λ_{max} of the absorption parallel to the plane was almost constant (2580 to 2670 A). On the basis of this evidence, they assign the perpendicular transition to a $5d_{z^2}(a_{1g}) \rightarrow 6p_z(a_{2u})$ transition of the central metal (Pt) ion and the parallel transition to a $5_{d^2}(a_{1g}) \rightarrow \pi^*(e_u)$ charge-transfer transition (between the Pt and CN group).

According to Pringsheim (P1), the solution absorption spectra, which is presumed to be due to the $Pt(CN)_4$ group alone, shows a large peak at 2500A and a small one at 2800 A, with cut-off at 3400 A.

Very different values of τ_{fl} (at room temperature) for the barium salt are quoted in the literature, e.g. $10^{-6} - 10^{-7}$ sec. (G6), $3\ 10^{-10}$ sec. (P1) and (L1) quote the decay as being complete in 10^{-5} sec. Moncuit (G8) does not quote τ_{fl} for either of the transitions. Pringsheim also states that there is considerable confusion in the literature concerning even the colour of the

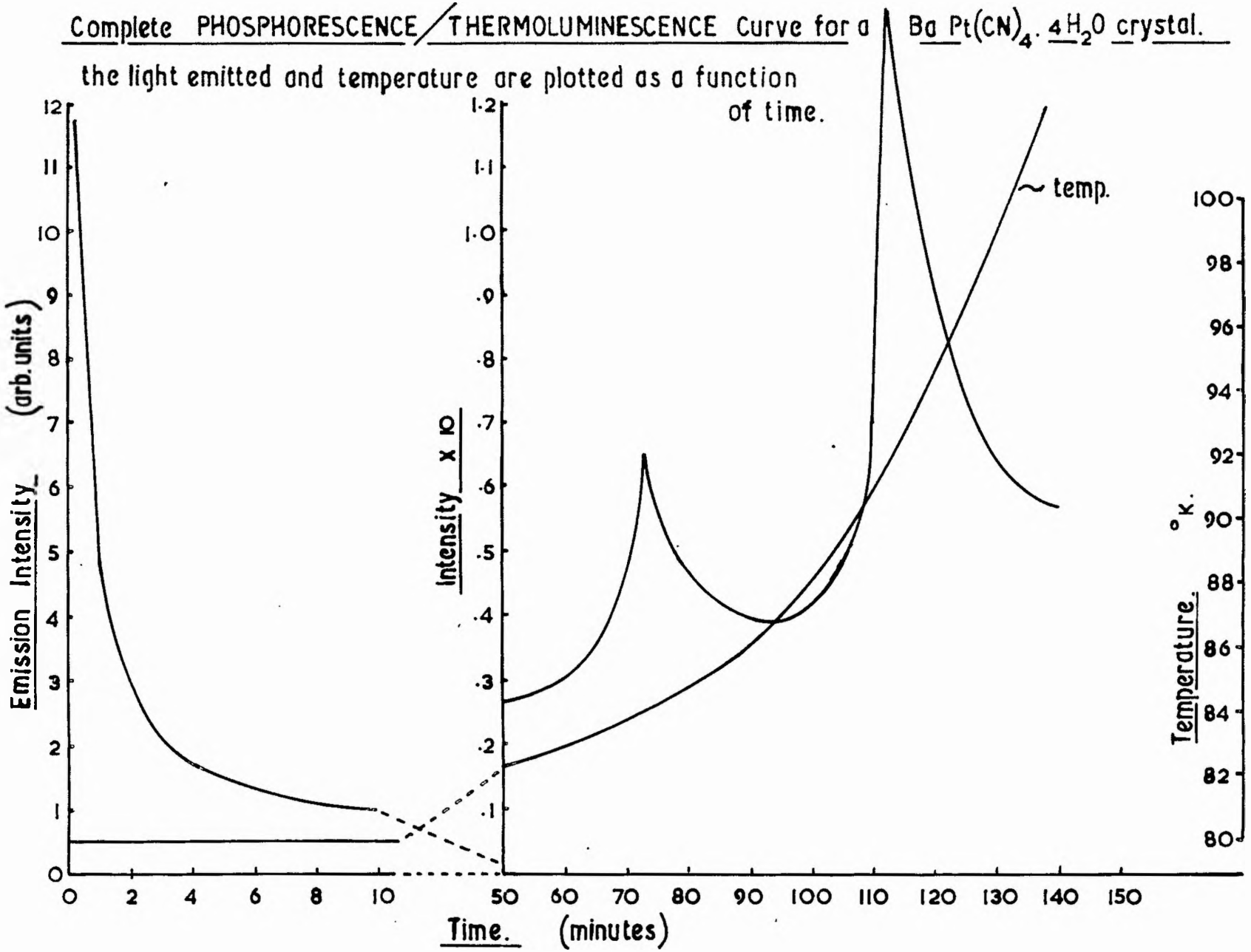
Complete PHOSPHORESCENCE / THERMOLUMINESCENCE Curve for a Ba Pt(CN)4. 4H2O crystal.
the light emitted and temperature are plotted as a function of time.
Emission Intensity (arb. units)
Intensity X 10
~ temp.
Temperature °K.
Time. (minutes)
0 2 4 6 8 10 50 60 70 80 90 100 110 120 130 140 150
0 1 2 3 4 5 6 7 8 9 10 11 12
.1 .2 .3 .4 .5 .6 .7 .8 .9 1.0 1.1 1.2
80 82 84 86 88 90 92 94 96 98 100

Figure IX 1

crystals. There does not seem to be any recorded measurement of the photoconductivity.

(b) 2. Experimental work (optical). The author measured the phosphorescence/thermoluminescence of the crystals and the results are given in Table IX 1. The crystals all gave similar results. The underlying reason for doing this work was to make an estimate of the number of active centres in the crystal.

The phosphorescence could only be stimulated by short wave-length u.v. light (< 3300A), and no emission was observed on irradiation at 4500A.

The decay time of the phosphorescence was measured using the photomultiplier circuit, keeping the temperature constant (80°K) until the emission intensity fell to a very low value, and then the temperature was allowed to rise slowly so that the thermoluminescent emission could be measured. A typical example of a combined phosphorescence/thermoluminescence curve is shown in Figure IX 1. (The error in the amplitude measurements is ± .03 units, and in time ± 5 sec.). There is no other emission up to 300°K. The decay curve at constant temperature could not be made to fit any of the theoretical decay systems discussed in (IX (a)), but finally two separate exponential curves were superimposed, one of decay time 2.5

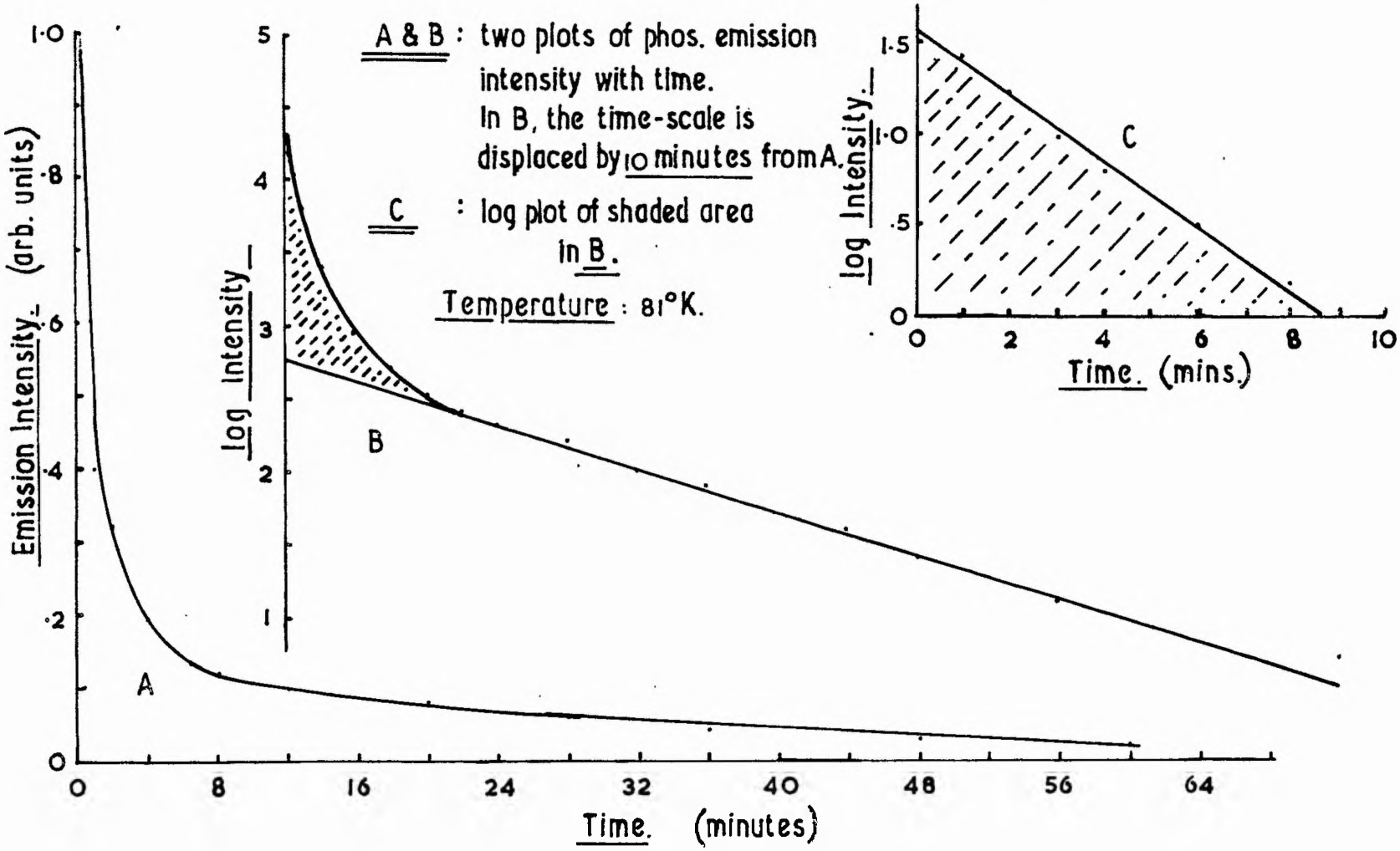
Phosphorescent decay with time of a single crystal of $BaPt(CN)_4.4H_2O$.
A & B : two plots of phos. emission intensity with time.
In B, the time-scale is displaced by 10 minutes from A.
C : log plot of shaded area in B.
Temperature : 81°K.
Emission Intensity (arb. units)
log Intensity
log Intensity
Time. (minutes)
Time. (mins.)
A
B
C

Figure IX 2

minutes and the other of 18 minutes. Figure IX 2 shows a set of experimental results plotted in this manner, and as can be seen a good fit was obtained (the error in the amplitude measurements is ± .003 units and in time ± 5 sec.).

If this division of the decay was correct, then the thermoluminescence curve should show the existence of two traps. Heating at a rate of 2.2°/min. had revealed only a single peak, but when the heating rate was slowed down to .46°/min. a second peak was resolved on the low temperature side of the major peak. Since the T^m and τ values are known, equations (9.6, 9.7) can be solved simultaneously, and it was found that s has a value of $10^9 \pm .3$ sec^{-1}., and that the trap depths are .195 and .180 ev. for the long and short decays respectively. It is rather difficult to estimate the absolute error in these values of the trap depth, but it seems to be within ± 5%. The value calculated from equation (9.8) is shown in Table IX 1 for comparison.

In experimental work on thermoluminescence, it is often impossible to solve these equations explicitly; hence the use of semi-empirical equations such as (9.8) and (9.9). The value of s used in these semi-empirical equations is usually selected as that which gives the best fit to the experimental data. Values of s between 10^9 - 10^{10} sec^{-1}, are commonly used. From Table IX 1 it can be seen that equation (9.8) gives the correct value within 10 - 20% (when the correct value of s is known).

Table IX 1

		T^m	dT	E ev.	method
.46°/min.	18 min.	93°K	6°	.195	(9.6; 9.7)
2.2°	"	97°	5°	.195	(")
.46°	2.5	86°	-	.180	(")
.46°	18	93°	6°	.22	(9.8)
.6°/sec.	Tolstoi	125°	16°	.25	(9.8)

This work was done early in the project and some time later a paper by Tolstoi and Ageeva was published (115), in which the thermoluminescence of the barium salt was measured. Their results are also given in Table IX 1 (recalculated) for comparison. These authors used a much higher warming-up rate and detected only a single peak, which has a greater trap depth than that measured by the author, using the same equation, but this discrepancy may be within the error involved in the use of this empirical equation.

The total number of quanta involved in the phosphorescent decay and thermoluminescence processes was estimated in the manner described in Appendix 4, and found to be $5\ 10^{12}$ in a crystal of volume .08 cc., which gives the density of phosphorescent centres in the crystal as being of the order of 1 in $3\ 10^{8}$ Ba $Pt(CN)_4$ molecules. From this it is obvious that

the phosphorescence is unlikely to be directly related to the platinum co-ordination group.

(b) 3. Experimental work. (e.s.r.). As can be seen above, the spin concentration is very low. Since the phosphorescence is stimulated only by short wavelength u.v., the crystal had to be studied at liquid nitrogen temperatures, and at this temperature the absolute number of spins in the sample is very close to the absolute spectrometer sensitivity. Several samples were studied, but on no occasion was any resonance observed, at any orientation of the magnetic field to the $Pt(CN)_4$ plane.

(b) 4. Conclusion. In view of the small number of active centres, the absence of a detectable e.s.r. signal cannot be considered to be of any real significance. It would seem, however, from the absorption and spin-density data that the phosphorescence is not a property of the platino-cyano groups per se. The existence of two distinct traps in the crystal is of interest, indicating that particular defects must be recurring through the crystals. The strictly exponential nature of the decay at 80°K must also be considered, for it suggests that re-trapping is not significant in this crystal. It was not possible with the limited equipment available to make a further study of these traps.

If the value of the deeper trap depth (.195 ev.) is taken, together with its associated decay time at 80°K, and equation

(9.2) is used to calculate the decay time of an electron trapped in the same state at 300°K, the value obtained is $5\ 10^{-7}$ sec. This value can be compared with the various values of τ_{fl} quoted in (IX (b) 1) and it will be seen that it is the same as that quoted by some authors as being the fluorescence lifetime. It seems probable therefore that these authors may not have been measuring the true fluorescence lifetime at all. More detailed optical work is obviously needed on these particular crystals. The assignation by Moncuit of the absorption spectra parallel to the $Pt(CN)_4$ plane to a charge-transfer state might be worth re-examining. The phosphorescence studied by the author is most unlikely to be due to a charge-transfer state as this state does not provide any mechanism for the observed temperature dependence. Conversely, however, a lattice trapping mechanism could equally well explain the constant energy required for this transition, since the energy required to remove an electron from the $Pt(CN)_4$ group will be as constant in terms of energy as the postulated charge-transfer mechanism.

IX (c). Uranyl nitrate hexahydrate.

(c) 1. Introductory. Another family of compounds which is said to exhibit phosphorescence due to an internal effect is the uranyl group. In this family it is well established that a phosphorescence of about 10^{-3} sec. is observed at room temperature. These salts were first studied by Bequerel (H1), and received a

great deal of attention from Nicholls & Merritt (H2) about 1910, but the results they obtained are of little use since at that time a correct understanding of the processes involved was impossible (their results, in fact, show some remarkable efforts at adapting the facts to fit the theory, e.g. experimentally observed exponential decay curves (which are correct) are divided into three straight sections, varying as $t^{-\frac{1}{2}}$) (see H3)). It is, however, generally agreed that the UO_2 group is responsible for the phosphorescence, since the decay curve is strictly exponential and the emission can be observed in solution as well in crystals (L1). The decay time has been measured at various temperatures and shows that there is relatively little change (H10):-

Uranyl nitrate	$\tau_{77^\circ K}$: $\tau_{293^\circ K}$ ::	1.15 : 1
Potassium uranyl nitrate	$\tau_{77^\circ K}$: $\tau_{293^\circ K}$ ::	1.63 : 1
	$\tau_{4^\circ K}$: $\tau_{77^\circ K}$ ::	1.17 : 1

which again strengthens the forbidden-transition explanation of the emission. There is no observed photoconductivity on irradiation (L1).

The UO_2 group is a linear one, the U-O bond distance being 1.90A (H4). For an up to date summary on uranyl salts see (H13). As far as the author could find there was no reported examination of the family for thermoluminescence effects. The salt

$(UO_2)(NO_3)_2.6H_2O$ was chosen for examination, as it was thought to be a typical example. This salt crystallizes readily from aqueous solution, forming regular green orthorhombic crystals (a = 11.42, b = 13.15, c = 8.02) which are slightly deliquescent (G3,H5).

Uranyl salts have a very small paramagnetism (about 57 10^{-6}) which can be related to the uranyl group. Theoretical studies showed that it could be explained as being due to an f-orbital motion (H11, H9), although it has recently been shown that it could equally well be due to a d-orbital (H12). However there is no detectable e.s.r. signal from the UO_2 group and it has been used as a non-paramagnetic dilutant in some studies (Q7).

(c) 2. Experimental results (optical). The crystals were studied using the methods discussed in (V (c)), but an unexpected result was obtained - the crystal showed a triboluminescent effect. (When a crystal emits light spontaneously on cooling, heating, being crushed or undergoing some other mechanical - as opposed to chemical - process, this emission is known as triboluminescence. A review of triboluminescent phenomena is given in section (c) 3.).

Further research on triboluminescent phenomena finally revealed that the effect had been reported over 50 years ago by Dewar (M8) and Bequerel (M9) who had also plunged crystals of uranyl nitrate into liquid air. (They also reported a similar

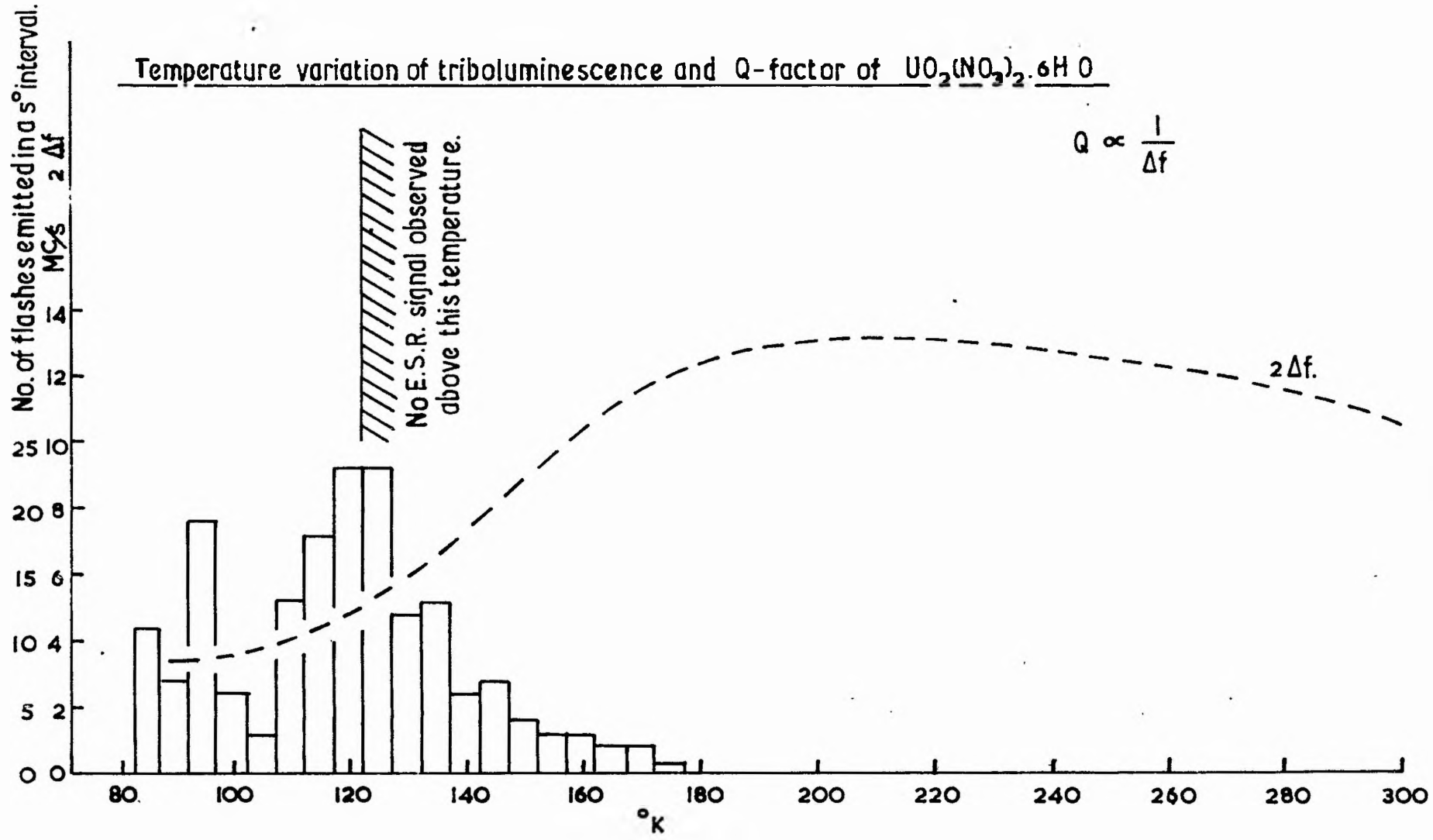
Temperature variation of triboluminescence and Q-factor of $UO_2(NO_3)_2.6H_2O$
No. of flashes emitted in a 5° interval.
M/s
2 Δf
No E.S.R. signal observed above this temperature.
$Q \propto \frac{1}{\Delta f}$
2 Δf.
0 0
5 2
10 4
15 6
20 8
25 10
12
14
80
100
120
140
160
180
200
220
240
260
280
300
°K

Figure IX 3

effect with barium platinocyanide crystals - an effect which was not observed by the author).

The author studied this phenomenon and found the following points of interest. The triboluminescent emission observed in these experiments is asymmetric in time, with a sharp leading edge and an exponential decay with period τ of .0023 ± .0005 secs. (τ for the apparatus = .0003 secs.) (see Figure VII 5g). This decay time was found to be the same as that for flashes emitted when grinding the crystals to destruction (Figure VII 5g) - the difference being that the cooling/heating effect was non-destructive and could be repeated many times (although after some time the crystals began to show signs of physical deterioration). An example of a histogram of the number of flashes measured over 5° intervals as a crystal warmed up from $77^{\circ}K$ (at a rate of 2°/sec. (approx.)) is shown in Figure IX 3. Both peaks are reproducible with different samples (although the relative intensity of the lower temperature peak is sometimes smaller than that shown).

The energy released in a single flash is some $3\ 10^{-12}$ ergs, giving approximately 10^{8} quanta involved in each flash. The number of flashes of this energy recorded (on a movie camera) on warming up seemed to be around 200. An indeterminate number of lower energy flashes also occurred which could not be resolved by the apparatus. The effect was also shown by samples which

had been ground to as fine a powder as possible.

These experiments were repeated with other materials known to be triboluminescent on grinding, e.g. acenaphthene, barium chlorate, sucrose, uranyl acetate etc., but no evidence of triboluminescence on cooling/heating was found.

On irradiating the samples of uranyl nitrate with short-wave u.v. before warming up, no thermoluminescent emission could be observed.

(c) 3. Review of triboluminescent mechanisms. The normal triboluminescent effect (i.e. that obtained on grinding the crystals) was first reported by Herschel (M1). The subject has received little serious attention (see references M3 - 7) and at present seems to be studied only by Wolff (M2) who has studied some 1883 (unnamed) compounds with no definite conclusions. It is thought to be caused by (i) unstable excited centres and/or (ii) stable heat resistant centres and/or (iii) electrical discharges, etc. etc.

In the author's opinion, triboluminescence in general however appears to be due to lattice dislocations in the crystals. Dislocations can cause intense local electric fields, and the dissipation of the energy stored in these fields can be sufficient to cause luminescence (Destriau effect). (It is perhaps significant in this context to note that the emission from uranyl nitrate is blue-white and not green). There seems to be

no need to invoke special (andunique) centres to explain the mechanism. An electrical breakdown of this nature would give the observed intensity variation with time of the emission.

It is interesting to note (see references in M7) that when uranyl nitrate is dropped into liquid nitrogen, it becomes electrically charged, and sticks to the wall of the dewar instead of dropping to the foot. It is also reported to clear up cloudy liquid nitrogen by attracting the (ice ?) particles. The phenomenon was suggested to be pyroelectric or piezoelectric in origin.

(c) 4. Experimental results. (dielectric constant). Also shown on Figure IX 3 is the variation of the resonant cavity's Q-factor with temperature when it contained a sample of uranyl nitrate. The corresponding frequency change was small. These changes were not shown by samples of other materials. The cause of these changes, which are related to the dielectric constant of the crystals, is considered in detail in section ((c) 6 (ii)).

(c) 5. Experimental results. (e.s.r.). When crystals of uranyl nitrate were examined in the spectrometer, it was found that below a temperature of approximately 115°K an e.s.r. absorption was found. The line had the following constants:-

$$g = 2.015 \pm .010$$

$$\text{line-width} = 120 \pm 10 \text{ oe.} \ (\text{mod}^{n}\cdot 10 \text{ oe.})$$

apparent spin density = about 1 in 10^6 nitrate molecules.

No change in any of these values was observed when the samples were irradiated with u.v. light. Nor was there any evidence of anisotropy when the crystals were rotated in any plane, or of any line structure. The line was rather small, but was reproducible in all the crystals which were examined.

(c) 6. Discussion. The following points arise from the above observations:-

(i) There is no evidence of thermoluminescence in the optical region.

(ii) dielectric changes. The Q-factor of the cavity is proportional to $(\tan \delta)^{-1}$, where $\tan \delta$ is defined as e_2/e_1, where e_1 is the dispersive part and e_2 the absorptive part of the complex dielectric constant. It can be shown, to a reasonable approximation, that e_1 equals $(1 + KN)$ and e_2 equals $(K \tau N)$ where K is a constant, N is the number of electrons involved (which need not all be in the same configurational assignment) and τ is the relaxation time of the electrons (T52). The absolute magnitudes of de_1 and de_2 were not found in the author's experiments since the crystals used were only in a part of the microwave E field, and an accurate measurement would have involved some major modifications to the existing equipment. It cannot be decided therefore, from the above evidence, whether dQ is due to a decrease in τ or N.

(iii) Triboluminescent considerations suggest that some particular phenomenon, which is dictated primarily by the crystal structure, is involved.

(iv) E.S.R. The appearance of an e.s.r. signal could presumably be due to two causes, either a change in the UO_2 group or to the presence of unpaired spins. In the former case, it is difficult to see why only 1 in 10^6 molecules would be involved and the latter theory would seem to be the more probable. The experimental evidence suggests that these unpaired spins are in fact trapped electrons, since the g-value obtained for the spins indicates that they are almost completely free.

If the spin density and the crystal volume are considered, a value for the average separation of the spins can be found to be about 1000A. At distances of this magnitude, most forms of broadening can be neglected. The observed line however is very broad, and this needs some explanation. Three possible mechanisms can be postulated: (a) the line is saturation broadened, (b) it is interacting with the surrounding nuclei (N and/or H) or (c) the spins are not uniformly distributed throughout the crystal and are either in little groups or in different sites. Due to the low spin density, however, it was not possible to carry out experiments to distinguish between these possibilities.

The approximate trap depth can be estimated from equation (9.1) to be about .2 ev. Mott & Gurney (T51) have shown that if an electron is held in a potential hole where the binding energy is relatively small (< .5 ev.) its orbit will be quite large and markedly affected by any electric fields present. The orbits are said to be of the order of several lattice spacings (T52) and this would mean that the line could be severely broadened by nuclear interactions (see also the calculation in IX (g)).

(v) The pyro/piezo-electric effect mentioned in ((c) 3) supports the view that electric charges are present when the crystal is cold and not when it is at room temperature.

(vi) Summary. In view of the above evidence, the following explanation seems to be the most reasonable:-

When the uranyl nitrate is cooled down, stresses in the crystal are relieved. The lattice cannot withstand the change and cracks along random planes. These dislocations naturally break bonds in the crystal and create potential hollows, which are deep enough to trap some bonding electrons. These electrons were originally charge compensated, so that now the crystal acquires a "permanent" electric moment. These conditions persist until the crystal is warmed up, when the traps are no longer sufficient to contain the electrons. The fact that the crystals begin to show some physical deterioration after repeated cooling and heating supports this explanation. Another possible

mechanism is that the crystal undergoes a phase change. Some support for this mechanism can be found from the existence of a fairly sharp transition point and also from the observation that the magnitude of the e.s.r. absorption was (as far as could be ascertained) independent of the temperature range through which the crystal was cooled. If this is the correct explanation, evidence of the phase change should be found in the warming-up curve. However, with the apparatus available, it was not possible to check this.

IX (d). di-Potassium Uranyl Nitrate.

(d) 1. Introductory. Wick & McDowell (H7) mention briefly that with certain uranyl salts a long persistence phosphorescence was observed when the sample was bombarded by cathode rays, while immersed in liquid air (see also (H8) for the same effect in uranyl silicate). It occurred to the author that since quartz dewars would be a rarity at that time, the phosphorescence might be stimulated by short wave u.v. as well as by cathode rays. This proved to be the case, except that since liquid nitrogen was used, the phosphorescence was frozen in. The crystals used were di-potassium uranyl nitrate ($K_2(UO_2)(NO_3)_4$). The crystal system is monoclinic (a:b:c:: .639:1: .619, $\beta = 90^{\circ}$). Two modifications can be grown, depending on the percentage of nitric acid in the solution from which the crystals are grown. Both types were examined

in the experimental work detailed below, but no significant differences were observed. The crystals can be grown from solution with some difficulty.

TABLE IX 2

Peak	T^*	β	E ev.	method
larger	109°K	1.7°/sec.	.20	(9.8)
smaller	136°K	"	.26	(9.8)

(d) 2. Experimental results (optical). For these crystals, the phosphorescence lifetime is very long at 77°K, so that all the stored energy is released as the crystal is allowed to warm up. The samples were irradiated with short wavelength u.v. and the thermoluminescence curves recorded photographically. The emission showed two peaks (see Figure VII 5 h) and the trap depths are given in Table IX 2 (with an absolute error of ± 20%). The area under the second peak is about .05 that of the larger. No other peaks were observed up to room temperature. These crystals are very stable and can be repeatedly cooled.

Thermoluminescence curves were taken after different periods of irradiation, varying from 15 sec. to 15 min. No variation of T^* was observed, indicating that retrapping does

not play a significant part in the decay mechanism. The thermoluminescence could be stimulated only with short wavelength u.v. (< 3400A).

An estimation of the number of quanta emitted gave 10^{12} quanta (after 14 minutes irradiation). Therefore the ratio of supposed luminescent centres to total number of molecules present is 10^{-8} (approx.). Thus, it can be seen that only a very few centres are active. Hence, it seems unlikely that the trapping state is in any way connected with the uranyl ion.

(d) 3. Experimental results (e.s.r.). Since the wavelengths needed to stimulate the phosphorescence are too short, it is not possible to use the glass dewars, and as can be seen above the spin density is almost that of the spectrometer at liquid nitrogen temperatures. Nevertheless, some specimens were examined at various orientations, but even after prolonged irradiation no e.s.r. signal was observed. The temperature was kept below $88^{\circ}K$, at which temperature τ should be >100 secs.

(d) 4. Conclusion. When the evidence given above is taken into consideration, the phosphorescent emission from this substance certainly seems to be due to an electron trapping mechanism. The disturbing effect of the potassium ions on the regularity of the lattice may be a contributory factor but it is obviously not the prime reason, since in this case there would be many more traps. It is also interesting to note that these crystals

did not show any triboluminescent effect. (See also the comments in IX (g).

IX (e). KCl(TlCl).

(e) 1. Introductory. Potassium chloride is a very well known material in optical spectroscopic work and has been studied extensively for many years, primarily because of its simple cubic lattice structure and also because it can be treated to form a number of interesting cases (D2, D3). It is normally grown from the melt and often an excess of potassium or other elements is added. Pringsheim (O1) noted however that if KCl and TlCl were co-precipitated from a saturated aqueous solution, a very long lived phosphorescence could be observed in crystals which were taken from the first 5% deposited. The remaining 95% of the crystals contains very little TlCl. Pringsheim found that while the excitation spectra are the same, the complete phosphorescent decay took about 1 min. for those grown from the melt, and several hours for those that were microcrystalline. As explained in (V (b) 2), reasonably sized crystals of this salt were grown by the author.

The phosphorescent emission spectra of these crystals is given in (O2), where it can be seen that there is also considerable u.v. emission at 3050A, in addition to the strong visible emission at 4800A. The thermoluminescence of these crystals has been measured before (L2B) and results indicative

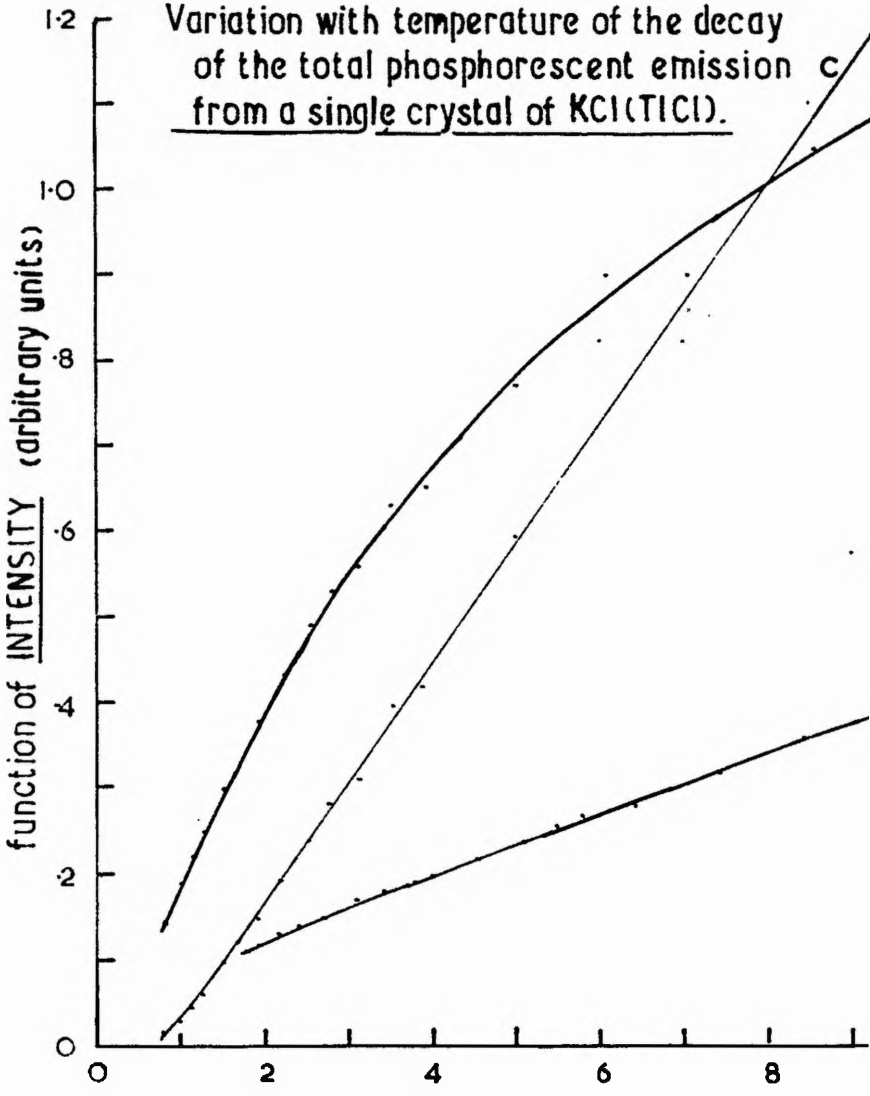
Variation with temperature of the decay
of the total phosphorescent emission
from a single crystal of KCl(TlCl).
function of INTENSITY (arbitrary units)
1·2
1·0
·8
·6
·4
·2
0
0
2
4
6
8

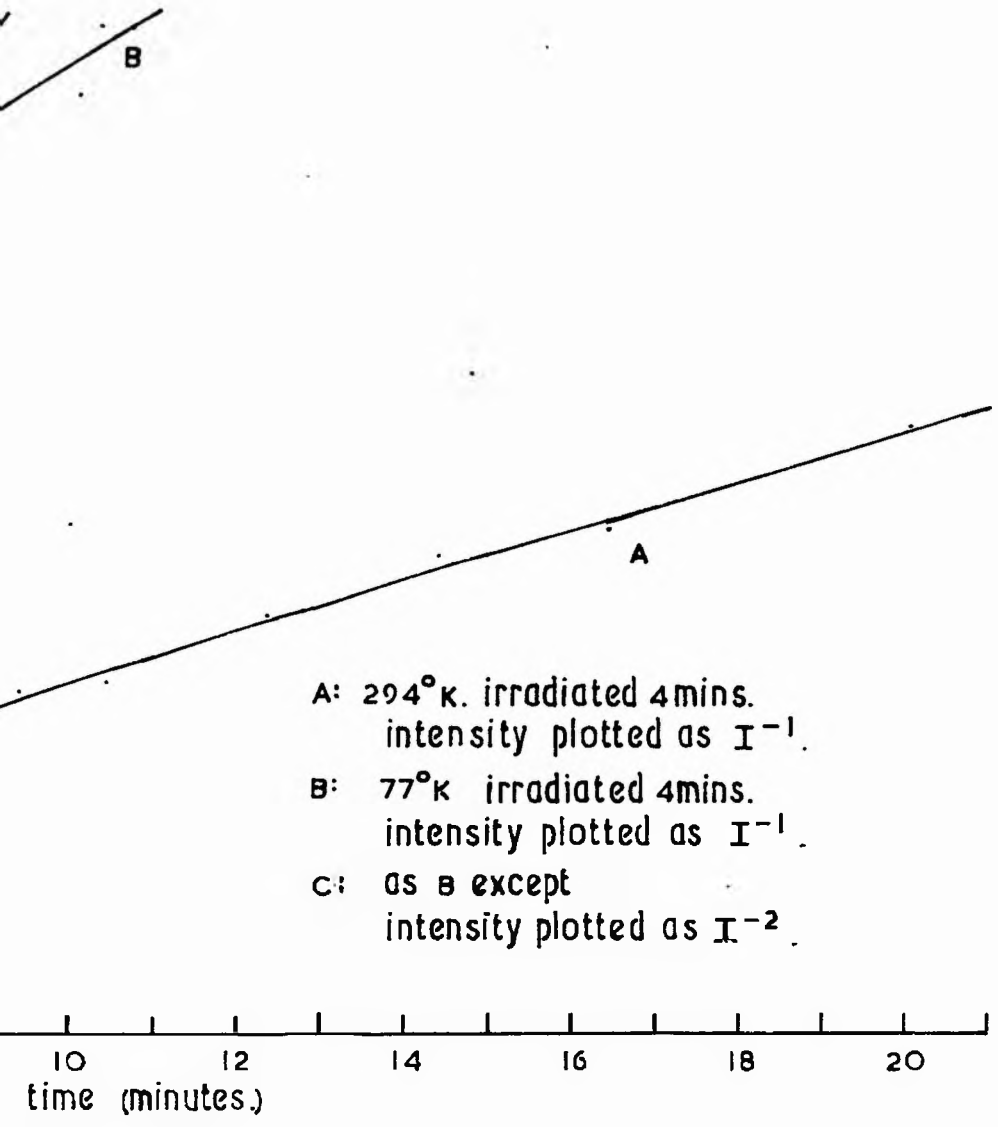
B
A
A: 294°K. irradiated 4mins.
intensity plotted as I^{-1}.
B: 77°K irradiated 4mins.
intensity plotted as I^{-1}.
C: as B except
intensity plotted as I^{-2}.
10
12
14
16
18
20
time (minutes.)

Figure IX 4

of a very wide trap distribution were obtained - there being no observable T^{*}.

The u.v. emission spectrum has been explained by several authors in terms of metastable states of the free thallous ion, and for a review see (L3C). Recently Ewles & Joshi (02) have published data which throws doubt on this explanation, concluding that metastable states cannot be responsible for this emission, and they suggest that the emission is due to traps caused by lattice distortions due to the Tl^{+} ions. Ewles' theory also provides a reasonable mechanism for the visible emission, which is unexplained in the meta-stable state theories, but it offers no explanation for their observation that there was no detectable photoconductivity - at least down to 10^{-14} amp.

Vrehen (03) has recently studied the magnetic properties of the Tl^{+} ion in KCl crystals using an optical method. His results suggested that the ^{3}P state (the proposed metastable state) is non-paramagnetic and he suggests that this may be due to non-thermalization of the spins (i.e. a Boltzmann distribution is not attained).

(e) 2. Experimental results (optical). The decay curves of the visible emission for these crystals were measured at 305° and $77^{\circ}K$, and are shown in Figure IX 4 (the error in the intensity

measurements is ± .03 units and in time measurements is ± 5 secs.) At room temperature, the decay curve can be described by a t^{-1} relationship, while at 77°K by a t^{-2} relationship. (Ewles (02) quotes a $t^{-\frac{1}{2}}$ decay for microcrystalline samples at room temperature).

At 77°K the decay is shorter, indicating that the trap distribution is different from that at room temperature. It was also noticed that the lifetime of the phosphorescence decreased with an increasing period of irradiation, i.e. there was bleaching of some of the centres by the irradiating light.

(e) 3. Experimental results (e.s.r.). The samples yielded no observable e.s.r. signal at room or nitrogen temperatures, in any orientation or with differing TlCl concentrations.

(e) 4. Conclusions. The absence of e.s.r. in this sample is particularly disappointing. Of all the crystals considered in the present chapter, these were the most promising in view of the known large light sum contained, the absence of photoconductivity, ease of stimulation at room temperature etc. However, the apparent presence of a large spread of trapping mechanisms in these crystals may well be an inhibiting factor, since this could lead to a wide spread in g-values and/or line-widths for the various spins, which in turn would probably broaden the resonance line to such an extent that it would be undetectable.

IX (f). Lanthanum fluoride, doped with Praseodymium.

(f) 1. Introduction. There has been recently some interest in the investigation of lanthanon salts, as several of them were thought to be of use in lasers. These salts can be doped with other rare earth ions without charge compensation, and as such may show e.s.r. absorptions due to transitions in the lowest lying levels of the impurity ions. Because of the screening effect of the 4f electrons, the spin-lattice interaction is strong, and hence the spectra can be observed only at low temperatures. In addition, the g-values depart widely from the free-spin value, and are usually very anisotropic (Q2).

Crystals of lanthanum tri-fluoride have been grown by Dr. D. A. Jones (Aberdeen) (J2) who supplied one which was known to contain Praseodymium. The author studied this crystal, since it was a possible example of Class 2C phosphors. The ion, Pr^{3+}, has an even number of electrons in the 4f shell, and should therefore have only a singlet level. It has been found in some cases however, that the Jahn-Teller splitting of the lowest doublet is small, and is capable of microwave stimulation; e.g. in $LaCl_3(Pr^{3+})$, a resonance was observed at $4^{\circ}K$, having $g_{//} = 1.035$, $g_{\perp} = .1$ ($\nu = 9.5$kMc/s.) (J3, J4). However, in $LaF_3(Pr^{3+})$, Baker & Rubins report that there is no resonance down to $14^{\circ}K$ (J5).

The crystal structure of the lanthanum tri-fluorides has also been under investigation. Earlier work showed a hexamolecular unit cell, with C6/mcm symmetry (G3), but a recent paper by Schlyter has given crystallographic evidence for a bimolecular unit cell, with C6/mmc symmetry (J6). E.S.R. work on the Gd^{3+} doped salt has favoured the hexamolecular unit cell (J2) and one of lower symmetry for Ce, Nd, Dy, Er and Yb doping (J5).

(f) 2. Optical details of the crystal.

Experimental. The crystal was investigated by the author for phosphorescence. When the sample was irradiated with light of wave-length shorter than 3000A at 77°K, a green phosphorescence of half-life about 5 sec. was observed. It was not observed at 293° or 195°K (solid CO_2/acetone bath). The number of phosphorescent centres (estimated from the recorded data) was found to be about 1 in 10^{10} LaF_3 molecules.

Discussion. Spectroscopic investigations of LaF_3(Pr) crystals show that the highest discrete energy band is at 4,400A, wavelengths shorter than this raising the electron into the continuum, as can be seen from the energy level diagrams given in (J7,J8). From these diagrams, it can be seen that those transitions which correspond to a green emission are forbidden. These metastable states are known to have a mean lifetime which does

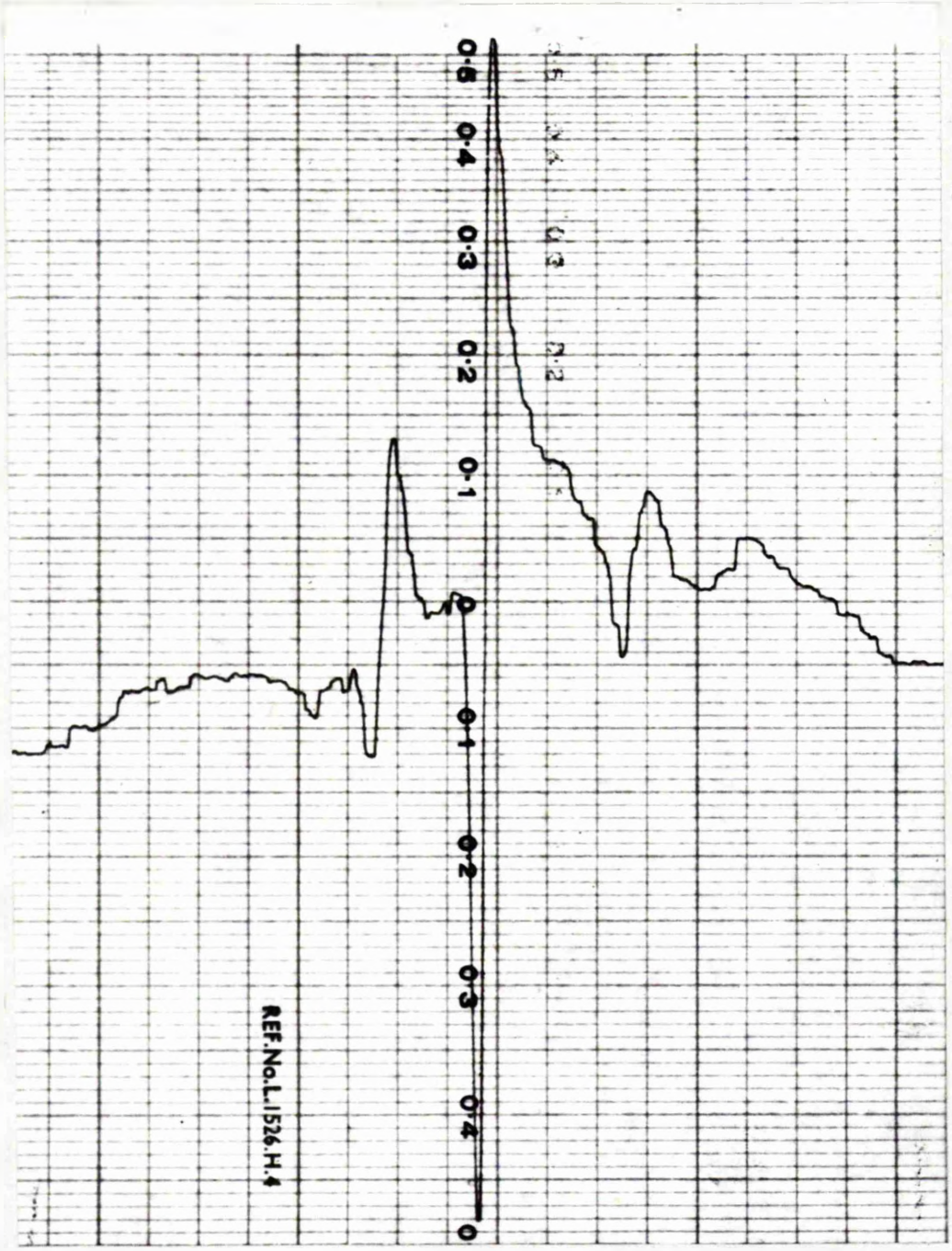

Figure IX 5.

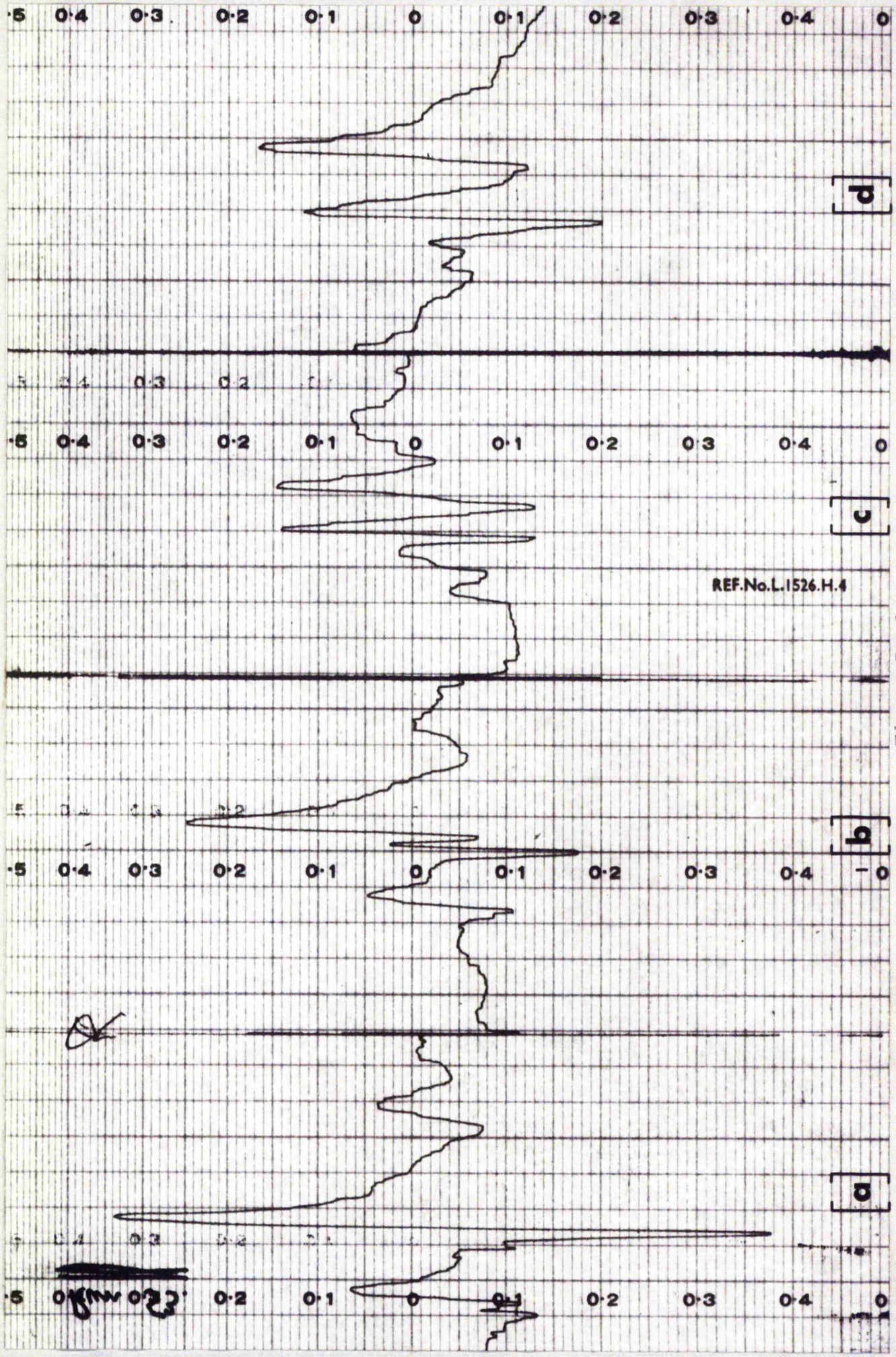

Figure IX 6

Figures IX 5 and IX 6.

Sample : $LaF_3(Pr^{3+})$, single crystal.

Temperature : 80° (± 2°) K.

Orientation: IX 5 = X- and Y- crystal axes parallel to the "b" and "a" dimensions of the microwave cavity.

IX 6 (a - d) = Spectra obtained when the crystal is rotated in the X-Y plane with successive increments of 10.35°.

Field sweep: full field sweep. Each trace is calibrated individually, and the approximate extent of the sweep in each recording is given below.

The sweep is linear (± 3 oe.) between 2500-4000 oe.

" " " " (± 20 oe.) between 1600-4300 oe.

In the linear region, 1 division on the pen-recording equals approximately 150 oe.

IX 5. field swept between 1600-4500 oe.

IX 6a. " " " 2650-4000 oe.

6b. " " " 2500-3900 oe.

6c. " " " 2620-3950 oe.

6d. " " " 2640-4100 oe.

Field direction: Increasing left to right.

Mod^{n} = 10 oe. τ = 1 sec. dH/dt = 5oe/sec.

$Frequency_{KL}$ = 9476 Mc/s.

not exceed a few hundredths of a second (e.g. P2). The extremely low number of phosphorescent centres is further evidence against a metastable state theory. These internal forbidden transitions should also be temperature independent as discussed in Chapter VI, although it is always possible that lowering the temperature decreases significantly the radiationless probability transfer. On balance, it seems however that another mechanism, probably lattice trapping, is responsible.

(f) 3. Emerimental work (e.s.r.). The crystal was examined under a polarizing microscope by the author and the optic axis was found. The specimen was then examined in the e.s.r. spectrometer in two orientations: (i) with the optic axis parallel to the r.f. field (X-axis) and (ii) with the optic axis perpendicular to the r.f. field (Y- and Z-axes). The angle between the X-axis and the optic axis is θ. A resonance was found to occur at 293° and 77°K. Since at 293°K the signal was very small and observable only in favourable orientations, most of the work was done at 77°K.

The microwave spectrum shows that there are six types of magnetically distinct centres, each with electronic spin $\frac{1}{2}$, but with differently orientated axes of magnetic symmetry. Typical examples of the e.s.r. spectra are shown in Figures IX 5 and 6. The measurements suggest that the magnetic level of each unit

can be described by the spin Hamiltonian

$$\mathcal{H} = g_{//} \underline{H} \cdot \underline{S} + g_{\perp} \underline{H} \cdot \underline{S} \qquad (9.10)$$

where $g_{//} = 2.08 \pm .01$, $g_{\perp} = 2.02 \pm .01$, $\theta = 10 \pm 3^{\circ}$. No other resonance was found within the range of the magnet (500 - 6000 gauss).

From these observed g-values, it is clear that the spectra obtained are quite obviously not due to a resonant absorption by the Praseodymium ion. Moreover, they strongly suggest that the resonance is due to an electron being trapped on impurity sites (J1) (see next section).

From the spectra, the number of spins observed in the sample was calculated to be 10^{16}, giving a spin density of about 1 in 10^5 LaF_3 molecules. This value compares with the doping density suggested by Dr. Jones. Since Pr^{3+} has a nuclear spin of 5/2, h.f.s. on the resonance line is possible, but no conclusive evidence for this was obtained (due to the small size of the e.s.r. signal, limiting the amount by which the modulation depth could be reduced).

When the sample is mounted with the optic axis perpendicular to the r.f. field, the resonance showed 120° rotational symmetry, which relates to a hexamolecular cell. The recording, Figure IX 5, shows, as an example, the spectrum obtained with the X-

and Y-axes parallel to the "b" and "a" dimensions of the cavity respectively, and demonstrates clearly the three lines expected from a hexamolecular unit cell. The pen-recording, Figure IX 6, shows the effect of rotation of the crystal in the same plane at 10^{o} intervals. The line can be seen splitting into two components, of approximately equal intensity. This further splitting shows that the centres are not paired, but that the symmetry is even lower. These spectra show that this extra distortion is perpendicular to the Y-Z plane. This evidence suggests that the electron trapping site found in this crystal is similar to that occupied by impurity rare earth ions in this host lattice.

It can also be noted from Figure IX 6 that the two lines have different line-widths, in the ratio of about 2:1. The narrower line in Figure IX 6 (d) has a width of 35 ± 5 oe. ($mod^{n.}$ 7 oe.). When the sample was allowed to warm up slowly (2^{o}/min.), it was found that between 125 - 130°K, the broader line disappeared, leaving only the narrower, which remained, although diminishing in intensity, up to 293°K. These observations seem to be indicative of a trap emptying. The difference in line-width also suggests two different trapping sites. Using equation (9.1), one can make an approximate calculation using the above data, which suggests that one trap has a depth of .29 ± .05 ev., and the other a depth greater than .85 ev.

Summary of experiments carried out on inorganic phosphors.

Phosphor	Approx Temp. °K	Dewar.	absorption band Å	Lamp.	method of observation	Crystals.	Angular rotation	calculated spin density.	spectrometer sensitivity. S:N::1:1 ΔH:1.	τ
$Ba\ Pt\ (CN)_4.4H_2O$	77	metal	<3400	medium pressure Hg lamp.	video & pen-recording.	single. 2 modifications.	0 – 360° 2 orthog. planes	$5\ 10^{12}$	5:1	2·5 min.
$UO_2(NO_3)_2.6H_2O$	77 4	metal glass	—			single.	0 – 360° 2 orthog. planes	—	—	—
$K_2(UO_2)(NO_3)_4$	77	metal	<3400			single. 2 modifications.	0 – 360° 2 orthog. planes	10^{14}	200:1	∞
KCl (TlCl)	305 77	metal	<3400			single. 2 concentrations	0 – 360°	not estimated	—	20 min.
$LaF_3\ (Pr^{3-})$	77	metal	<3400			single.	0 – 360° 2 orthog. planes	10^{11}	1:1	5 sec.
Anthracene et al.	305	—	<3400			single.	0 – 360°	—	—	—

Figure IX 7

Irradiation with u.v. light produced no observable effect on the e.s.r. signal, nor was any new resonance detected. Since the extinction coefficient of the wavelength needed to excite the phosphorescence is not known, it is not clear whether or not enough light was available or not, and the wavelengths involved precluded the use of lower temperatures. Nor did the author study the crystal at 1.6°K in an effort to find a Pr^{3+} absorption, since the g-values expected were beyond the range of the spectrometer (observable $g_{min} = 1.0$).

IX (g) Conclusion. A summary of the experimental work tackled in this chapter is given in Figure IX 7. The optical work suggests that (except for uranyl nitrate) these phosphors all belong to Class 1, and as has been indicated in the individual sections on these phosphors, the probability of observing e.s.r. is not high, due to the low spin density, but for the sake of completeness a summary is given below of the various factors which could inhibit the detection of e.s.r. in these samples:-

i) Strong spin-lattice interaction; to increase the broadening to 100 oe., the magnetic spin state lifetime must be shortened to the order of 10^{-9} sec.

ii) Saturation broadening; this implies the reverse condition to (i), i.e. a very long lifetime for the spin state and is more likely with this type of experiment.

iii) Dipolar broadening; this is proportional to r^{-6} where r is the distance between the interacting spins.

iv) Electrons in a wide variety of traps, so that the number in any one set is low. This situation could lead to a spread in g-values and in line-widths which could make the line undetectable.

v) If the spin state has a quantum number of one or more, zero-field splitting could be significant, so that an e.s.r. absorption could not be detected with the present X-band equipment.

vi) Nuclear interaction broadening; Curie (L3D) gives the following relations:-

for an electron constrained to a hydrogen-like model of localized states,

$$a = .53\ K' \text{ (angstroms)} \qquad (9.11)$$

$$E = 13.5\ K'^{-2} \text{ ev.} \qquad (9.12)$$

where a = the orbital radius of the electron and K' = the effective dielectric constant.

K' can be eliminated from these equations and for a trap depth of .2 ev. (as commonly found in this chapter) a can be found to be approximately equal to 4A. So it can be seen that an electron in such a trap travels over a fairly large volume. Thus it may be expected to suffer considerable interaction with neighbouring nuclei (if they possess a nuclear spin) and certainly

the orbit will be considerably disturbed.

vii) In the work on ZnS(Cd) (Cl0), it was found that the majority of crystals did not give any e.s.r. signal, the experimental data being confined to a single specimen. These authors attributed the absence of a signal to a coupling of trapped electrons and ionized activators to form a low lying (diamagnetic) singlet state.

Thus it may be seen that there are many varied reasons for the absence of e.s.r. In general it is very difficult to distinguish between the different ones. It is still possible that an increase in sensitivity (see Chapter 11) might lead to detectable absorptions in some cases, and if the work could be carried out in the metal dewar at 1.6^{o}K this might help even further by completely freezing in the phosphorescence.

CHAPTER X

Miscellaneous samples.

In this chapter, the results are given of preliminary e.s.r. work on some other specimens which have been studied by the author. These samples, which have no connection with phosphorescent phenomena, were:-

X (a) Three charge-transfer complexes.

X (b) Lead di-fluoride (doped with Cerium).

X (c) BAAACP.

X (a). Charge-transfer complexes.

At the suggestion of Dr. Read (Chem. Dept.) three C-T complexes were studied. The donor and acceptor components are shown in Appendix 7. The solvent used was acetonitrile, a very lossy liquid which limited the permissible sample volume. A single narrow absorption line was observed for the tri-methyl-amine - dichloroquinone (D.D.Q.) complex, but no line was detected for the others. Dilution to a concentration of somewhat less than 10^{-4}m/l, failed to reveal any hyperfine structure on the observed line. The g-value was found to be 2.026 ± .003, while the line-width was some 3 oe. (mod^{n}. 1.5 oe.). An estima-

tion of the spin density showed that only about 1% of the molecules present were forming a complex at this concentration.

Discussion. The g-value found for the resonance line indicates that the charge-transfer electron has very little residual spin-orbit coupling.

The resonance line has a very narrow line-width and the general shape is Lorentzian rather than Gaussian, which suggests that considerable exchange narrowing was still occurring. The reason for this, however, is not clear, since at the concentrations used, the effect of this mechanism should be small. D.D.Q. is a much stronger reducing agent than T.C.P.A., having a larger redox potential than chloranil. Brown (S1) has discussed the action of D.D.Q. on sodium, p-phenylenediamine and tetramethyl-p-phenylenediamine, obtaining a similar narrow line for all three. The lack of resolved h.f.s. was attributed to an exchange mechanism between the D.D.Q. molecules, since at the dilutions used (as here) other broadening mechanisms should be small.

Since the spectrometer was not designed for lossy work, and was fitted with a fixed length cavity, further dilution of the sample could not be attempted. Recent work has shown that for maximum sensitivity with this type of solvent, a flat rectangular cell, capable of accurate positioning in the cavity,

should be used (R31, R32).

X (b). Lead fluoride (cerium doped).

This sample was also grown (from the melt) by Dr. Jones of Aberdeen (D11). The cerous ion has a spin of 5/2, but previous work in other host lattices (Q7) has shown that the crystal field splitting is small and that it is necessary to work at low temperatures to resolve the resonance lines. Even so, the e.s.r. absorption line, which should split into a lower quartet and an upper doublet (from crystal field theory), still shows evidence of considerable spin-orbit coupling (D12).

The concentration of cerium in the sample was .5%, but the crystallographic axes (of the sample) were not known since an X-ray study has not yet been made. The crystal structure of pure PbF_2 is cubic, but that of the doped salt is unlikely to be as simple since charge compensation must occur with cerous (Ce^{3+}) impurity ions.

Nevertheless, a sample was studied several times at 1.6°K, at different orientations, in the hope that it might have split along a cleavage plane (although it is known that PbF_2 does not do so readily). Strong resonances were observed, but as these were very complex, no interpretation has been possible, since it is difficult to follow a set of anisotropic lines on rotation, especially if the crystal is not aligned along an axis.

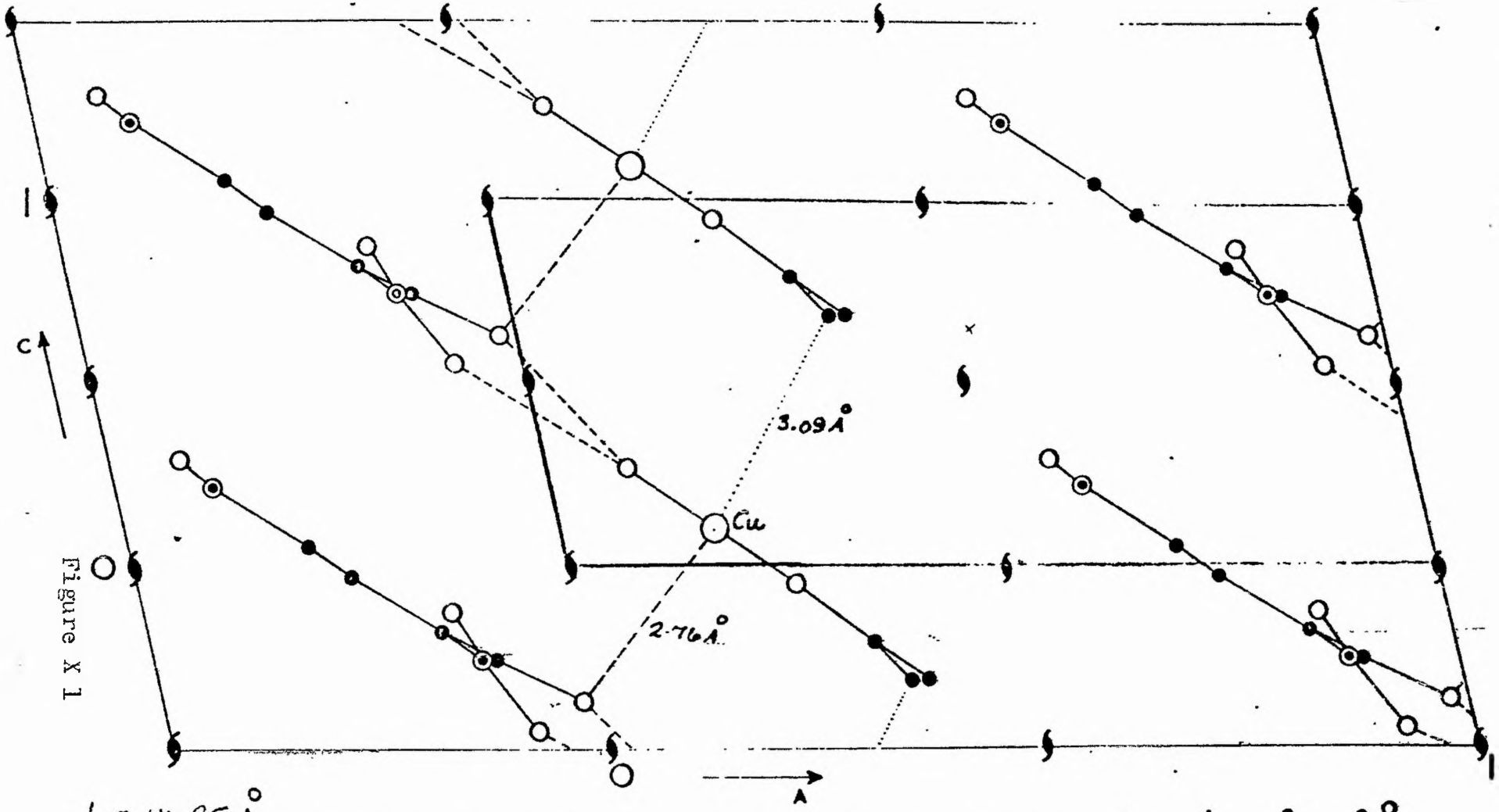

Figure X 1

One layer of molecules showing co-ordination around Copper.

○ = Cu ○ = O ◎ = N ● = C

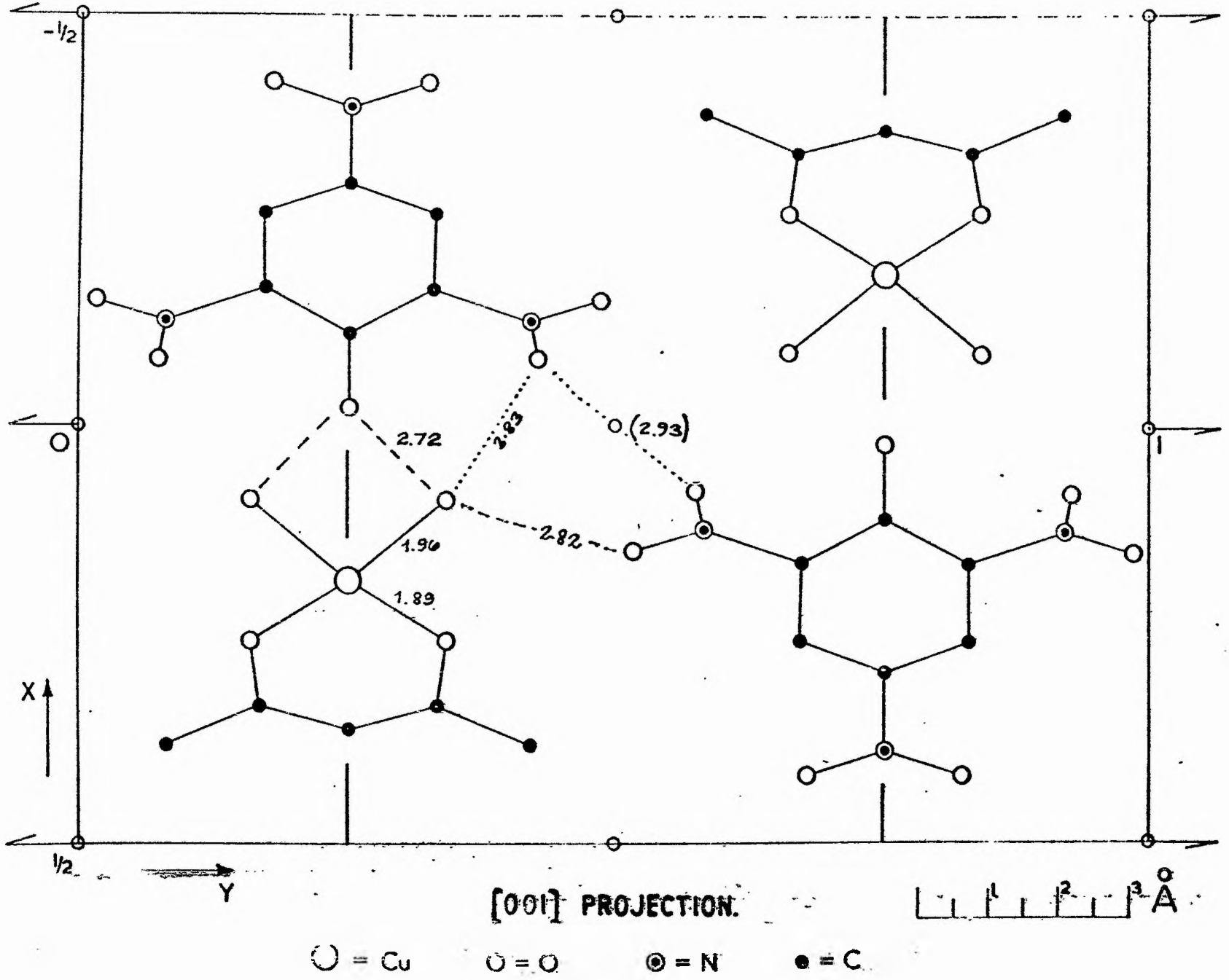

Figure X 2

However, it did seem that there were two distinct sets of resonances occurring between g = 2.7 - 2.1 and g = 1.8 - 1.5, values which are similar to those found for CaF_2(D13).

Since it was apparent that little real progress could be made with this particular sample until the crystallographic axes and the symmetry of the impurity site were found, a more detailed study was not attempted.

X (c). bis-aquo-acetylacetonate-Copper(II) picrate. (BAAACP)

(c) 1. Introduction. This substance was supplied by Gillard and Rogers who first prepared it; they also supplied the crystallographic data used below (K1). Two of their structural drawings are reproduced in Figures X 1 and 2, and show that the molecule is a large planar one, in which one of the acetylacetonate groups has been replaced by a picrate group. The bright green crystals are monoclinic with a cell dimension, a = 11.36A, b = 14.95A, c = 4.17A, $\beta = 103^{\circ}$, containing two formula units/cell. The symmetry is $P_{21/m}$.

The main points of interest for an e.s.r. investigation which were raised by the crystallographic study are:-

i) the molecule is nearly a planar structure, and stacked in sheets almost parallel to the (201) direction at a separation of about 3.4A.

ii) each copper atom is octahedrally co-ordinated to a fifth oxygen, the phenolic oxygen in an adjacent sheet. This link is

not quite normal to the plane of the four main Cu-O bonds (about 3 - 4° off normal), and is apparently fairly strong since it has dragged the oxygen out of the plane of the molecule. iii) the γ-carbon of the acetylacetonate ligand lies .13A out of the plane of the otherwise excellently planar ligand, and the question arises whether this is an example of a copper-carbon bond, which apparently has not been previously reported (although platinum-carbon bonds have been studied).

An e.s.r. study might be useful in settling this question.

(c) 2. Previous work. Cu (II) has been studied extensively by e.s.r. techniques, being amongst the earliest investigated. This ion, as well as forming essentially ionic compounds, can also form covalent bonds. Cu (II) has nine electrons in its 3d shell, and in a tetragonal or rhombic crystalline field the splitting is such that the ion has an effective spin of $\frac{1}{2}$. The bonding in transition metal ions can be described in terms of the ligand field theory. This theory regards the central transition metal ion as a positive ion surrounded by negatively charged atoms, even when the bonding is known to be appreciably covalent. The theory considers the effect of the electrostatic field due to the ligands upon the d orbitals of the central metal atom (K2). For an octahedral arrangement of ligands on Cu(II) ions, it can be shown that for both weak and strong ligand fields, the natural filling order of the levels is disturbed, the six

d_ϵ (d_{xy}, d_{yz}, d_{zx}) levels being filled before 3 of the 4 d_γ ($d_{x^2-y^2}$, d_{z^2}) levels. (where x, y and z represent a rectangular co-ordinate system). The result of this is that the postulated octahedral arrangement is disturbed along the z-axis, but in the x-y plane the location of the ions remains almost four-square. Such a co-ordination of Cu is quite common, but a detailed X-ray investigation usually reveals that the square is slightly distorted (as it is here). For an octahedral covalent bonding arrangement the hybridized orbital is sp^3d^2.

It has always been a problem to distinguish adequately between ionic and covalent bonding. Pauling's original work (G3) used the four-square arrangement to distinguish between them, but later work has shown that this structure could result from crystalline field theory (K3). The only real difference between the two types of bonding lies in the spatial location of the unpaired electron. E.s.r. techniques may throw some light on the properties of the electronic orbit.

The location of the unpaired spin can be deduced from the anisotropy of the g-value. The distorted octahedral arrangement discussed in the above paragraph is an example of (crystallographic) tetragonal symmetry, and in many cases of this symmetry class it has been found that the axes of the g-tensor coincide with

the crystallographic axes. If this is so, then $g_z = g_{//}$ and $g_x \sim g_y = g_{\perp}$.

For purely ionic bonding, Abragam & Price (K9) have shown that $g_{//}$ should have a value of approximately 2.4 and $g_{\perp}$ about 2.1, whereas on the basis of covalent bonding it can be shown that the expected values should be $g_{//} \sim 2.0$ and $g_{\perp} \sim 2.1$ (K7).

E.s.r. studies have been made on Cu(II) bis-acetylacetonate (K4). On assuming tetragonal symmetry, the results showed that in this case the bonding was partly ionic, partly covalent, the g-values obtained being: $g_{\perp} = 2.075 \pm .001$ and $g_{//} = 2.254 \pm .008$. The resonance line showed considerable narrowing.

The only other comparable molecule which has been studied in detail is Cu(II) phthalocyanine, in which the four ligating atoms are nitrogens. The phthalocyanine molecules show much more aromatic character than the chelates and behave differently in comparison with the salts above (e.g. K5).

(c) 3. Experimental work and discussion. The crystals of EAAACP are in the form of needle-shaped laths, with the (010) face well developed. The (101) or (201) edge is also prominent and allows a correct assignment of the crystal axes. The crystals, however, are rather small, the biggest being (.08 x .002 x .0005 cm.), which means that the number of Cu(II) ions in the specimen is only $2\ 10^{14}$. Some preliminary work was done using an assembly of 10 crystals aligned under a microscope, but because of their

Figure X 3 (a).

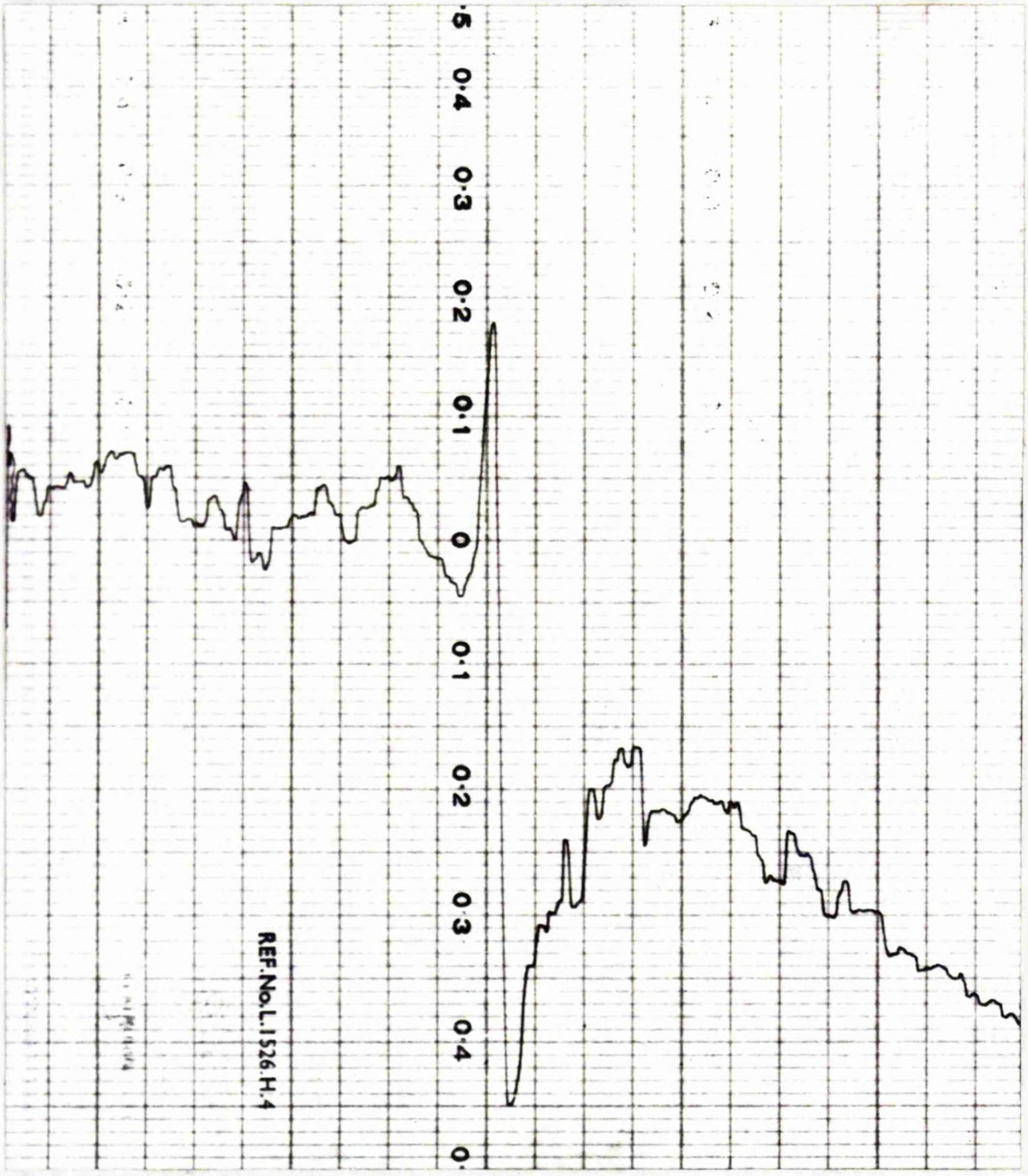

Sample : BAAACP. single crystal. Temperature : 110°K.
Orientation : the recording shows the narrowest line-width found when the crystal was rotated in the b-c plane. (see Figure X 6).
Field sweep : electronic. Field swept = ~2560 - 3890 oe. (linear ± 3 oe.) 1 division on recording = 65 oe.
Field direction : increasing left to right.
Mod$^{n.}$ = 10 oe. τ = 1 sec. dH/dt = 4.3 oe/sec.
ν = 9427 Mc/s. centre of line at 3209 ± 10 oe.

Figure X 3 (b).

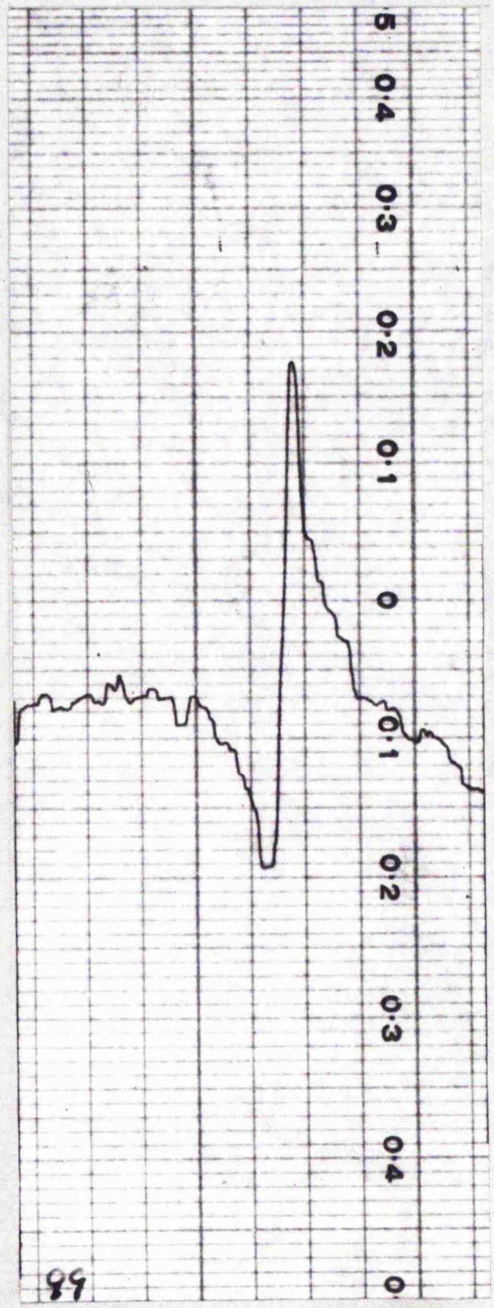

Sample : BAAACP. single crystal.
Temperature : 110°K
Orientation : crystal rotated in the a - c plane. The recording shows a typical broad line (~200 oe) (at position marked on Figure X4.)
Sweep : electronic sweep mechanism. This recording was one of a series taken for line-shape studies and is not of the accuracy used in g-value and line-width measurements.

centre of line at 3200 ± 30 oe.
1 division of paper = ~500 oe.
Field direction : increasing left to right.
Mod$^{n.}$ = 10 oe. τ = 1 sec.
dH/dt = 20 oe./sec.
ν = 9480 Mc/s.

extreme smallness and fragility it was rather difficult to ensure parallelism. It was, however, just possible to obtain spectra from a single crystal, as shown in Figure X 3, although to observe the signal at all orientations it was necessary to work near 100°K. As far as could be ascertained, there was no difference between the spectra obtained at 100° and at 300°K.

(c) 3.1 g-values. The g-values were measured in the a - c and b - c crystallographic planes. The values measured in the a - c plane are given in Figure X 3, where it can be seen that the variation found on rotation of the sample is very small. Due to the relatively large field-measurement error (see below) in comparison with the observed variation, it was not possible to measure the maximum and minimum values of the g-value to the same accuracy as was attained in other experimental work. The g-variation measured in the b - c plane (not shown) is also very small and can be taken to be almost constant at 2.09 ± .02. The large error in g-value measurement was a consequence of the very wide line-widths of the e.s.r. absorptions; with such large line-widths, it is very difficult to establish a base-line with normal e.s.r. apparatus, especially at high sensitivity.

Discussion. With crystals of BAAACP, it is not possible to postulate confidently any type of g-tensor symmetry for the Cu ions, due to the unknown effect of the different ligating atoms (O and C) in the z-direction. The tetragonal symmetry

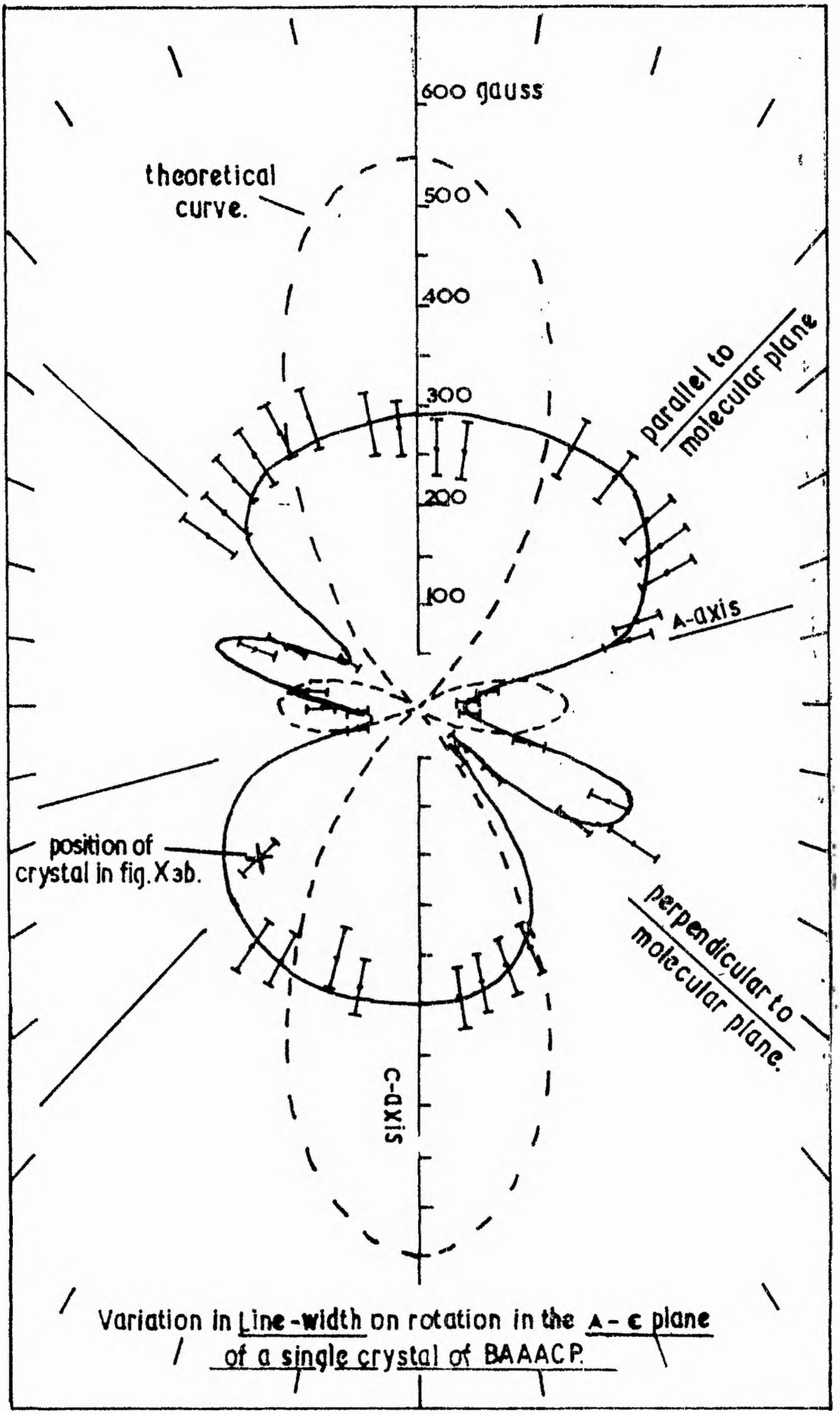
600 gauss
500
400
300
200
100
theoretical curve.
parallel to molecular plane
A-axis
position of crystal in fig. X3b.
perpendicular to molecular plane.
C-axis
Variation in Line-width on rotation in the A - C plane of a single crystal of BAAACP.

Figure X 4

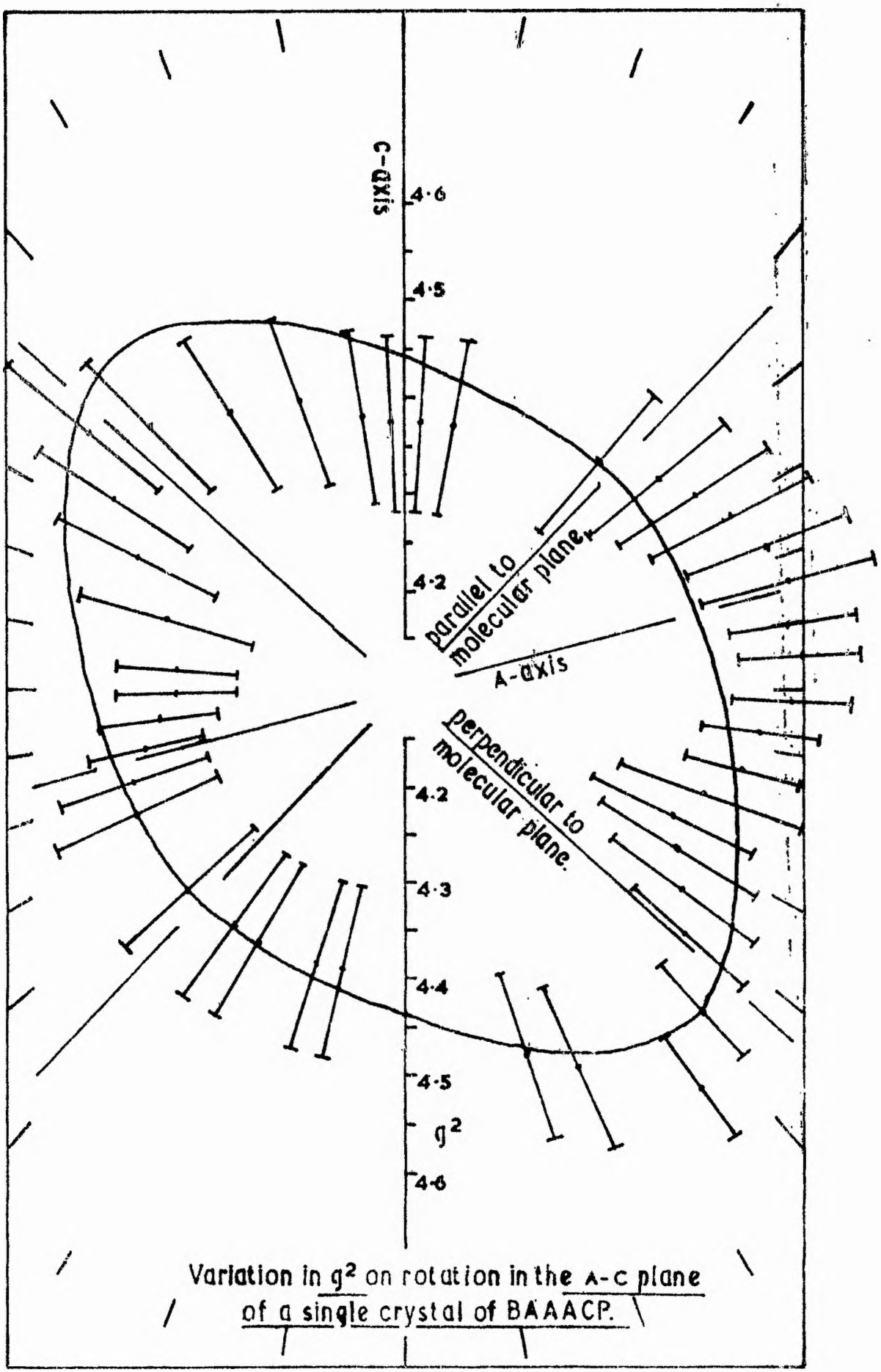

Variation in g^2 on rotation in the A-C plane of a single crystal of BAAACP.

Figure X 5

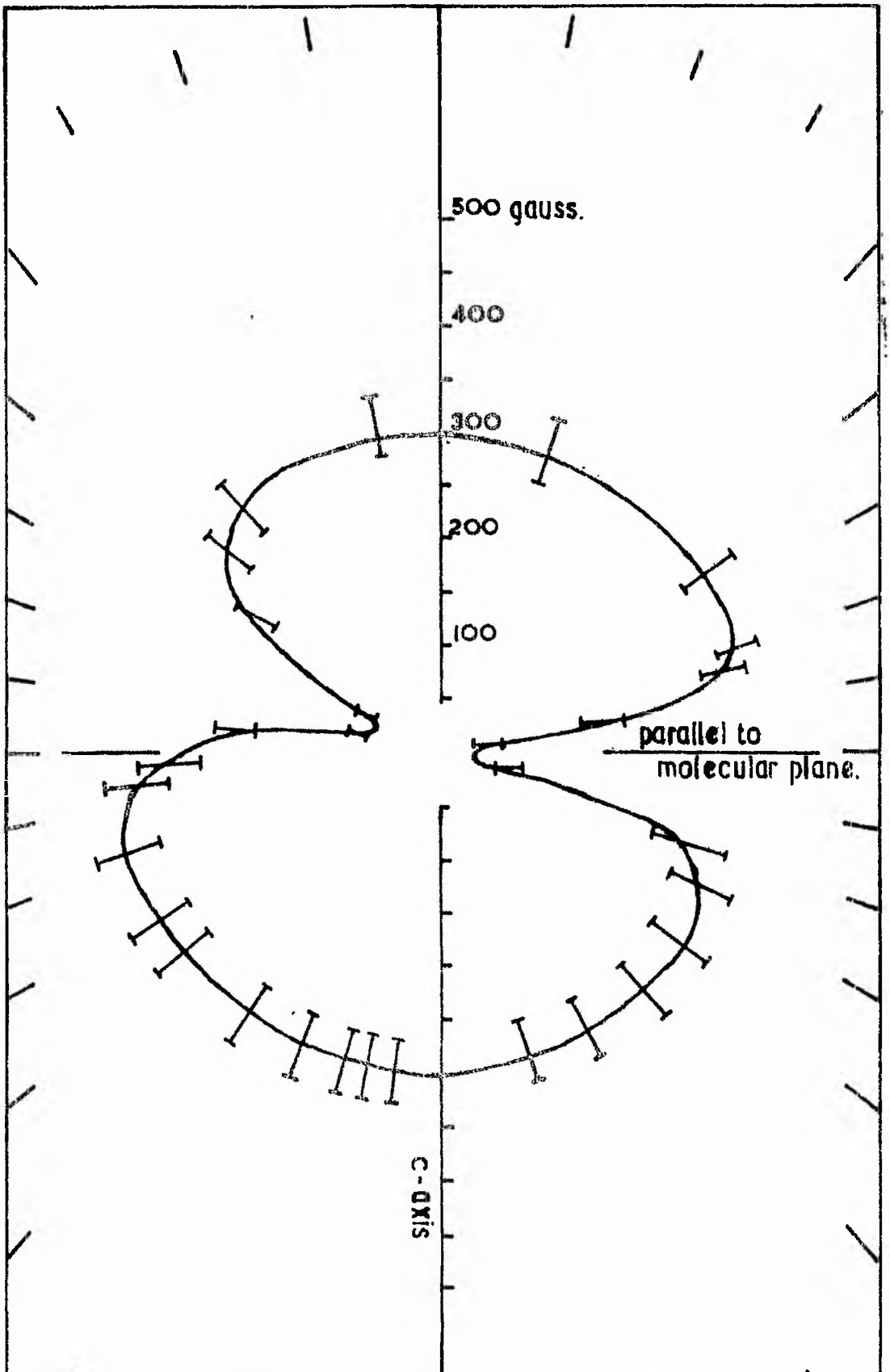

Variation in Line width on rotation in the B-C plane of a single crystal of BAAACP.

Figure X 6

which was found for Cu(II) bis-acetylacetonate cannot be expected to hold in the case of BAAACP. In fact, a lower symmetry can be expected (i.e. one in which the x, y and z-susceptibility axes, although still forming an orthorhombic system, will no longer have any direct relationship with the crystallographic axes (see K8, p. 323)).

The absence of any marked variation in the g-value makes it very difficult to draw any conclusions on the actual molecular symmetry around the copper ion. However, since all the g-values observed in both planes fall within $g = 2.11 \pm .04$, it seems that ionic coupling (leading to values of $g \sim 2.4$) is not at all probable, but it is not possible to estimate the degree of covalency on the evidence available.

(c) 3.2 Line-width variations. The observed variations of the line-width of this salt, measured in the a - c and b - c planes are shown in Figures X 4 and 6. Also shown on Figure X 4 is the theoretical curve which would have been expected on the basis of pure dipole-dipole interaction. This theoretical curve was first applied by Bleaney (K8) who was working with Cu doped Tutton salts. As can be seen, there is considerable distortion and dissymmetry in the observed curve, although much less so than in the case of Tutton salts.

The theoretical variation of the line-width with angle due to dipole-dipole interaction alone can be calculated from

the formula due to van Vleck (see K8):-

$$(\Delta H^2)_{av} = \tfrac{3}{4} g^2 \beta^2 S(S+1) \sum_j (1 - 3\cos^2 \theta_{ij})^2 r_{ij}^{-6} \quad (10.3)$$

where $(\Delta H^2)_{av}$ is the "mean square moment" and θ_{ij} is the angle between the magnetic field and a line joining spins i and j.

In the crystals of BAAACP, the nearest neighbours are at 4.75 ± .15 A, while the next nearest neighbours (the Cu ions of the other molecule in the unit cell) are at 8.9 A. Since the mean square width varies as the sixth power of the Cu-Cu spacing, it is only necessary to consider (to a first approximation) the nearest neighbours at (0,0, ± 1). Substitution of the approximate quantities in equation (10.3) yields (along the Cu-Cu axis) a value of 257 ± 25 oe.

$\left[(\Delta H^2)_{av}\right]^{\frac{1}{2}}$ can also be evaluated from the experimentally observed line-width using the definition (K10):-

$$(\Delta H^2)_{av} = -.3 \int_0^{\infty} (\Delta H)^3 \frac{dg(\nu)}{d\nu} \cdot d\nu \quad (10.4)$$

Because of the rather low S:N ratio obtained for the absorption along the Cu-Cu axis, it has not been possible to evaluate this equation with any confidence. van Vleck has shown that, if the line has a Gaussian distribution

$$\Delta H_{\text{max. slope}} = 2\left[(\Delta H^2)_{av}\right]^{\frac{1}{2}} \quad (10.5)$$

The measured line-width for this salt along the Cu-Cu axis in the case of a Gaussian distribution should therefore be

about 550 ± 50 oe., instead of the experimental value of 300 oe., indicating the presence of some other factors.

The observed line-shape in fact does not seem to be constant on rotation (although this is difficult to judge for the wider lines) and in fact appears to be somewhat asymmetric at certain positions (including that along the Cu-Cu axis). These variations are possibly due to unresolved hyper-fine structure on the line.

(c) 4. Conclusion. The preliminary study of this material has shown that e.s.r. techniques may be used. It has not been possible at this stage, however, to obtain any significant information on the nature of the Cu - C bond. It can be seen from the work above that to obtain more detailed information from these samples, a larger crystal is necessary. The author tried unsuccessfully to grow larger crystals by recrystallization methods. A magnetically dilute crystal, containing a single Cu isotope, would also be preferable - palladium might be a suitable non-paramagnetic ion (see e.g. K6). It might be possible thus to obtain more detailed information on the degree of covalency of the bonding using such a crystal.

CHAPTER XI

Summary and suggestions.

The work which has been done has revealed that the application of electron spin resonance to the field of phosphorescence is possible in a few selected cases. Work on organo-phosphors is by far the most promising at the moment, as can be seen from the volume of work being published. The study which has been initiated on the problems of charge-transfer complexes has already raised a number of interesting problems. The use of e.s.r. absorption resonances to separate complexed and uncomplexed emissions is an example of a situation which could be tackled by e.s.r. alone and not by spectroscopic work, which could measure only the total emission.

The work done on the so-called "pure" inorganic phosphors suggests that it is doubtful if significant e.s.r. results could be obtained. The work in this field, especially, has emphasized the difficulty of obtaining reliable data. The compilation of a catalogue of phosphors, together with their characteristics, would surely be of great help to many workers. The advance in understanding of phosphorescent processes has

nullified much of the earlier work, principally because strict control of the preparation of the phosphors was not observed. It seems that an accurate measurement of the total light sum (a very simple experiment) could yield much useful data. The work done by the author has been restricted by the absence of relevant optical data, and it is fairly obvious that the setting up of an optical arrangement, capable of studying absorption, total and phosphorescent emissions, decay period and polarization data, etc., would be highly advantageous.

Several modifications to the spectrometer have also become obviously necessary during the work carried out. The spectrometer was in the first place designed on the assumption that reasonably large spin densities would be available. In fact, this expectation has not been fulfilled except in only a few examples. In view of this experience, it seems desirable that the sensitivity should be increased wherever this is possible. In certain circumstances, a more highly powered klystron might be profitably used, while a balanced mixer unit, with more sensitive detecting crystals, is essential.

One of the disadvantages of the present A.F.C. circuit is that, in common with all sample cavity systems, it depends on an error signal of reasonable amplitude, so that, if saturation is suspected, it is not possible to reduce the power to a

sufficiently low level. An external reference-cavity system, would be a great help in such circumstances.

The success of the gas-flow system suggests that a more sophisticated system could be usefully set up, possibly using liquid hydrogen as the refrigerant. A dewar, with a quartz optical system, functioning at liquid helium temperatures, is also needed.

Finally, the desirability of evolving some method of establishing the purity of the samples must also be considered. Although there is no evidence of (unknown) impurities being significant in the present work, it is a possibility which should be recognized and taken into account.

Appendix 1

Design details of the K1.A.F.C. circuit

1 (a). Derivation of the modulated carrier-wave

The V.S.W.R. of a cavity is given by

$$\frac{\frac{1}{Q_{ext}}}{j\left(\frac{\omega}{\omega_o} - \frac{\omega_o}{\omega}\right) + \frac{1}{Q_o}} \qquad (A1.1)$$

where Q_{ext} = external Q, Q_o = unloaded Q, and ω_o = resonant frequency of the cavity.

The reflection coefficient $/^-$ is defined as

$$/^- = \frac{V.S.W.R. - 1}{V.S.W.R. + 1} \qquad (A1.2)$$

Substituting (A1.1) into (A1.2),

$$/^- = \frac{\frac{2}{Q_{ext}}}{\left(\frac{1}{Q_{ext}} + \frac{1}{Q_o}\right) + j\left(\frac{\omega}{\omega_o} - \frac{\omega_o}{\omega}\right)} - 1 \qquad (A1.3)$$

Near resonance $\omega \rightarrow \omega_o$, and $Q_{ext} \approx Q_o$, so (A1.3) can be rewritten:-

$$/^- = \frac{1}{1 + Qj\left(\frac{\omega}{\omega_o} - 1\right)} = \frac{1}{1 + jd} - 1 \qquad (A1.4)$$

where d is defined as $Q\left(\frac{\omega}{\omega_o} - 1\right)$ (A1.5)

On rationalizing,

$$/^- = \frac{-d^2}{1 + d^2} - j\,\frac{d}{1 + d^2} \qquad (A1.6)$$

The carrier wave of the klystron can be written as $V = B \cos \phi(t)$, where $\phi(t) = \int \omega_i dt$; with no frequency modulation, ω_i = a constant, ω . If the frequency of this carrier wave is modulated by a lower frequency wave, $A_1 \cos pt$, then $\omega_i = \omega + \Delta\omega \cos pt$ where $\Delta\omega$ = the maximum deviation of ω_i from ω .

Thus, V can be written as

$$V = B \cos(\omega t + \frac{\Delta\omega}{p} \sin pt) \qquad \text{(A1.7)}$$

where $\frac{\Delta\omega}{p} = m_f$, commonly known as the modulation index.

$\Delta\omega$ is found by the relation, (in the case of the K302 klystron):-
1 volt change applied to the repeller = 2Mc/s. frequency change of carrier.

By Fourier analysis, equation (A1.7) can be written:-

$$V = BJ_o(m_f) \cos \omega t + B \sum_{n=1}^{\infty} \left[J_n(m_f) \cos(\omega + np)t + (-1)^n \cos (\omega - np)t \right] \qquad \text{(A1.8)}$$

1 (b). Evaluation of equation (A1.8)

Typical values of $J(m_f)$ are:-

Sidebands (Mc/s.)	Energy in band as a % of the total energy		
	$m_f = 5$	$m_f = .5$	$m_f = .05$
0	12%	80%	98%
± 5	22	20	2
10	3	-	-
15	25	-	-
20	28	-	-
25	18	-	-
30	9	-	-

At $m_f = .05$ it can be seen that there is no significant power lost in the sidebands and so the sensitivity of the spectrometer is unimpaired. Using a modulation frequency of 5Mc/s. (see III (d) 3), this value of m_f means that $\frac{\Delta\omega}{2\pi} = .25$Mc/s., which corresponds to an amplitude modulation on the repeller of the order of 100mv.

1 (c). Application of equation (A1.8) to the present circuit.

If a value of $m_f = .05$ is used, equation (A1.8) can be written as:-

$$V^i = BJ_o \cos\omega t + BJ_1 \cos(\omega + p)t - BJ_1 \cos(\omega - p)t \quad \text{(A1.9)}$$

The voltage which reaches the cavity will be $V^{ii} = V^i/\sqrt{2}$, due to the magic tee, and the voltage reflected by the cavity will now be

$$V^{iii} = \frac{B}{\sqrt{2}}\left(J_o \bar{/}_1 \cos\omega t + J_1 \bar{/}_2 \cos(\omega + p)t + J_1 \bar{/}_3 \cos(\omega - p)t \right) \quad \text{(A1.10)}$$

where $\bar{/}_a = \frac{d_a^2}{1 + d_a^2} - j\frac{d_a}{1 + d_a^2}$ $\quad (a = 1, 2, 3)$ $\quad \text{(A1.11)}$

where $d_1 = Q\left(\frac{\omega}{\omega_o} - 1\right) = Q\frac{d\omega}{\omega_o}$ $\quad \text{(A1.12a)}$

$$d_2 = d_1 + d_p \quad \text{(A1.12b)}$$

$$d_3 = d_1 - d_p \quad \text{(A1.12c)}$$

$$d_p = Q_p/\omega_o \quad \text{(A1.12d)}$$

The signal then goes through a 10db. coupler, so $V^{iv} = V^{iii}/3.2$.

Thus the voltage reaching crystal X1 is

$$V^{iv} = R\cos\omega t + S\cos(\omega + p)t + T\cos(\omega - p)t \quad \text{(A1.13)}$$

where $R = \frac{BJ_o \bar{/}_1}{\sqrt{2}\ \ 3.2}$, etc.

1 (d). Rectification by the crystal

The rectified current given by the crystal can be described by a characteristic of the form, $i = av + bv^2$. (A1.14)

By substituting (A1.13) into (A1.14), and averaging out factors involving ω, (as this frequency is smoothed out by the relatively long time-constant of the crystal) and also ignoring factors in 2 pt (as they are not passed by the following tuned amplifier, which also removes all constant (i.e. d.c.) terms), it is found that

$$i = \frac{b}{2} R(S + T) \cos pt \qquad (A1.15)$$

1 (e). Numerical evaluation of equation (A1.15)

Using equation (A1.13), $R(S - T) = .05\, B^2 J_o J_1 \bar{/}_1(\bar{/}_2 - \bar{/}_3)$

and from equations (A1.11 and A1.12),

$$\bar{/}_1(\bar{/}_2 - \bar{/}_3) = \frac{-2d_1 d_p + 2jd_1^2 d_p}{1 + d_p^2} \qquad (A1.16)$$

using the assumptions $d_1^2 \ll d_p^2$ (See 1 (f).)

$$d_1^2 \ll 1$$

Equation (A1.16) has a modulus $\frac{2d_1 d_p}{1 + d_p^2}$, and an amplitude $\tan\theta = d_1$.

Therefore, cos pt is shifted to $\cos(pt + \tanh d_1) \approx \cos(pt + d_1)$ (A1.17)

And so combining equations (A1.15, 16 and 17), it is found that

$$i = \frac{.025\, B^2 b\, J_o J_1\, 2\, d_1 d_p \cos(pt + d_1)}{1 + d_p^2}$$

B can be replaced by PZ_o, where P is the output power of the klystron and Z_o the characteristic impedance of the waveguide. The value of b can be roughly obtained, since I = W in the microwatt region and $W = V^2/Z_o$, so $b = 1/Z_o$.

The input impedance of the amplifier is 70 ohms, so V_1, the input voltage to the amplifier is

$$V_1 = \frac{i}{70} = \frac{3.5\ P\ J_o J_1\ d_1 d_p\ \cos(pt + d_1)}{1 + d_p^2} \qquad (A1.18)$$

which can be written as

$$V_1 = A_2\ d_1\ \cos(pt + d_1)$$

1 (f). Desired stability

This is one of the design conditions, and the value chosen was 1 in 10^6, i.e. 10kc/s., since this frequency is the smallest change in frequency which can be detected by the wavemeter, and it was known that changes of this magnitude have no effect on the balance conditions of the spectrometer. So substituting the appropriate values in equation (A.18) it is found that

$$V_1 = 1.5\ \ 10^{-6} \text{ volts} \qquad (\cos(pt + d_1) = 1) \qquad (A.19)$$

1 (g). Phase-sensitive detector

In 1 (e), the voltage developed at the input to the tuned amplifier has been found, and since the voltage applied to the repeller must be at least .5v/Mc/s., the next step is to calculate the input voltage to the P.S.D. to give a voltage change of the correct magnitude.

The phase-sensitive detector used is a pentode in which the signal (error) voltage is applied to the suppressor grid and a constant amplitude and phase voltage to the control grid.

Let the error voltage be represented as $GA_2d_1 \cos(pt + d_1)$ (cf. (A1.18)) and the reference voltage as $A_1 \cos pt$. (where G is the amplifier gain.)

The characteristics of a valve operating in this condition are fully discussed in (ref. T6), and if the input voltages given above are put into the relevant equations in (T6), the following result is obtained:-

$$\left[\Delta V_a\right] = \frac{g_c R\, R_a G A_1 A_2\, d_1 \cos d_1}{2\,(R + R_a)} \qquad (A1.20)$$

where $\left[\Delta V_a\right]$ = the change in anode voltage, R = the anode load, R_a = the anode slope resistance, g_c = the combined mutual conductance for the valve operating in this condition and has to be estimated graphically. Substituting in the values for this valve (R = 100K, R_a = 1M, $d_1 \ll 1$, $g_c = 25\ 10^{-6}$ amp/volt^2), it is found that

$$\left[\Delta V_a\right] = GA_1A_2\, d_1 \text{ volts.} \qquad (A1.21)$$

But it is already known that for a frequency change of 10kc/s. the control voltage on the repeller $\left[\Delta V_a\right]$ must change by $5\ 10^{-3}$ v., and if the reference voltage is 10v.(p.t.p.), then

$$GA_2 = \frac{5\ 10^{-4}}{d_1} \text{ volts.} \qquad (A1.22)$$

A_2 has already been calculated in equations (A1.18 and 19), and is approximately $5\ 10^{-4}$v. So the necessary gain required from the tuned amplifier is

$$G = \frac{1}{d_1} = 300 \qquad \text{(A1.23)}$$

Thus, the minimum gain needed for the tuned amplifier has been fixed, but in fact the straight gain of the amplifier has to be greater than this, because the tuned loads have to be adjusted slightly to ensure the correct phase change round the loop; also, a higher gain is desirable in order to provide a more positive correction.

Appendix 2.

Design details of the K2.A.F.C. circuit.

In this circuit, the frequency difference must also be held to within 10Kc/s., i.e. 1 in 3 10^3. However the problem is much simpler than in the K1.A.F.C. circuit, because here the input signal is of a constant and finite magnitude. The power falling on the crystal X_4 is around 1.5mW, giving a voltage signal of about 10mV. It is desirable to provide some amplification to ensure that the valve diodes work at their optimum, since they are inherently noisy devices. The pre-amp gives a gain of 30x, which is sufficient (R29).

The input signal then has to be multiplied by a factor dG/df, where G is the gain of the coil system; for the one built G_{max} = 4 at 30 ± 1 Mc/s. The phase-sensitive signal at this point therefore has a value of 1v/Mc/s., but $\frac{3}{4}$ of this is lost in the voltage level changing stage. The voltage needed on the K2 repeller is $\frac{1}{2}$v/Mc/s., so the d.c. amplifier must have a minimum gain of 2. As before extra amplification leads to a more positive response. The amplifier has a gain of 100x, which should give a voltage correction curve of 25v/Mc/s. The value obtained is in good agreement with this. For a stability of 10Kc/s, the voltage at the pre-amp at 30.010 Kc/s. should be greater than the noise voltage, i.e.

the noise voltage should be less than 3μv. The r.m.s. noise voltage of the pre-amp is of this order (R30).

Appendix 3

Design details of the 280c/s. circuit

Low frequency oscillators, because of the necessity of using only resistive and capacitive components, are not so stable as those operating at higher frequencies. The generally quoted figure for the frequency stability of oscillators of this type is .1%. In this circuit small frequency instabilities of the oscillator are unimportant in so far as the phase-shifter, power amplifier and P.S.D. are concerned since these are not particularly frequency sensitive devices. However the narrow-band amplifier is different.

From the equations given in (T9), it can be shown that for a frequency drift of .1c/s (.03%), the change in voltage output is .6% and the phase-change is .2%. The reason why changes of such magnitude are not serious is due to the general pick-up of the system. The amplifier itself, as has been noted in (III (g) 3), has a residual oscillation of the order of 10mv. This is permissible because amplification of the Johnson noise of the spectrometer, pick-up by the cavity from the coils and general pick-up throughout the apparatus is such that the quiescent output voltage of the amplifier is 10x this value. Thus if the frequency drift mentioned above is considered, it can be seen to manifest itself only as a small change in a

relatively large quantity, whereas the signal to be observed from the spectrometer is given by a relatively large change in a small quantity. I.e., if the gain of the spectrometer is arranged so that, after amplification, a change in frequency of 10Kc/s. gives a deflection of the pen-recorder of 1 division (full-scale = 100 divisions) this means that the output of the amplifier has gone up from 100mv. to 200mv. Under these circumstances the change in amplitude of .6% is negligible; similarly the phase change makes no significant difference, provided it does not actually cause a phase-change.

This study also shows that the maximum output from the narrow-band amplifier should be as large as possible, consistent with gain linearity. The maximum output from the amplifier built was 60v., implying that S:N ratios of up to 600:1 can be displayed by the pen-recording system.

Appendix 4

An approximate estimation of the total number of quanta emitted by a phosphorescence sample

The first step is to calculate the fraction of light which the cathode of the photomultiplier tube collects. This is done by the usual formula

$$dF = \frac{Fo\ ds_1\ ds_2 \cos\theta_1 \cos\theta_2}{r^2} \qquad (A4.1)$$

where ds_1 = area of sample, ds_2 = area of the cathode = .25 sq. cm., r = distance between ds_1 and ds_2. θ is the angle between the normal to ds and r. The result can be written as $F_o = k\ dF$, where the constant k will also include an estimate for any light lost from reflections, etc.

The rest of the problem is concerned with estimating dF from the results obtained. These are plotted as a graph whose area (A sq. cm.) is obviously proportional to the light output. If the ordinate is in volts and the abscissa in seconds, A = I volt-sec. If the voltage was measured by the potentiometer method, the p.m. anode current is I/R amp-sec., where R is the grid-leak of V1. If it was measured on the scope, it is given by I/GR amp-sec., where G is the amplifier gain. Therefore the total cathode current of the p.m. tube is I/GRL, where L is the current gain of the tube. The characteristics for this tube show a current gain of 10^6 at 100v/dynode (T7, T8).

The next step is to convert the cathode current into lumens, and for this it is necessary to know the cathode sensitivity and the spectral response. From these the cathode response can be found, and for the tube used is $6\ 10^{-7}$ amp/lumen at a wavelength of 5500A. So $A = (I/GR)\ 3\ 10^{-1}$ lumen-sec.

Lumens can be converted into ergs/sec., using the definition of a lumen (650 lumen = 1 watt at 5500A), so $A = I\ 10^{5}/2\ GR$ ergs.

The energy of 1 photon at 5500A = $3.3\ 10^{-12}$ ergs, so the number of photons (n_p) detected by the p.m. tube is

$$n_p = \frac{I\ 1.5\ 10^{16}}{GR}. \qquad (A4.2)$$

And the total number of photons emitted $\sum n_p = k\ dF\ n_p$.

If the crystal absorbs light at 5500A, a further correction has to be made:

$$\phi = \int_{\text{front face}}^{\text{back face}} \phi_o\ e^{-\mu x}\ dx \qquad (A4.3)$$

where ϕ is the flux detected and ϕ_o the total flux; μ is the absorption coefficient.

The total quanta emitted therefore is given by

$$\sum n_p = \frac{\phi_o\ K\ dF\ I\ 1.5\ 10^{16}}{GR} \qquad (A4.4)$$

if the results are plotted as volts/sec.

This calculation has been carried out for a wavelength of 5500A, and can be reworked for wavelengths significantly

different.

Accuracy of the method. It is fully appreciated that the method outlined above is by no means accurate; however it is not proposed to go over each step in detail, but only to indicate the two most serious ones:- the gain of the p.m. tube (which cannot be readily checked and may well be lower than that quoted due to the age of the tube used) and the linearity of the tube and measuring circuits. The total error is estimated to be:- plus a factor of 5 or minus a factor of 2.

Appendix 5.

Examples of Class 1 phosphors

Lenard phosphors:- these phosphors were mainly microcrystalline and of very varied constitution. A typical example is

$CaSO_4(Bi,Na_2B_4O_7,CaF)$ (fired) (P3)

ZnS(Zn), ZnS(Cu) etc. (fired) phosphors of this type are probably the most commonly known. (N1)

Be or Al nitrides (τ = 1 hr.) (fired). (N2)

Boron phosphors. e.g. borophenanthrene (τ = 2 secs.)

boronphosphate (Tl) (N3, N4)

CdI (thermoluminescent peak at 120°K) (fired) (N5, N6, N7)

$CdSO_4$ (anhydrous salt) (N8)

Double phosphors. e.g. SrS(Eu,Sm), SrS(Ce,Bi), $CdBr_2$(Pb,Mn) (fired) (these phosphors can often be stimulated by infra-red light) (N4)

Manganese halides (thermoluminescent effect, see also Class 2) (N9)

Sr,Br,Mn,Zn and Cd vanadates (V_2O_5) (apparently self-activated) (N4)

Blue fluorescent diamonds have a blue émission (τ = 1 sec.) and a yellow emission (τ = 30 min.) (P5)

Many naturally occurring minerals, e.g. Kunzite (lithium aluminium silicates) (P6)

Calcium phosphate (thallium) (an example of a phosphor with pure u.v. emission (3200A) (τ = 10 mins.) (P7)

	Phosphor.	Absorption spectra. log ε 4 2	Fluorescence s.w.l.	Phosphorescence s.w.l.	$\frac{Q_{phos}}{Q_{fl}}$	τ secs.	E.S.R.	fl. line-splitting
1	NAPHTHALENE.	(1	(3 ·30 μ.	s.w.l. (3 ·47 μ.	·09 (30 ·05 (52 ·1 (4	2·6 (4 2·6 (5 2·3 (30	A1. A5. A9.	n-PENTANE.
2	CORONENE.	(1	—	(50 ·53	—	9·4 (5 9· (50 7·9 (A5	A5. A9. A18.	n-HEXANE.
3	TRIPHENYLENE.	(1	(7 ·35	(7 ·42	·51 (4	15·9 (4 15·9 (5	A5. A9.	
4	PHENANTHRENE.	(1	(3 ·35	(3 ·46	1·1 (35	3·3 (5 3·3 (35 2·8 (0	A9. A11. A18.	
5	CARBAZOLE.	(1	(3 ·34	(30 ·41	·55 (2	10 (4 7·6 (2 7·25 (30	A9.	
6	DIPHENYL	(24	(7 ·35	(13 ·44	·8 (30	4·3 (30	A9.	n-HEPTANE
7	FLUORENE.	(1	(7 ·4	(14 ·41	<·05 (2	4·9 (50 6·9 (2 5 (14	A9.	
8	BENZENE.	—	(3 ·27	(3 ·31	·3 (4	7 (4 7 (5	A6. A9.	
9	CHRYSENE.	(1	(7 ·38	(9 ·50	—	2·5 (5 4·5 (12	A5. A9.	n-HEXANE
10	HEXAMETHYL-BENZENE.	—	(7 ·30	—	-	8·3 (12	A6.	

·22 · 28 · 34 · 4 μ

s.w.l: short wave-length limit.
all refererences from Section E.

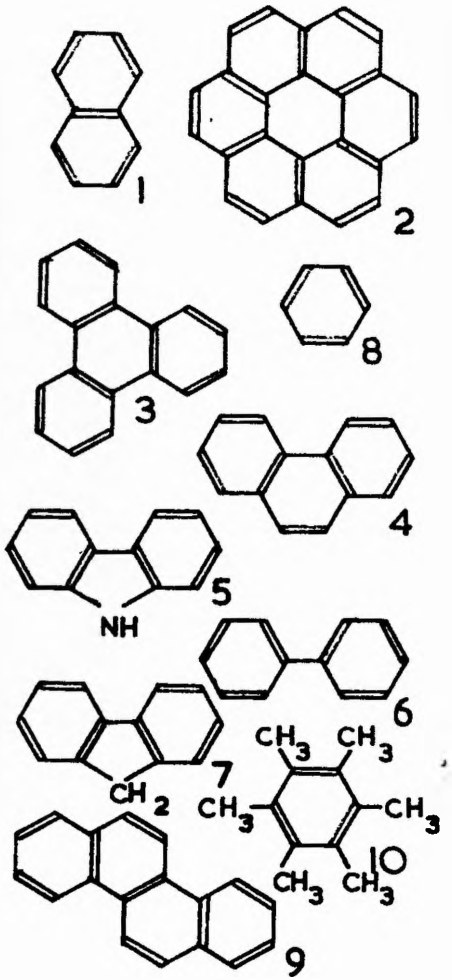

	Phosphor.	emission (max).	τ sec.	Structure.
1	Toluene.	~·34 μ	8·6	
2	Durene.	~·45 μ	4·	
3	Benzophenone.	~·45 μ	4·7ms.	
4	T.C.P.A.	~·43 μ	·5	

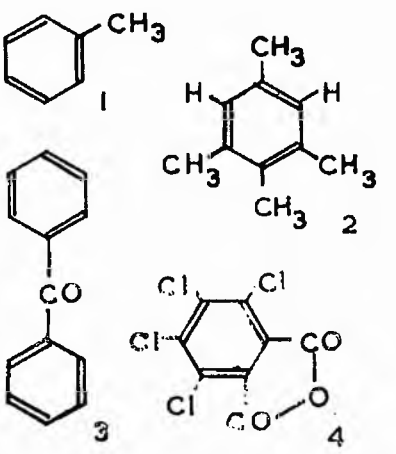

Appendix 7

Three Charge-transfer complexes referred to in Chapter X

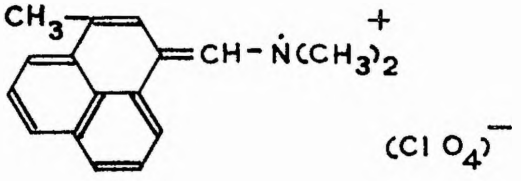

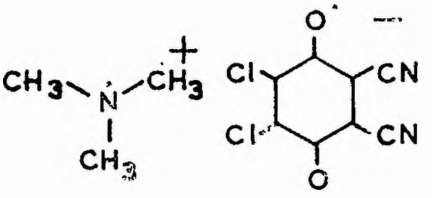

only the above complex gave E.S.R. absorption.

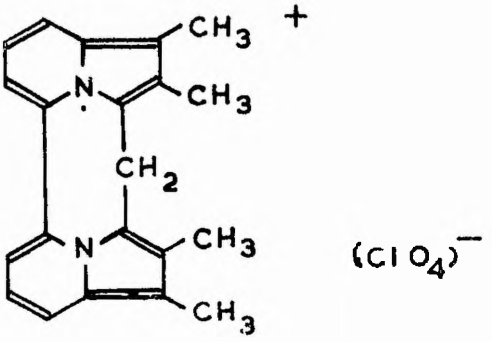

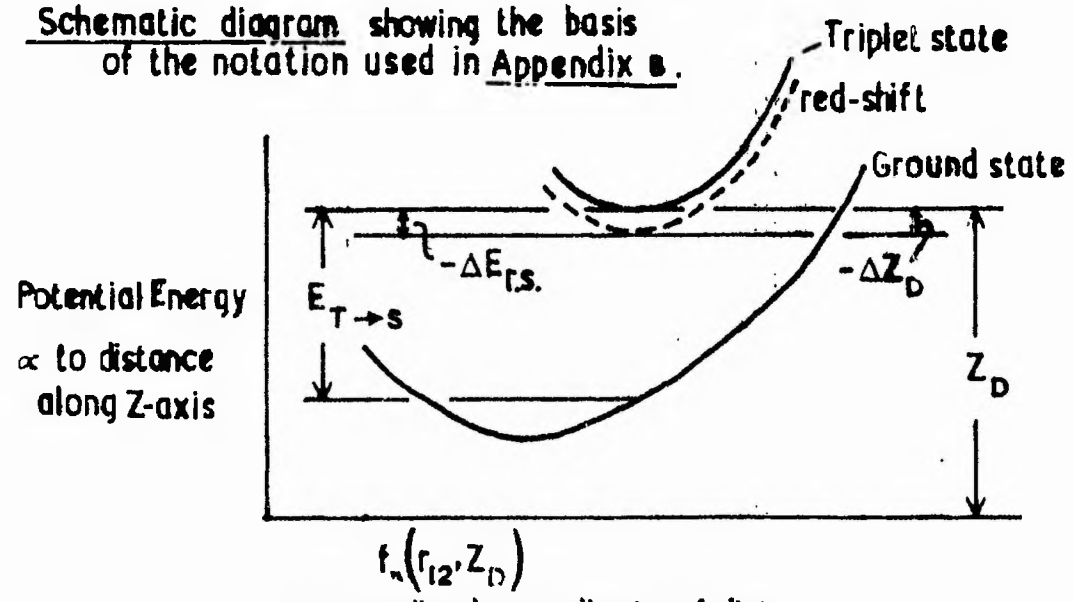

Figure A8.1

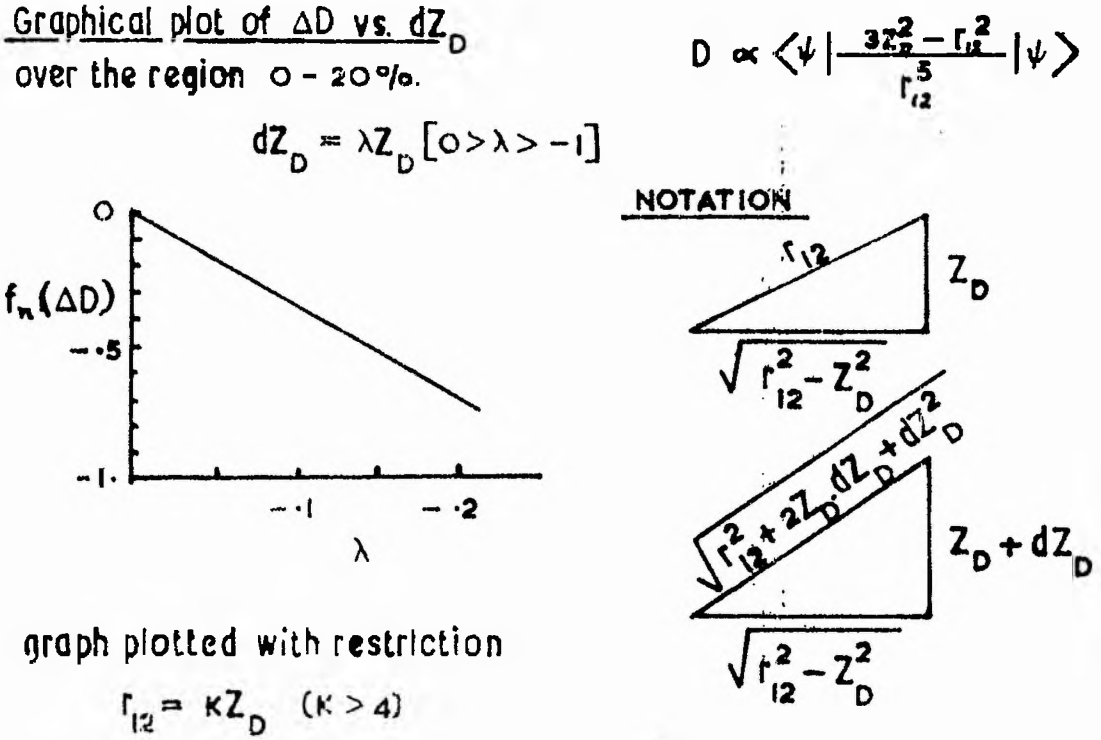

Figure A8.2

Appendix 8

A discussion on the significance of changes in $\underline{D}^*$.

In the following section, an attempt is made to show that the magnitude of the red-shift change which is found on complexing indicates that the change in $\underline{D}^*$ which also occurs on complexing cannot be wholly due to a change in $\underline{D}$, but must be mainly due to a change in $\underline{E}$. A qualitative proof can be carried out as follows:-

Firstly, two assumptions will be made:-

Assumption (i). The fractional change in energy $\left[\frac{\Delta E_{r.s.}}{E_{T\rightarrow S}}\right]$ given by the red-shift is wholly due to a change $(-\Delta z_{r.s.})$ along the z-axis of the molecule. (These terms are defined in Figure A8.1). Thus, this assumption expresses a limiting case of the probable cause of the red-shift.

Experimentally, for naphthalene-T.C.P.A.,

$$\left[\frac{\Delta E_{r.s.}}{E_{T\rightarrow S}}\right] = .2\% \quad (F2).$$

Assumption (ii). The fractional change in $\underline{D}^*$ is wholly due to $z_{r.s.}$, i.e. $\left[\frac{\Delta \underline{D}^*}{\underline{D}^*}\right] = \left[\frac{\Delta \underline{D}}{\underline{D}}\right]$.

Since $\underline{D}$ is proportional to $\left\langle \psi \left| \frac{3z_D^2 - r_{12}^2}{r_{12}^5} \right| \psi \right\rangle$,

assumption (ii) implies that $\Delta Z_{r.s.} = \Delta Z_D$.

Experimentally, for naphthalene-T.C.P.A., $\left[\frac{\Delta \underline{D}^*}{\underline{D}^*}\right] = 10\%$.

The next step is to consider the behaviour of

(a) $dE_{r.s.}$ vs. $dZ_{r.s.}$

and (b) $d\underline{D}$ vs. dZ_D

The conclusions will then be applied to the observed rates of change for $\Delta E_{r.s.}$ and $\Delta \underline{D}^*$.

(a) $\underline{dE_{r.s.} \text{ vs. } dZ_{r.s.}}$ Since $\Delta E_{r.s.}$ is due to a change in the potential energy of the electron, $dE_{r.s.}$ vs. $dZ_{r.s.}$ should be approximately constant over the initial range (0 - 5%).

(b) $\underline{d\underline{D} \text{ vs. } dZ_D}$ Since $\Delta \underline{D}$ is proportional to $\Delta\left\langle \psi \left| \frac{3z_D^2 - r_{12}^2}{r_{12}^5} \right| \psi \right\rangle$, the easiest method of evaluating $d\underline{D}$ vs. dZ_D is to evaluate $\Delta \underline{D}$ vs. ΔZ_D graphically. This is shown in Figure A8.2, where it can be seen that over the range of interest $d\underline{D}$ vs. dZ is approximately constant.

Now if assumptions (i) and (ii) are correct, it can be seen, by applying the conclusions from (a) and (b), that the rate of

change of $\left[\frac{\Delta E_{r.s.}}{E_{T\rightarrow S}}\right]$ is inconsistent with the rate of change of $\left[\frac{\Delta \underline{D}^{*}}{\underline{D}^{*}}\right]$; since a .2% change in $Z_{r.s.}$ is postulated to lead to a 10% change in $Z_{\underline{D}}$, a 2% change in $Z_{r.s.}$ would lead to a 100% change in $Z_{\underline{D}}$ (viz. $\underline{D}^{*} = 0$).

This result, however, is the reverse of that expected, as reference to Figure A8.1 shows. Clearly, as $\left[\frac{\Delta E_{r.s.}}{E_{T\rightarrow S}}\right] \rightarrow 0$, $\left[\frac{\Delta \underline{D}}{\underline{D}}\right] \rightarrow$ to a constant non-zero value.

This suggests therefore that either assumption (i) or (ii) is wrong. A consideration of these (q.v.) shows that a change in assumption (i) would not improve the above disparity in the results and thus assumption (ii) must be in error.

It seems reasonable to postulate, therefore, on the basis of the above discussion, that there must be considerable change in the $\underline{E}$ component of $\underline{D}^{*}$.

REFERENCES

Section A **Experimental e.s.r. work on the triplet state**

A1) Hutchison & Mangum	J.C.P. 34 908
A2) " " "	J.C.P. 32 1261
A3) " " "	J.C.P. 29 952
A4) de Groot & Van der Waals	Mol. Phys. 2 335
A5) " " " " " "	Mol. Phys. 3 190
A6) " " " " " "	Proc. XIth. Colloque Ampere. Eindhoven. 1962 p. 379
A6B)	discussion on above
A7) " " " " " "	Mol. Phys. 4 189
A8) Yager, Wasserman & Cramer	J.C.P. 37 1148
A9) Smaller	J.C.P. 37 1578
A10) Farmer, Gardner & McDowell	J.C.P. 34 1058
A11) Brandon, Gerkin & Hutchison	J.C.P. 37 447
A12) Piette et al.	J.C.P. 36 3094
A13) Varian advertisement	Physics Today 16 95
A14) Shigorin	O.i.S. 12 369
A15) Ptak & Douson	C.R. 257 438 Nat. 199 1092
A16) Smaller	Nat. 195 593
A17) Vincent & Maki	J.C.P. 39 3088
A18) Foerster	Z.f.N. 18A 620
A19) Thomson	J.C.P. 41 1
A20) Hornig & Hyde	Mol. Phys. 6 33

A21) de Groot & van der Waals — Mol. Phys. 6 544

A22) Wasserman, Snyder & Yager — J.C.P. 41 1763

A23) Smaller (review) — Advances in Chemical Physics. VII 567

A24) Smaller — R.S.I. 24 991

Section B. Theoretical work on the triplet state

B1) Bernstein & Gouterman — J.C.P. 39 2443

B2) Ying-Nan Chiu — J.C.P. 39 2736

B3) McLachlan — Mol. Phys. 5 51

B4) Amos — Mol. Phys. 5 91

B5) Jablonskii — Zeits. Phys. 94 38

B6) Pariser — J.C.P. 24 250

B7) Wasserman et al — J.C.P. 41 1763

B8) Kottis & Lefebrve — J.C.P. 39 393

B9) van der Waals et al — Mol. Phys. 8 301

B10) Griffiths et al — Rept. Bristol Conf. on Defects in Crystalline Solids 1954 p. 81.

B11) Dexter — J.C.P. 21 836

B12) Kottis & Lefebrve — J.C.P. 41 3660

Section C. E.S.R. work on other phosphors

C1) Low — P.R. 98 426

C2) Dubinin & Trapeznikova — O.i.S. 9 187
O.i.S. 9 245

C3) " " " — O.i.S. 9 279

C4) Garlick, Cunliffe & Jones — P.P.S. 79 223

C5) Herschberger & Leifer — P.R. 88 714

C6) N.M.R. & E.S.R. Spectroscopy — Varian Bros. p. 249 Pergamon 1961

C7) Ingram et al — Nat. 176 1227

C8) Otomo et al — P.L. 4 228

C9) Rauber & Schneider — P.L. 3 230

C10) Kallman et al — Magnetic & Electric Resonance and Relaxation (ed) Smidt. 1963 p. 414

C11) Dielman — ibid. p. 409

E.S.R. work on Cr^{3+} phosphors

C20) Manenkov & Prokhorov — J.E.T.P. 1 611

C21) Geusic — J.E.T.P. 4 288 P.R. 102 1252

C22) Mairman — P.R.L. 4 654

C23) Wieder — P.R.L. 3 469

C24) Geshwind & Schawlow — P.R.L. 3 545

Section D. Other e.s.r. work

D1) Shigorin et al — O.i.S. 10 315

D2) Kawamura & Ishiwatari — J.P.S.J. 13 33

D3) Smaller et al — P.R. 104 599, 605

D4) Hahn & Walstedt — Helv. Phys. Acta. 35 255

D5) Bijl et al — J.C.P. 30 765

Cerous salts

D11) Jones — P.P.S. 68 165

D12) Baker, Jones et al — P.P.S. 73 942

D13) Dvir & Low — P.P.S. 75 136

Section E. Optical work on the triplet state

E1) Friedel & Orchin — U.V. Spectra. Wiley 1951

E2) Ermolaev — O.i.S. 11 266

E3) Kasha — Chem. Rev. 41 401

E4) McLure — J.C.P. 20 829

E5) McLure — J.C.P. 17 905

E6) Gilmore et al — J.C.P. 20 829
J.C.P. 23 399

E7) Sangster & Irvine — J.C.P. 24 670

E8) McLure — J.C.P. 19 670

E9) Nurmukhametov et al — O.i.S. 9 313

E10) Spooner — Luminescence. p. 143
Kallman & Spruch. (ed.)
Wiley. 1962.

E11) O'Dwyer et al — J.C.P. 36 1395

E12) Olness & Spooner — J.C.P. 38 1779

E13) Lewis & Kasha — J.A.C.S. 66 2100
J.A.C.S. 67 994

E14) Heckman — J. Mol. Spec. 2 27

E15) Ermolaev — O.i.S. 9 183

E16) Ferguson — J.C.S. 1954 3160

E17) Ferguson — J. Mol. Spec. 3 177

E18) Piatnitskii — Doklady 1 451

E19) Balikova — O.i.S. 6 72

E20) Freed — Science 128 1341

E21) Spooner & Kanda — J.C.P. 40 778

E22) Trusov & Teplyakov — Ukranian Fiz. Zh. 8 1008

E23) Wolf — Z.f.N. 10A 3

E24) Landolt-Bornstein — Springer-Verlag 1960-

E25) Lewis, Lipkin & Magel — J.A.C.S. 63 1941

E26) Porter & Windsor — J.C.P. 21 2088

Energy transfer (intermolecular)

E30) Terenin & Ermolaev — T.F.S. 52 1042

E31) Ermolaev — O.i.S. 6 417

E32) Kallman et al — Luminescence (see R0) p. 244

E33) Ermolaev & Sheshnikova — Doklady 8 375

E34) Eisenthal — J.C.P. 39 2108

E35) Ermolaev — Uspekhi 6 333

E36) Roy & El-Sayed — J.C.P. 40 3442

E37) Hochstrasser — J.C.P. 39 3153
J.C.P. 40 1038

Energy transfer (intramolecular)

E40) Ermolaev & Terenin — Uspekhi 3 423
J. Chim. Phys. 55 698

Quasi-linear emission spectra

E50) Shpol'skii & Klimova — Doklady 1 782

E51) Bowen & Brocklehurst — J.C.S. 1955 4320
J.C.S. 1954 3875

E52) Bolotnikova — O.i.s. 7 138

E53) Shpol'skii — Uspekhi 3 372

Paramagnetism of the triplet state

E60) Lewis, Calvin & Kasha — J.C.P. 17 804

E61) Evans — Nat. 176 777

Theoretical

E70) Kasha — Chem. Rev. 41 401
D.F.S. 9 14

E71) Foester — Naturwissen 36 240

E72) Reid — Quarterly Reviews No. 12

E73) Reid — Excited States in Chemistry & Biology. Butterworths. 1956.

E74) Mokeeva & Sveshnikov — O.i.S. 10 41

E75) Philipovitch & Sveshnikov — Doklady 3 286

E76) Wolf. — Solid state physics 9 1

E77) Ganguly & Chaudbury — Rev. Mod. Phys. 31 990

E78) McLure — Solid state physics. 8 1

E79) El-Sayed — Nat. 167 481

Polarization of spectra

E80) Krishnan & Seshan — Current Science 3 26

E81) Albrecht — J. Mol. Spec. 6 84

E82) Williams — J.C.P. 30 233

E83) Hochstrasser — J.C.P. 40 1041

E84) Krishna & Goodman — Nat. 191 800

E85) Philipovitch — O.i.S. 10 104

E86) Platt — J.C.P. 17 484 et seq.

E87) McLure — J.C.P. 22 1668

E88) El-Sayed — J.O.S.A. 53 797

Miscellaneous

E90) Kallman, Kramer & Sucov — J.C.P. 23 1043

E91) Giordmaine — Sc. Am. 210 4 38

Section F. Molecular complexes

F1) Briegleb — Electron-Donor-Acceptor-complexes. p. 88. Springer. Berlin.

F2) Czekalla & Briegleb — Z. Elecktrochem. 61 1053; 63 623; 63 712.

F3) McGlynn & Boggus — J.A.C.S. 58 5096

F4) McGlynn, Boggus & Elder — J.C.P. 32 357

F5) McGlynn & Christodouleas — J.C.P. 40 166

F6) Buu-Hoi — Bull. Chim. Soc. 1960 1714

F7) McGlynn — Luminescence (see E10) pp. 284, 289.

F8) Reid — J.C.P. 20 1212

F9) Chowdhury & Basu — T.F.S. 56 335

F10) Benesi-Hildebrand — J.A.C.S. 71 2703

F11) Murrell — The Theory of the Electronic Spectra of Organic Molecules. Methuen. 1963. Chapter 13.

F12) Mulliken — J.A.C.S. 74 811
J.P.C. 56 801

F13) Nakamoto — J.A.C.S. 74 1739

F14) Wallwork — J.C.S. 1961 494

Section G. Platinocyanides

G1) Levy — J.C.S. 93 Trans. 1446; J.C.S. 93 Proc. 178

G2) Pauling — Nature of the Chemical Bond p. 98 (Oxford 1940)(see also Ch. XI)

G3) Wyckoff — Crystal structures. 1951.

G4) Brasseur — C.R. 196 2015

G5) Tolstoi, Tkachuk & Ageeva — O.i.S. 14 85

G6) Tolstoi et al — J.E.T.P. 2 331

G7) Dewar — Chem. News 70 252

G8) Moncuit & Poulet — J. Phys. Rad. 23 358

Section H. Uranyl salts

H1) Bequerel — C.R. 75 296; C.R. 152 511

H2) Nichols & Howes — Fluorescence of Uranyl Salts. Carnegie Inst. 1919.

H3) Wawilow & Lewschin — Z. Phys. 48 397

H4) Dieke & Duncan — Spectroscopic properties of Uranium compounds. McGraw-Hill. 1949.

H5) Pauling & Dickinson — J.A.C.S. 46 1615

H6) Coustal — C.R. 187 1139

H7) Wick & McDowell — P.R. 11 et seq.

H8) — O.i.s. 3 234

H9) Bleaney — D.F.S. 19 112

H10) Hall & Dieke — J.O.S.A. 47 1092

H11) Eisenstein & Pryce — P.R.S. A229 20

H12) Belford — J.C.P. 34 314.

H13) Rabinowitch & Belford — Spectrochemistry & Photochemistry of Uranyl compounds. Pergamon. 1964.

Section J. Rare-earth trifluorides

J1) Griffiths, Owen & Ward — Nat. 173 439

J2) Jones, Baker & Pope — P.P.S. 74 249

J3) Hutchison & Wong — J.C.P. 29 754

J4) Bleaney & Scovil — Phil. Mag. 43 999

J5) Baker & Rubins — P.P.S. 78 1353

J6) Schlyter — Arkiv. fur Kemi. 5 786

J7) Wong et al — J.C.P. 39 786

J8) Sayer & Freed — J.C.P. 23 2066

Section K. Transition metal chelates

K1) Gillard, Rogers et al — Private communication

K2) Addison — Structural Principles in Organic Compounds. Longmans. 1962. p. 124.

K3) Orgel — J.C.S. 1952 4756

K4) Maki — J.P.C. 60 71

K5) Harrison & Assour — Paramagnetic Resonance. Low (ed.) p. 855. Academic Press. 1963.

K6) Maki & McGarvey — J.C.P. 29 31

K7) Okmura & Data — P.R. 94 314

K8) Bleaney et al — P.R.S. A198 416

K9) Abragam & Price — P.R.S. A206 173

K10) Pake & Purcell — P.R. 74 1184

Section L. Phosphorescence and thermoluminescence

L1) Randall & Wilkins — P.R.S. A184 366

L2) Garlick — Luminescent Materials. Oxford. 1949

L2B) — ibid. p. 54

L3A) Curie — Luminescence in crystals. Methuen. 1963. p. 162

L3B) — ibid. Chapters 3 and 4

L3C) — ibid. p. 32

L4) Wrzesinska — Acta. Phys. Pol. 15 151

L5) Grossweiner — J. Appl. Phys. 24 1306

L6) Garlick & Wilkins — P.R.S. A 184 411

Section M. Triboluminescence

M1) Herschel (1899) — Nat. 60 29

M2) Wolff et al (1955) — Z.f. Electrochemie 59 346

M3) Longchambon (1922) — C.R. 174 1633

M4) Nelson (1926) — R.S.I. 12 207

M5) Bhatnagar et al (1932) — Z.f. Phys. Chem. 163A 18

M6) Wick (1937) — J.O.S.A. 27 275

M7) Wick (1940) — J.O.S.A. 30 302

M8) Dewar (1901) — Nat. 64 244

M9) Bequerel (1901) — C.R. 133 199

Section N. Inorganic Phosphors

N1) Bowen — Chemical Aspects of Light. Oxford. 1949 p. 181.

N2) Satoh — Nat. 133 837

N3) Khalupovskii — O.i.S. 9 274

N4) Brit. J. Applied Physics — Supplement No. 4. 1955.

N5) Monod-Herzan et al — C.R. 252 3618

N6) Balin — O.i.S. 6 495

N7) Kutzelnigg — Z. Agnew. Chem. 50 366, 49 267.

N8) Waggoner — P.R. 31 358

N9) Randall — P.R.S. A184 421

N10) Beard — J. Appl. Phys. 33 144

N11) Cook — P.P.S. 68 148

N12) Przibram — Irradiation Colours & Luminescence. Pergamon. 1956.

Section O. KCl phosphors

O1) Pringsheim — Rev. Mod. Phys. 14 32

O2) Ewles & Joshi — P.R.S. A254 366

O3) Vrehen — Paramagnetic resonance of Eu in $PbCl_2$ & Fluorescence of Tl in KCl. Rotterdam. 1963.

O4) Schlesiger & Halperin — P.R.L. 11 360

Section P. References from Pringsheim

(P0) Fluorescence & Phosphorescence. Pringsheim. Interscience. 1949.

P1) p. 373; P2) p. 515; P3) p. 594; P4) p. 658; P5) p. 654; P6) p. 659; P7) p. 629; P8) p. 505; P9) p. 502.

Section Q. General references on e.s.r.

Q1) Feher	B.S.T.J. 36 449
Q2) Ingram	Spectroscopy at Radio & Microwave Frequencies. Butterworths. 1955.
Q3) Ingram	Free Radicals. Butterworths. 1958.
Q4) Goldsburgh & Mandel	R.S.I. 31 1044
Q5) Wertz	Chem. Rev. 55 829
Q6) Squires	Introduction to microwave spectroscopy. Newnes 1963.
Q7) Bowers & Owen	Rep. Prog. Phys. 18 304
Q8) Bleaney & Stevens	Rep. Prog. Phys. 16 108

Section R. References on e.s.r. spectrometers

R1) Smidt et al	R.S.I. 32 1421
R2) Mishra	R.S.I. 29 590
R3) Daniels & Farrach	R.S.I. 32 1262
R4) Whiffen et al	T.F.S. 54 1129
R5) Strandberg et al	R.S.I. 27 596
R6) Smith	J.S.I. 39 127

R7) Gambling & Wilmshurst — J.S.I. 38 334

R8) Henning — R.S.I. 32 1262

R9) Stoodley — Research & Development 5 74

Variable Couplers

R11) Gordon — R.S.I. 32 658

R12) Faulkner — J.S.I. 40 205

Sensitivity

R21) Ehrenberg — Advances in Chem. Phys. VII 606

R22) Fraenkel — Techniques of Organic Chemistry. Pt. IV. p.2801 Weissberger (ed.) Interscience. 1959.

R23) Lyons & Watson — J. Polymer. Sci. 18 141

R24) Gardner & Fraenksl — J.A.C.S. 76 5891 J.A.C.S. 78 3279

R25) Wilmshurst & Ingram — J. Electronics & Control 13 339.

R26) Yariv & Gordon — R.S.I. 32 462

R27) Bleaney & Bleaney — Electricity & Magnetism p. 482. Oxford. 1959.

R28) Low Noise Amplifier Design — M-O valve Co. London.

R29) Robinson — Noise in Electrical Circuits. Oxford. 1962.

R30) Parker — Electronics. Arnold. 1960.

R31) Stoodley — J. Electronics & Control 14 531

R32) Cook & Mallard — Nat. 198 145

R33) de Groot — Private communication

R34) Kohnlein & Mullen — Physics in Medicine & Biology. 6 599.

R35) Bijl — Private communication

Section S. Previous St. Andrews group work

S1) Brown — Ph.D. Thesis

S2) Campbell — Ph.D. Thesis

S3) Firth — Ph.D. Thesis

S4) Taylor — M.Sc. Thesis

S5) Bevridge — M.Sc. Thesis

Section T. Miscellaneous

T1) Sealy — Electron-Tube Circuits. p. 624.

T2) Valley & Wallman — Vacuum-tube Amplifiers. McGraw-Hill. 1948.

T3) Hickman — W.W. 65 550

T4) Williamson — W.W. 53 118, 161 and 282

T5) Schuster — R.S.I. 22 254

T6) Williams — Thermionic Valve Circuits p. 233. Pitman. 1955.

T7) Engstrom — J.O.S.A. 37 420

T8) Curran — Luminescence & Scintillation Counters. Butterworth. 1963.

T9) Zepler & Punnett — Electronic Circuit Technique p. 102

Chemical Actinometers

T11) Techniques of Organic Chemistry — Vol. II. Interscience. p. 103. 1950.

T12) Bowen — Chemical Aspects of Light. p. 283. Oxford. 1949.

Filter Combinations

T21) Kasha — J.O.S.A. 38 929

T22) Bowen — See T12, Appendix.

Mechanical

T31) Roberts — J.S.I. 31 251

T32) Henry & Dolecek — R.S.I. 21 496

T33) White — Experimental Techniques in Low Temperature Physics. Oxford. 1959.

Crystal Growing

T41) Symposium — D.F.S. 5

T42) Fonda & Seitz — Preparation and Characteristics of Solid Luminescence Materials. Wiley. 1948.

T43) Holden & Singer — Crystals & Crystal Growing. Heinemann. 1961.

T44) Gilman — The Art & Science of Growing Crystals. Wiley. 1963.

T51) Mott & Gurney — Electronic Processes in Ionic Crystals. Oxford. 1940.

T52) Kittel — Solid State Physics. Wiley. 1959.

T61) Ellenbass — Physica. 3 859

T62) " — The High Pressure Mercury Vapour Lamp. Amsterdam.

T63) Koller — U.V. Radiation. Wiley. 1952.

T71) Grebenkemper & Hagan — P.R. 80 89.

Personal Acknowledgements

During the course of my research studentship at St. Andrews, I was helped by many people, far too numerous to mention individually, but I would particularly like to thank Professor J. F. Allen, F.R.S., and my supervisor Dr. D. Eijl, F.R.S.E., for their unfailing interest and encouragement, as well as supplying the necessary equipment. The design and construction of the cryogenics was only possible due to the help freely given by Mr. R. H. Mitchell. I would also like to thank Mr. H. Cairns for generously lending some of the electrical equipment. The photographs, etc., in the thesis are due to Messrs. J. Gerrard and J. Sparks. I am also grateful to the University of St. Andrews and the Department of Scientific and Industrial Research for the award of maintenance grants.

During the final year of my research, I was very grateful for the assistance given by Mr. I. D. Campbell, who is now carrying on the research project, and I wish him well!